Hydrological response of Icelandic river basins to projected climate change during the 21st century. A case study.

Philippe Crochet

Report number: 2022-RD-01	Date: December 2022	Number of pages:168	Distribution: Public

Report title:
Hydrological response of Icelandic river basins to projected climate change during the 21st century. A case study.

Author:
Philippe Crochet
philippec@simnet.is

Abstract:

This study presents an analysis of the hydrological response of three Icelandic river catchments to projected climate change in the 21st century. The catchments are located in the north and southeast of the country and their current hydrological regimes are influenced by snow seasonality. Daily streamflow series were simulated over the period 1981-2100 with the HYPE hydrological model forced with an ensemble of regional climate projections from CORDEX, under two greenhouse gas emission scenarios. Changes affecting near surface air temperature and precipitation and their impact on mean and extreme streamflow characteristics were analysed. There is a consensus that air temperature will rise in the future, leading to shorter snow seasons and less snow storage. The projected changes in climatic conditions are expected to impact the hydrological characteristics of the three studied catchments but the timing, magnitude and direction of the response vary with the season and catchment.

Prepared for:
The research fund of the Icelandic Road and Coastal Administration

Keywords:
Iceland - Hydrology - Climate change - CORDEX - HYPE model

Executive summary

This study presents an analysis of the hydrological response of three Icelandic river catchments to projected climate change in the 21st century. The catchments are located in the north (Svartá and Fnjóská) and southeast (Laxá) of the country and their drainage areas range from 52 to 1130 km^2. The snow accumulation and melt cycle has a strong influence on the hydrological regimes of the Svartá and Fnjóská catchments under present climate conditions, whereas the Laxá catchment has a more mixed rainfall/snowmelt regime. In order to infer the likely hydrological response of these catchments to projected climate change and its evolution throughout the 21st century, an ensemble of daily streamflow series was simulated over the period 1981-2100, with the HYPE hydrological model forced with an ensemble of regional climate projections from CORDEX, for two possible greenhouse gas emission scenarios referred to as Representative Concentration Pathways (RCPs 4.5 and 8.5). Changes affecting near surface air temperature and precipitation and their impact on mean and extreme streamflow characteristics were analysed, considering moving 30-year periods. The reference period was taken as the 1981-2010 period.

A significant warming is expected in the 21st century, more or less pronounced according to the season, catchment location and emission scenario (0.295°C/decade for the RCP4.5 emission scenario and 0.473°C/decade for the RCP8.5 emission scenario, on average over all months and catchments). The temporal variability of precipitation is mainly characterised by decadal to multi-decadal oscillations and no clear long-term trend is emerging in most cases, except in summer and/or autumn in the Svartá and Fnjóská catchments, depending on the emission scenario, where mean precipitation is projected to increase, leading to an increase in mean annual precipitation as well.

The rise in temperature leads to an increase in the fraction of annual precipitation falling as rain, at the expense of snow, which, in turn, leads to shorter snow seasons and less snow storage. These changes, in turn, are projected to lead to changes in the streamflow regimes of the studied catchments in the future, but the timing, magnitude and direction of the hydrological response vary with the emission scenario, season and catchment.

The results indicate that mean seasonal river flow is likely to increase in autumn and winter and decrease in spring, in the future, in the three catchments. Mean seasonal river flow is likely to decrease in summer in the Fnjóská and Laxá catchments, whereas in the Svartá catchment, no significant change is projected under the lowest emission scenario and a moderate increase is projected in the second-half of the 21st century under the highest emission scenario. The peak of mean daily flow caused by spring snowmelt will most likely be reduced and shifted earlier, in the three catchments, due to snow storage depletion. The projected changes in mean seasonal flow are not necessarily gradual along the projection horizon, like warming, because precipitation fluctuations contribute to modulate these changes.

The results also indicate that flood risk is likely to change in the future. In the Svartá catchment, annual maximum floods are projected to occur less and less frequently in spring and more and more often in the other seasons, especially in winter, and their magnitude is projected to decrease, owing to the projected reduction in snow storage and subsequent decrease in spring snowmelt. In the Fnjóská catchment, annual maximum floods are projected to occur less and less frequently in spring and summer, and more and more often in autumn and winter, especially under the highest emission scenario, and their magnitude is also projected to decrease, owing to the projected reduction in snow storage. In contrast, the Laxá catchment is projected to remain under the dominating influence of rainfall-generated annual maximum floods in autumn but a slight magnitude increase is likely to be expected in some future periods, probably because of rainfall intensification.

Projected changes in streamflow characteristics are usually more pronounced and/or start earlier under the highest emission scenario than under the lowest one because a greater warming is projected, leading to larger changes in the ratio of rainfall and snowfall and to a larger decrease in snow storage. The uncertainties associated with the streamflow projections reflect the uncertainties associated with the emission scenarios, climate projections and hydrological modelling.

1 Introduction

Global warming caused by human influence is unequivocal (IPCC 2021). Numerous studies have been undertaken worldwide to investigate the impact of projected climate change on hydrology and associated extreme events such as floods and droughts (e.g. Habets et al. 2013; Arheimer and Lindström 2015; Vetter et al. 2015; Vormoor et al. 2015; Wanders and Wada 2015; Naz et al. 2016; Frans et al. 2018; Osuch et al. 2018; Wan et al. 2018; Somers et al. 2019; Zhao et al. 2019; Lane and Kay 2021; and many others). Changes affecting hydrological processes are likely to have implications for water resource management, the operation of reservoirs and existing hydropower installations and flood and drought risks. Thus, providing a comprehensive overview of climate change impact on future hydrological conditions is imperative in order to adapt water management strategies and anticipate mitigating actions that may have to be taken to make the society resilient to these changes.

In Iceland, several studies have analysed recent and projected climate changes and their impact on glaciers and hydrology (e.g. Jóhannesson et al. 2007; Einarsson and Jónsson 2010; Thorsteinsson and Björnsson Eds. 2011; Gosseling 2017; Björnsson et al. 2018; Aðalgeirsdóttir et al. 2020; Crochet 2013, 2020, 2021). Of particular importance, the projected warming in the coming decades is expected to lead to less snow storage, shorter snow seasons and the retreat of glaciers. With increased glacier melting owing to higher temperatures, the runoff from glaciers is projected to first increase and later decline because the glaciers will retreat and eventually disappear (e.g. Jóhannesson et al. 2007). At the catchment scale, the hydrological response to projected climate change is likely to depend on the catchment properties and current hydro-climatic characteristics (e.g. Einarsson and Jónsson 2010; Crochet 2020, 2021). For example, temperature-driven changes affecting streamflow seasonality such as changes in the phase of precipitation, amount of snow accumulation and snow and glacier melt, are likely to vary according to the altitude distribution of the catchments and their fraction of glacier coverage if any. Therefore, in order to continue the work initiated in Crochet (2020) and expand our knowledge of the hydrological response to projected climate change in Iceland, three new catchments are investigated in this study.

The methodology adopted in this study is based on a multi-model approach. An ensemble of six locally-adjusted CORDEX climate projections are used to force a hydrological model (HYPE) and produce an ensemble of hydrological projections. The climate projections have been obtained by the combination of two global climate models (GCMs) and four regional climate models (RCMs) for two possible emission scenarios known as Representative Concentration Pathways (RCPs 4.5 and 8.5). The hydrological model is run with two different parameter sets. This type of multi-model ensemble approach has been widely used (see for instance Vormoor et al. 2015). It allows to take into account various sources of uncertainties in the modelling chain (future emission scenarios, global and regional climate modelling, hydrological model parameterisation) and is thus expected to provide a plausible range of hydrological projections for the coming decades.

This report is organised as follows. Section 2 presents the studied catchments and Section 3 presents the data and methods. Section 4 is dedicated to the calibration of the hydrological model and Section 5 to the analysis of the climate projections. The hydrological response to projected climate change is analysed in Sections 6 and 7 and Section 8 concludes this report.

2 The investigated catchments

The three studied catchments are situated in different regions and their drainage areas range from 52 to 1130 km^2 (Figure 1 and Table 1). Svartá is located in the north of Iceland, west of the Tröllaskagi mountain range; Fnjóská is located in the north of Iceland, east of the Tröllaskagi mountain range; Laxá í Nes is located in the southeast of Iceland, east of the Vatnajökull ice-cap. The streamflow gauging stations are located at the outlet of the catchments and monitored by Veðurstofa Íslands (Icelandic Met. Office).

Icelandic rivers are usually classified in three main categories according to the origin of flow: direct runoff rivers (D), glacial fed rivers (J), groundwater fed rivers (L) and whether they flow through lakes (S). In practise, rivers are often a combination of several of these categories. According to Hróðmarsson and Þórarinsdóttir (2018), the Svartá river at gauging site vhm10 is a combination of two categories (L, D), the Fnjóská river at gauging site vhm200 and the Laxá river at gauging site vhm74 are classified as direct runoff rivers. According to the Corine Land Cover data (Árnason and Matthíasson, 2017), the Svartá catchment is mainly covered with vegetated land followed by poorly vegetated or barren areas and by some cultivated land; the Fnjóská catchment is dominated by poorly vegetated or barren areas followed by vegetated land; the Laxá catchment is mainly covered with vegetated land followed by poorly vegetated or barren areas. According to the soil map of Iceland (Arnalds and Óskarsson, 2009; Arnalds, 2015), the prevailing soil type found in the Svartá catchment is made of a composition of brown, histic and gleyic andosols, followed by cambic vitrisol; the three dominating soil types found in the Fnjóská catchment are i) a composition of brown, histic and gleyic andosols, ii) leptosol and iii) cambic vitrisol; the prevailing soil type found in the Laxá catchment is made of leptosol followed by a composition of brown, histic and gleyic andosols.

Table 1: Discharge gauging stations and main characteristics of catchments

Name of river and location of gauging station	ID	River type	Drainage area (km^2)	Mean elevation (m.a.s.l)
Svartá, Skagafirði; Reykjafoss	vhm10	L, D	390	526
Laxá í Nesjum	vhm74	D	52	389
Fnjóská; above Árbugsár	vhm200	D	1130	729

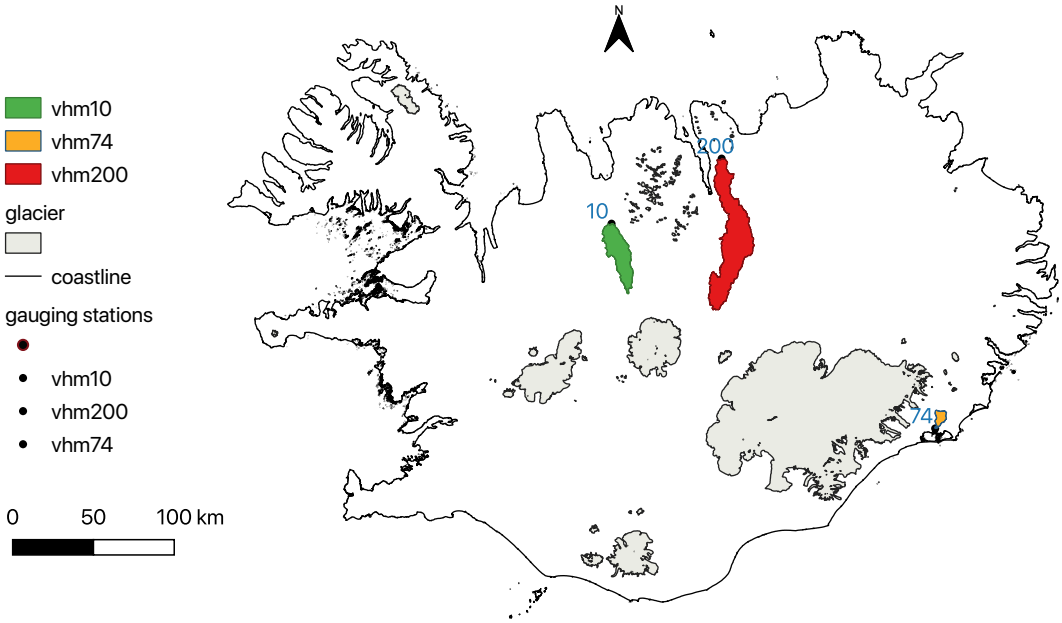

Figure 1: Overview of the studied catchments. Glaciers and coastline from National Land Survey of Iceland. Catchment delineation based on ArcticDEM (Porter et al., 2018).

3 Data and methods

3-1 Method overview

The methodology adopted in this study is similar to the one used in Crochet (2020, 2021). An ensemble of daily hydrological projections was obtained for the period 1981-2100, using the following well-established modelling chain (see for instance Arheimer and Lindström, 2015):

"Emission scenario → global climate model → regional downscaling → bias correction → hydrological model → analysis"

The HYPE hydrological model was used in this study (see Section 3-2). The model was calibrated over two consecutive periods, leading to two parameter sets. The use of two parameter sets is expected to improve the reliability of the hydrological simulations.

The climate forcing was provided by an ensemble of six regional climate projections from the CORDEX framework for two possible emission scenarios (see Section 3-3). These climate projections were obtained from four regional climate models (RCMs) driven by two global climate models (GCMs) and their precipitation and temperature outputs were then locally adjusted using a statistical technique to improve their applicability at the catchment scale (see Section 3-7). Using an ensemble of climate projections rather than a single one gives a better representation of possible future states of the climate system under study and allows a more reliable evaluation of its future temporal evolution.

In total, an ensemble of twelve daily hydrological projections (or twelve ensemble members) was obtained for the period 1981-2100 and each emission scenario. The spread of the ensemble provides a measure of the projection uncertainty. Various hydro-climatic indicators were then extracted from these projections and their characteristics analysed considering a moving-window approach based on 30-year periods (1981-2010; 1991-2020; 2001-2030; 2011-2040; 2021-2050; 2031-2060; 2041-2070; 2051-2080; 2061-2090; 2071-2100). The reference or baseline period is defined as the 1981-2010 period.

The hydro-climatic indicators considered in this study are:

- Air temperature (catchment-averaged)
- Precipitation (catchment-averaged)
- Rainfall (catchment-averaged)
- Snowfall (catchment-averaged)
- Snow storage, in snow water equivalent (SWE, catchment-averaged)
- Snow melt (catchment-averaged)
- River discharge at the catchment outlet

For each hydro-climatic indicator (except snow storage), monthly and/or seasonal and annual values were calculated by averaging daily values from each month, season and water year, respectively, and then the 30-year mean calculated in each period. The water year is defined from October of year *i* to September of year *i*+1 and the four seasons are October to December (OND), January to March (JFM), April to June (AMJ) and July to September (JAS). These seasons will sometimes be referred to as autumn, winter, spring and summer, respectively. In order to analyse changes in more details, 30-year mean daily discharge and snow storage were also calculated for each day of the water year.

The annual maxima of the daily river discharge series (annual maximum floods, AMFs) were also extracted and changes in the timing and magnitude of these extreme events examined. Changes in the timing of AMFs were analysed in order to examine possible changes in the flood-generating mechanisms. To investigate changes in the timing of AMFs, the day in the water year when annual maximum discharge occurred was assigned to the corresponding season. The frequency with which AMFs occurred in each season for each 30-year projection period was then calculated. To analyse changes in the magnitude of extreme flood events, a Gumbel distribution was fitted to the AMFs (Stephenson 2002; Delignette-Muller and Dutang 2015) and the magnitude of the T-year flood (for T=10 and 50 years) estimated in each 30-year period. Finally, the flood magnitude Q was fixed and the corresponding return period T(Q) estimated in each 30-year period.

Changes affecting the hydro-climatic indicators were evaluated by comparing each future 30-year period to the reference period (1981-2010). A two-sided Mann-Whitney test with a 5% significance level was used to compare the 30-year mean daily snow storage and river discharge ensembles, respectively, between the reference and future periods. The null hypothesis being that the ensembles in the reference and future periods are drawn from populations having the same distribution and the alternative hypothesis being that the two populations differ. Two one-sided Mann-Whitney tests with a 5% significance level were used to compare the ensembles of 30-year mean seasonal and annual temperature, precipitation, rainfall, snowfall, snowmelt and discharge and the T-year flood ensembles, respectively, between the reference and future periods. The null hypothesis being that the ensembles in the reference and future periods are drawn from populations having the same distribution and the alternative hypothesis either being that the population in the future period tends to be shifted towards larger values (increase) or towards lower values (decrease), compared to the population in the reference period. The two one-sided tests were run consecutively. When the null hypothesis was not rejected by both tests, it was reasonably concluded that the ensemble members from the two periods were drawn from the same population, and no change was likely projected between the two periods. When the null hypothesis was rejected in favour of the alternative hypothesis, it was reasonably concluded that an increase or decrease had likely been projected in the future period, compared to the reference period, depending on the selected alternative hypothesis.

For the seasonal frequencies of occurrence of AMFs, changes between the reference and future periods were considered significant when at least 2/3 of the ensemble members were shifted in the same direction (frequency increase or decrease).

Then, changes affecting the 30-year mean of each hydro-climatic indicator and the T-year flood magnitude between reference and future periods were quantified. To do so, the future values of each ensemble member were compared with the value of the same member in the reference period, by calculating the difference (future minus reference) or relative difference in percent (100*(future minus reference)/reference), and the ensemble median of the difference or relative difference calculated.

A detailed analysis of the contribution of individual sources of uncertainty in the modelling chain to the overall uncertainty of the hydrological projections is beyond the focus of this study and therefore not undertaken. This aspect has been investigated in a number of studies. For instance, in a study focused on river basins in Northern and Central Europe, Graham et al. (2007) found that the choice of GCM had more impact on projected hydrological change than the choice of emission scenario or RCM used for downscaling. Gosling et al. (2011) found that the GCM uncertainty was greater than the hydrological model uncertainty when analysing river runoff projections obtained with a global hydrological model and several catchment-scale hydrological models, for a set of catchments located in various regions of the world. The study of Ott et al. (2013) in Germany came to different conclusions depending on the season considered, with the main contribution to overall uncertainty of the climate change signal attributed to the RCMs in summer, whereas in winter, the largest contribution to overall uncertainty was attributed to natural variability.

3-2 The HYPE hydrological model

HYPE (Hydrological Predictions for the Environment) is a conceptual, spatially semi-distributed hydrological model developed by the Swedish Meteorological and Hydrological Institute (SMHI) to assess water resources and water quality. It is forced with time series of precipitation and near surface air temperature, typically on a daily time step, to simulate water flow and nutrients concentrations at the catchment scale. The catchment to be modelled may be divided into sub-catchments which, in turn, are divided into land cover and soil type classes. The soil classes can contain up to three layers. A detailed description of the model can be found in Lindström et al. (2010) and on the HYPE wiki page (http://www.smhi.net/hype/wiki/doku.php). The HYPE model has already been used in climate change impact studies (e.g. Arheimer and Lindström 2015).

3-3 Climate projections

The climate projections for daily precipitation and near surface air temperature used to force the hydrological model are based on the CORDEX framework (Coordinated Regional Climate Downscaling Experiment) (www.cordex.org). This framework has provided an ensemble of high-resolution regional climate projections over several regions of the world for use in impact and adaptation studies (Giorgi et al., 2009). The CORDEX projections were obtained by dynamical

downscaling of a set of coarse global climate simulations made with different global climate models (GCMs), with a set of regional climate models (RCMs), assuming various greenhouse gas emission scenarios referred to as Representative Concentration Pathways (RCPs). The set of global climate model simulations used within CORDEX are part of the fifth phase of the Climate Model Inter-comparison Project (referred to as CMIP5), planned in support of the IPCC Fifth Assessment Report. The RCPs correspond to prescribed greenhouse-gas concentration pathways throughout the 21st century leading to different radiative forcing levels by the year 2100, relative to pre-industrial conditions (see for instance Giorgi et al., 2009; Benestad et al., 2017). Two RCPs emission scenarios are considered in this study in order to account for the uncertainty about future emissions. The first one (RCP4.5) assumes a warming scenario with a stabilisation of radiative forcing by the end of the 21st century at 4.5 W/m² and the second one (RCP8.5) represents very high greenhouse gas emissions and assumes a radiative forcing by the end of 21st century at 8.5 W/m² which continues to rise after 2100. In this project, the climate projections are taken from the European branch of CORDEX, EURO-CORDEX (www.euro-cordex.net) (Jacob *et al.*, 2014), as this region includes Iceland and is available at a very high horizontal resolution (0.11°, about 12.5 km).

The CORDEX projections consist of a historical period (1976-2005) and a projection period (2006-2100) assuming a given RCP. The projections in the historical period (1976-2005) do not correspond to the actual reality as it took place day after day but represent a possible realisation of what could have taken place. Evaluation series driven by the European Centre for Medium-Range Weather Forecasts (ECMWF) ERA-Interim reanalyses (Dee et al., 2011) and dynamically downscaled with the selected RCMs are available for the 1981-2010 period and have been used in this study to investigate the intrinsic quality of these RCMs.

Tables 2 and 3 present the GCMs and RCMs used in this study. The two selected GCMs are those suggested by Gosseling (2017) as the best GCMs for the Icelandic domain, namely MOHC-HadGEM2-ES and MPI-ESM-LR. Each CORDEX projection is considered equally likely.

Table 2: List of CORDEX GCMs and RCMs

Model	Type	Institution	Reference
ERA-Interim	Reanalysis	ECMWF	Dee et al. (2011)
MOHC-HadGEM2-ES	GCM	Met Office Hadley Centre	Jones et al. (2011)
MPI-ESM-LR	GCM	ESM of the Max-Planck-Institut fur Meteorologie	Giorgetta et al. (2013)
CCLM4-8-17	RCM	CLMcom	Rockel et al. (2008)
RCA4	RCM	SMHI	Kupiainen et al. (2011) Samuelsson et al. (2011)
RACMO22E	RCM	KNMI	van Meijgaard et al. (2012)
REMO2009	RCM	MPI-CSC	Jacob et al. (2012)

Table 3: List of CORDEX GCM-RCM combinations and emission scenarios (RCP)

		RCP	RCM			
			CCLM4-8-17	RCA4	RACMO22E	REMO2009
Forcing GCM	ERA-Interim (evaluation)		x	x	x	x
	MOHC-HadGEM2-ES	RCP4.5 & RCP8.5	x	x	x	
	MPI-ESM-LR	RCP4.5 & RCP8.5	x	x		x

3-4 Reference climate data

Daily precipitation and 2m-temperature from the high-resolution (2.5 km) ICRA climate reanalysis (Nawri et al., 2017) produced by Veðurstofa Íslands constitute the historical meteorological data of reference (1981-2017) used i) as input to calibrate the HYPE hydrological model ii) to verify the credibility of the CORDEX climate projections in the historical period and iii) to statistically bias-correct the CORDEX climate projections prior to use them as input to the hydrological model.

3-5 Hydrological data

Daily-averaged discharge series from three gauging stations monitored by Veðurstofa Íslands (Fig. 1) were used to calibrate HYPE and verify the credibility of the simulated streamflow series in the historical period when the hydrological model was forced with the CORDEX climate projections.

3-6 Other data

The hydrological modelling with HYPE requires the use of a land cover map and a soil map. The Corine Land Cover data updated for the reference year 2012 (Árnason and Matthíasson, 2017) were used and obtained from the download page of the National Land Survey of Iceland. The soil map of Iceland compiled by the Agricultural University of Iceland (Arnalds and Óskarsson, 2009; Arnalds, 2015) was used and downloaded from http://rangarvellir.ru.is. A digital elevation model (DEM) with resolution 10m obtained from ArcticDEM (Porter et al., 2018) was used for the delineation of the catchments and sub-catchments borders and extraction of various hydrologic and physiographic information. A DEM with resolution 10m obtained from the download page of the National Land Survey of Iceland (http://atlas.lmi.is/LmiData/) was used to calculate the average elevation of the catchments (cf. Table 1). Additional information about coastline, glaciers and water bodies were also obtained from the download page of the National Land Survey of Iceland. The delineation of the catchment borders and extraction of all required hydrologic and physiographic information was done with QGIS.

3-7 Local bias-adjustment method

The CORDEX daily precipitation and air temperature projections have been locally adjusted prior to be used as input to the hydrological model. This adjustment is necessary in order to correct systematic biases and guaranty consistency between the climate projections and the ICRA reference climate used in the calibration of the HYPE model. The local adjustment was based on quantile mapping (QM) (Gudmundsson et al. 2012; Gudmundsson 2016), which is a distribution-based adjustment method. A specific QM adjustment was defined for each month. The adjustment coefficients were estimated by comparing the CORDEX climate series to the ICRA climate reanalysis in the common 1981-2005 period. The adjustment was then applied to the entire projection period (1976-2100).

4 Calibration and validation of the hydrological model

For the hydrological modelling with HYPE, the Svartá catchment (vhm10) was divided into three sub-basins, the Laxá catchment (vhm74) was divided into two sub-basins and the Fnjóská catchment (vhm200) was divided into four sub-basins.

The HYPE model parameters were inferred through optimisation using the PEST software package (Doherty, 2021). The CMA-ES global optimisation scheme, which stands for "covariance matrix adaptation - evolutionary strategy" was considered, using the Nash-Sutcliffe (NSE) efficiency criterion (Nash and Sutcliffe 1970) between observed and simulated discharges as the objective function. In order to deal with the uncertainty of model parameters, the calibration was performed over two consecutive periods of similar duration, leading to two best performing parameter sets and therefore two simulated discharge series for each model and catchment. Note that among the optimised parameters, a correction for precipitation was included. This means that after passage into the hydrological model, the output precipitation series will be differently modified depending on the associated parameter set.

The validation was then performed for different periods. Tables 4 to 7 summarise the results of the daily discharge simulations for the different calibration/validation periods (water years). Figs. 2 to 8 present the results for the longest validation period. The criteria are i) the NSE and ii) the percent bias (RE):

$$NSE = 1 - \frac{\sum_{i=1}^{n} \left(Qsim_i - Qobs_i\right)^2}{\sum_{i=1}^{n} \left(Qobs_i - E[Qobs]\right)^2} \qquad (1)$$

$$RE(\%) = 100 \times \frac{\sum_{i=1}^{n} \left(Qsim_i - Qobs_i\right)}{\sum_{i=1}^{n} Qobs_i} \qquad (2)$$

where *Qobs* and *Qsim* denote observed and simulated discharge respectively and *n* the number of days. The NSE criterion can take values ranging from $-\infty$ to 1. A value lower than 0 means that the HYPE discharge simulations are worst than an estimate derived from the mean of the observations (E[*Qobs*]), a value of 0 means that the HYPE simulations are as accurate as an estimate derived from the mean of the observations, a value greater than 0 means that the HYPE simulations are better than an estimate derived from the mean of the observations and a value of 1 corresponds to a perfect simulation of observed discharges.

The overall NSE and RE criteria were calculated using all available daily discharge observations in each validation period whereas the annual NSE was only calculated in water years for which daily discharge observations were available in more than 300 days.

- Daily discharge simulations
    - Svartá catchment (vhm10)

The HYPE model calibrated in the two different periods performs reasonably well with respect to NSE in the different validation periods. A negative bias is often observed but the percent bias is in most cases within ±12.5 %. The seasonality of mean daily flow in the period 1981-2016 is also reasonably well reproduced.

    - Fnjóská catchment (vhm200)

The HYPE model performs reasonably well with respect to NSE but there is some lack of consistency when the simulations made with the two parameter sets are compared in the validation periods 1996-2002 and 2003-2009. The streamflow simulations are reasonably unbiased on average in most validation periods and the percent bias is within ±5 %. The seasonality of mean daily flow in the water years 1981-2016 is reasonably well reproduced but some over-estimation is observed in Sep-Oct-Nov with both HYPE simulations.

    - Laxá catchment (vhm74)

The HYPE model performs reasonably well with respect to NSE and the streamflow simulations are unbiased on average. The seasonality of mean daily flow in the period 2006-2016 is also reasonably well reproduced.

- Annual Maximum Floods (AMFs)

The plots of the magnitude versus occurrence day of AMFs are shown in Figs. 6 to 8 and Appendix 1 presents the plots of the simulated vs. observed magnitude of AMFs. The catchments experience AMFs in different seasons, associated with different underlying generating mechanisms (rainfall, snowmelt, combined rainfall and snowmelt). AMFs occurring in spring are expected to be primarily generated by snowmelt, sometimes combined with rain. AMFs occurring in summer and autumn are expected to be primarily generated by rainfall, sometimes combined with snowmelt. AMFs occurring in winter are expected to be generated by a combination of rainfall and snowmelt. In the Svartá catchment (vhm10), a large majority of AMFs occurred in spring and a few in winter. In the Fnjóská catchment (vhm200), AMFs occurred in spring and early summer. In the Laxá catchment (vhm74), the majority of AMFs occurred from late summer to autumn and a few in winter.

Overall, the seasonality of the timing of AMFs is reasonably well reproduced by the HYPE simulations in all three catchments, meaning that the different types of AMFs are usually simulated with the correct proportions by the model calibrated in the two different periods. Note however that AMFs occurring in winter are sometimes difficult to detect correctly in the Svartá catchment.

In the Svartá catchment (vhm10), the magnitude of AMFs is reasonably well simulated when the HYPE model is calibrated in the 1996-2002 period and a tendency towards an underestimation of the magnitude of AMFs is observed when HYPE is calibrated in the 2003-2009 period. In the Fnjóská catchment (vhm200), the magnitude of AMFs is reasonably well simulated but the most extremes AMFs are underestimated by both model simulations. In the Laxá catchment (vhm74), the magnitude of AMFs tends to be underestimated by both model simulations.

- Conclusion

The HYPE hydrological model reproduces the observed daily streamflow characteristics reasonably well. The performances of the model simulations in the validation periods are usually consistent with their performances in the calibration periods but some fluctuations in the results were observed in the Fnjóská catchment, which could be related to a lack of robustness in model parameters when applied in periods with hydro-climatic conditions significantly different from those encountered in the calibration period. Therefore, the use of two parameter sets obtained from different calibration periods is expected to provide more reliable hydrological simulations than if one parameter set only was used. The robustness of hydrological model parameters for climate change impact studies is an important issue (see e.g. Brigode et al. 2013; Vormoor et al. 2015).

Table 4: Catchment vhm10 (Svartá): Calibration and validation results for a daily time step (text in bold indicates when the calibration and validation periods are the same).

vhm10	**HYPE**			
	Calibration period 1996-2002		Calibration period 2003-2009	
Validation period:	NSE	RE (%)	NSE	RE (%)
1981-2016	0.699	-1.39	0.675	-8.2
1981-1995	0.726	-5.8	0.685	-12.5
1996-2002	**0.693**	**-1.12**	0.613	-7.69
2003-2009	0.652	9	**0.702**	**1.9**
2010-2016	0.648	-1.95	0.703	-8.94

Table 5: Catchment vhm200 (Fnjóská): Calibration and validation results for a daily time step (text in bold indicates when the calibration and validation periods are the same).

vhm200	**HYPE**			
	Calibration period 1996-2002		Calibration period 2003-2009	
Validation period:	NSE	RE (%)	NSE	RE (%)
1981-2016	0.73	-2.1	0.702	0.33
1981-1995	0.742	-1.02	0.699	0.56
1996-2002	**0.713**	**-0.71**	0.579	2.02
2003-2009	0.589	-4.06	**0.775**	**-0.18**
2010-2016	0.783	-3.36	0.758	-1.11

Table 6: Catchment vhm74 (Laxá): Calibration and validation results for a daily time step (text in bold indicates when the calibration and validation periods are the same).

vhm74	**HYPE**			
	Calibration period 2006-2011		Calibration period 2012-2016	
Validation period:	NSE	RE (%)	NSE	RE (%)
2006-2016	0.701	-0.83	0.715	-0.32
2006-2011	**0.688**	**-0.39**	0.675	0.1
2012-2016	0.715	-1.28	**0.758**	**-0.75**

Table 7: Annual NSE statistics for water years with more than 300 valid discharge observations. Validation results for a daily time step.

	HYPE	
vhm10 (1981-2016)	Calibration period 1996-2002	Calibration period 2003-2009
NSE min	0.34	0.262
NSE median	0.674	0.662
NSE max	0.853	0.813
vhm200 (1981-2016)	Calibration period 1996-2002	Calibration period 2003-2009
NSE min	0.225	-0.05
NSE median	0.719	0.674
NSE max	0.903	0.883
vhm74 (2006-2016)	Calibration period 2006-2011	Calibration period 2012-2016
NSE min	0.52	0.583
NSE median	0.654	0.678
NSE max	0.838	0.864

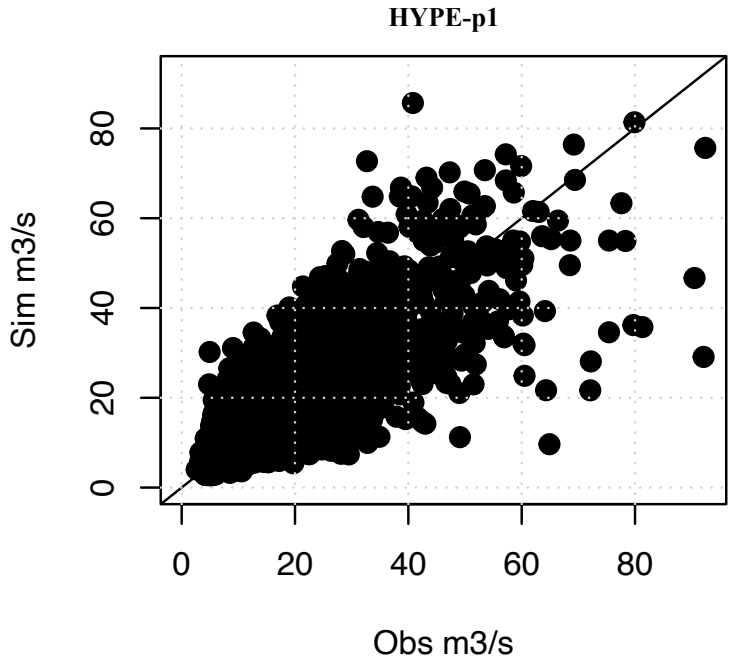

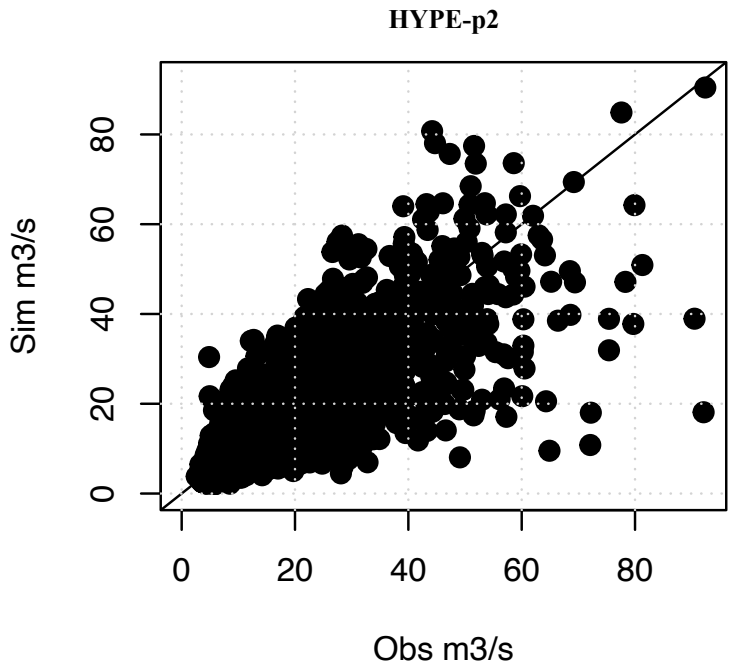

Fig. 2: Catchment vhm10 (Svartá): Simulated vs. observed daily discharge in the water years 1981-2016. Top: HYPE with parameter set calibrated in 1996-2002. Bottom: HYPE with parameter set calibrated in 2003-2009.

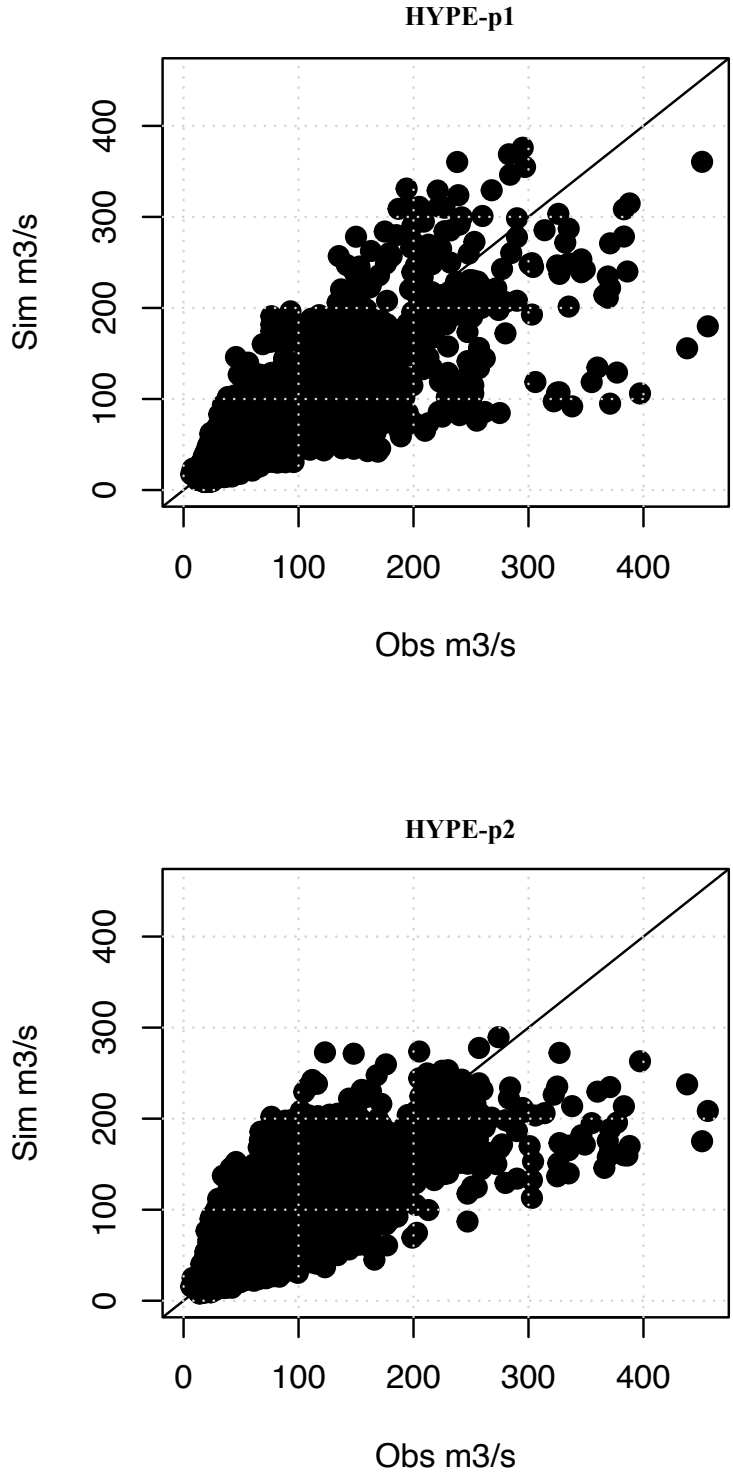

Fig. 3: Catchment vhm200 (Fnjóská): Simulated vs. observed daily discharge in the water years 1981-2016. Top: HYPE with parameter set calibrated in 1996-2002. Bottom: HYPE with parameter set calibrated in 2003-2009.

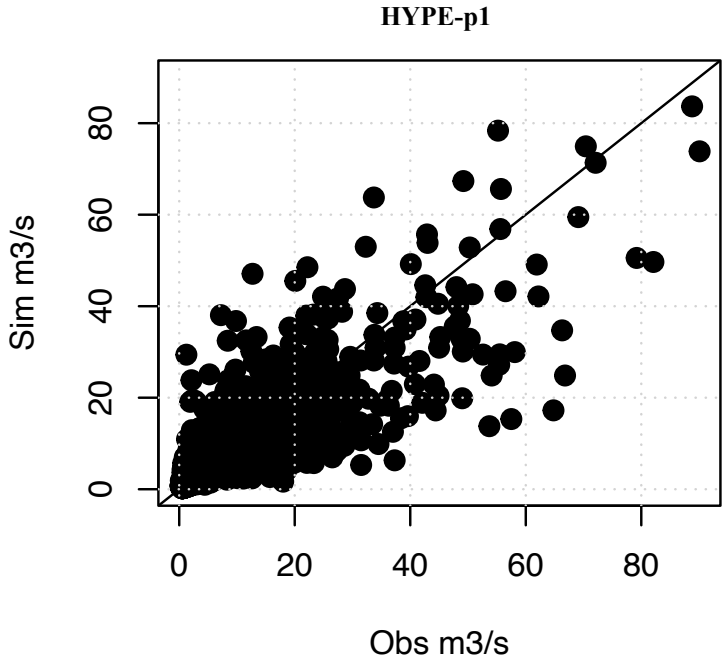

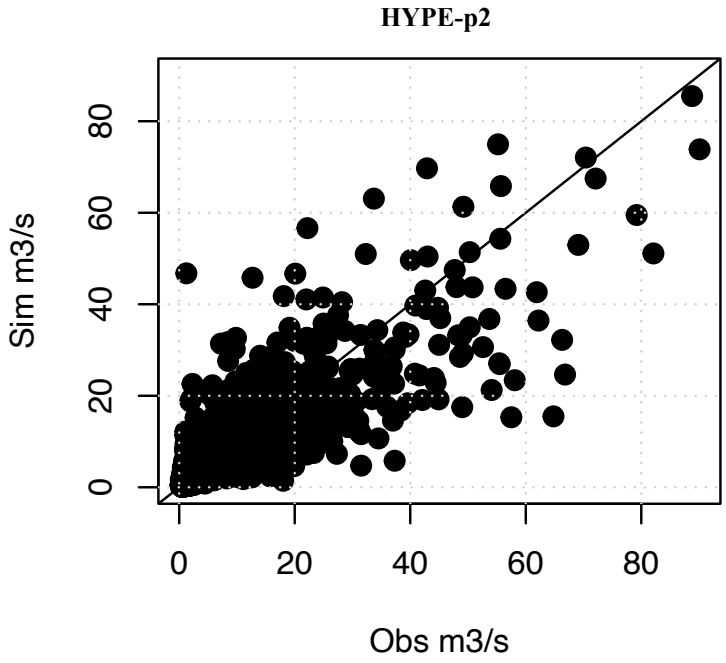

Fig. 4: Catchment vhm74 (Laxá): Simulated vs. observed daily discharge in the water years 2006-2016. Top: HYPE with parameter set calibrated in 2006-2011. Bottom: HYPE with parameter set calibrated in 2012-2016.

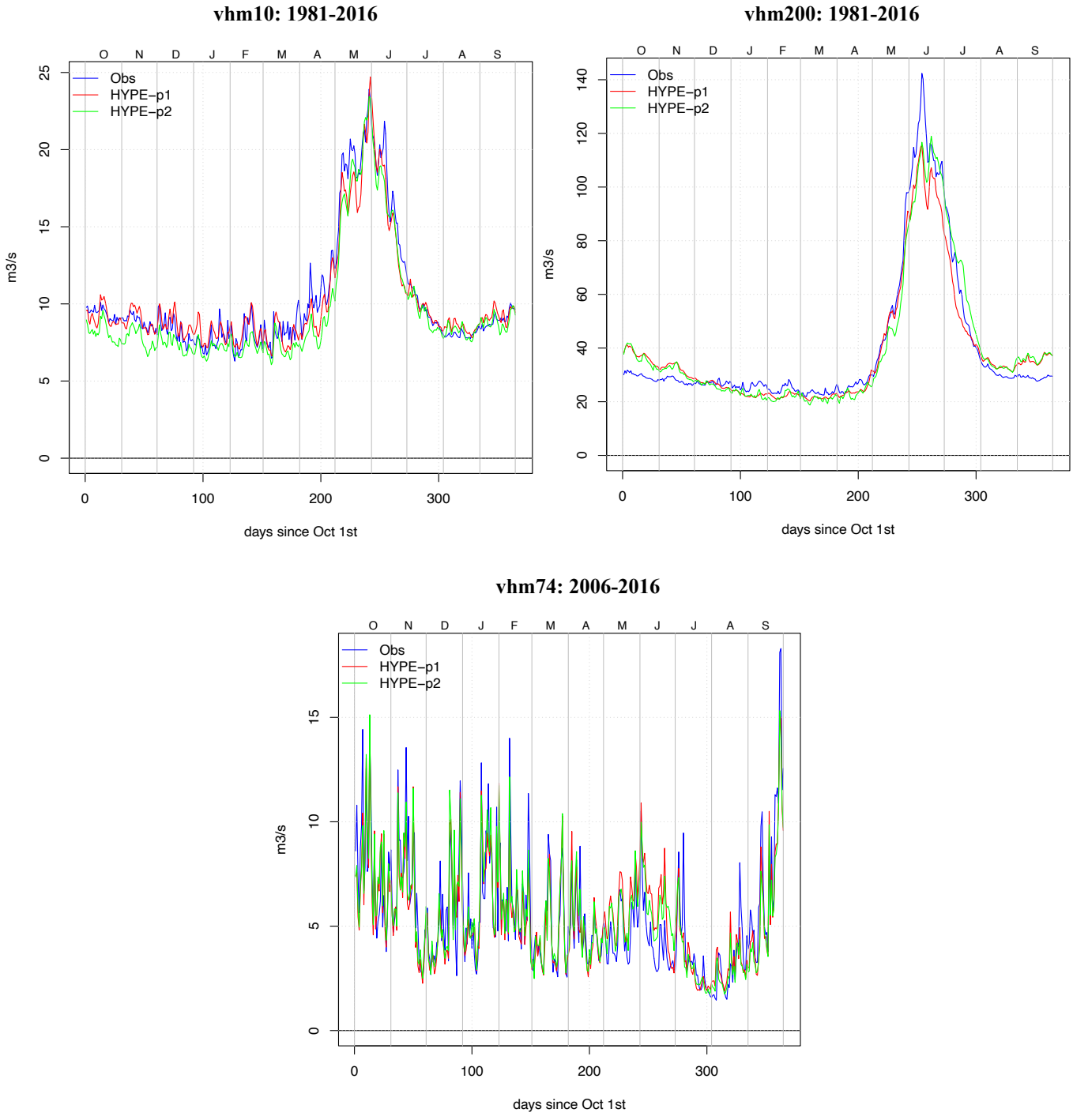

Fig. 5: Seasonality of mean daily discharge. Observed discharge (blue), HYPE discharge simulations using first (red) and second (green) parameter sets; vhm10 (top-left); vhm200 (top-right); vhm74 (bottom). The day=1 for October 1st and 365 for September 30th.

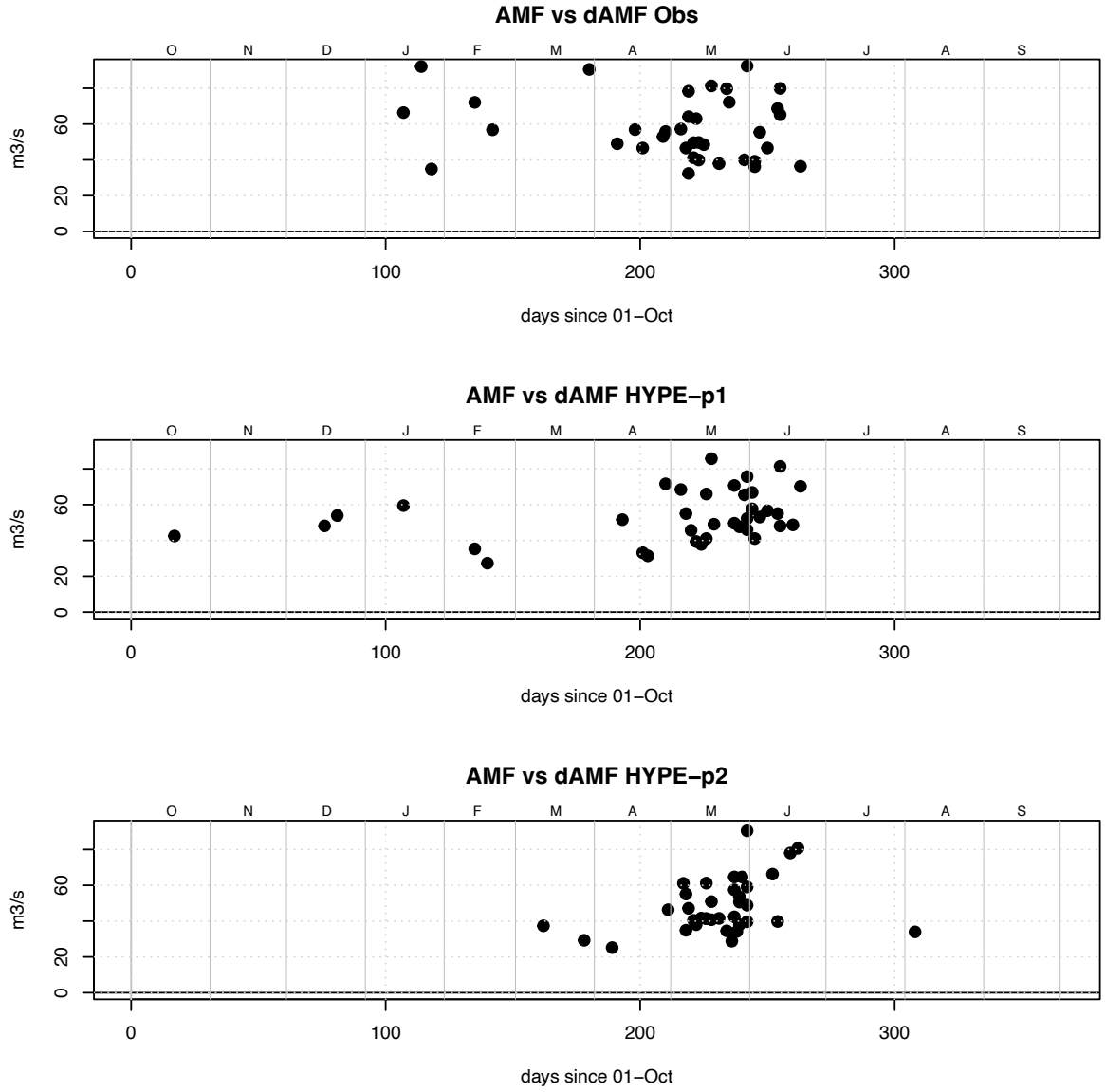

Fig. 6: Svartá catchment (vhm10): Magnitude vs. day of occurrence of AMFs (water years 1981-2016). Observed (top), HYPE with parameter set calibrated in 1996-2002 (middle), HYPE with parameter set calibrated in 2003-2009 (bottom). The day=1 for October 1st and 365 for September 30th.

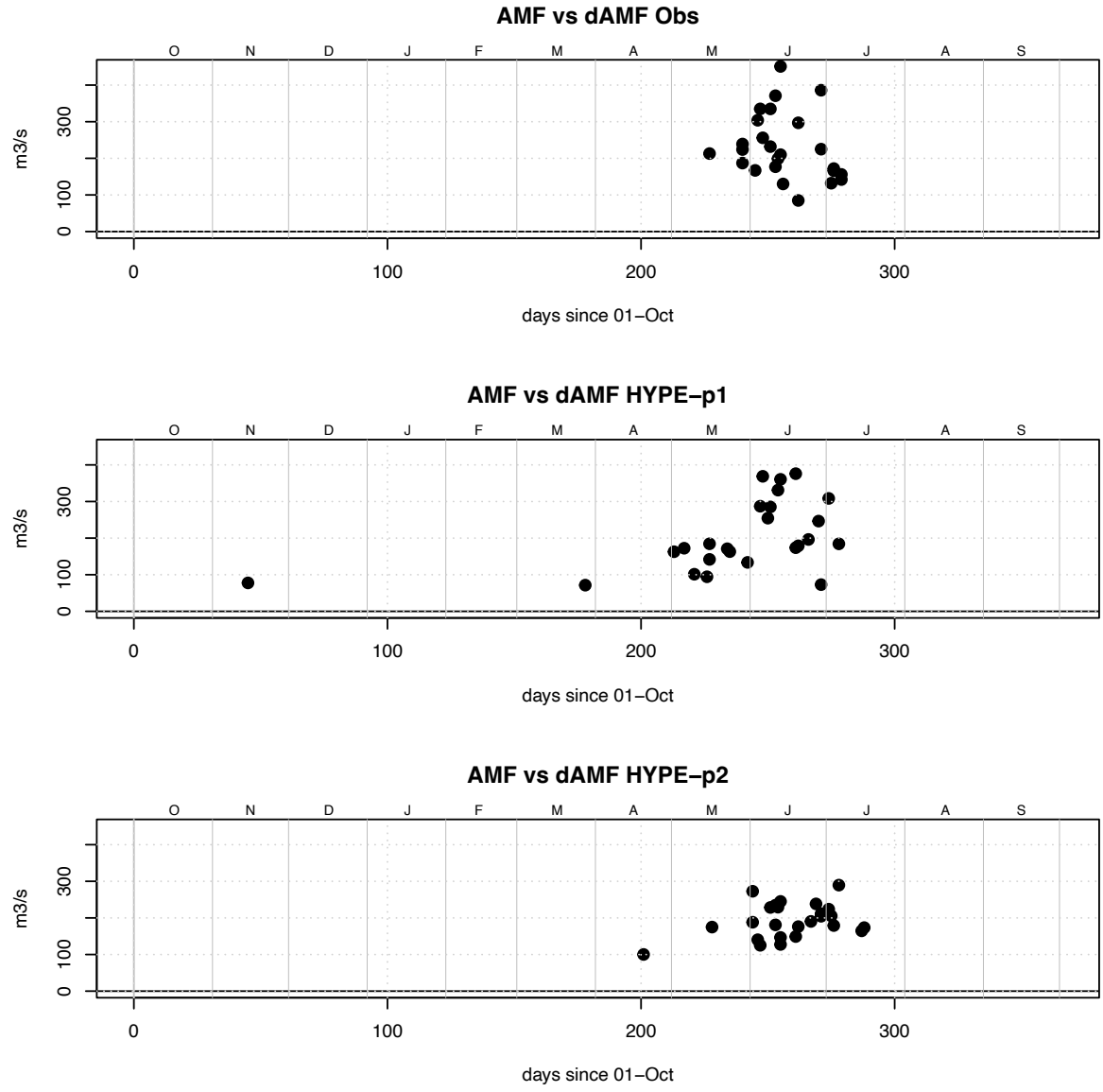

Fig. 7: Fnjóská catchment (vhm200): Magnitude vs. day of occurrence of AMFs (water years 1981-2016). Observed (top), HYPE with parameter set calibrated in 1996-2002 (middle), HYPE with parameter set calibrated in 2003-2009 (bottom-right). The day=1 for October 1st and 365 for September 30th.

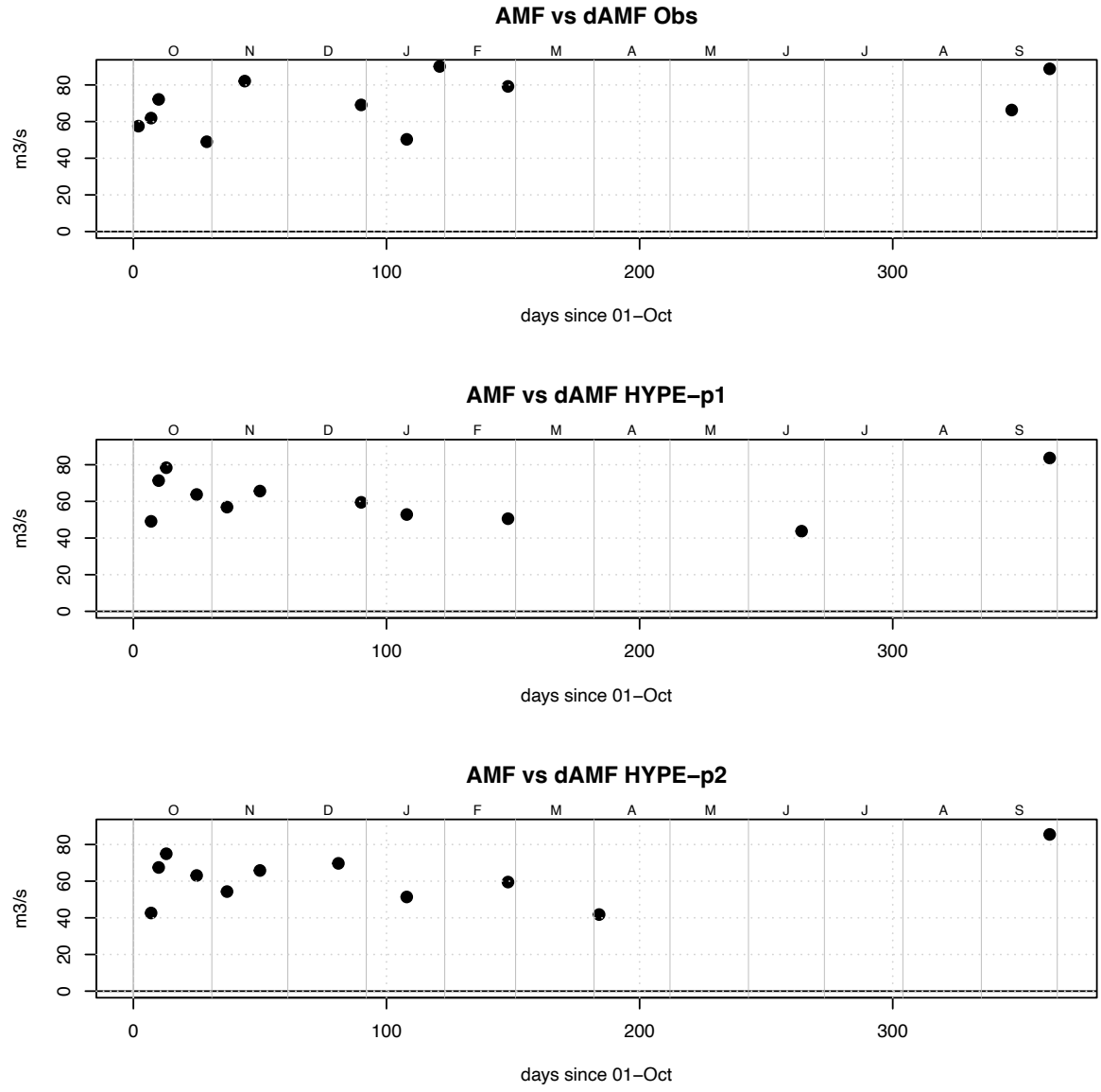

Fig. 8: Laxá catchment (vhm74): Magnitude vs. day of occurrence of AMFs (water years 2006-2016). Observed (top), HYPE with parameter set calibrated in 2006-2011 (middle), HYPE with parameter set calibrated in 2012-2016 (bottom). The day=1 for October 1st and 365 for September 30th.

5 EURO-CORDEX climate projections

The ICRA and CORDEX precipitation and temperature series were first area-averaged over each sub-basin (see Section 4 above) and a specific QM-based adjustment calculated for each sub-basin, as in Crochet (2020, 2021). Note that for precipitation, the original ICRA data were used to define the QM adjustment coefficients, not the corrected ICRA-precipitation after passage in the hydrological model. Therefore, the results presented below correspond to the original ICRA temperature and precipitation data and the corresponding QM-adjusted CORDEX projections, before their passage into the hydrological model. After passage into the hydrological model, the ICRA and QM-adjusted CORDEX precipitation series will be further corrected according to a specific correction parameter that depends on each associated parameter set (these results will be presented in Section 6).

5-1 RCMs evaluation and skill of the local bias-adjustment method

In order to evaluate the intrinsic quality of the different RCMs (see Tables 2 and 3) and the skill of the quantile mapping (QM) method at removing local biases, a comparison was made between the ICRA reanalysis and the CORDEX evaluation series obtained by dynamical downscaling of ERA-interim reanalyses with the selected RCMs. The CORDEX evaluation series are synchronised with observed climate, making a direct comparison with ICRA reanalysis possible. QM-based adjustment coefficients were defined by comparing ICRA data in the 1981-2010 period to the CORDEX evaluation series in the available period (1981-2010 or 1989-2008, depending on the RCM). Only results related to daily temperature and precipitation area-averaged over the entire catchment are presented.

The following evaluation statistics were calculated in the period 1989-2008 common to all daily temperature and precipitation evaluation series:

$$\text{Mean error: } ME = E[CORDEX - ICRA] \tag{3}$$

$$\text{Root-mean-square error: } RMSE = \sqrt{E[(CORDEX - ICRA)^2]} \tag{4}$$

5-1-1 Temperature

The seasonality of ME and RMSE before and after local bias-adjustment by QM is presented in Appendix 2. The CCLM-4-8-17 evaluation series display a positive temperature bias in all three catchments in spring/summer and are relatively unbiased in other months. The REMO2009 evaluation series display a positive temperature bias in all three catchments in spring/summer and are slightly negatively biased in autumn/winter except in the Laxá catchment (vhm74) where the bias is positive in all months. The RCA4 evaluation series are negatively biased in most months in the Svartá (vhm10) and Fnjóská (vhm200) catchments and unbiased in the Laxá catchment (vhm74). The RACMO22E evaluation series are negatively biased in a majority of months and all three catchments. These biases are partly related to differences between the ICRA and CORDEX terrain elevations caused by a difference of spatial resolutions. Quantile mapping eliminates the bias, on average, and reduces RMSE in months where ME was large. After bias-correction, the

different evaluation series are relatively similar in terms of RMSE, with an advantage for CCLM-4-8-17.

5-1-2 Precipitation

The seasonality of ME and RMSE before and after local bias-adjustment by QM is presented in Appendix 3. The results vary with the catchments and RCMs. The biases are usually not of a systematic nature as for temperature and the scatter plots indicate either over- or under-estimation depending on the days (not shown). For the Svartá catchment (vhm10), three RCMs (CCLM-4-8-17, RCA4 and RACMO22E) behave similarly with a positive bias on average in autumn/winter and a negative bias on average in summer while REMO2009 is relatively unbiased on average in most months. Precipitation over the Fnjóská catchment (vhm200) tends to be underestimated on average with REMO2009 and is relatively unbiased on average with the other three RCMs. Precipitation over the Laxá catchment (vhm74) tends to be underestimated on average in most months with RCA4 and in autumn/winter with CCLM-4-8-17, unbiased with RACMO22E and overestimated in autumn/winter with REMO2009. Quantile mapping eliminates the bias, on average and either reduces RMSE, when the bias is large and systematic, or keeps it similar to its original level or even increase it slightly, when the bias is low or not systematic. Overall, the different bias-corrected evaluation series are relatively similar in terms of RMSE and no RCM dominates in all months and catchments.

5-2 Climate projections

Comparisons between CORDEX climate projections and ICRA reference climate in the 1981-2010 period confirms i) the presence of biases in the original CORDEX temperature and precipitation series and ii) the efficiency of the QM adjustment method at eliminating these biases on average (see Appendix 4 and 5). The biases depend both on the RCM and the driving GCM. After local bias-adjustment, a temporal trend test based on ordinary least squares linear regression was applied to catchment-averaged monthly temperature and precipitation projections in the 1981-2100 period and the significance of the trend estimated at a 5% significance level (p value lower than 0.05).

5-2-1 Temperature trends

A significant warming is projected in all months and catchments, more or less pronounced according to the emission scenario and the month under consideration (see Table 8). On average over all months and catchments, a warming rate of 0.295°C/decade is projected with the RCP4.5 emission scenario and 0.473°C/decade with the RCP8.5 emission scenario. The lowest warming rate is projected in the Laxá catchment (vhm74) and the largest one is projected in the Fnjóská catchment (vhm200). The warming rate is usually larger for scenarios driven by HadGEM2ES GCM than for those driven by MPI−ESM−LR GCM (not shown). Note also that the warming rate estimated from the locally-adjusted temperature series is systematically greater than the one derived from the original temperature series, especially for the Fnjóská catchment and the RCP8.5 emission scenario.

In addition to the presence of long-term trends, oscillations are observed in the temperature series reflecting natural climate variability (not shown). The locally-adjusted temperature series are more or less grouped according to the driving GCM and the two groups of projections do not necessarily vary in phase with each other. The projected warming in the 21st century is also well reflected in the evolution of the mean temperature cycle (see Appendix 6).

5-2-2 Precipitation trends

Monthly precipitation projections do not exhibit any significant linear trend in most months and catchments (see Table 9). The main features characterising the variability of monthly precipitation projections are decadal to multi-decadal oscillations, especially in autumn-winter, corresponding to a succession of “wet” and “dry” periods. These oscillations are characteristic of the natural variability of precipitation in the Icelandic domain (see for instance Crochet, 2007). The oscillations often depend on the driving GCM and the two groups of precipitation projections driven by the two GCMs do not always vary in phase with each other. The fact that no consistent linear precipitation trend is detected in a majority of projections for a given month does not mean that no significant change is affecting precipitation in some particular periods. Changes in 30-year mean annual and seasonal precipitation are studied in Section 6 using the Mann-Whitney test.

To illustrate the temporal variability of precipitation, Appendix 7 presents the time-series of locally-adjusted monthly precipitation in February, June and October for the RCP4.5 scenario. A 5-year moving average was applied to the monthly series in order to make the oscillations appear more clearly. Similar results were observed for the RCP8.5 scenario (not shown).

Table 8: Ensemble average warming rate in degree Celsius/decade estimated from the locally-adjusted monthly temperature series (1981-2100). All six ensemble members display a statistically significant trend (slope of the linear regression statistically different from zero at the 5% level). The average warming rate estimated from the original temperature series before local bias-adjustment is also given for comparison (Mean DMO).

Month	vhm10		vhm200		vhm74	
	RCP4.5	RCP8.5	RCP4.5	RCP8.5	RCP4.5	RCP8.5
Jan	0.30	0.40	0.30	0.42	0.27	0.33
Feb	0.29	0.44	0.29	0.46	0.25	0.41
Mar	0.30	0.46	0.29	0.46	0.28	0.40
Apr	0.28	0.44	0.27	0.43	0.25	0.34
May	0.32	0.50	0.30	0.52	0.24	0.34
Jun	0.30	0.45	0.40	0.70	0.24	0.38
Jul	0.31	0.54	0.44	0.75	0.24	0.46
Agu	0.28	0.51	0.44	0.78	0.27	0.58
Sep	0.29	0.46	0.37	0.58	0.24	0.42
Oct	0.33	0.50	0.38	0.58	0.25	0.38
Nov	0.26	0.46	0.30	0.52	0.22	0.34
Dec	0.27	0.44	0.31	0.49	0.25	0.38
Mean	**0.294**	**0.467**	**0.339**	**0.556**	**0.251**	**0.397**
Mean DMO	**0.28**	**0.430**	**0.290**	**0.466**	**0.230**	**0.350**

Table 9: Locally-adjusted monthly precipitation projections (1981-2100): Average trend (mm/day / decade) when more than 50% of the six ensemble members have a statistically significant trend (slope of the linear regression statistically different from zero at the 5% level). Number of members with a significant trend is given in brackets.

Month	vhm10		vhm200		vhm74	
	RCP4.5	RCP8.5	RCP4.5	RCP8.5	RCP4.5	RCP8.5
Jan	/	/	/	/	/	/
Feb	/	/	/	/	/	/
Mar	/	/	/	/	/	/
Apr	/	/	/	/	/	/
May	/	/	/	/	/	/
Jun	/	/	/	/	/	/
Jul	/	/	/	/	/	/
Agu	/	0.1 (5)	/	/	/	/
Sep	0.08 (5)	0.11 (6)	/	/	/	/
Oct	/	/	/	/	/	/
Nov	/	/	/	/	/	/
Dec	/	/	/	0.13 (4)	/	/

6 Hydrological projections

An ensemble of twelve daily hydrological projections was obtained for the period 1981-2100 and each emission scenario, by forcing the HYPE model with the ensemble of locally-adjusted CORDEX daily precipitation and temperature projections (six climate projections x two HYPE parameter sets).

6-1 Comparison with reference hydrological series

In order to evaluate the skill of the quantile mapping method used to locally adjust the CORDEX precipitation and temperature projections and how the adjustment is propagated into the modelling chain, the hydrological series obtained by forcing HYPE with the CORDEX projections in the reference period (1981-2010) were compared to the reference series obtained by forcing HYPE with the ICRA reanalysis in the same period. Figs 9 to 11 present the seasonality of mean daily discharge and snow storage (snow water equivalent, SWE). Appendix 8 presents the comparisons of the seasonal frequencies of occurrence of AMFs and the comparisons of the empirical frequency distributions of the magnitude of AMFs. The hydrological projections are identical in the 1981-2005 historical period but differ thereafter because the CORDEX RCPs 4.5 and 8.5 emission scenarios differ, hence results from the two RCPs are presented together with the results from the evaluation series.

The current streamflow seasonality of the Svartá and Fnjóská catchments is governed by the seasonality of snow accumulation and melt, leading to a strong contrast between low flows in winter when snow accumulates and high flows in spring when snow melts, whereas the Laxá catchment has a more mixed rainfall/snowmelt regime with high flows in autumn due to rainfall and high flows in spring due to snowmelt. The seasonality of mean daily flow and SWE projections in the 1981-2010 reference period offers a reliable estimation of the seasonality of the reference mean daily flow and SWE in that period. The seasonal frequencies of occurrence of AMFs and the empirical frequency distributions of the magnitude of AMFs are usually reasonably well reproduced when the HYPE hydrological model is forced with the locally-adjusted CORDEX projections in the reference period (1981-2010), although some overestimation in the magnitude of AMFs is observed for the Laxá catchment (vhm74). The spread of the ensembles reflects the uncertainties associated with the climate projections, their local-adjustment, and the hydrological model parameterisation. Overall, these results can be considered as a reasonable proof of credibility of the local-adjustment method applied to the CORDEX climate projections and its transmission into the modelling chain. It is assumed in the rest of the study that the local-adjustments of CORDEX precipitation and air temperature by quantile mapping hold for the entire projection period and that the HYPE parameter sets are sufficiently robust to be transferable over the entire projection period.

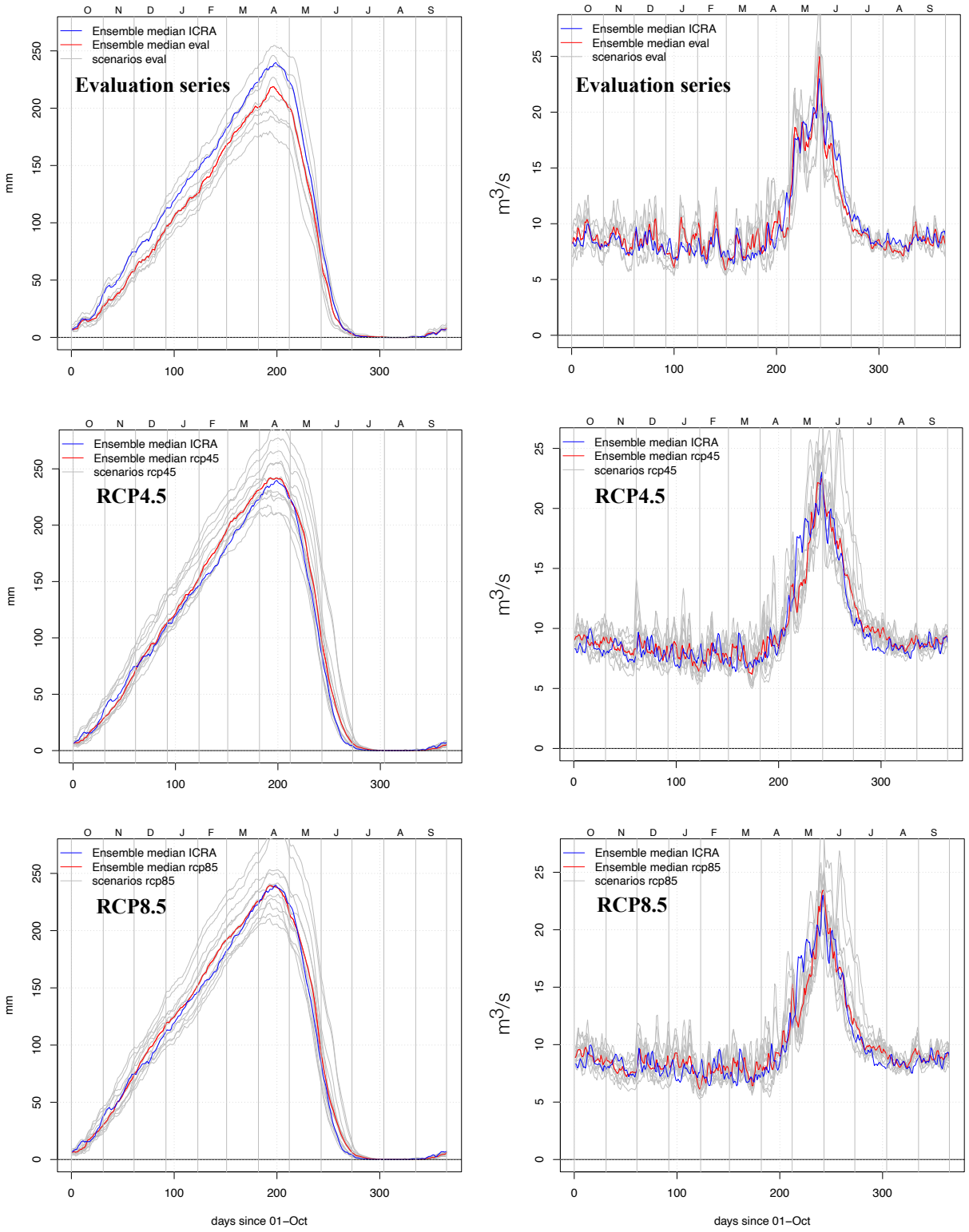

Fig. 9: Svartá catchment (vhm10): Mean daily snow storage (SWE) (left panel) and river discharge (right panel). Estimations derived from the HYPE hydrological model forced with the ICRA reanalysis (blue line) and with the locally-adjusted CORDEX projections (grey lines) in the 1989-2007 period (evaluation series) and 1981-2010 period (RCPs 4.5 & 8.5). The ensemble median of the mean daily projections is coloured in red. HYPE model forced with CORDEX evaluation series (top), CORDEX RCP4.5 series (middle), CORDEX RCP8.5 series (bottom). The day=1 for October 1st and 365 for September 30th.

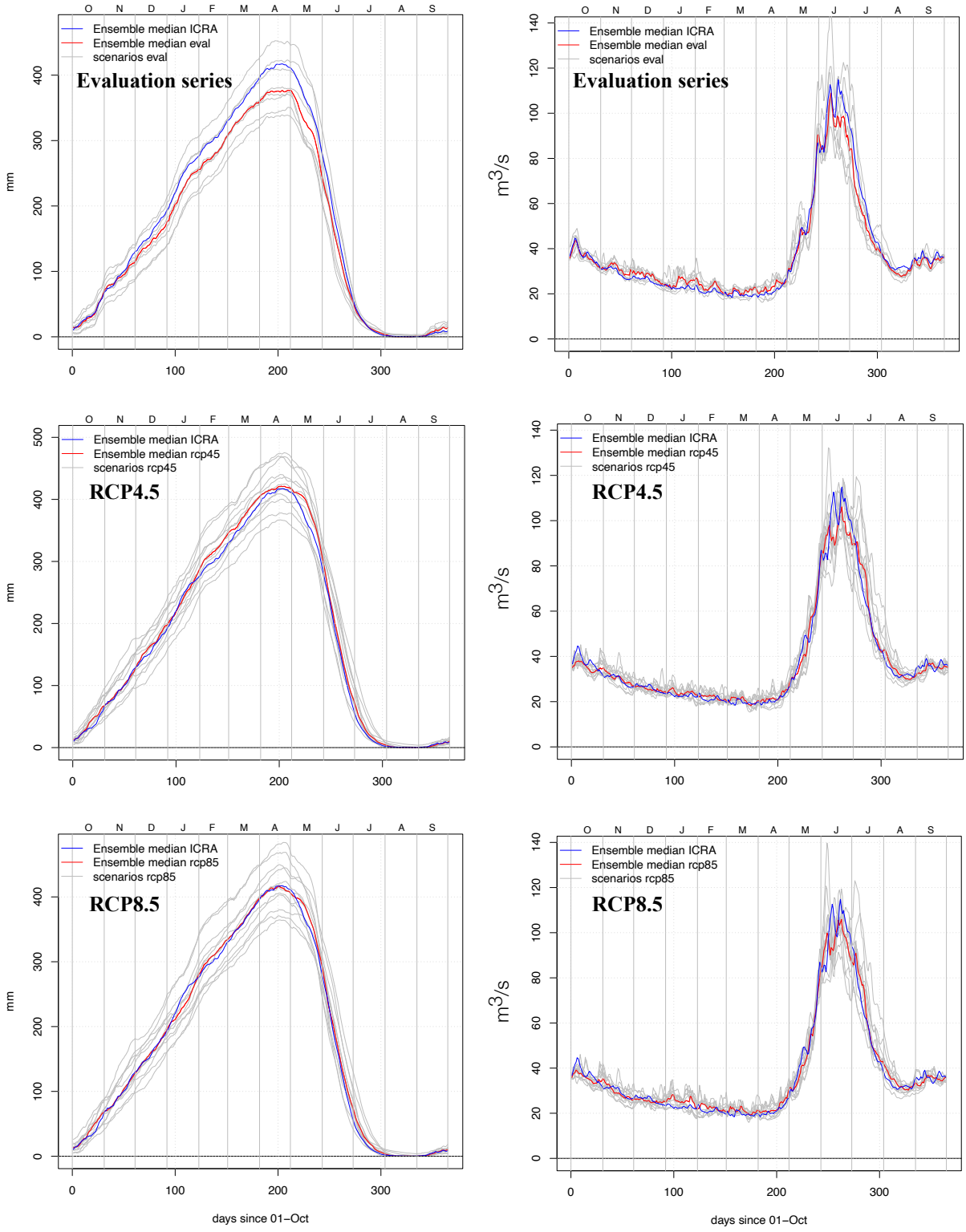

Fig. 10: Fnjóská catchment (vhm200): Mean daily snow storage (SWE) (left panel) and river discharge (right panel). Estimations derived from the HYPE hydrological model forced with the ICRA reanalysis (blue line) and with the locally-adjusted CORDEX projections (grey lines) in the 1989-2007 period (evaluation series) and 1981-2010 period (RCPs 4.5 & 8.5). The ensemble median of the mean daily projections is coloured in red. HYPE model forced with CORDEX evaluation series (top), CORDEX RCP4.5 series (middle), CORDEX RCP8.5 series (bottom). The day=1 for October 1st and 365 for September 30th.

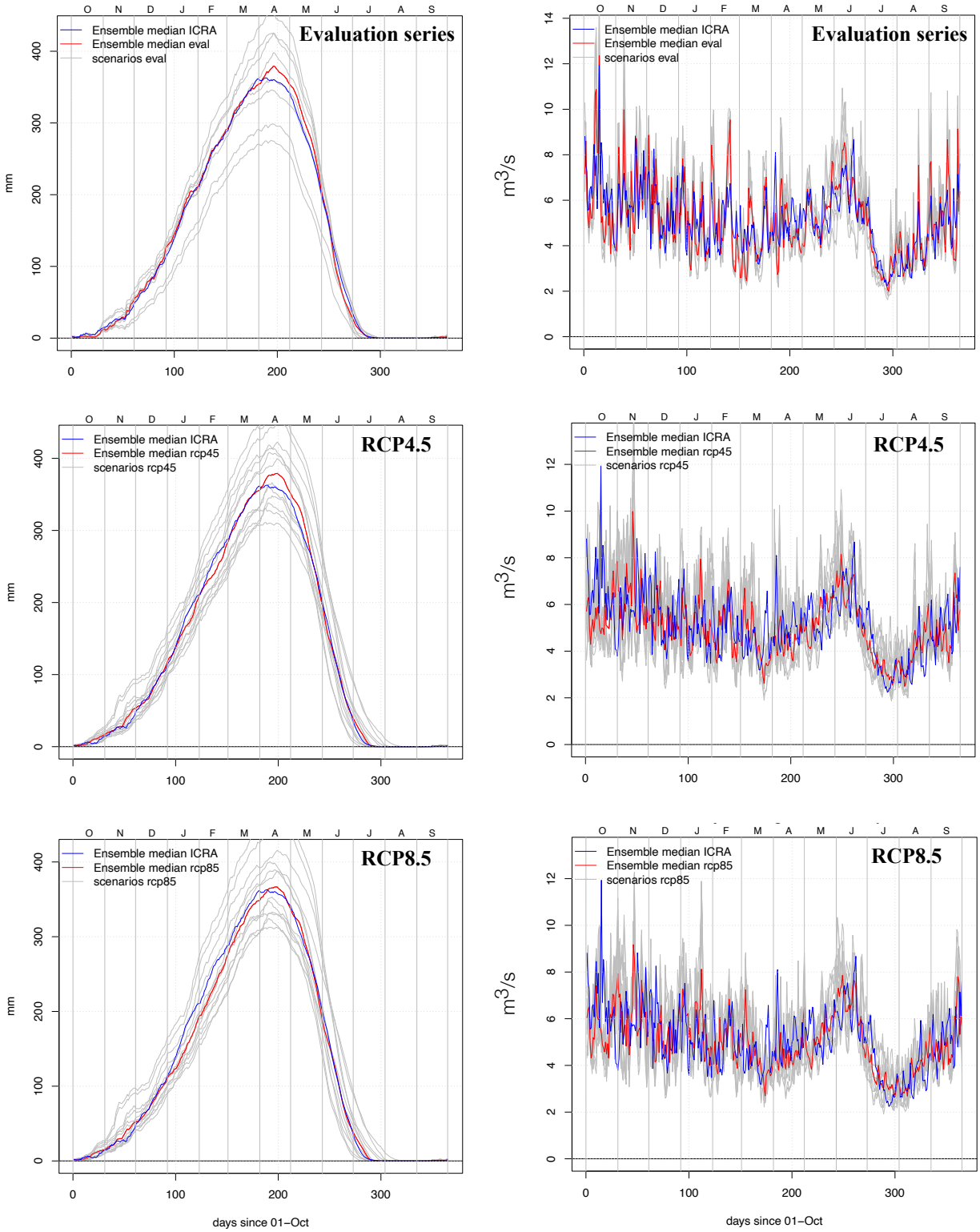

Fig. 11: Laxá catchment (vhm74): Mean daily snow storage (SWE) (left panel) and river discharge (right panel). Estimations derived from the HYPE hydrological model forced with the ICRA reanalysis (blue line) and with the locally-adjusted CORDEX projections (grey lines) in the 1989-2007 period (evaluation series) and 1981-2010 period (RCPs 4.5 & 8.5). The ensemble median of the mean daily projections is coloured in red. HYPE model forced with CORDEX evaluation series (top), CORDEX RCP4.5 series (middle), CORDEX RCP8.5 series (bottom). The day=1 for October 1st and 365 for September 30th.

6-2 Hydrological response to projected climate change

This section examines the hydrological impact of projected climate change in the 21st century.

6-2-1 Changes in mean daily flow and snow storage

Projected changes in the seasonality of mean daily snow storage and river discharge are presented in Figs. 12 to 23. First the evolution of the ensemble median is presented for all 30-year periods and then detailed results with all the ensemble members are presented for two periods: near future (2021-2050) and far future (2071-2100). The spread of the ensemble provides an estimate of the overall uncertainty associated with these projections. The percentage of days in the water year for which the mean daily snow storage or discharge ensembles differ significantly between the reference (1981-2010) and future periods is also indicated for these two periods.

The three river catchments are found to respond to projected climate change and in particular to warming. As the projection horizon increases, the rise in temperatures (see Appendix 6) gradually leads to shorter snow seasons combined with less snow storage. By the end of the 21st century, the mean daily snowpack is projected to drastically shrink in all three catchments, especially under the RCP8.5 emission scenario.

In the reference period, the hydrological regimes of the Svartá and Fnjóská catchments are strongly influenced by the seasonality of snow accumulation and melt, leading to a strong contrast between low flows in winter when snow accumulates, and high flows in spring when snow melts, whereas the Laxá catchment has a more mixed rainfall/snowmelt regime with high flows in autumn due to rainfall, and high flows in spring due to snowmelt. As a result, a well defined peak of mean daily discharge caused by snowmelt-induced runoff can be observed in May/June in the three catchments. As the projection horizon increases, the mean daily flow pattern of the three catchments is projected to change. Mean daily discharge is mainly projected to increase from October to April in the Svartá and Fnjóská catchments, likely because the number of rainfall and/or snowmelt events is increasing with the projected warming, whilst the evolution is more variable in Laxá. In May, mean daily discharge either experiences an increase or decrease depending on the day of the month, projection horizon and catchment, likely in relation to snowmelt changes. The peak of mean daily discharge in May/June is projected to gradually decrease and shift earlier in the three catchments and eventually disappear in the Laxá catchment, because of the projected snow storage reduction. Mean daily discharge is projected to decrease in June and July in the three catchments in relation to the snow storage reduction whilst the evolution in August and September is more variable, depending on the catchment, period and emission scenario. A period of low flow is developing towards the end of the century, from ca. May/June to July/August, depending on the catchment, because snowmelt contribution to streamflow is strongly reduced. The largest relative changes in mean daily discharge are usually projected in June/July in the three catchments (median reduction of -50% or more by the end of the century), caused by the reduction in snow storage and subsequent decrease in snowmelt, and in winter (median increase of more than +50%, towards the end of the century) likely caused by an increase in the number of rainfall and snowmelt events. The larger warming projected with the RCP8.5 scenario also leads to larger changes in snow storage and streamflow seasonality than the RCP4.5 scenario.

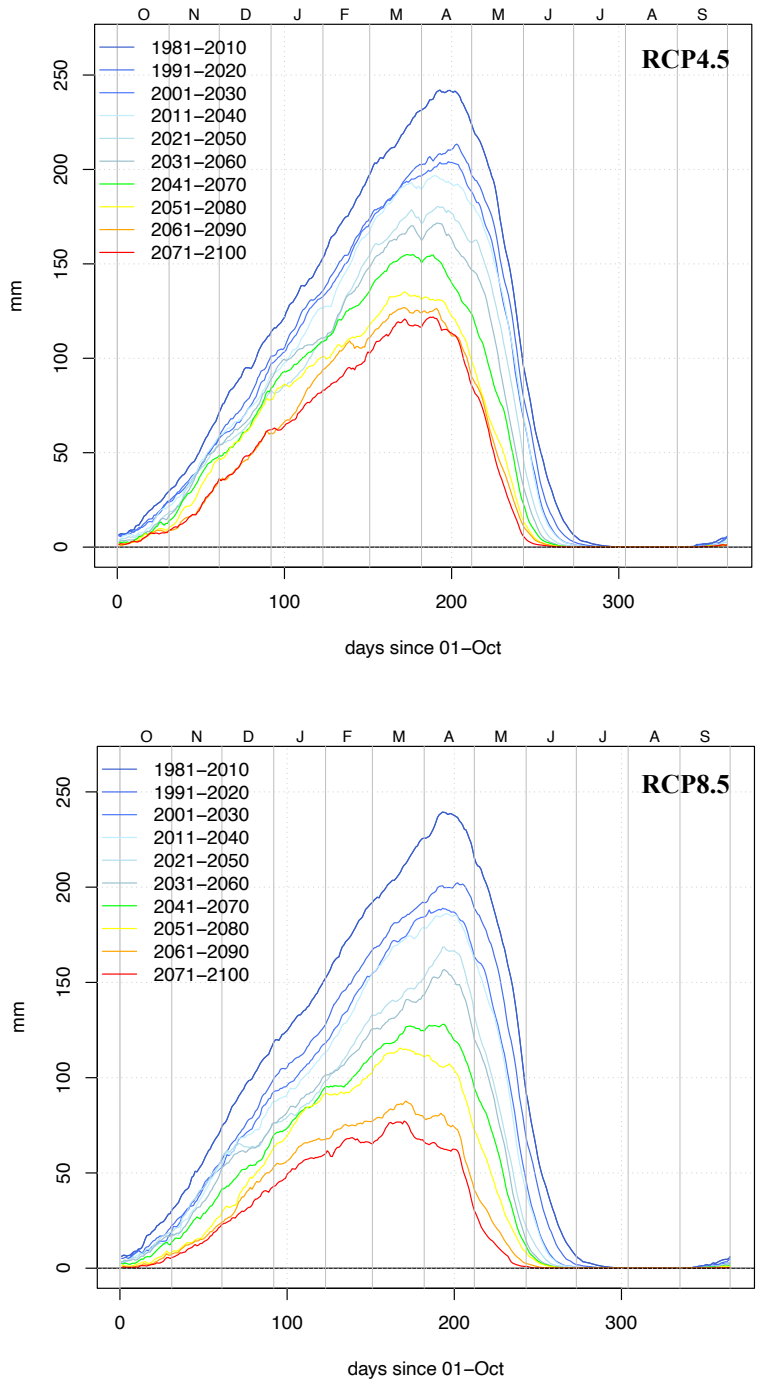

Fig. 12: Svartá catchment (vhm10): Ensemble median of the projected seasonality of mean daily snow storage (SWE) under the RCP4.5 emission scenario (top) and RCP8.5 emission scenario (bottom). Each colour corresponds to a 30-year period: from dark blue (1981-2010) to red (2071-2100). The day=1 for October 1st and 365 for September 30th.

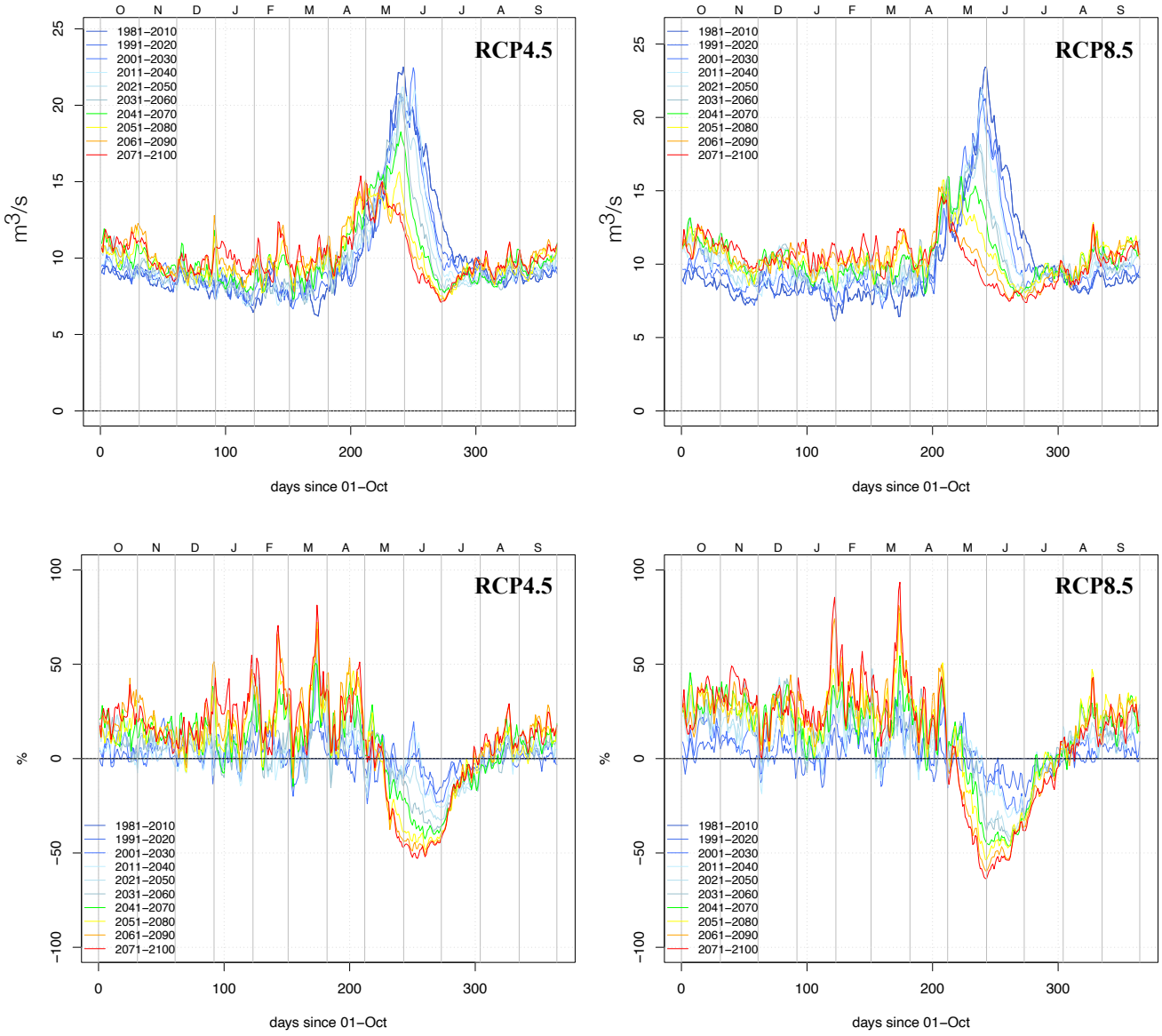

Fig. 13: Svartá catchment (vhm10): Ensemble median of the projected seasonality of mean daily discharge (top-panel) and percent change in the ensemble median of mean daily discharge relative to the reference period 1981-2010 (bottom-panel). Left-panel: RCP4.5 emission scenario. Right-panel: RCP8.5 emission scenario. Each colour corresponds to a 30-year period: from dark blue (1981-2010) to red (2071-2100). The day=1 for October 1st and 365 for September 30th.

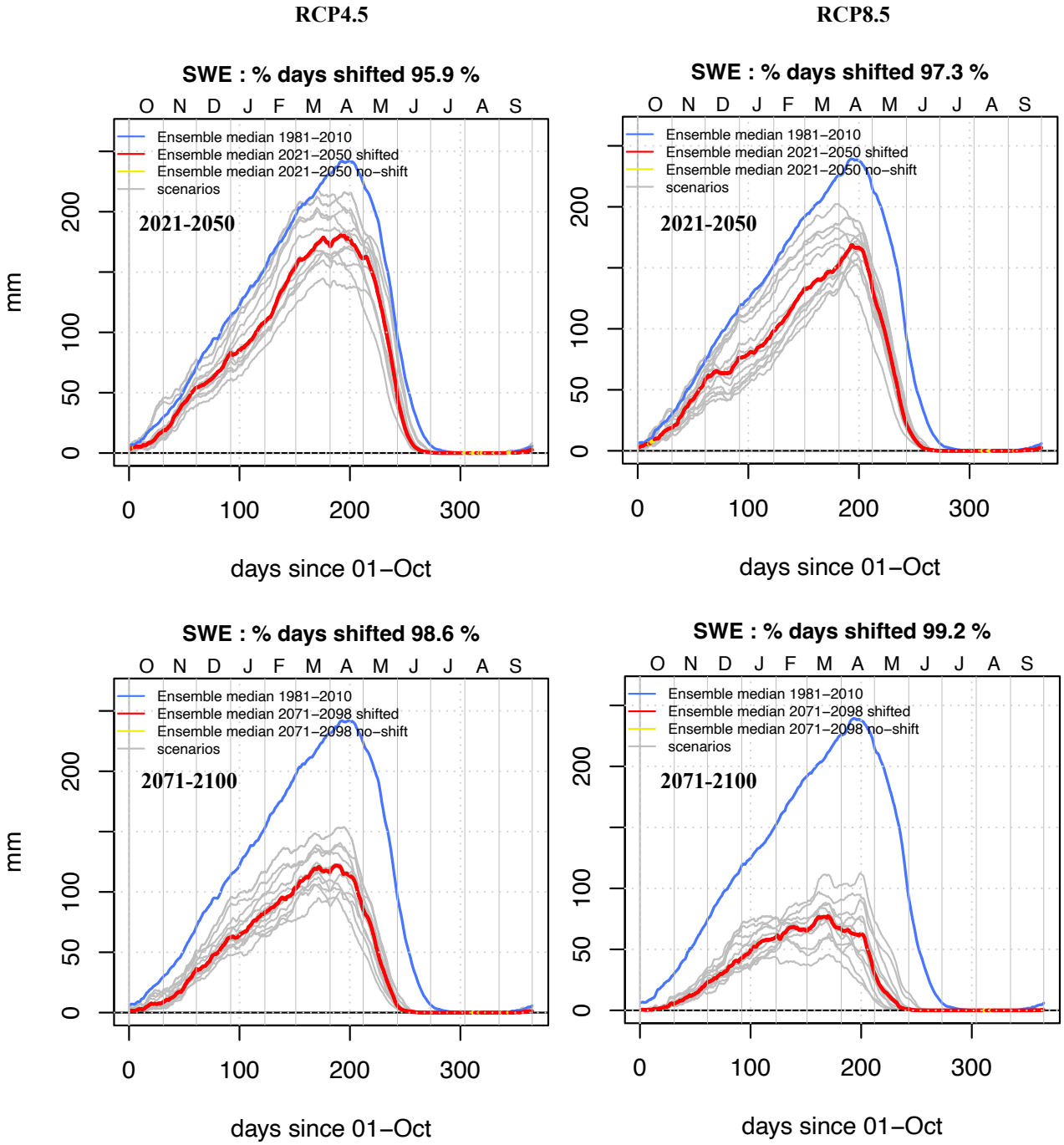

Fig. 14: Svartá catchment (vhm10): Projected seasonality of mean daily snow storage (SWE) under the RCP4.5 emission scenario (left-panel) and the RCP8.5 emission scenario (right-panel). Projection periods: 2021-2050 (top-panel) and 2071-2100 (bottom-panel). Individual ensemble members are coloured in grey. The ensemble median in each projection period is coloured in red for days when the Mann-Whitney test detected a significant shift in the mean daily snow storage ensemble, compared to the reference period (1981-2010) and yellow otherwise. The ensemble median in the reference period is shown in blue. The percentage of days in the water year when a significant shift in mean daily snow storage is detected by the Mann-Whitney test is also indicated. The day=1 for October 1st and 365 for September 30th.

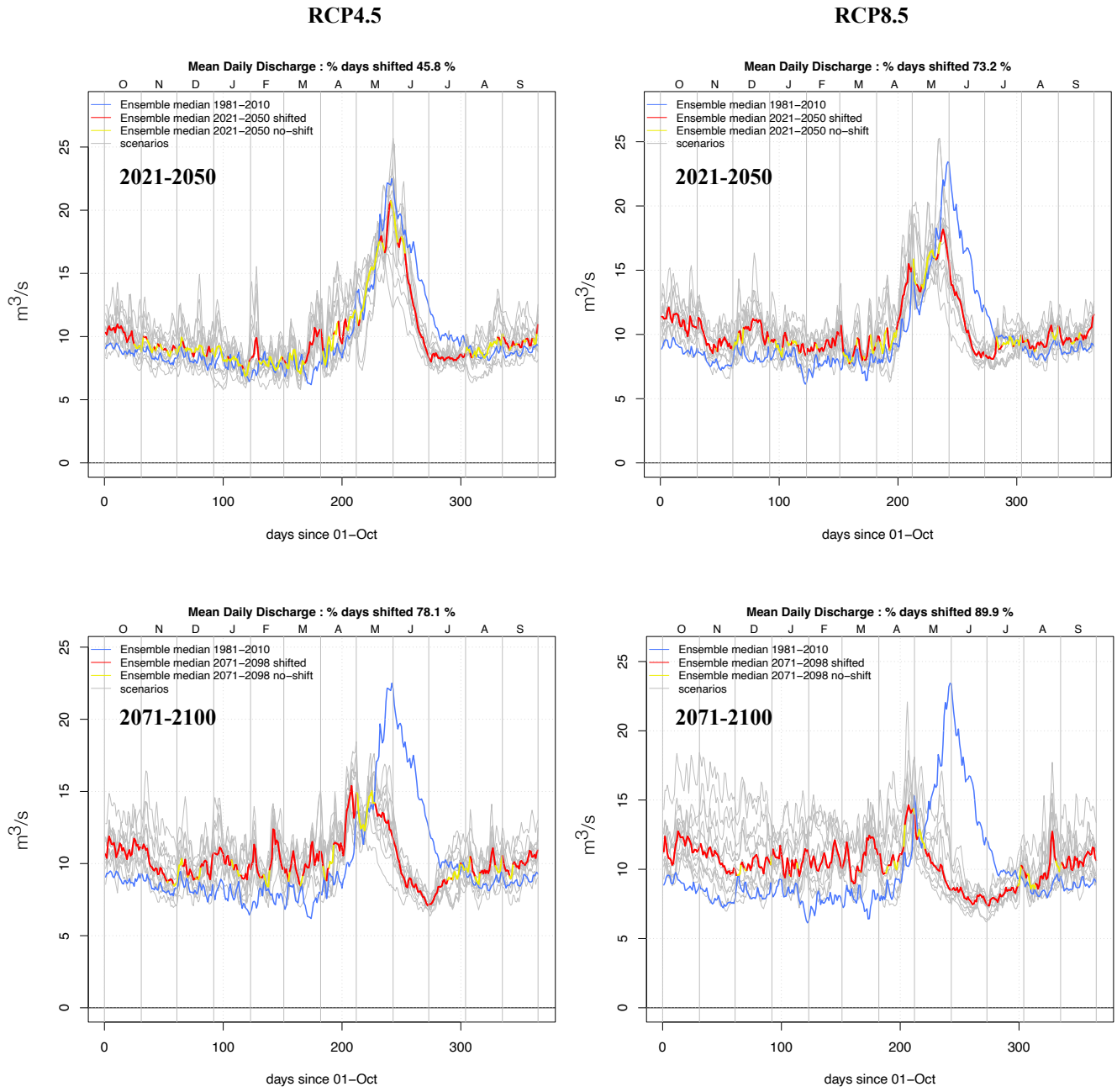

Fig. 15: Svartá catchment (vhm10): Projected seasonality of mean daily discharge under the RCP4.5 emission scenario (left-panel) and the RCP8.5 emission scenario (right-panel). Projection periods: 2021-2050 (top-panel) and 2071-2100 (bottom-panel). Individual ensemble members are coloured in grey. The ensemble median in each projection period is coloured in red for days when the Mann-Whitney test detected a significant shift in the mean daily discharge ensemble, compared to the reference period (1981-2010) and yellow otherwise. The ensemble median in the reference period is shown in blue. The percentage of days in the water year when a significant shift in mean daily discharge is detected by the Mann-Whitney test is also indicated. The day=1 for October 1st and 365 for September 30th.

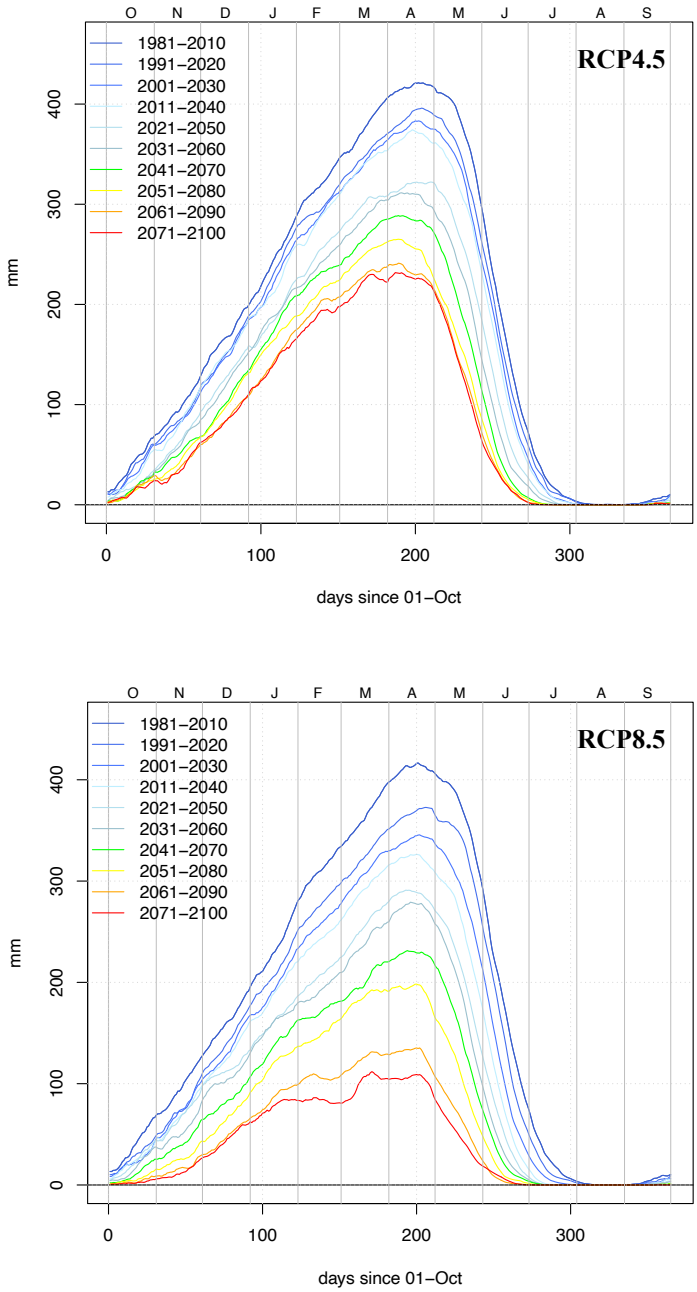

Fig. 16: Fnjóská catchment (vhm200): Ensemble median of the projected seasonality of mean daily snow storage (SWE) under the RCP4.5 emission scenario (top) and RCP8.5 emission scenario (bottom). Each colour corresponds to a 30-year period: from dark blue (1981-2010) to red (2071-2100). The day=1 for October 1st and 365 for September 30th.

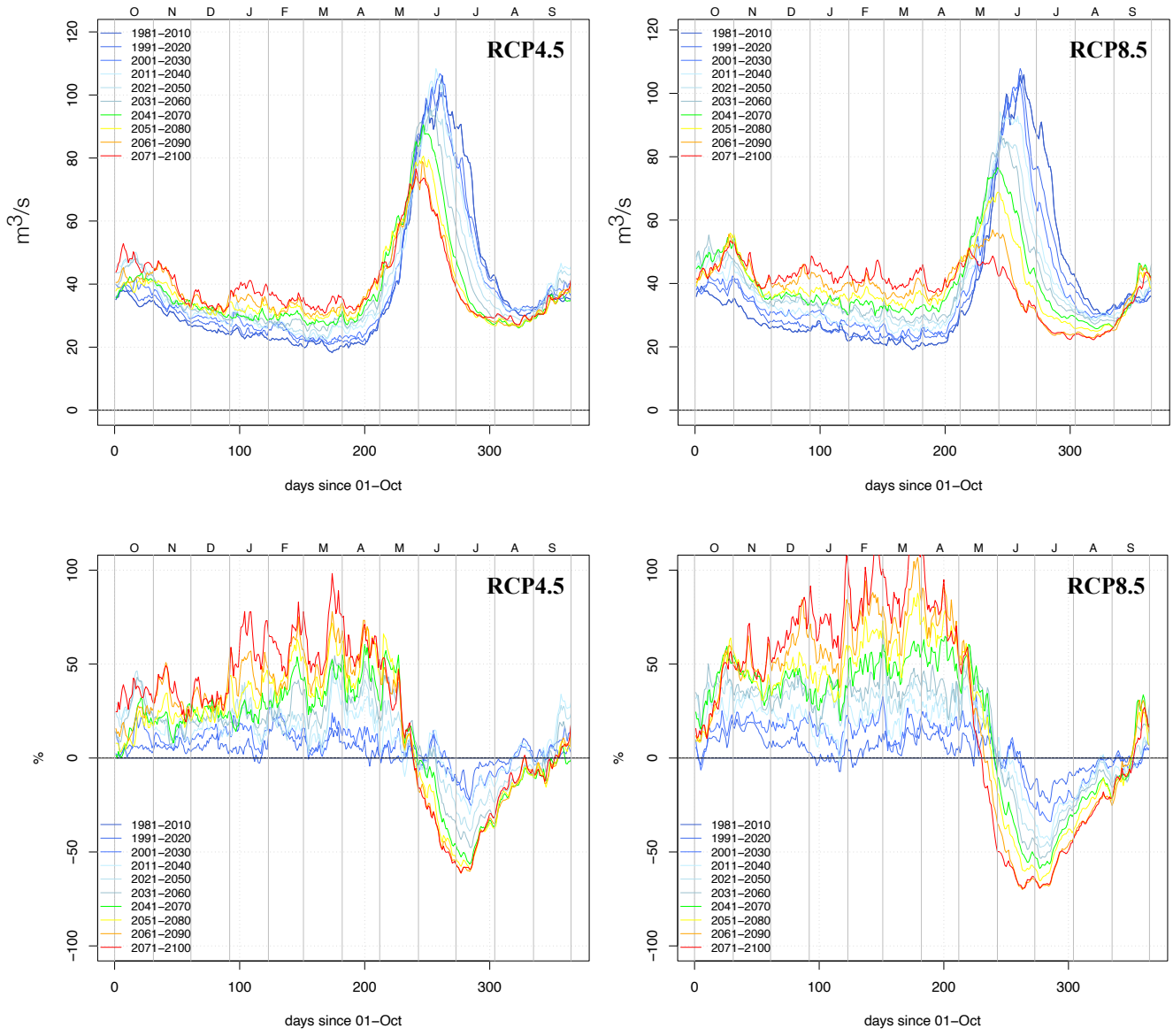

Fig. 17: Fnjóská catchment (vhm200): Ensemble median of the projected seasonality of mean daily discharge (top-panel) and percent change in the ensemble median of mean daily discharge relative to the reference period 1981-2010 (bottom-panel). Left-panel: RCP4.5 emission scenario. Right-panel: RCP8.5 emission scenario. Each colour corresponds to a 30-year period: from dark blue (1981-2010) to red (2071-2100). The day=1 for October 1st and 365 for September 30th.

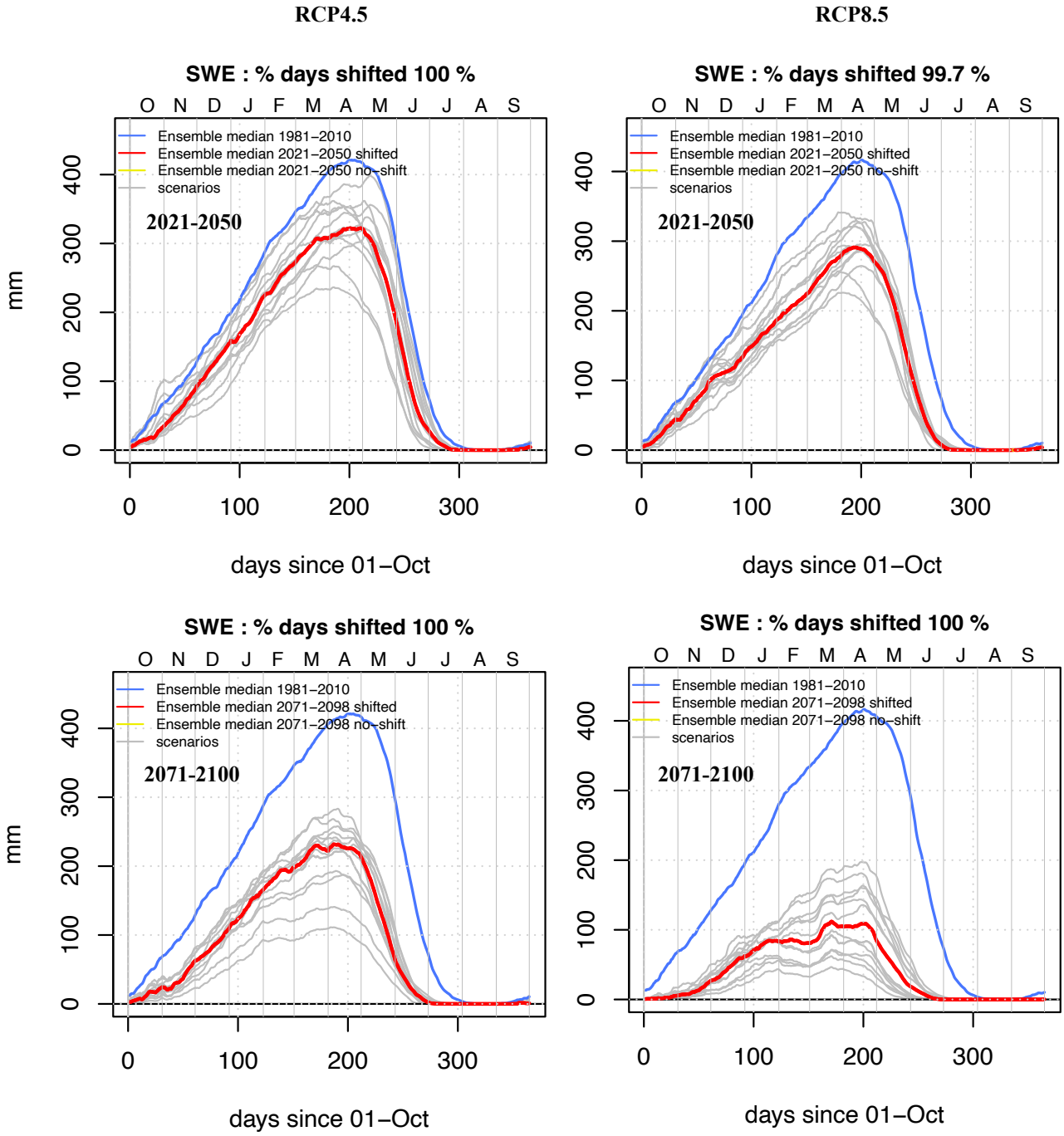

Fig. 18: Fnjóská catchment (vhm200): Projected seasonality of mean daily snow storage (SWE) under the RCP4.5 emission scenario (left-panel) and the RCP8.5 emission scenario (right-panel). Projection periods: 2021-2050 (top-panel) and 2071-2100 (bottom-panel). Individual ensemble members are coloured in grey. The ensemble median in each projection period is coloured in red for days when the Mann-Whitney test detected a significant shift in the mean daily snow storage ensemble, compared to the reference period (1981-2010) and yellow otherwise. The ensemble median in the reference period is shown in blue. The percentage of days in the water year when a significant shift in mean daily snow storage is detected by the Mann-Whitney test is also indicated. The day=1 for October 1st and 365 for September 30th.

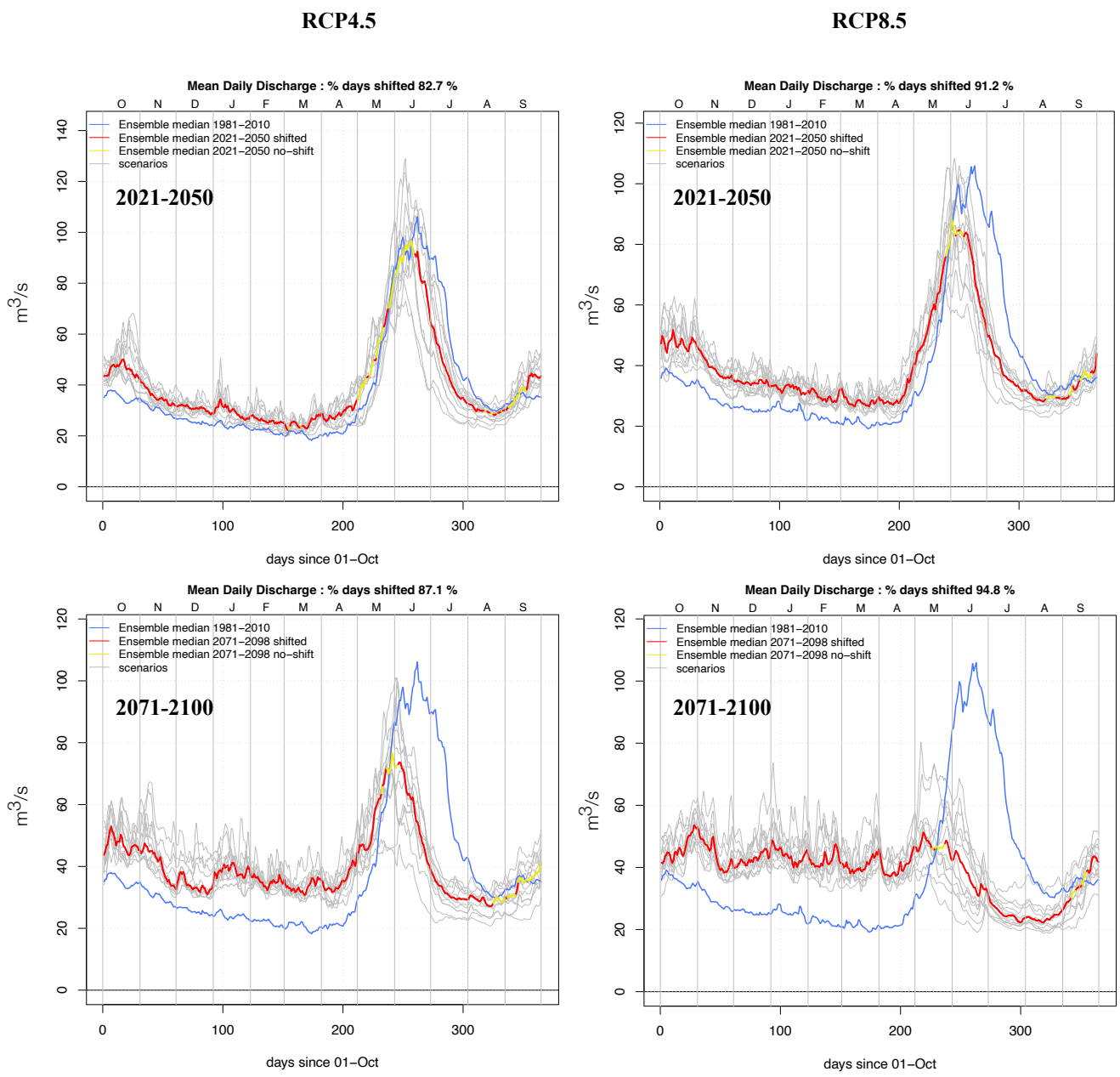

Fig. 19: Fnjóská catchment (vhm200): Projected seasonality of mean daily discharge under the RCP4.5 emission scenario (left-panel) and the RCP8.5 emission scenario (right-panel). Projection periods: 2021-2050 (top-panel) and 2071-2100 (bottom-panel). Individual ensemble members are coloured in grey. The ensemble median in each projection period is coloured in red for days when the Mann-Whitney test detected a significant shift in the mean daily discharge ensemble, compared to the reference period (1981-2010) and yellow otherwise. The ensemble median in the reference period is shown in blue. The percentage of days in the water year when a significant shift in mean daily discharge is detected by the Mann-Whitney test is also indicated. The day=1 for October 1st and 365 for September 30th.

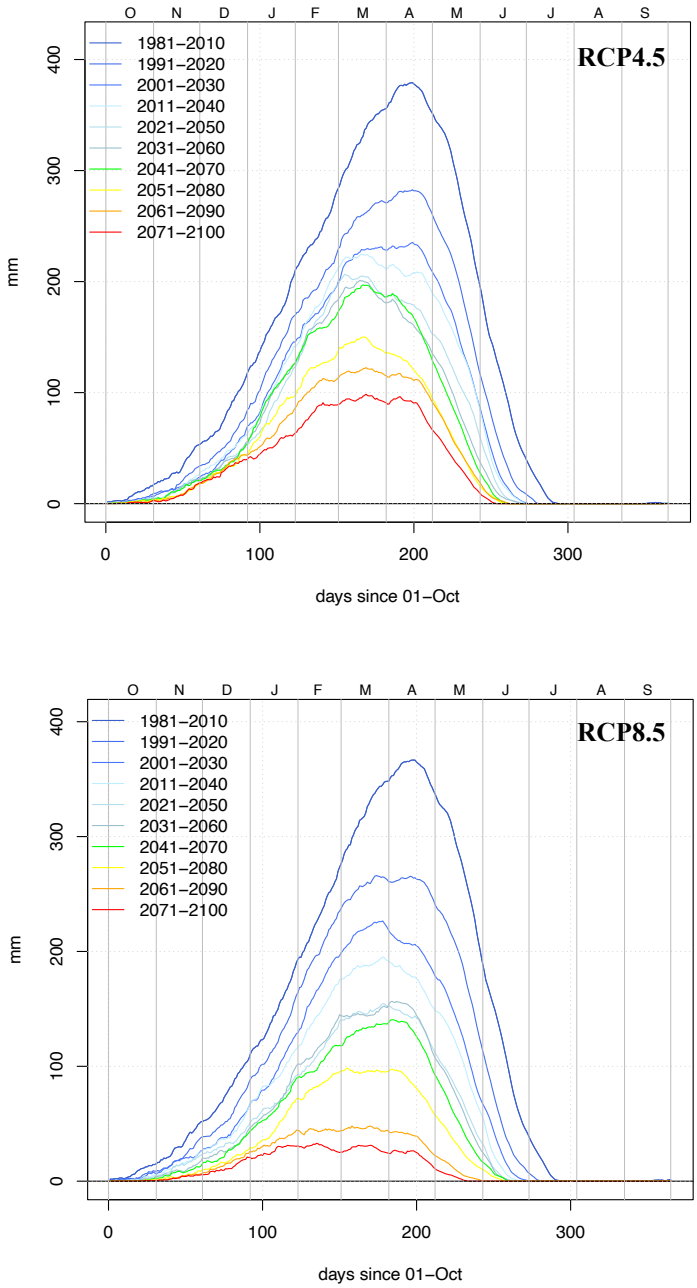

Fig. 20: Laxá catchment (vhm74): Ensemble median of the projected seasonality of mean daily snow storage (SWE) under the RCP4.5 emission scenario (top) and RCP8.5 emission scenario (bottom). Each colour corresponds to a 30-year period: from dark blue (1981-2010) to red (2071-2100). The day=1 for October 1st and 365 for September 30th.

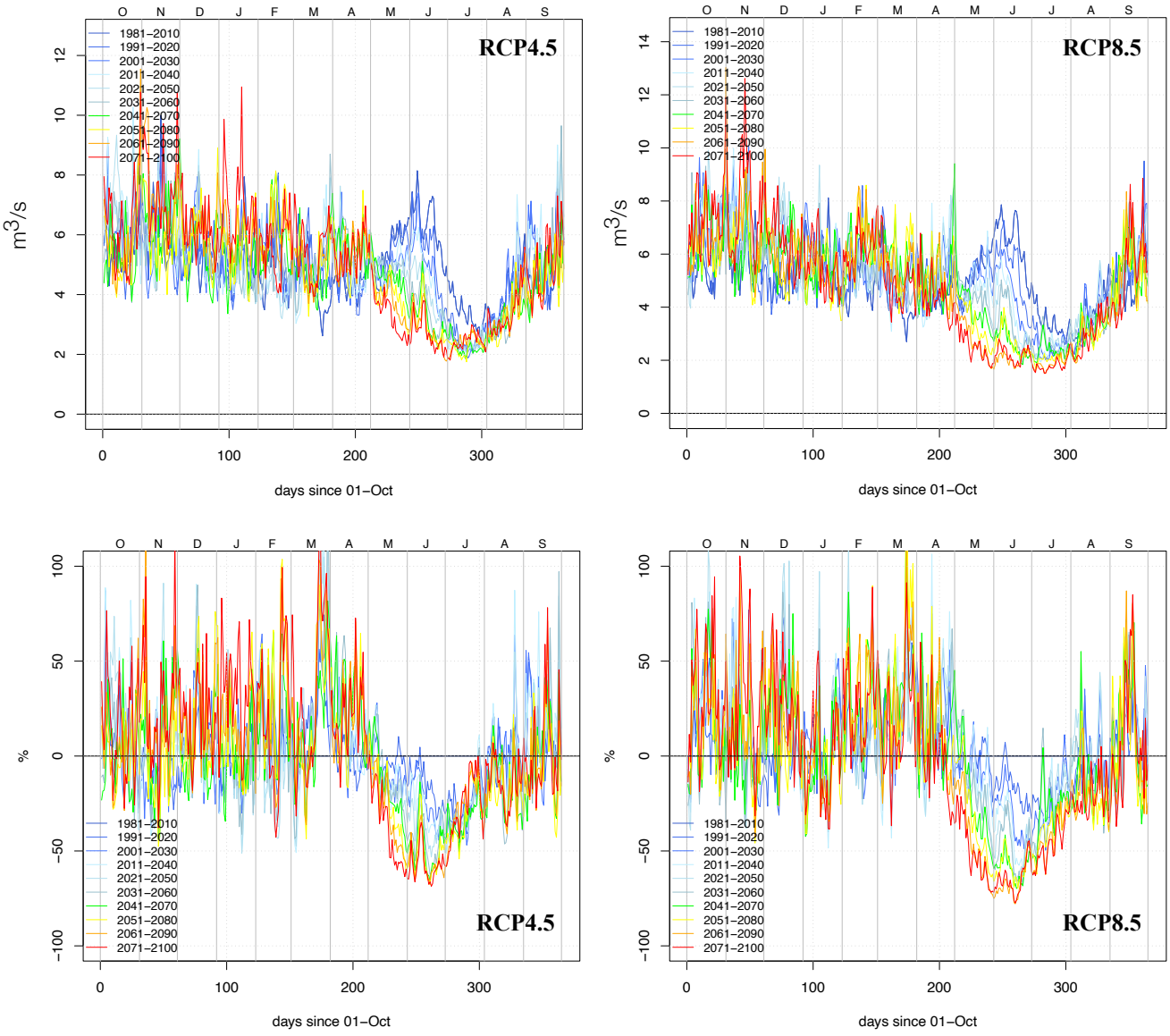

Fig. 21: Laxá catchment (vhm74): Ensemble median of the projected seasonality of mean daily discharge (top-panel) and percent change in the ensemble median of mean daily discharge relative to the reference period 1981-2010 (bottom-panel). Left-panel: RCP4.5 emission scenario. Right-panel: RCP8.5 emission scenario. Each colour corresponds to a 30-year period: from dark blue (1981-2010) to red (2071-2100). The day=1 for October 1st and 365 for September 30th.

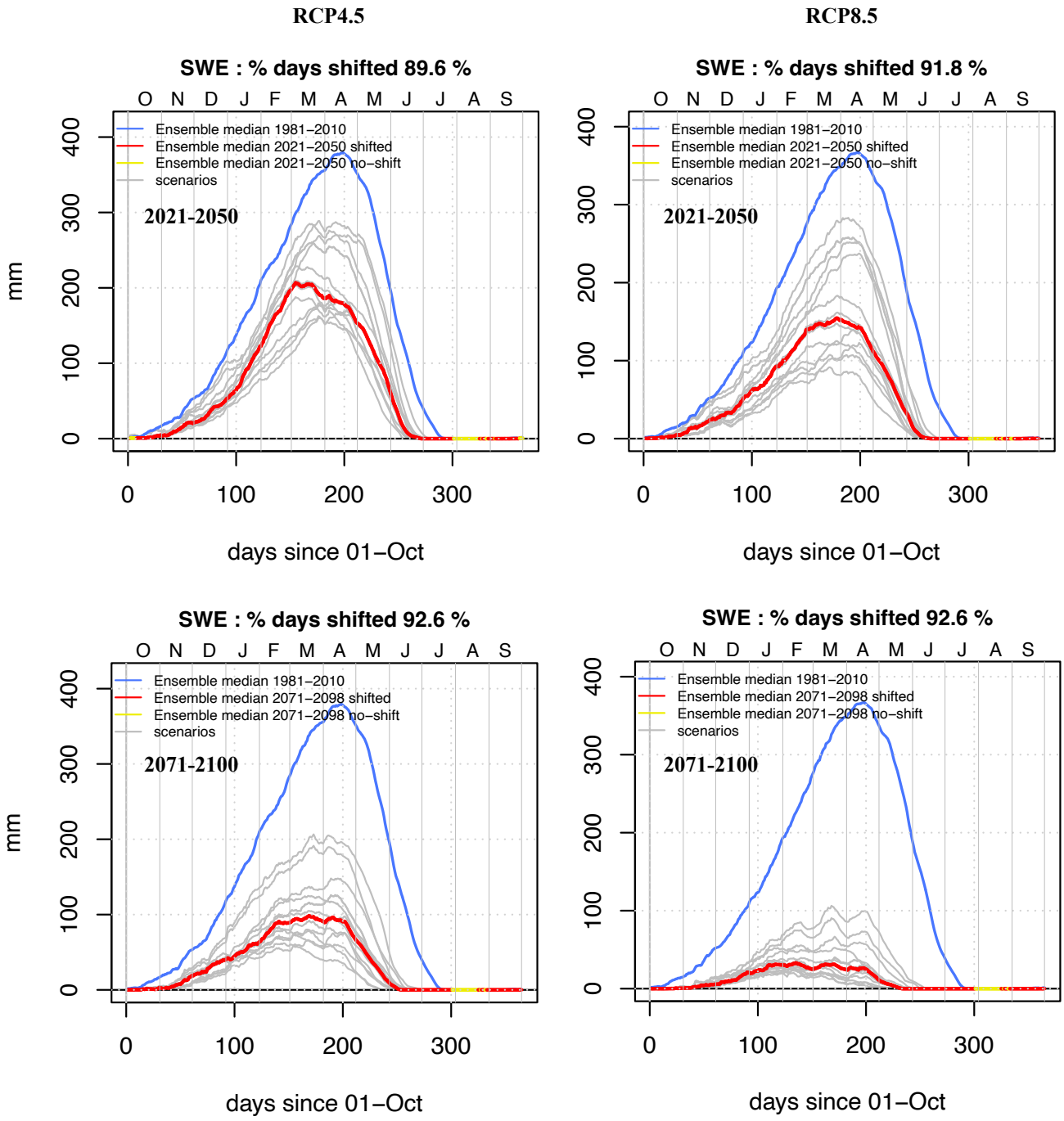

Fig. 22: Laxá catchment (vhm74): Projected seasonality of mean daily snow storage (SWE) under the RCP4.5 emission scenario (left-panel) and the RCP8.5 emission scenario (right-panel). Projection periods: 2021-2050 (top-panel) and 2071-2100 (bottom-panel). Individual ensemble members are coloured in grey. The ensemble median in each projection period is coloured in red for days when the Mann-Whitney test detected a significant shift in the mean daily snow storage ensemble, compared to the reference period (1981-2010) and yellow otherwise. The ensemble median in the reference period is shown in blue. The percentage of days in the water year when a significant shift in mean daily snow storage is detected by the Mann-Whitney test is also indicated. The day=1 for October 1st and 365 for September 30th.

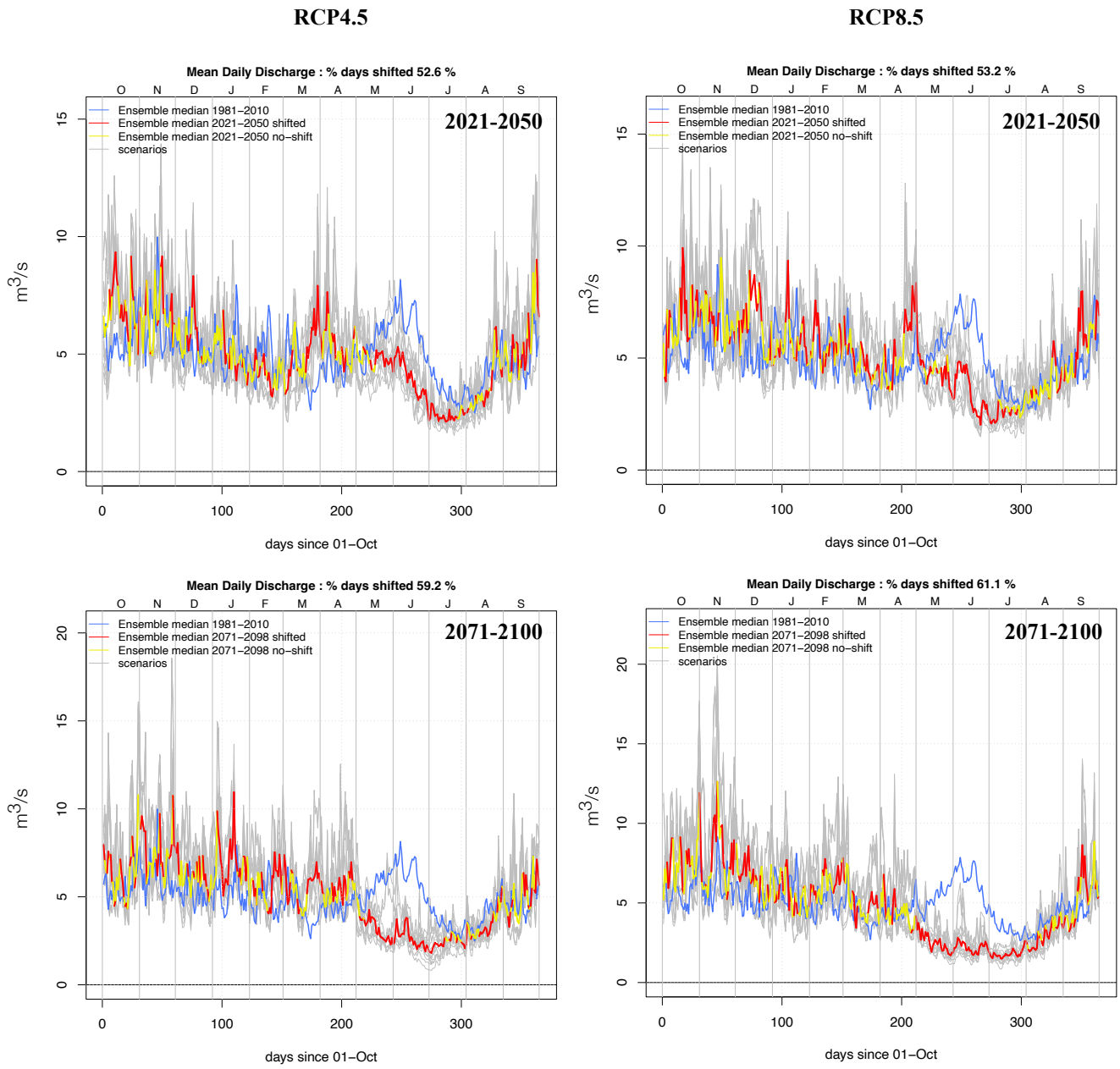

Fig. 23: Laxá catchment (vhm74): Projected seasonality of mean daily discharge under the RCP4.5 emission scenario (left-panel) and the RCP8.5 emission scenario (right-panel). Projection periods: 2021-2050 (top-panel) and 2071-2100 (bottom-panel). Individual ensemble members are coloured in grey. The ensemble median in each projection period is coloured in red for days when the Mann-Whitney test detected a significant shift in the mean daily discharge ensemble, compared to the reference period (1981-2010) and yellow otherwise. The ensemble median in the reference period is shown in blue. The percentage of days in the water year when a significant shift in mean daily discharge is detected by the Mann-Whitney test is also indicated. The day=1 for October 1st and 365 for September 30th.

6-2-2 Changes in mean annual and seasonal hydro-climatic characteristics

In order to obtain a more integrated view on the temporal evolution of the hydrological response to projected climate change and some insights into the mechanisms behind these changes, the ensembles of 30-year mean annual and seasonal flow projections were analysed with the corresponding ensembles of 30-year mean annual and seasonal temperature, precipitation, rainfall, snowfall and snowmelt projections. Projected changes between reference and future periods are presented in Figs. 24 to 53. For temperature, the changes are given in degree Celsius (future minus reference) and for the other indicators, the changes are given in percent relative to the corresponding reference (100*(future minus reference)/reference). The plots also show results from the one-sided Mann-Whitney tests used to compare the 30-year mean ensembles of each hydro-climatic indicator between the reference and future periods (see Methodology in Section 3-1). The analysis below summarises the results.

- **Svartá catchment (vhm10)**
  - Mean annual and seasonal surface air temperatures are projected to steadily rise along the 21st century. A median warming of about 2.5°C to 2.7°C is projected from 1981-2010 to 2071-2100 under the RCP4.5 scenario and about 3.8°C to 4.5°C under the RCP8.5 scenario, depending on the season (see also Table 8).
  - Mean annual precipitation projections fluctuate and remain close to their reference level until 2011-2040 under the RCP4.5 scenario and thereafter, a significant but moderate increase, not exceeding a median value of 10%, is projected. For the RCP8.5 scenario, results indicate a significant increase in mean annual precipitation along most of the century, reaching a median value of about 15%. The increase in mean annual precipitation is mainly driven by the projected mean precipitation increase in JAS. In that season, the largest median increases projected along the 21st century are estimated at about 25% with the RCP4.5 scenario and about 30% with the RCP8.5 scenario. A significant increase in mean precipitation is also projected in OND under the RCP8.5 scenario in a majority of projection periods and reaches a median value of about 20% in 2071-2100. Mean seasonal precipitation is not projected to change significantly in OND under the RCP4.5 scenario, and in JFM and AMJ under both emission scenarios, either because the ensemble spread is large and with a lack of consensus regarding the direction of change, making the outcome uncertain, or because the projections fluctuate closely around their reference level.
  - The rise in temperature has an impact on the fractions of seasonal precipitation falling as rain or snow. As a result, mean seasonal rainfall is projected to increase more or less gradually whereas mean seasonal snowfall is projected to decrease more or less gradually, along the projection horizon. These changes concern all seasons and a majority of projection periods, therefore, the annual means are impacted as well. The largest median relative increases in mean seasonal rainfall are projected in OND and JFM, in 2071-2100 (about 80% in OND and 90% in JFM with the RCP4.5 scenario, and about 150% in OND and 130% in JFM with the RCP8.5 scenario).

- The decrease in mean annual snowfall resulting from the projected warming leads to a reduction in snow storage (cf. Fig. 12) which, in turn, leads to a decrease in mean annual snowmelt. At the seasonal level, mean snowmelt variations are more complex: Results indicate that mean seasonal snowmelt is projected to increase first, before returning close to the reference level in OND, gradually increase in JFM and decrease in AMJ and JAS. The changes are usually greater under the RCP8.5 emission scenario than under the RCP4.5 emission scenario because the projected warming is greater. The projected increase in mean snowmelt in autumn/winter is likely caused by an increase in the number of warm spells leading to intermittent snowmelt events and/or a shift earlier in the onset of the snowmelt season, whereas the projected decrease in mean snowmelt in spring/summer is owing to the projected snow storage depletion caused by the projected decrease in seasonal snowfall and the increased number of snowmelt events in winter destabilising the build-up of the snowpack.
- Unlike mean annual precipitation, mean annual flow is not projected to change significantly along the 21st century under the RCP4.5 emission scenario and the median change remains close to zero percent. Similar results are projected under the RCP8.5 emission scenario except that a moderate mean annual flow increase is projected in some periods. The spread of the ensemble increases with the projection horizon under both emission scenarios. Note that increased evapotranspiration (not shown) caused by rising temperatures counteracts the increase in mean annual precipitation and contributes to reduce mean annual flow. At the seasonal level, the projections indicate a gradual increase in mean flow in OND and JFM, caused by the projected increase in rainfall and snowmelt; A gradual decrease in mean flow in AMJ, caused by the projected reduction in snowmelt not counteracted by increased rainfall; No significant change in JAS under the RCP4.5 emission scenario, and a moderate increase in mean flow under the RCP8.5 emission scenario in the second half of the projection horizon, depending on the balance between the increase in rainfall, the decrease in snowmelt and increased evapotranspiration (not shown). The changes in mean seasonal flow in OND, JFM and AMJ are significant in a majority of projection periods. The changes are usually more pronounced with the RCP8.5 emission scenario than the RCP4.5 emission scenario because the projected warming is greater and its impact on the change in the phase of precipitation and on snow storage larger. When significant, the largest mean flow changes are usually projected towards the end of the 21st century, if the changes are gradual, or possibly in some other future period, if they fluctuate. The largest median changes in mean seasonal flow, projected along the 21st century, have the following values:
  - RCP4.5: OND (about +15%), JFM (about +25%), AMJ (about -22%), JAS (about -2.5%)
  - RCP8.5: OND (about +25%), JFM (about +35%), AMJ (about -30%), JAS (about +10%)

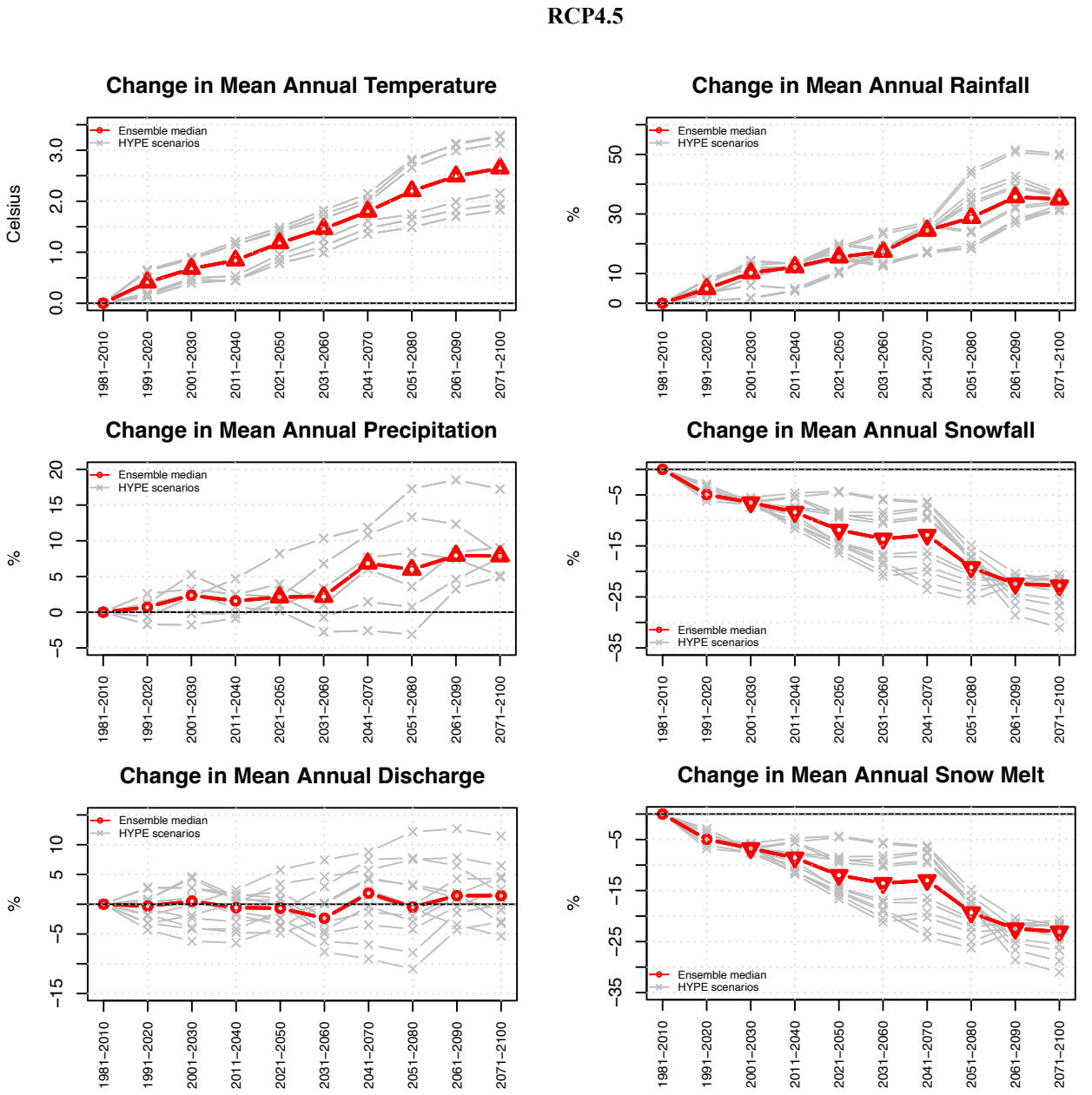

Fig. 24: Svartá catchment (vhm10): Projected changes in 30-year mean annual temperature, precipitation, rainfall, snowfall, snowmelt and river discharge under the RCP4.5 emission scenario, relative to the 1981-2010 reference period. Ensemble members (grey lines) and ensemble median (red line). The symbols on the ensemble median indicate whether the 30-year mean is likely to increase or decrease significantly or remain unchanged in the future periods compared to the reference period, according to the Mann-Whitney test (triangle point-up=increase; triangle point down=decrease; open circle=no significant change).

RCP4.5

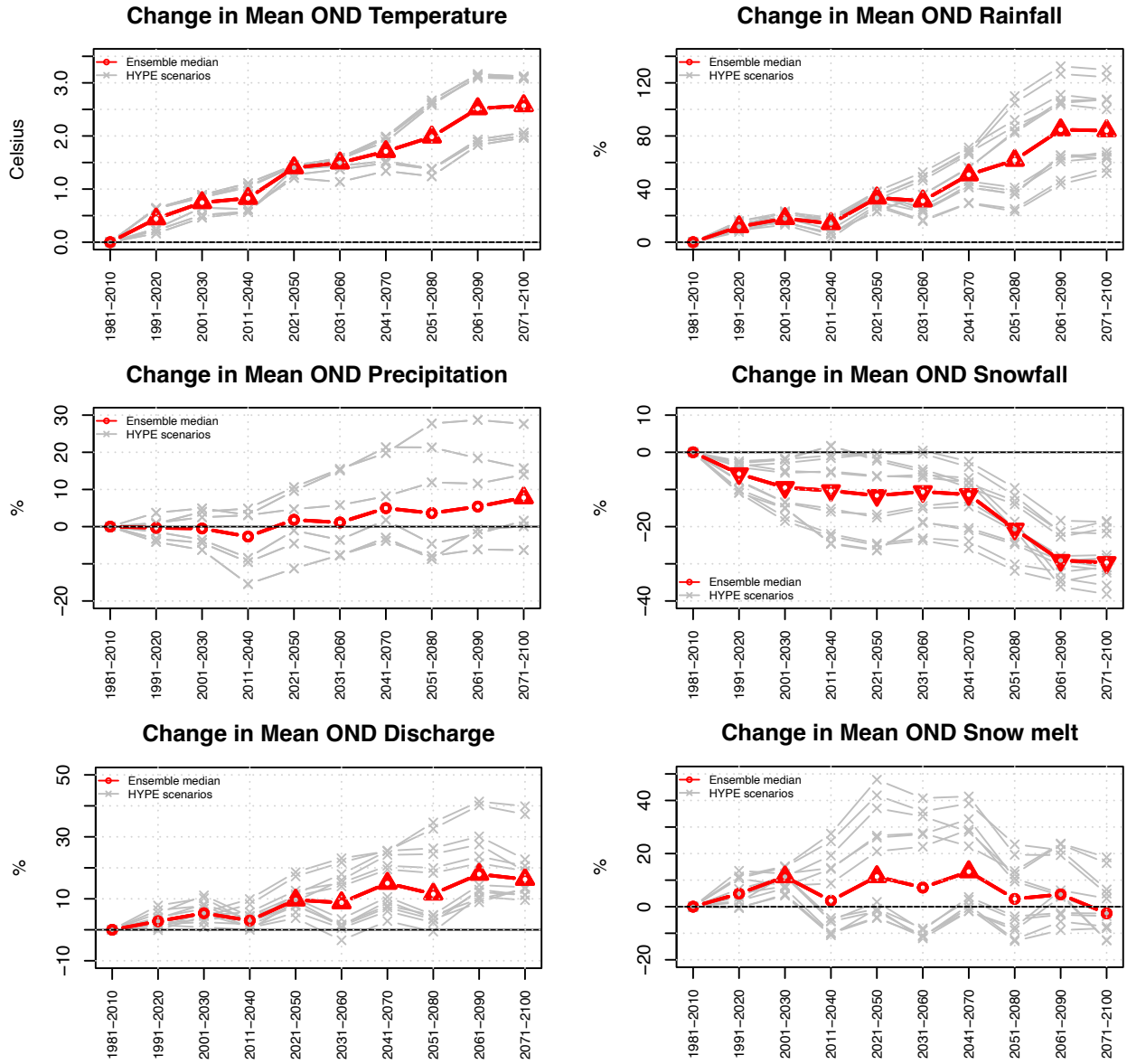

Fig. 25: Svartá catchment (vhm10): Projected changes in 30-year mean OND temperature, precipitation, rainfall, snowfall, snowmelt and river discharge under the RCP4.5 emission scenario, relative to the 1981-2010 reference period. Ensemble members (grey lines) and ensemble median (red line). The symbols on the ensemble median indicate whether the 30-year mean is likely to increase or decrease significantly or remain unchanged in the future periods compared to the reference period, according to the Mann-Whitney test (triangle point-up=increase; triangle point down=decrease; open circle=no significant change).

RCP4.5

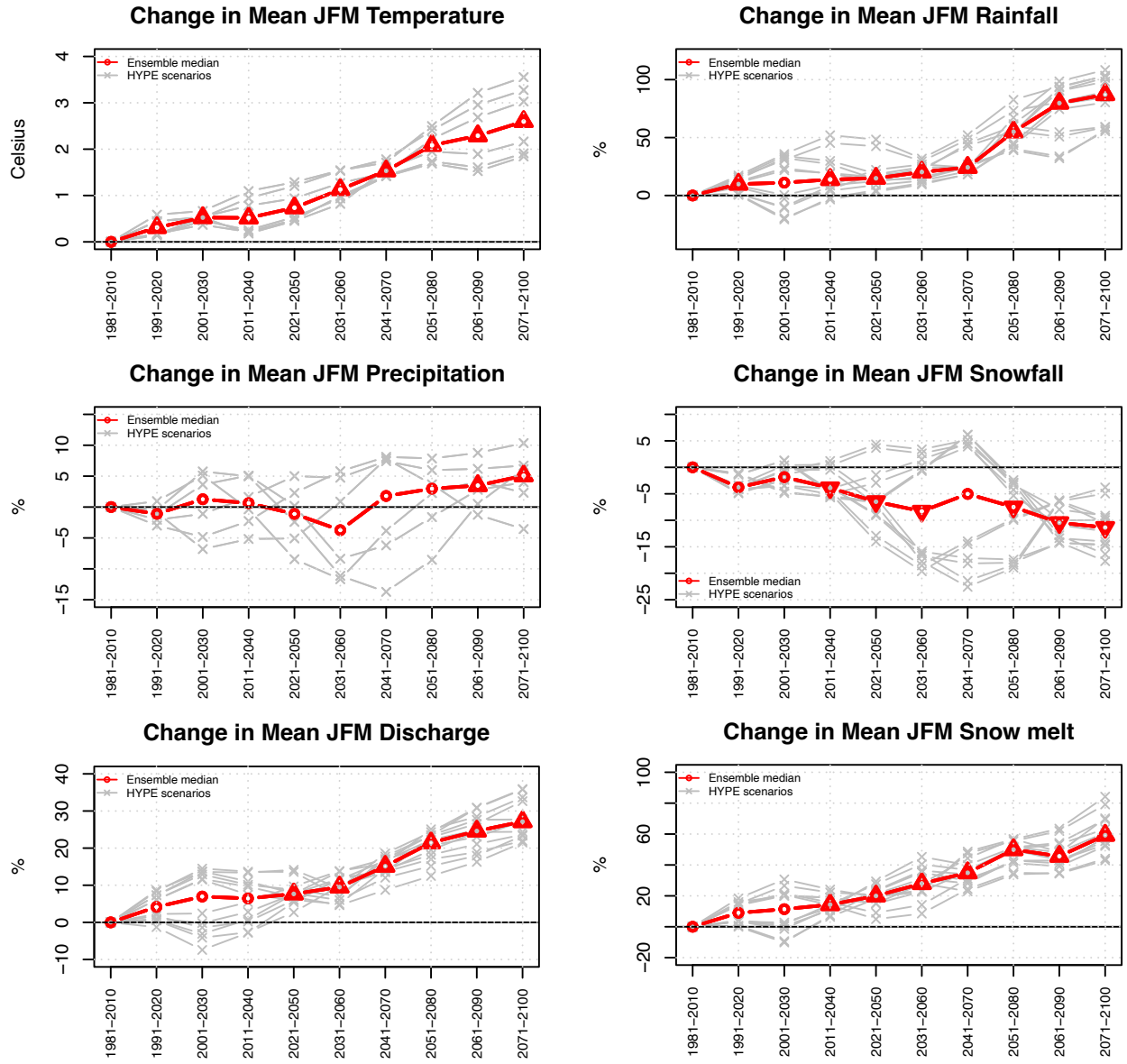

Fig. 26: Svartá catchment (vhm10): Projected changes in 30-year mean JFM temperature, precipitation, rainfall, snowfall, snowmelt and river discharge under the RCP4.5 emission scenario, relative to the 1981-2010 reference period. Ensemble members (grey lines) and ensemble median (red line). The symbols on the ensemble median indicate whether the 30-year mean is likely to increase or decrease significantly or remain unchanged in the future periods compared to the reference period, according to the Mann-Whitney test (triangle point-up=increase; triangle point down=decrease; open circle=no significant change).

RCP4.5

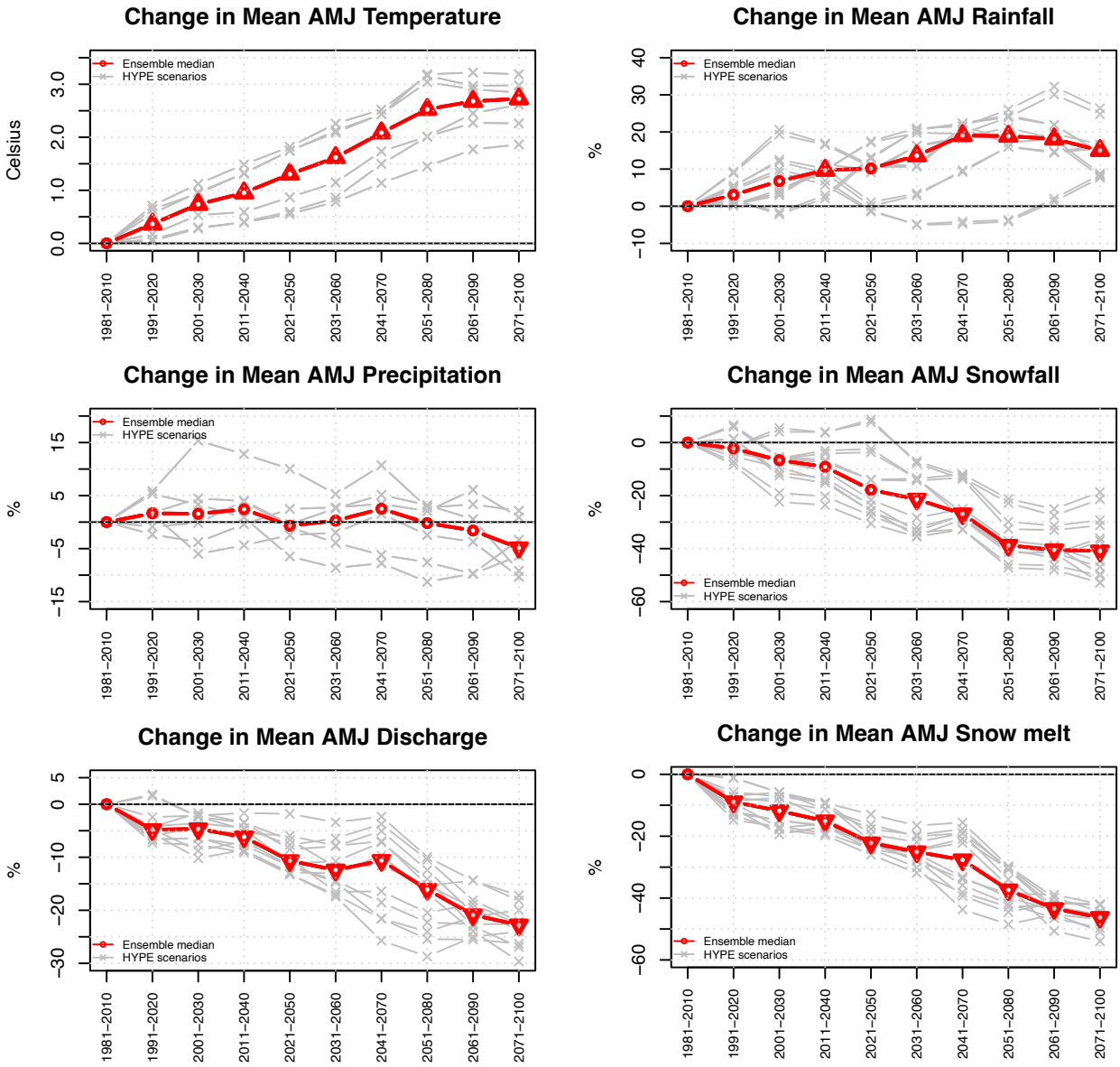

Fig. 27: Svartá catchment (vhm10): Projected changes in 30-year mean AMJ temperature, precipitation, rainfall, snowfall, snowmelt and river discharge under the RCP4.5 emission scenario, relative to the 1981-2010 reference period. Ensemble members (grey lines) and ensemble median (red line). The symbols on the ensemble median indicate whether the 30-year mean is likely to increase or decrease significantly or remain unchanged in the future periods compared to the reference period, according to the Mann-Whitney test (triangle point-up=increase; triangle point down=decrease; open circle=no significant change).

RCP4.5

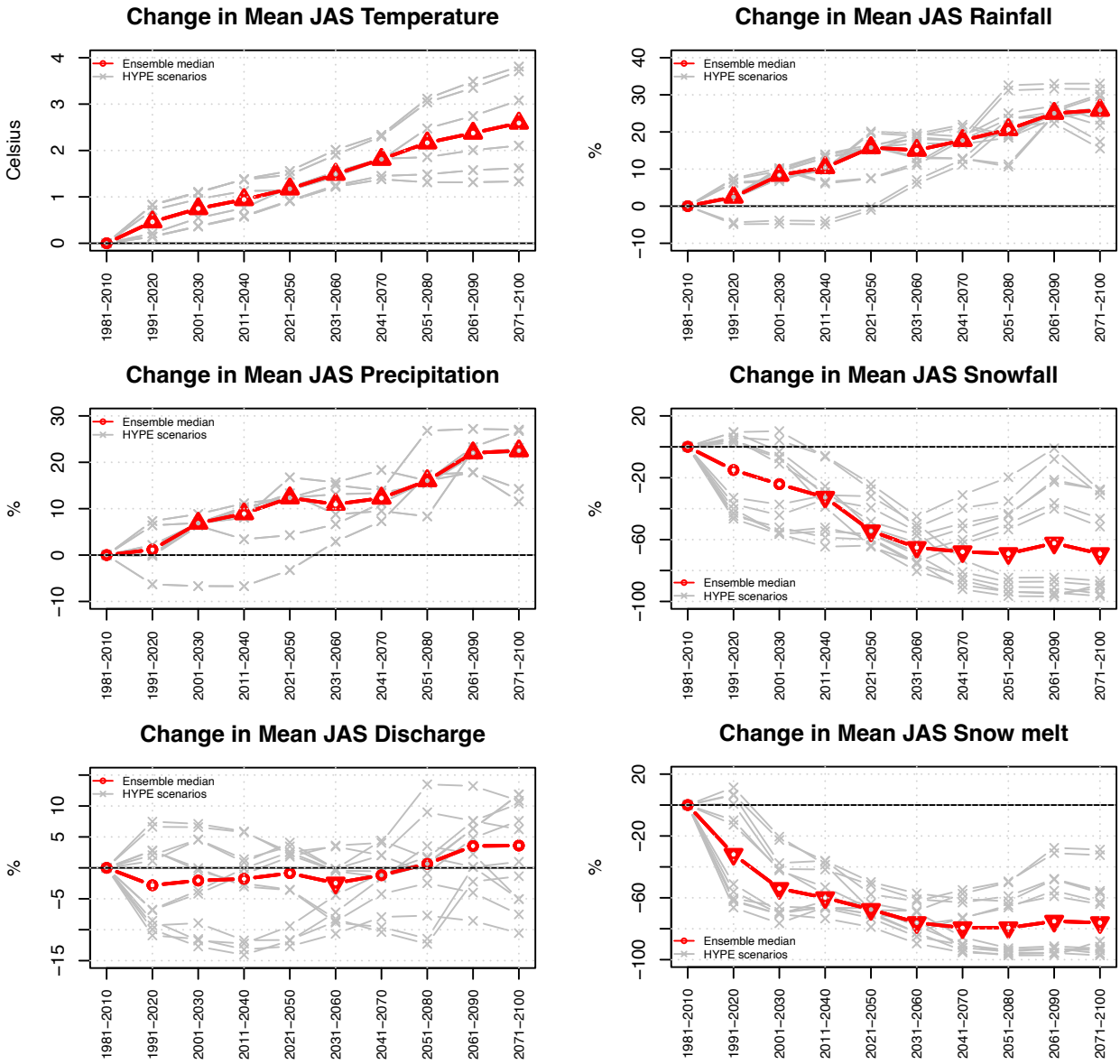

Fig. 28: Svartá catchment (vhm10): Projected changes in 30-year mean JAS temperature, precipitation, rainfall, snowfall, snowmelt and river discharge under the RCP4.5 emission scenario, relative to the 1981-2010 reference period. Ensemble members (grey lines) and ensemble median (red line). The symbols on the ensemble median indicate whether the 30-year mean is likely to increase or decrease significantly or remain unchanged in the future periods compared to the reference period, according to the Mann-Whitney test (triangle point-up=increase; triangle point down=decrease; open circle=no significant change).

RCP8.5

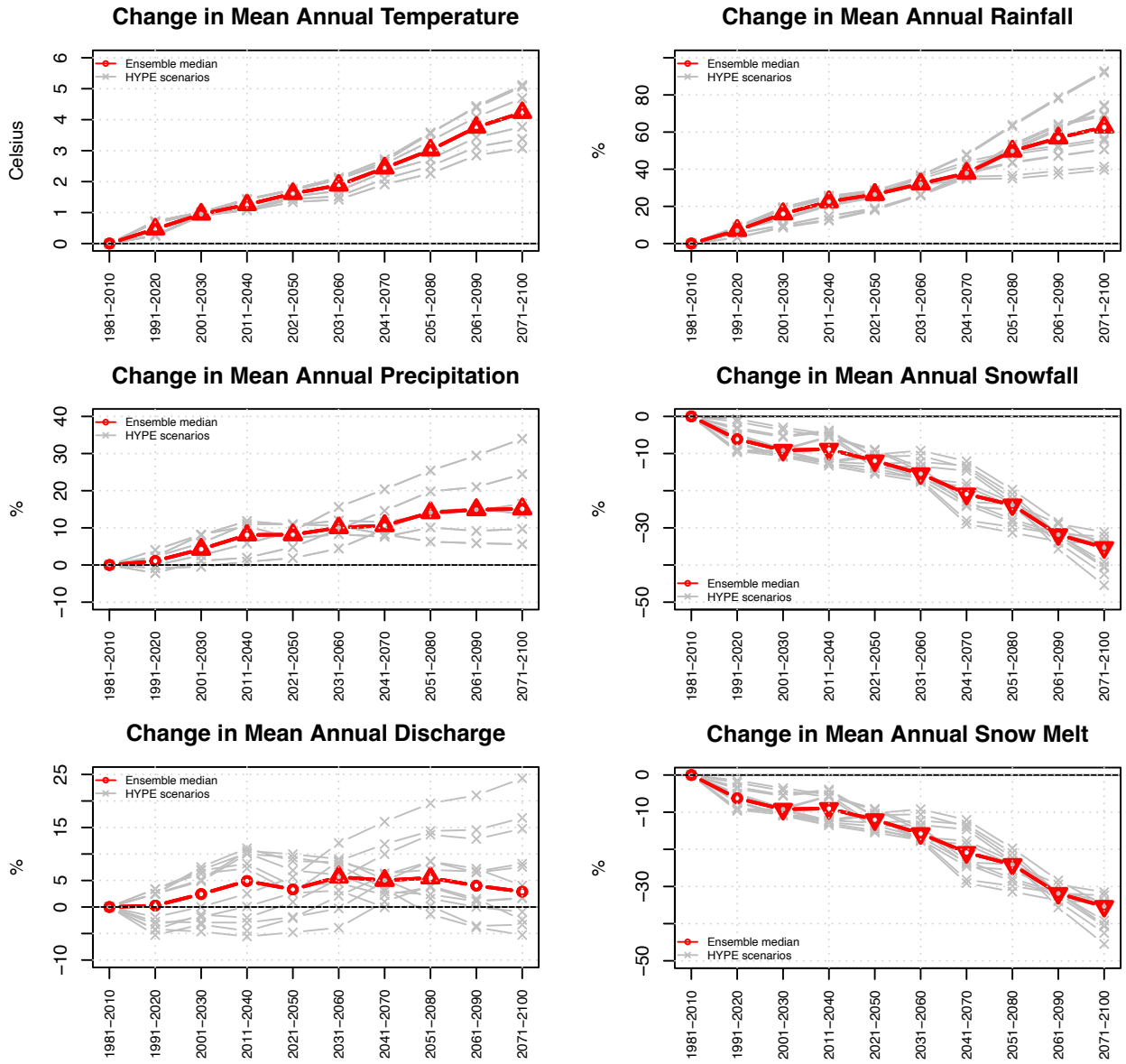

Fig. 29: Svartá catchment (vhm10): Projected changes in 30-year mean annual temperature, precipitation, rainfall, snowfall, snowmelt and river discharge under the RCP8.5 emission scenario, relative to the 1981-2010 reference period. Ensemble members (grey lines) and ensemble median (red line). The symbols on the ensemble median indicate whether the 30-year mean is likely to increase or decrease significantly or remain unchanged in the future periods compared to the reference period, according to the Mann-Whitney test (triangle point-up=increase; triangle point down=decrease; open circle=no significant change).

RCP8.5

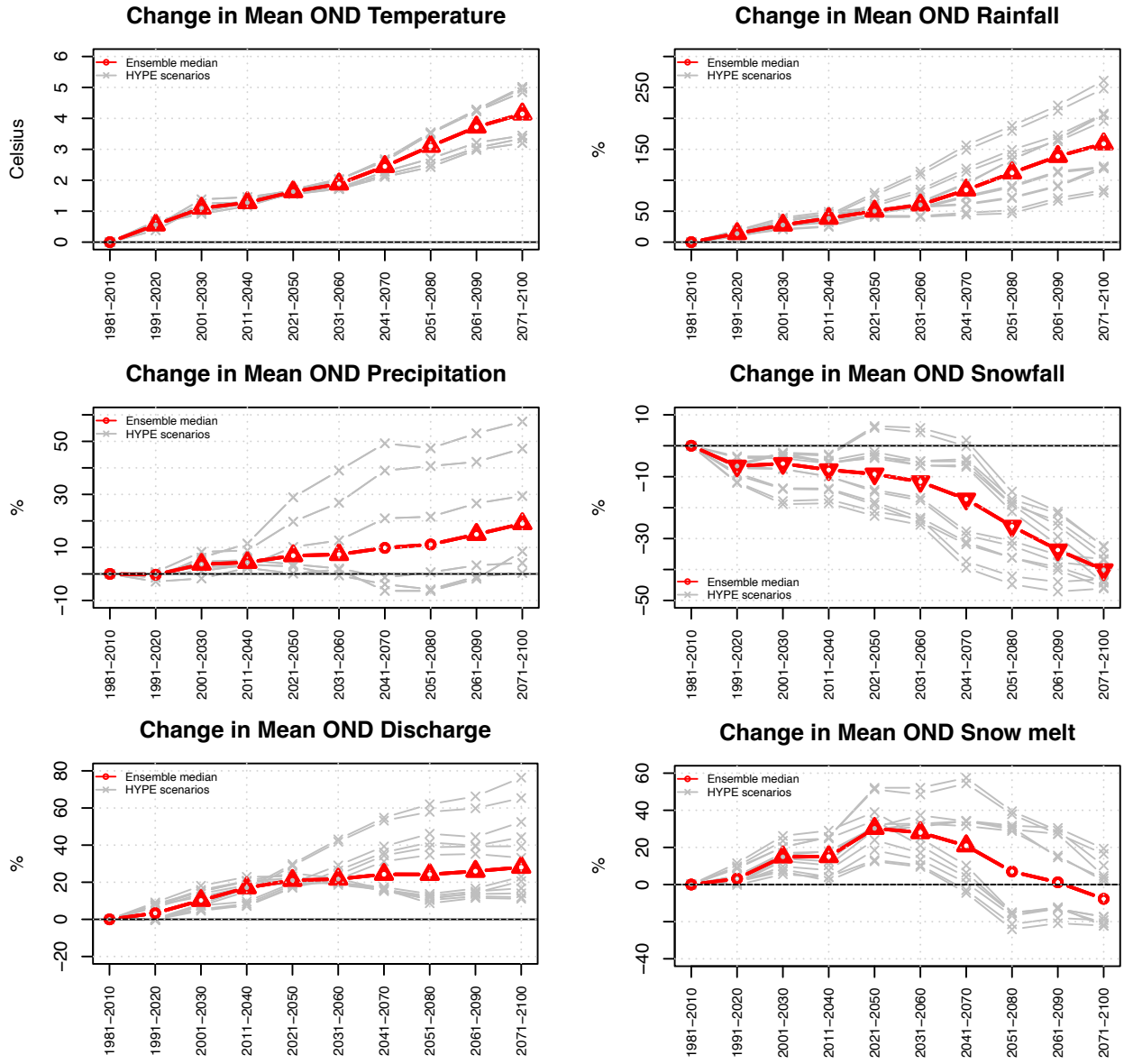

Fig. 30: Svartá catchment (vhm10): Projected changes in 30-year mean OND temperature, precipitation, rainfall, snowfall, snowmelt and river discharge under the RCP8.5 emission scenario, relative to the 1981-2010 reference period. Ensemble members (grey lines) and ensemble median (red line). The symbols on the ensemble median indicate whether the 30-year mean is likely to increase or decrease significantly or remain unchanged in the future periods compared to the reference period, according to the Mann-Whitney test (triangle point-up=increase; triangle point down=decrease; open circle=no significant change).

RCP8.5

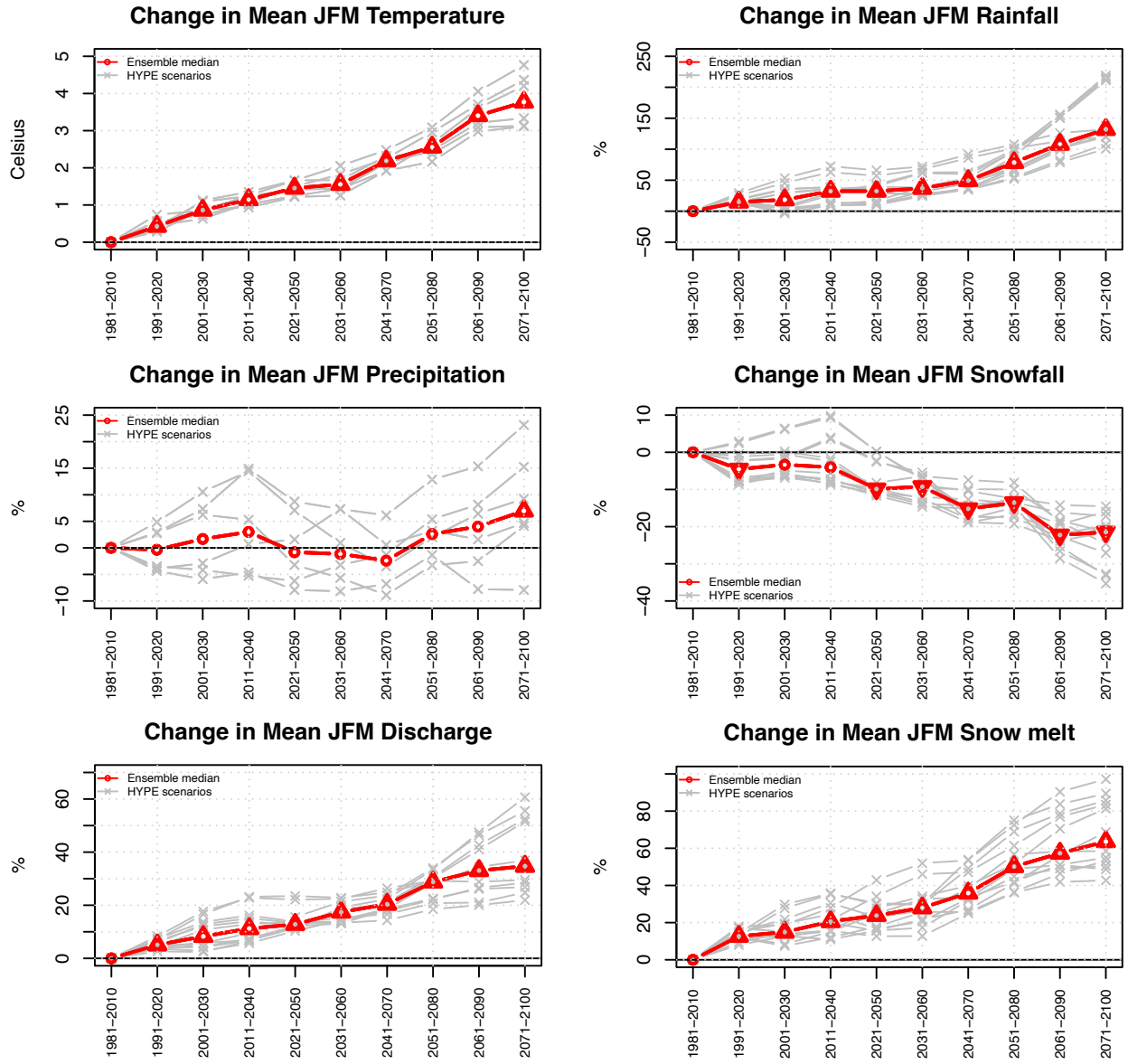

Fig. 31: Svartá catchment (vhm10): Projected changes in 30-year mean JFM temperature, precipitation, rainfall, snowfall, snowmelt and river discharge under the RCP8.5 emission scenario, relative to the 1981-2010 reference period. Ensemble members (grey lines) and ensemble median (red line). The symbols on the ensemble median indicate whether the 30-year mean is likely to increase or decrease significantly or remain unchanged in the future periods compared to the reference period, according to the Mann-Whitney test (triangle point-up=increase; triangle point down=decrease; open circle=no significant change).

RCP8.5

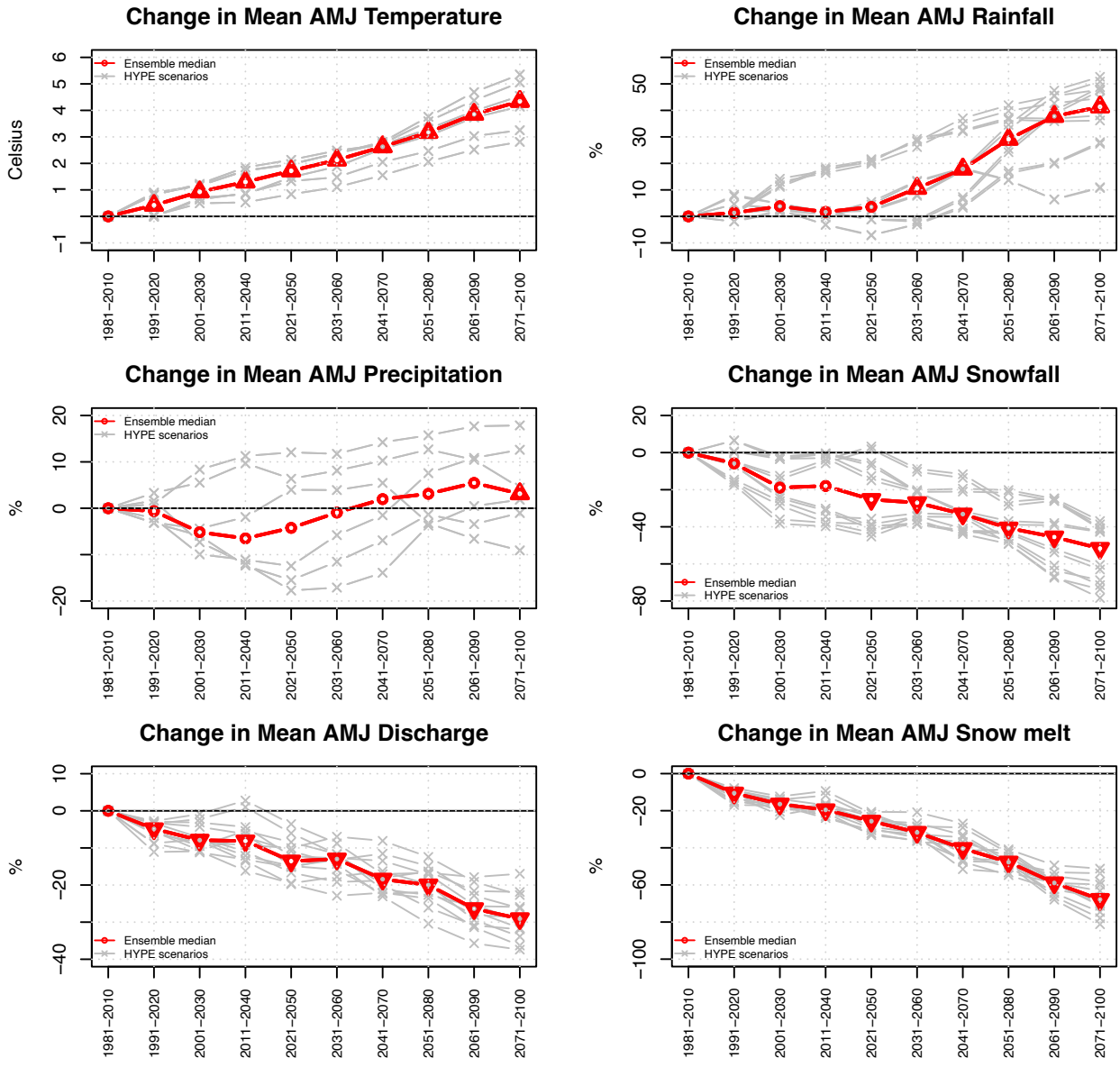

Fig. 32: Svartá catchment (vhm10): Projected changes in 30-year mean AMJ temperature, precipitation, rainfall, snowfall, snowmelt and river discharge under the RCP8.5 emission scenario, relative to the 1981-2010 reference period. Ensemble members (grey lines) and ensemble median (red line). The symbols on the ensemble median indicate whether the 30-year mean is likely to increase or decrease significantly or remain unchanged in the future periods compared to the reference period, according to the Mann-Whitney test (triangle point-up=increase; triangle point down=decrease; open circle=no significant change).

RCP8.5

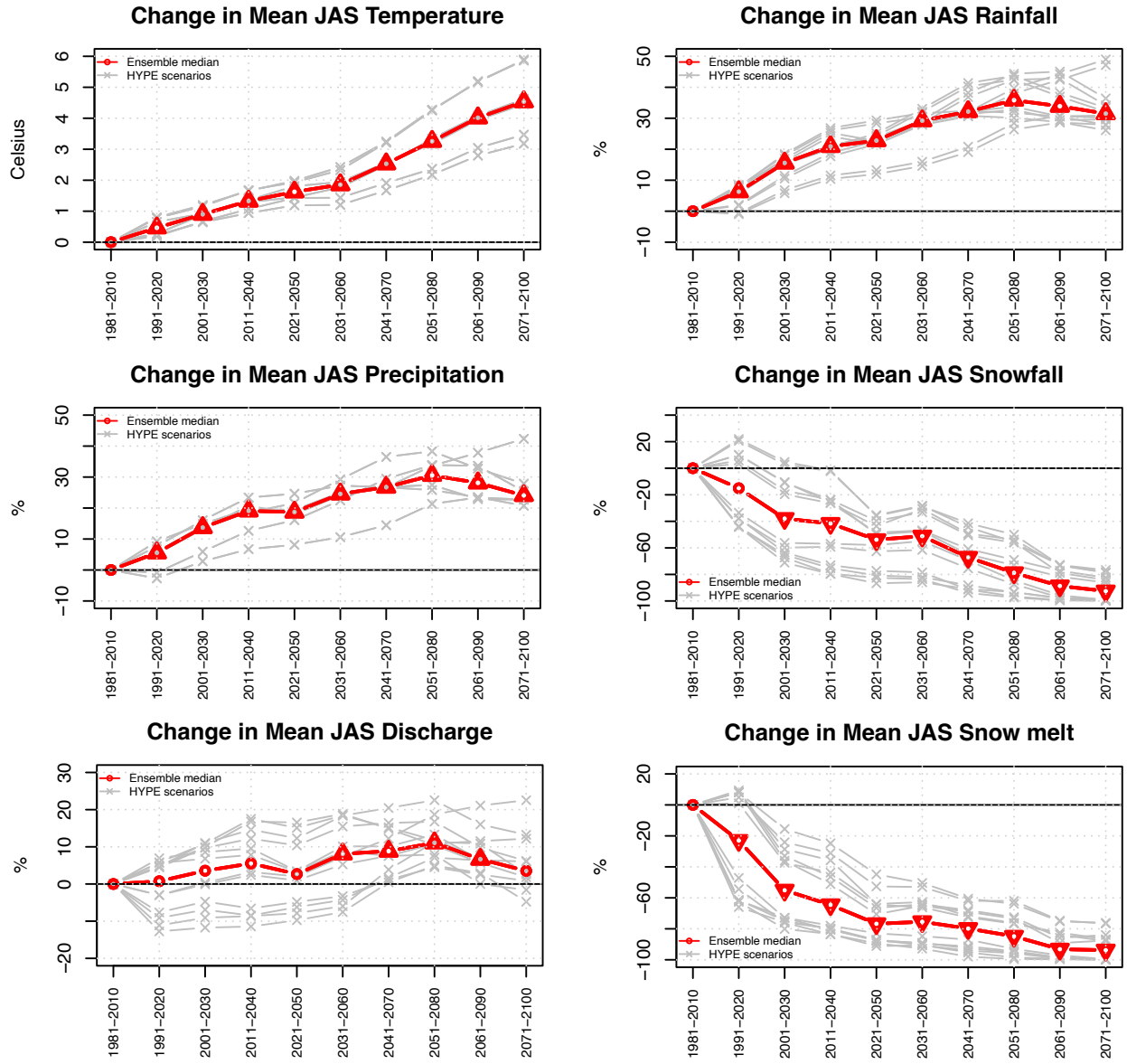

Fig. 33: Svartá catchment (vhm10): Projected changes in 30-year mean JAS temperature, precipitation, rainfall, snowfall, snowmelt and river discharge under the RCP8.5 emission scenario, relative to the 1981-2010 reference period. Ensemble members (grey lines) and ensemble median (red line). The symbols on the ensemble median indicate whether the 30-year mean is likely to increase or decrease significantly or remain unchanged in the future periods compared to the reference period, according to the Mann-Whitney test (triangle point-up=increase; triangle point down=decrease; open circle=no significant change).

- **Fnjóská catchment (vhm200)**
  - Mean annual and seasonal surface air temperatures are projected to increase along the 21st century. A median warming of about 2.5°C to 3.2°C is projected from 1981-2010 to 2071-2100 under the RCP4.5 scenario and about 4°C to 6°C under the RCP8.5 scenario, depending on the season (see also Table 8).
  - Mean annual precipitation is projected to increase moderately under the RCP4.5 scenario, and this increase reaches a median value of about 10% in 2071-2100. However, this increase is not gradual but fluctuates. A more gradual but moderate mean annual precipitation increase is projected along the 21st century under the RCP8.5 scenario, and reaches a median value of about 10% in 2071-2100. The increase in mean annual precipitation is mainly driven by the projected increase in mean seasonal precipitation in JAS and OND. In these two seasons, the largest median increases projected along the 21st century are estimated at about 15% in JAS and 10% in OND with the RCP4.5 scenario, and about 15% in JAS and 20% in OND with the RCP8.5 scenario. Mean precipitation is not projected to change significantly in JFM and AMJ along most of the projection horizon, under both emission scenarios, either because the ensemble spread is large and without any clear consensus regarding the direction of change, making the outcome uncertain, or because the projections fluctuate closely around their reference level.
  - The rise in temperature has an impact on the fractions of seasonal precipitation falling as rain or snow. As a result, mean seasonal rainfall is projected to increase more or less gradually whereas mean seasonal snowfall is projected to decrease more or less gradually, along the projection horizon. These changes often concern a majority of projection periods in most seasons. The largest median relative increases in mean seasonal rainfall are projected in OND and JFM, in 2071-2100 (about 120% in OND and 170% in JFM with the RCP4.5 scenario, and about 200% in OND and 260% in JFM with the RCP8.5 scenario). As these changes affect all seasons, the annual means are impacted as well: Mean annual rainfall is projected to increase along the projection horizon, whereas mean annual snowfall is projected to decrease after 2011-2040 under the RCP4.5 scenario, and along most of the century under the RCP8.5 scenario.
  - The decrease in mean annual snowfall resulting from rising temperatures leads to a reduction in snow storage (cf. Fig. 16) which, in turn, leads to a decrease in mean annual snowmelt, especially under the RCP8.5 scenario. Projected mean seasonal snowmelt variations are more complex: No significant change is projected in OND under the RCP4.5 scenario because the spread of the ensemble is large and the direction of the change varies with the members, whilst under the RCP8.5 scenario, a significant increase is detected first, in 2021-2050 and 2031-2060, followed then by a significant decrease towards the end of the century. Mean seasonal snowmelt is projected to gradually increase in JFM and gradually decrease in AMJ and JAS under both emission scenarios. The changes are usually more pronounced and/or start earlier with the RCP8.5 emission scenario than with the RCP4.5 emission scenario because the projected warming is greater. As for the Svartá catchment, the projected increase in mean JFM snowmelt is likely attributed to an increase in the number of

intermittent snowmelt events and/or a shift in the onset of the snowmelt season earlier, whereas the decrease in mean AMJ and JAS snowmelt is attributed to the projected snowpack depletion.

- Mean annual flow projections oscillate around or close to their reference level, under both emission scenarios, and a significant increase is projected in some periods, depending on the amplitude of the oscillations. The spread of the ensemble increases with the projection horizon making the outcome increasingly more uncertain. The pattern of mean annual flow change follows the pattern of mean annual precipitation change. Note that increased evapotranspiration (not shown) caused by rising temperatures counteracts the increase in mean annual precipitation and contributes to reduce mean annual flow. At the seasonal level, the projections indicate a gradual increase in mean flow in OND and JFM, caused by the projected increase in rainfall and snowmelt; No significant change in mean flow in AMJ until approximately the mid-century, followed by a significant decrease, caused by the projected decrease in snowmelt; A gradual decrease in JAS, caused by the decrease in snowmelt and increased evapotranspiration (not shown), not balanced by the increase in rainfall. The changes in mean flow in OND, JFM and JAS are significant in a majority of projection periods. The changes in mean seasonal flow are usually more severe and/or start earlier under the RCP8.5 emission scenario than under the RCP4.5 emission scenario because the projected warming is greater and its impact on the change in the phase of precipitation and on snow storage larger. When significant, the largest changes in mean flow are usually projected towards the end of the 21st century, if the changes are gradual, or possibly in some other future period, if they fluctuate. The largest median changes in mean seasonal flow, projected along the 21st century, have the following values:
  - RCP4.5: OND (about +30%), JFM (about +60%), AMJ (about -10%), JAS (about -30%)
  - RCP8.5: OND (about +45%), JFM (about +90%), AMJ (about -25%), JAS (about -35%)

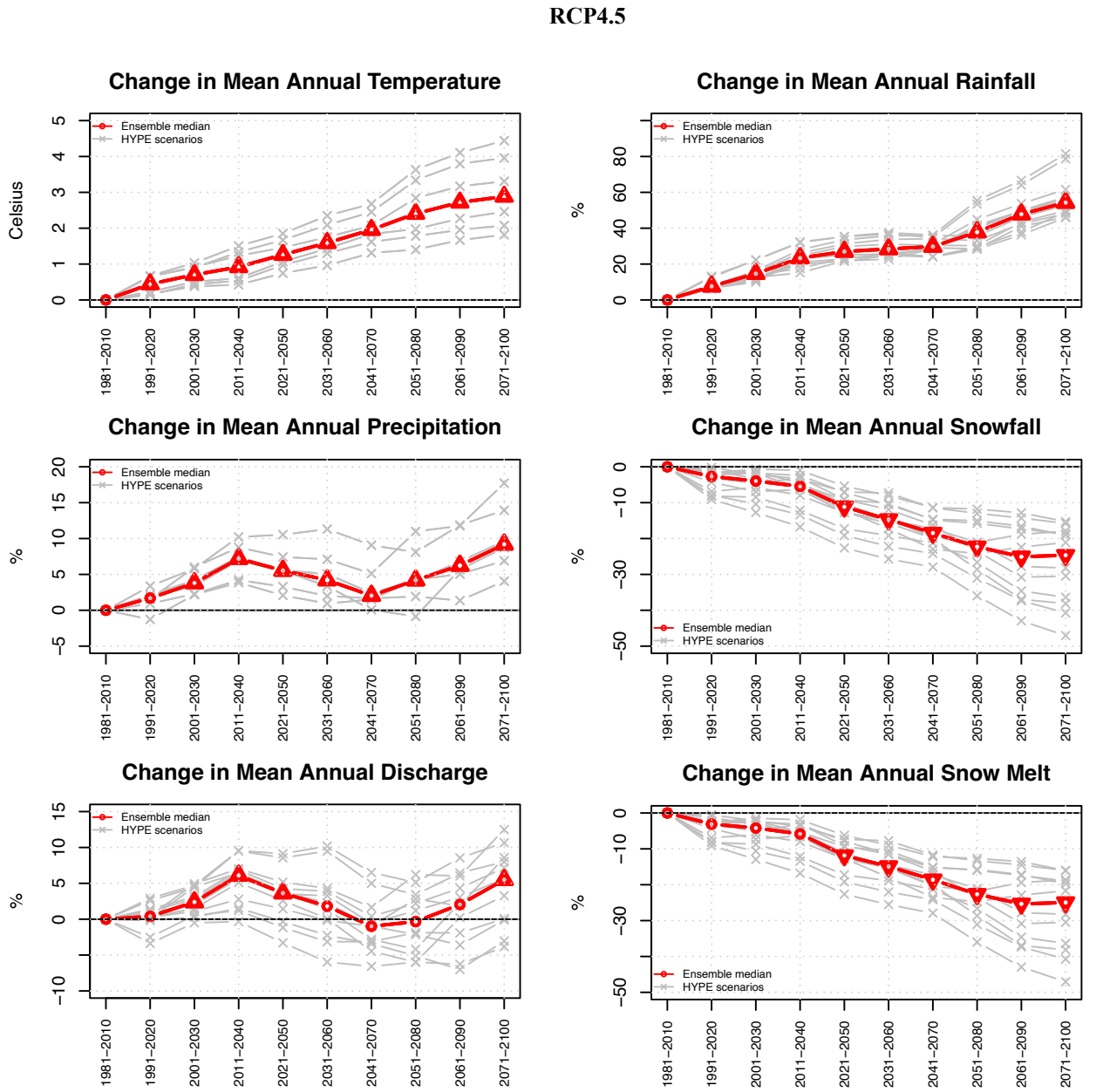

Fig. 34: Fnjóská catchment (vhm200): Projected changes in 30-year mean annual temperature, precipitation, rainfall, snowfall, snowmelt and river discharge under the RCP4.5 emission scenario, relative to the 1981-2010 reference period. Ensemble members (grey lines) and ensemble median (red line). The symbols on the ensemble median indicate whether the 30-year mean is likely to increase or decrease significantly or remain unchanged in the future periods compared to the reference period, according to the Mann-Whitney test (triangle point-up=increase; triangle point down=decrease; open circle=no significant change).

RCP4.5

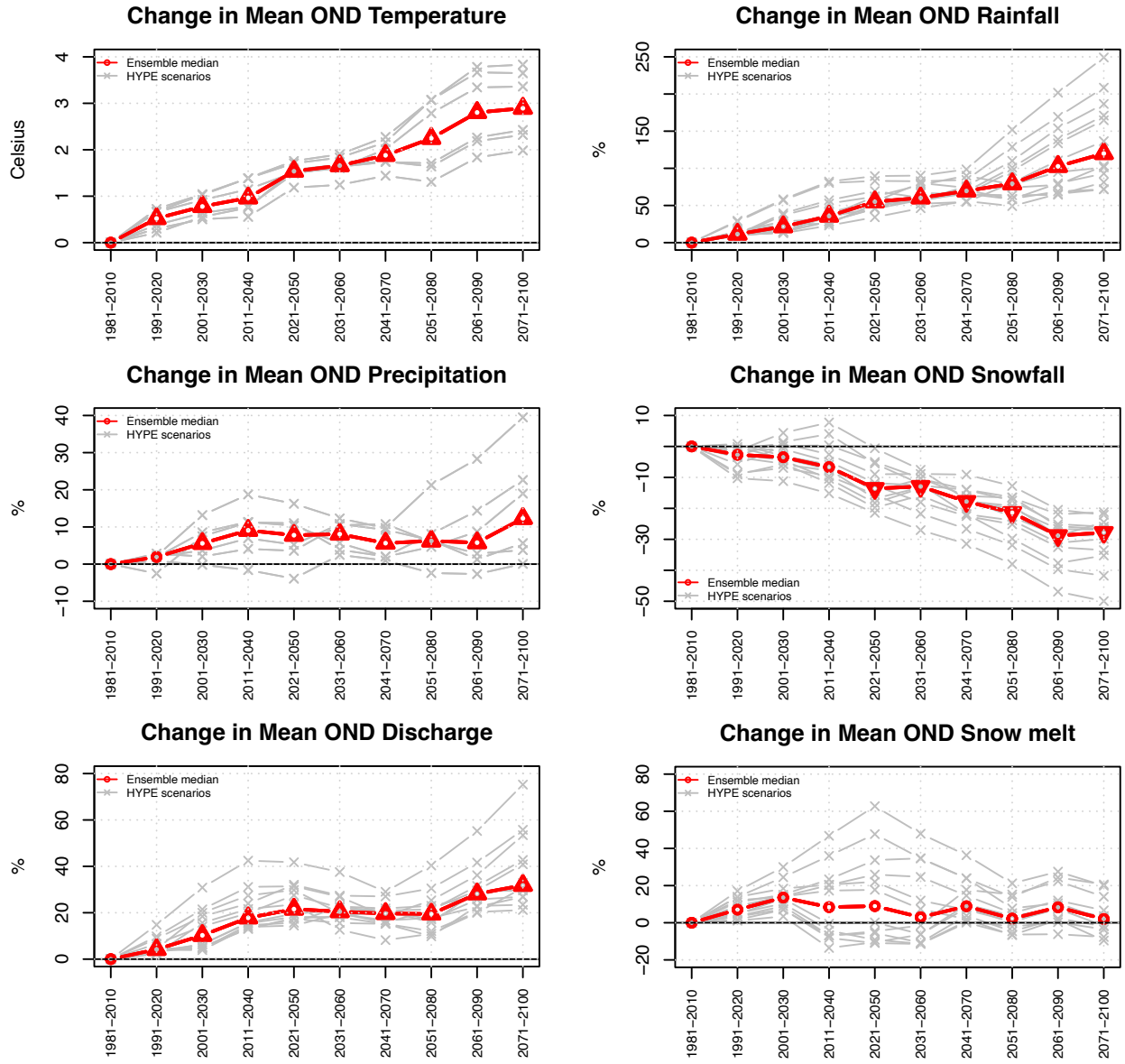

Fig. 35: Fnjóská catchment (vhm200): Projected changes in 30-year mean OND temperature, precipitation, rainfall, snowfall, snowmelt and river discharge under the RCP4.5 emission scenario, relative to the 1981-2010 reference period. Ensemble members (grey lines) and ensemble median (red line). The symbols on the ensemble median indicate whether the 30-year mean is likely to increase or decrease significantly or remain unchanged in the future periods compared to the reference period, according to the Mann-Whitney test (triangle point-up=increase; triangle point down=decrease; open circle=no significant change).

RCP4.5

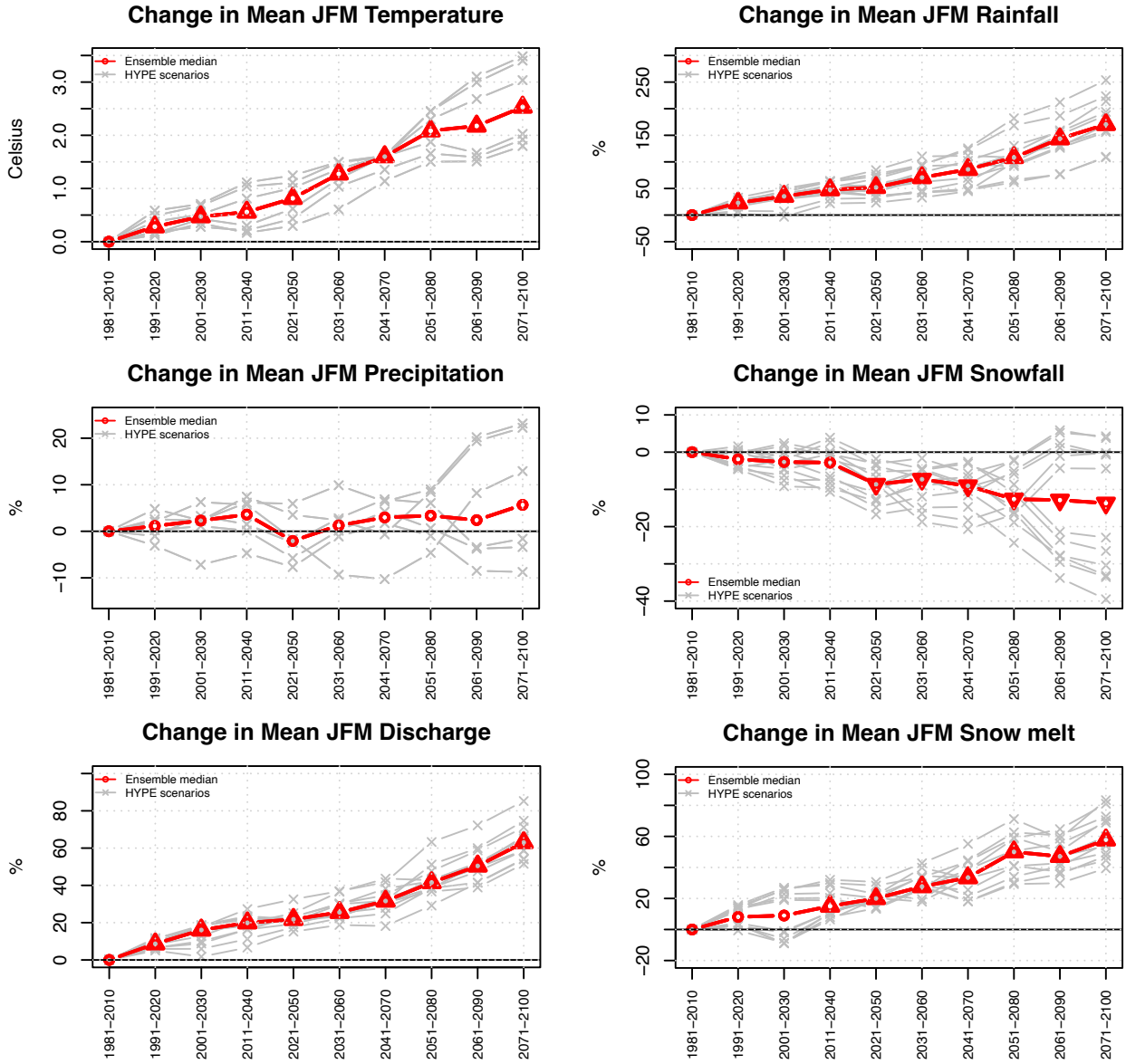

Fig. 36: Fnjóská catchment (vhm200): Projected changes in 30-year mean JFM temperature, precipitation, rainfall, snowfall, snowmelt and river discharge under the RCP4.5 emission scenario, relative to the 1981-2010 reference period. Ensemble members (grey lines) and ensemble median (red line). The symbols on the ensemble median indicate whether the 30-year mean is likely to increase or decrease significantly or remain unchanged in the future periods compared to the reference period, according to the Mann-Whitney test (triangle point-up=increase; triangle point down=decrease; open circle=no significant change).

RCP4.5

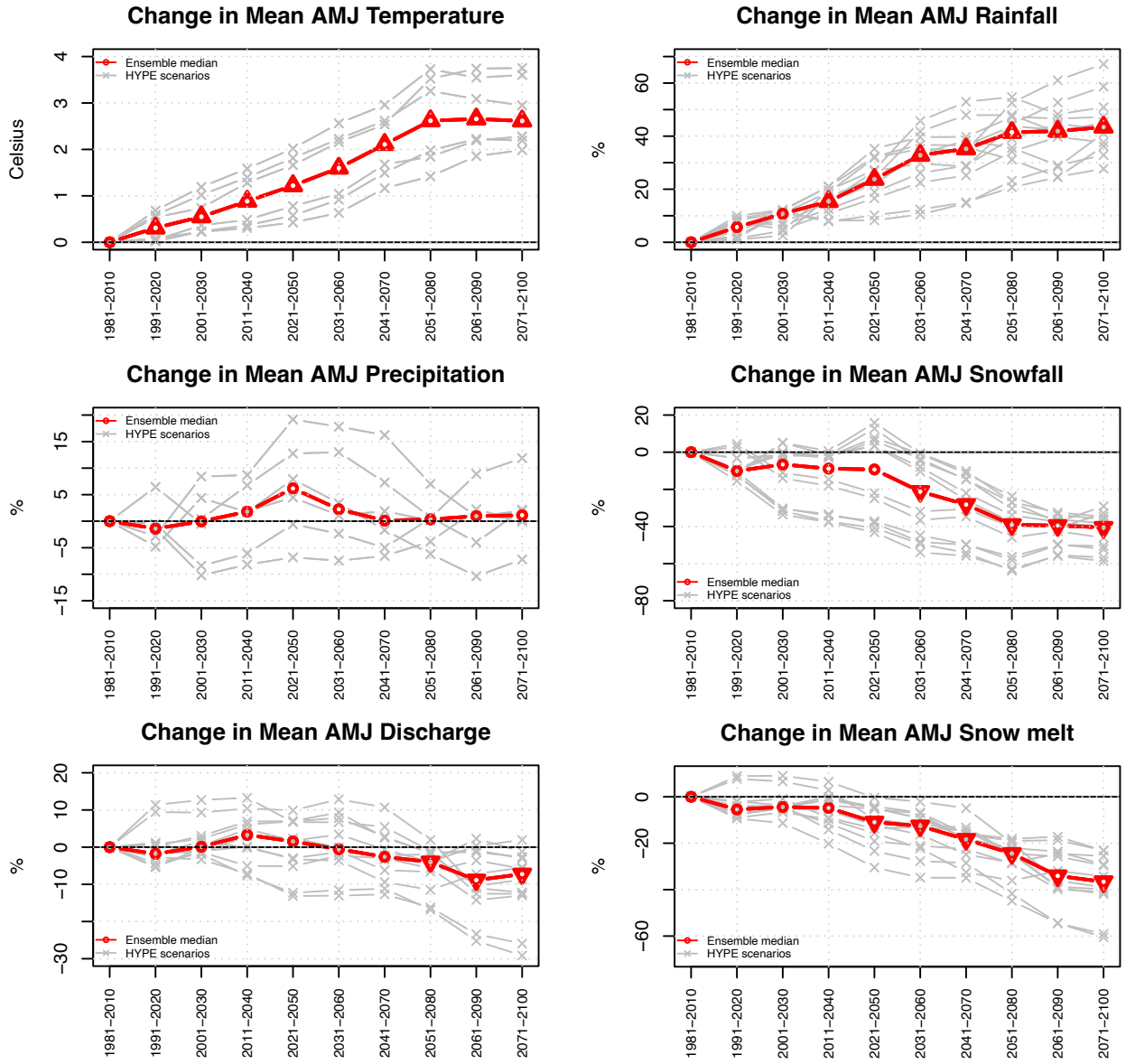

Fig. 37: Fnjóská catchment (vhm200): Projected changes in 30-year mean AMJ temperature, precipitation, rainfall, snowfall, snowmelt and river discharge under the RCP4.5 emission scenario, relative to the 1981-2010 reference period. Ensemble members (grey lines) and ensemble median (red line). The symbols on the ensemble median indicate whether the 30-year mean is likely to increase or decrease significantly or remain unchanged in the future periods compared to the reference period, according to the Mann-Whitney test (triangle point-up=increase; triangle point down=decrease; open circle=no significant change).

RCP4.5

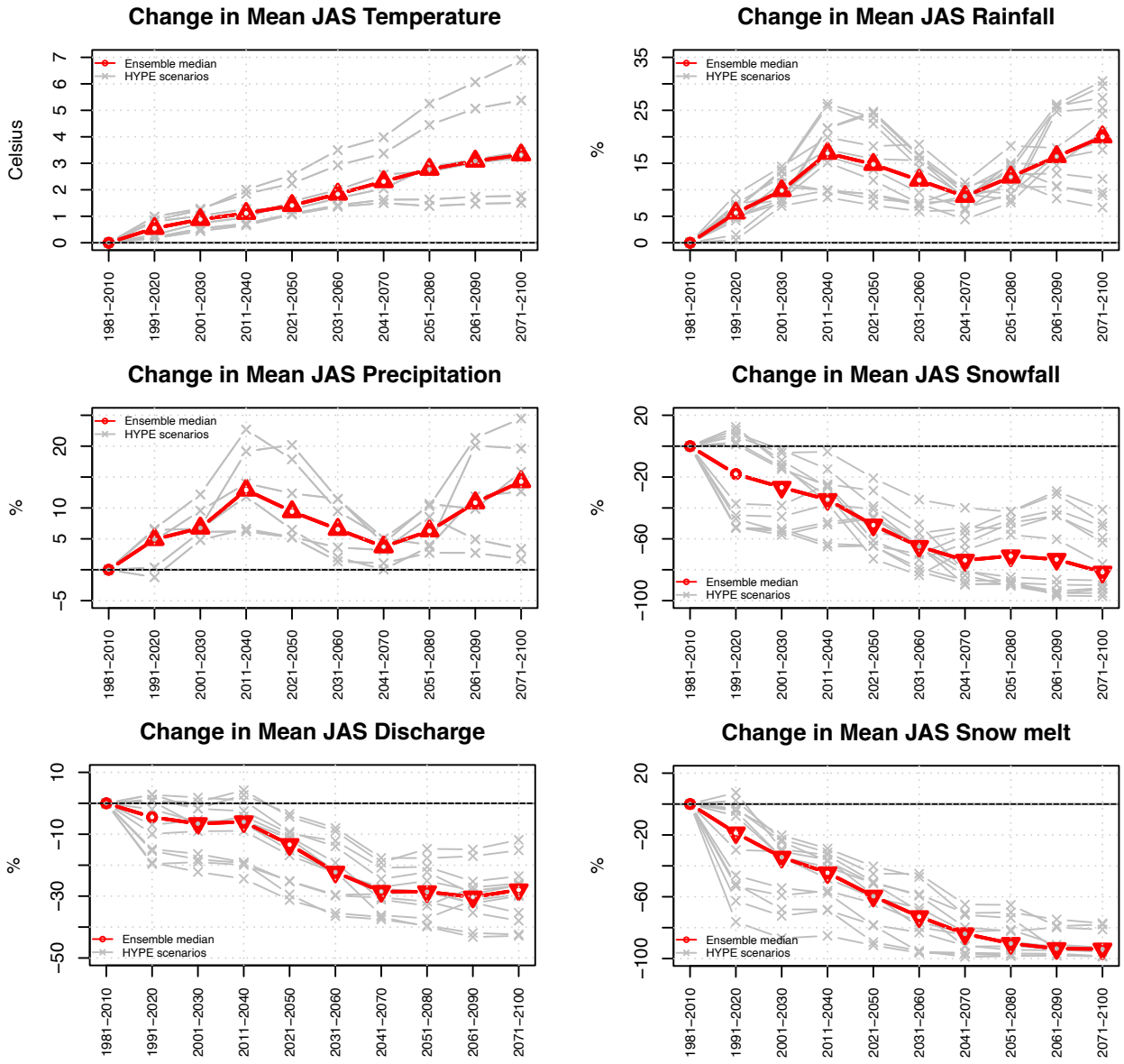

Fig. 38: Fnjóská catchment (vhm200): Projected changes in 30-year mean JAS temperature, precipitation, rainfall, snowfall, snowmelt and river discharge under the RCP4.5 emission scenario, relative to the 1981-2010 reference period. Ensemble members (grey lines) and ensemble median (red line). The symbols on the ensemble median indicate whether the 30-year mean is likely to increase or decrease significantly or remain unchanged in the future periods compared to the reference period, according to the Mann-Whitney test (triangle point-up=increase; triangle point down=decrease; open circle=no significant change).

RCP8.5

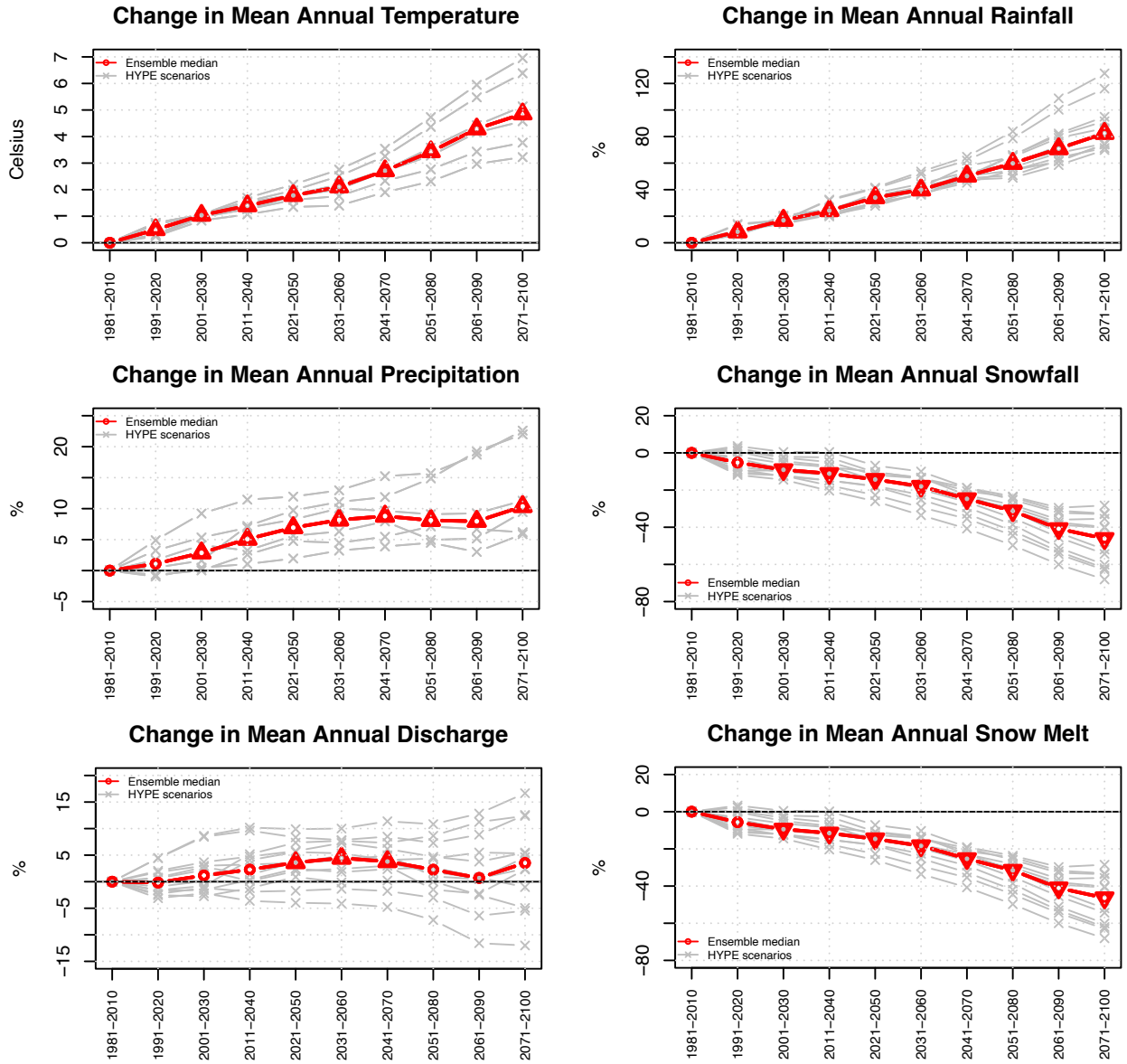

Fig. 39: Fnjóská catchment (vhm200): Projected changes in 30-year mean annual temperature, precipitation, rainfall, snowfall, snowmelt and river discharge under the RCP8.5 emission scenario, relative to the 1981-2010 reference period. Ensemble members (grey lines) and ensemble median (red line). The symbols on the ensemble median indicate whether the 30-year mean is likely to increase or decrease significantly or remain unchanged in the future periods compared to the reference period, according to the Mann-Whitney test (triangle point-up=increase; triangle point down=decrease; open circle=no significant change).

RCP8.5

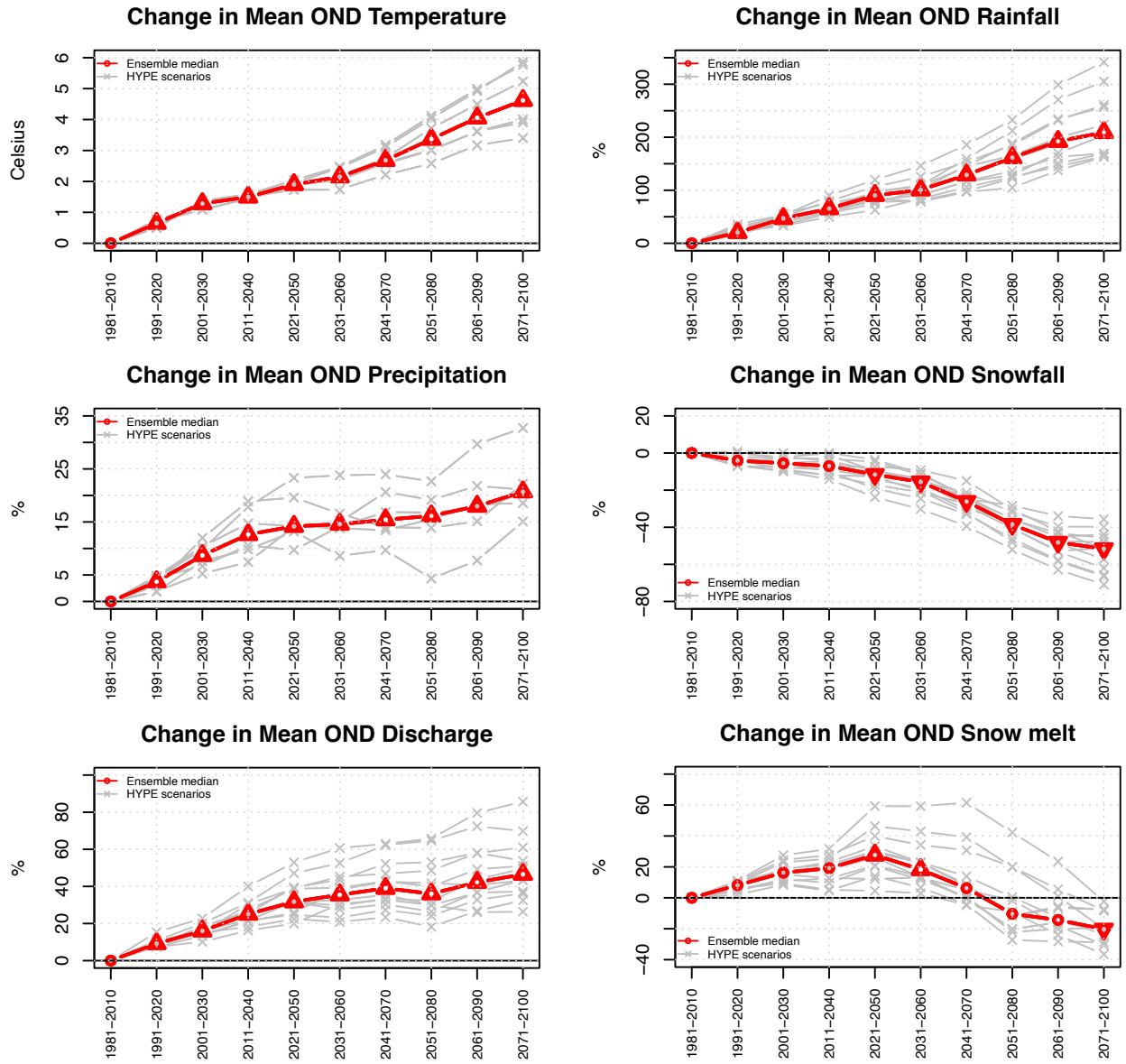

Fig. 40: Fnjóská catchment (vhm200): Projected changes in 30-year mean OND temperature, precipitation, rainfall, snowfall, snowmelt and river discharge under the RCP8.5 emission scenario, relative to the 1981-2010 reference period. Ensemble members (grey lines) and ensemble median (red line). The symbols on the ensemble median indicate whether the 30-year mean is likely to increase or decrease significantly or remain unchanged in the future periods compared to the reference period, according to the Mann-Whitney test (triangle point-up=increase; triangle point down=decrease; open circle=no significant change).

RCP8.5

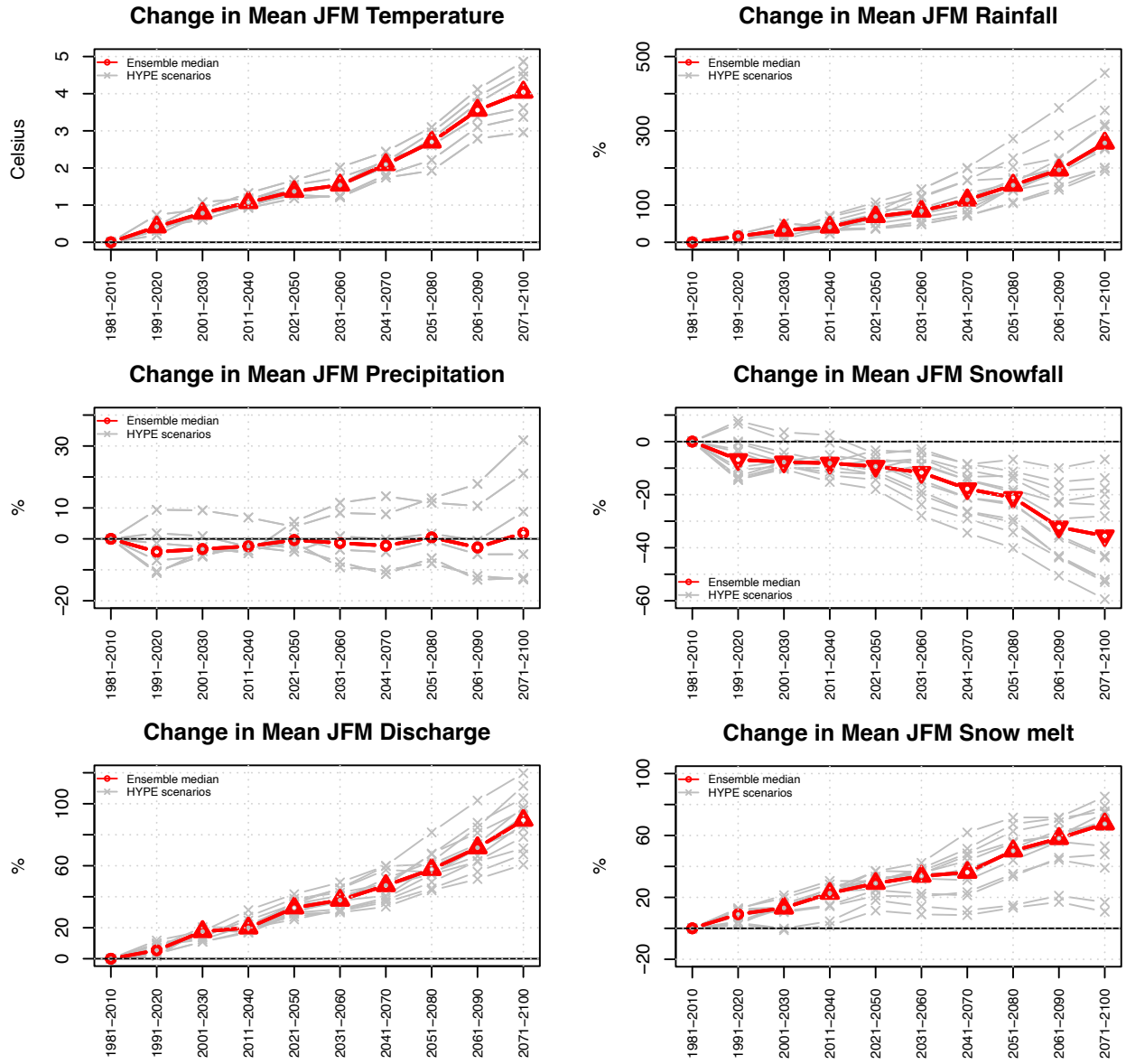

Fig. 41: Fnjóská catchment (vhm200): Projected changes in 30-year mean JFM temperature, precipitation, rainfall, snowfall, snowmelt and river discharge under the RCP8.5 emission scenario, relative to the 1981-2010 reference period. Ensemble members (grey lines) and ensemble median (red line). The symbols on the ensemble median indicate whether the 30-year mean is likely to increase or decrease significantly or remain unchanged in the future periods compared to the reference period, according to the Mann-Whitney test (triangle point-up=increase; triangle point down=decrease; open circle=no significant change).

RCP8.5

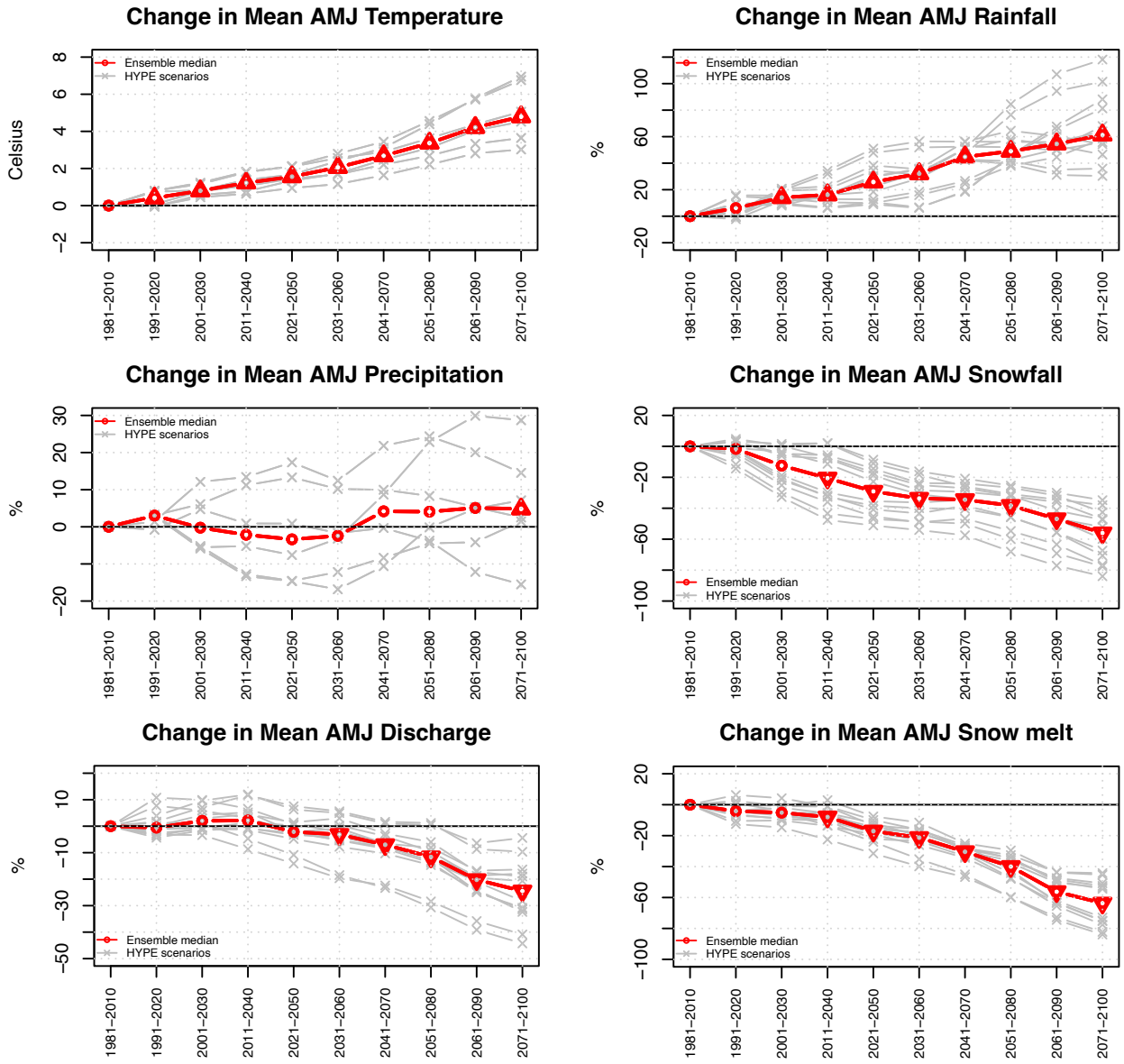

Fig. 42: Fnjóská catchment (vhm200): Projected changes in 30-year mean AMJ temperature, precipitation, rainfall, snowfall, snowmelt and river discharge under the RCP8.5 emission scenario, relative to the 1981-2010 reference period. Ensemble members (grey lines) and ensemble median (red line). The symbols on the ensemble median indicate whether the 30-year mean is likely to increase or decrease significantly or remain unchanged in the future periods compared to the reference period, according to the Mann-Whitney test (triangle point-up=increase; triangle point down=decrease; open circle=no significant change).

RCP8.5

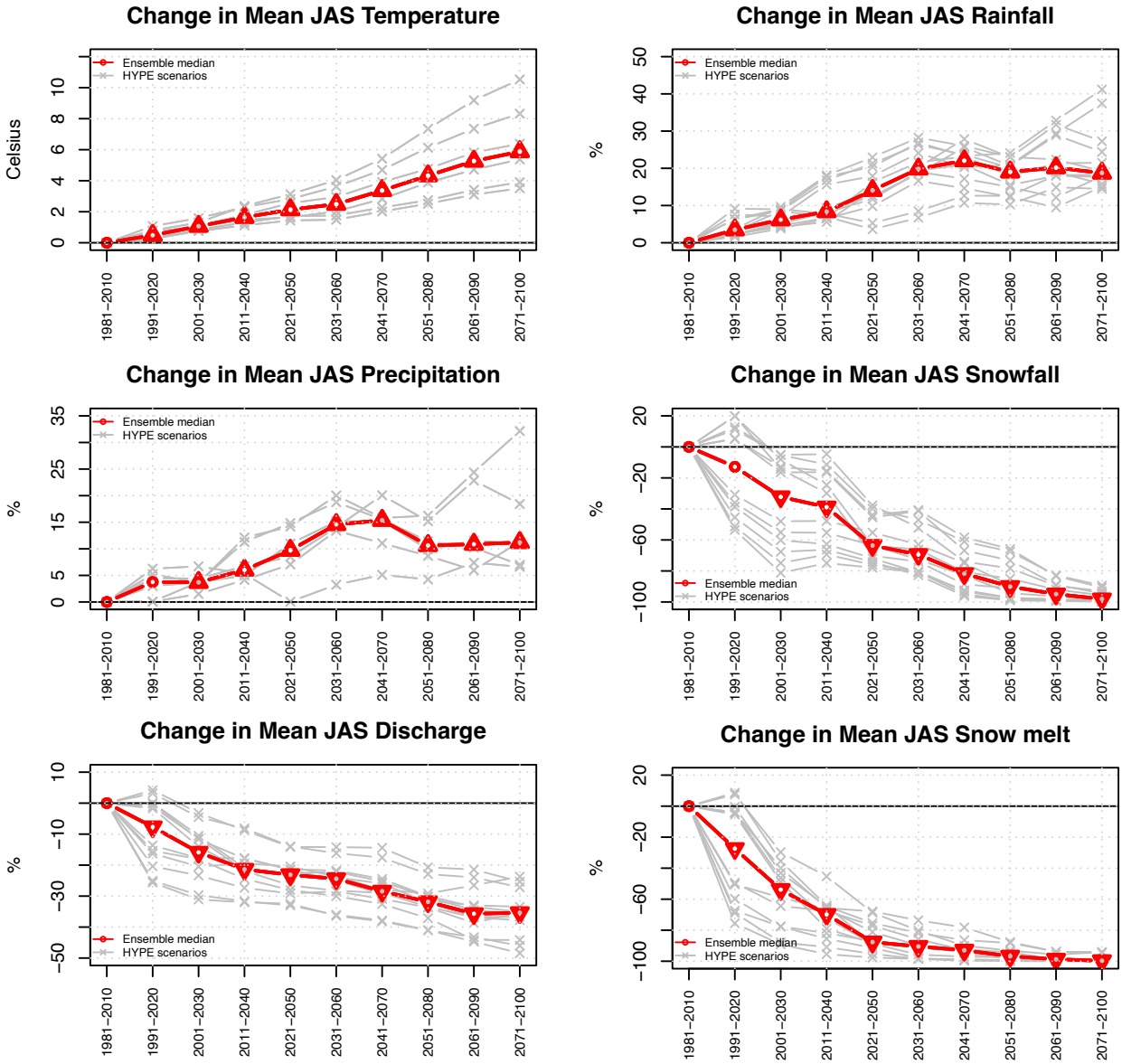

Fig. 43: Fnjóská catchment (vhm200): Projected changes in 30-year mean JAS temperature, precipitation, rainfall, snowfall, snowmelt and river discharge under the RCP8.5 emission scenario, relative to the 1981-2010 reference period. Ensemble members (grey lines) and ensemble median (red line). The symbols on the ensemble median indicate whether the 30-year mean is likely to increase or decrease significantly or remain unchanged in the future periods compared to the reference period, according to the Mann-Whitney test (triangle point-up=increase; triangle point down=decrease; open circle=no significant change).

- **Laxá catchment (vhm74)**
  - Mean annual and seasonal surface air temperatures are projected to rise along the 21st century. A median warming of about 2°C to 2.3°C is projected from 1981-2010 to 2071-2100 under the RCP4.5 scenario and about 3.2°C to 4.3°C under the RCP8.5 scenario, depending on the season (see also Table 8).
  - Mean annual precipitation projections fluctuate around or close to their reference level under both emission scenarios without any significant change towards a particular direction for the ensemble, and a large ensemble spread increasing with the projection horizon is observed, especially under the RCP8.5 emission scenario. Mean seasonal precipitation projections oscillate around their reference level and significant changes (increase or decrease) are sometimes detected in some periods and all seasons, depending on the phase and amplitude of these oscillations.
  - The rise in temperature has an impact on the fractions of seasonal precipitation falling as rain or snow. As a result, mean seasonal rainfall is projected to increase significantly in OND, JFM and AMJ, in a majority of projection periods, under both emission scenarios, whereas it is projected to oscillate around the 1981-2010 reference level in JAS, with or without any significant change (increase or decrease), depending on the phase and amplitude of these oscillations. Oscillations are also observed in OND, JFM and AMJ but the increasing trend dominates in a majority of periods (the largest median increases projected along the 21st century are estimated at about 20% in OND, 30% in JFM and 15% in AMJ with the RCP4.5 scenario, and about 45% in OND, almost 20% in JFM and almost 10% in AMJ with the RCP8.5 scenario). Mean seasonal snowfall is projected to decrease more or less gradually in all seasons and most projection periods under both emission scenarios.
  - The projected decrease in mean annual snowfall leads to a snow storage reduction (cf. Fig. 20) which, in turn, leads to a decrease in mean annual snowmelt. At the seasonal level, mean snowmelt is projected to gradually decrease in AMJ, JAS and OND in most projection periods. No significant change in mean snowmelt is projected in JFM under the RCP4.5 scenario whereas a slight increase is projected at the beginning of the 21st century under the RCP8.5 scenario, followed by a decrease towards the end of the century. The changes are usually more pronounced under the RCP8.5 scenario than under the RCP4.5 scenario because the projected warming is greater. The projected decrease in mean snowmelt in AMJ, JAS and OND is likely caused by the projected snow storage depletion.
  - Mean annual flow projections fluctuate around or close to their reference level under both emission scenarios, as mean annual precipitation, and a significant decrease is detected in some periods under the RCP4.5 scenario, but the spread of the ensemble becomes increasingly larger with the projection horizon, making the outcome increasingly more uncertain, especially under the RCP8.5 emission scenario. At the seasonal level, the projections indicate a significant increase in mean flow in OND and JFM, caused by the projected rainfall increase; A gradual decrease in mean flow in AMJ, caused by the projected snowmelt decrease; No change in mean flow in JAS in the first half of the projection horizon, followed by a significant decrease until the end of the century, caused by projected

rainfall variations combined with increased evapotranspiration (not shown). Note that the projected changes are not gradual in OND, JFM and JAS, but oscillate like mean seasonal rainfall. When significant, the largest changes in mean flow are usually projected towards the end of the 21st century, if the changes are gradual, or possibly in some other future period, if they fluctuate. The largest median changes in mean seasonal flow, projected along the 21st century, have the following values:

- RCP4.5: OND (about +15%), JFM (about +20%), AMJ (about -30%), JAS (about -17%)
- RCP8.5: OND (about +30%), JFM (about +12%), AMJ (about -40%), JAS (about -15%)

RCP4.5

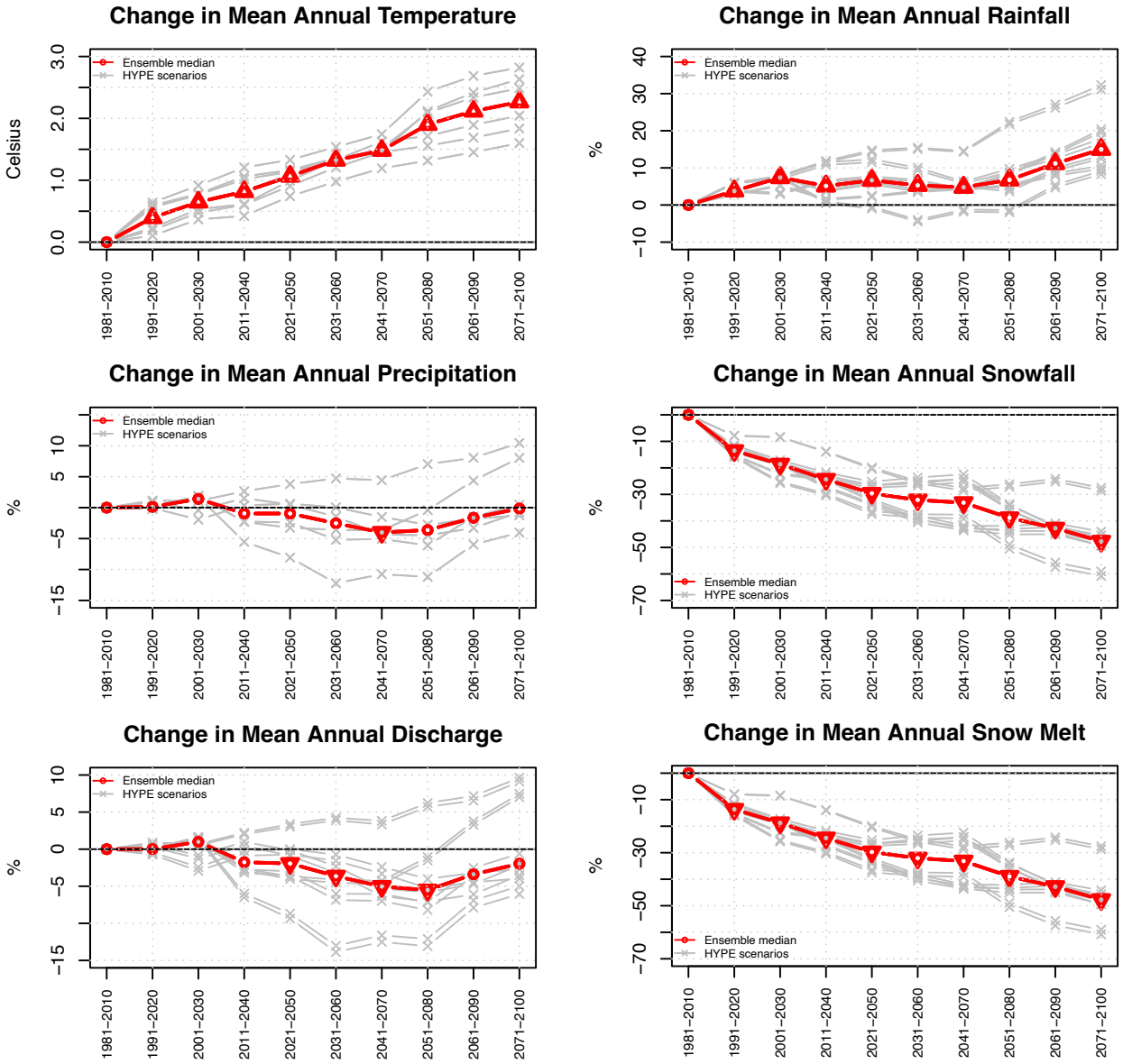

Fig. 44: Laxá catchment (vhm74): Projected changes in 30-year mean annual temperature, precipitation, rainfall, snowfall, snowmelt and river discharge under the RCP4.5 emission scenario, relative to the 1981-2010 reference period. Ensemble members (grey lines) and ensemble median (red line). The symbols on the ensemble median indicate whether the 30-year mean is likely to increase or decrease significantly or remain unchanged in the future periods compared to the reference period, according to the Mann-Whitney test (triangle point-up=increase; triangle point down=decrease; open circle=no significant change).

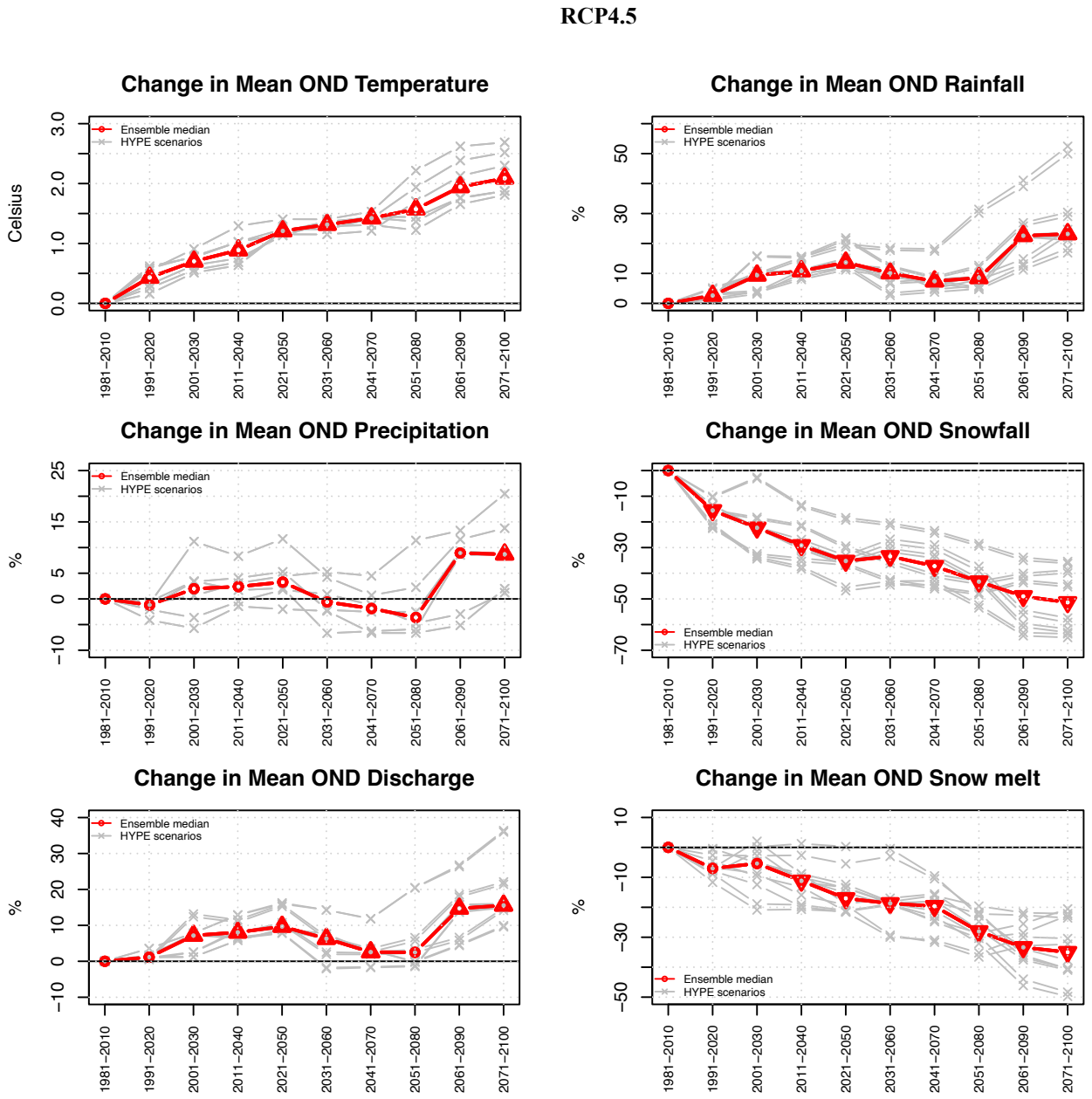

Fig. 45: Laxá catchment (vhm74): Projected changes in 30-year mean OND temperature, precipitation, rainfall, snowfall, snowmelt and river discharge under the RCP4.5 emission scenario, relative to the 1981-2010 reference period. Ensemble members (grey lines) and ensemble median (red line). The symbols on the ensemble median indicate whether the 30-year mean is likely to increase or decrease significantly or remain unchanged in the future periods compared to the reference period, according to the Mann-Whitney test (triangle point-up=increase; triangle point down=decrease; open circle=no significant change).

RCP4.5

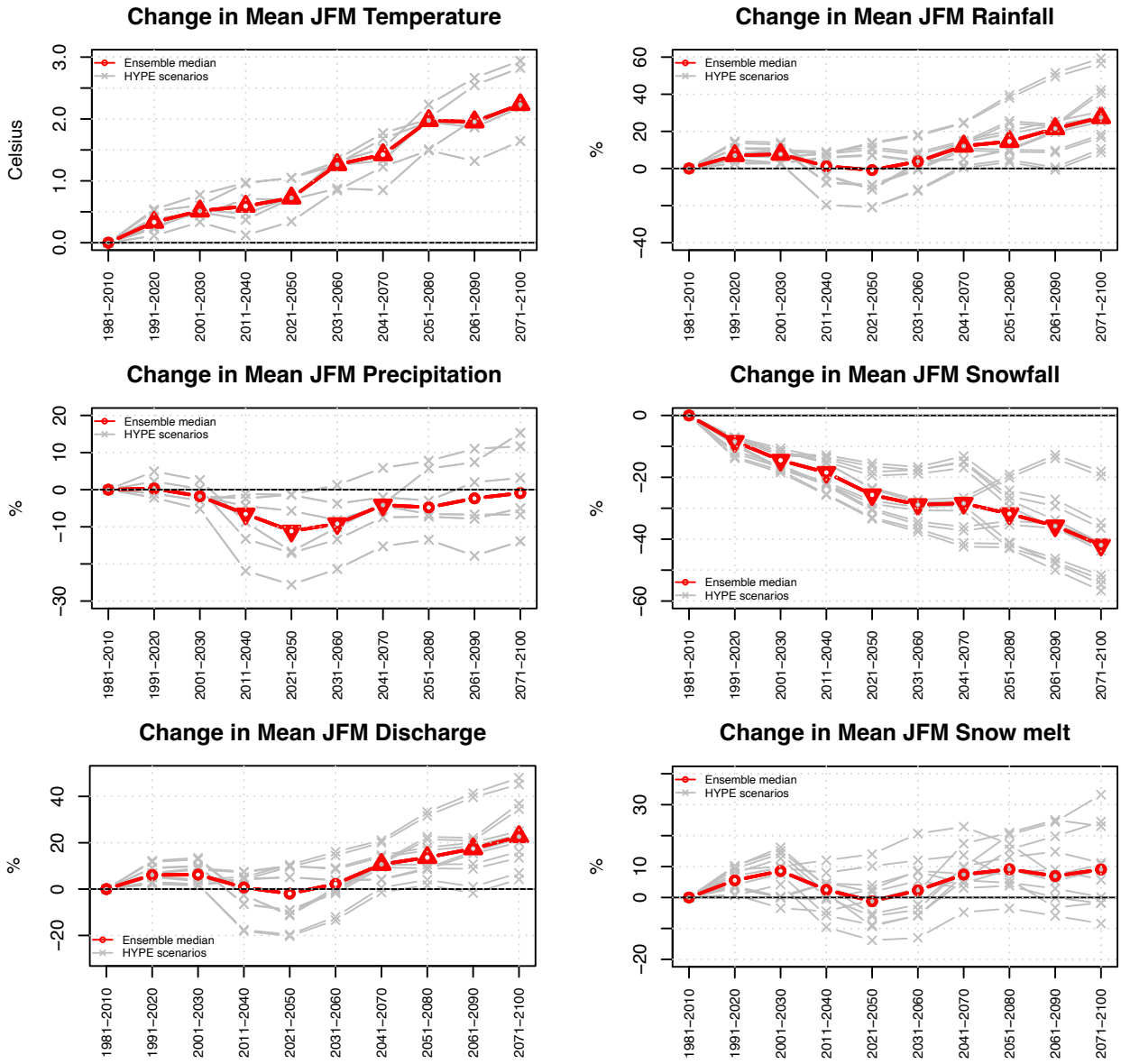

Fig. 46: Laxá catchment (vhm74): Projected changes in 30-year mean JFM temperature, precipitation, rainfall, snowfall, snowmelt and river discharge under the RCP4.5 emission scenario, relative to the 1981-2010 reference period. Ensemble members (grey lines) and ensemble median (red line). The symbols on the ensemble median indicate whether the 30-year mean is likely to increase or decrease significantly or remain unchanged in the future periods compared to the reference period, according to the Mann-Whitney test (triangle point-up=increase; triangle point down=decrease; open circle=no significant change).

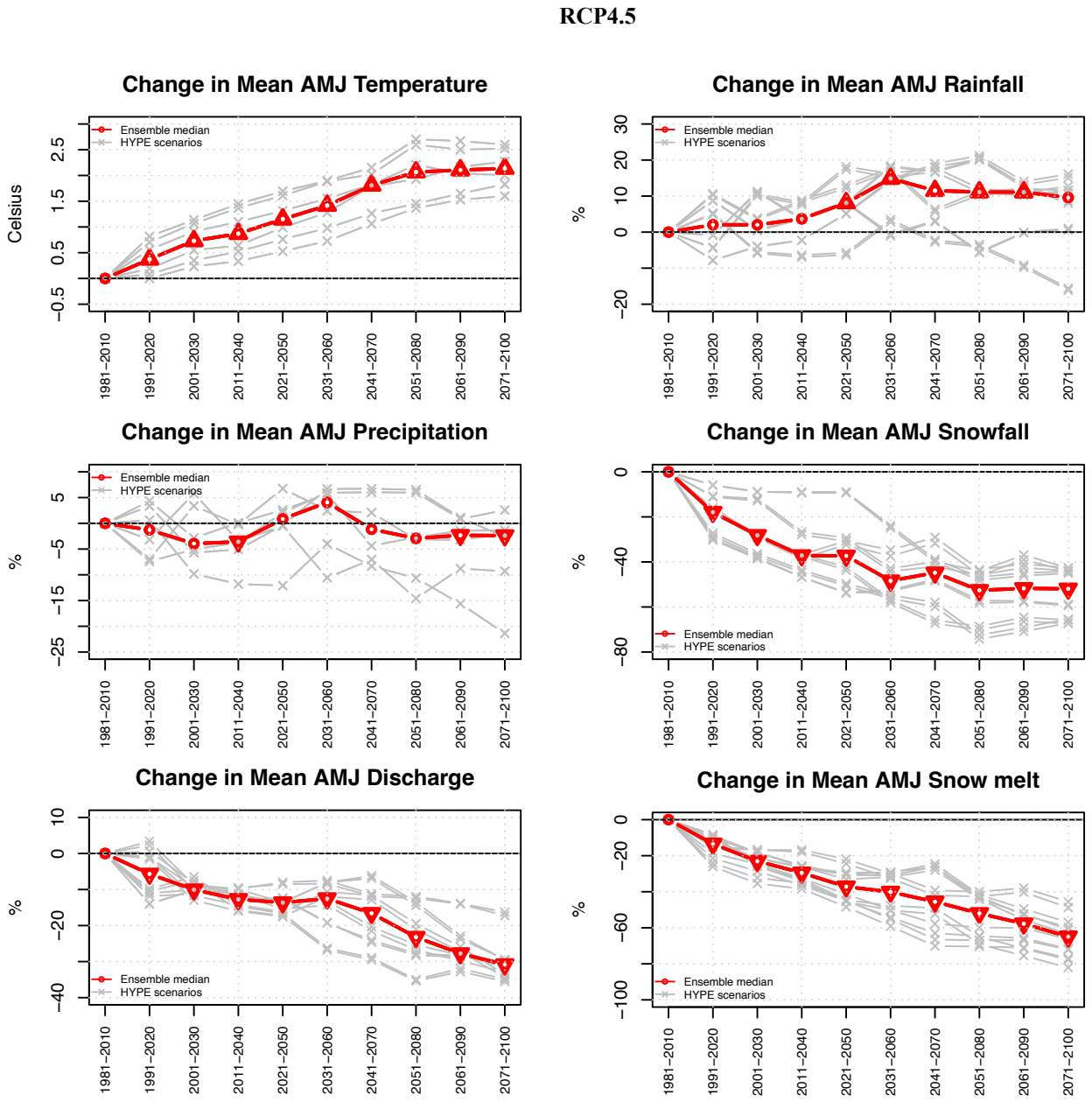

Fig. 47: Laxá catchment (vhm74): Projected changes in 30-year mean AMJ temperature, precipitation, rainfall, snowfall, snowmelt and river discharge under the RCP4.5 emission scenario, relative to the 1981-2010 reference period. Ensemble members (grey lines) and ensemble median (red line). The symbols on the ensemble median indicate whether the 30-year mean is likely to increase or decrease significantly or remain unchanged in the future periods compared to the reference period, according to the Mann-Whitney test (triangle point-up=increase; triangle point down=decrease; open circle=no significant change).

RCP4.5

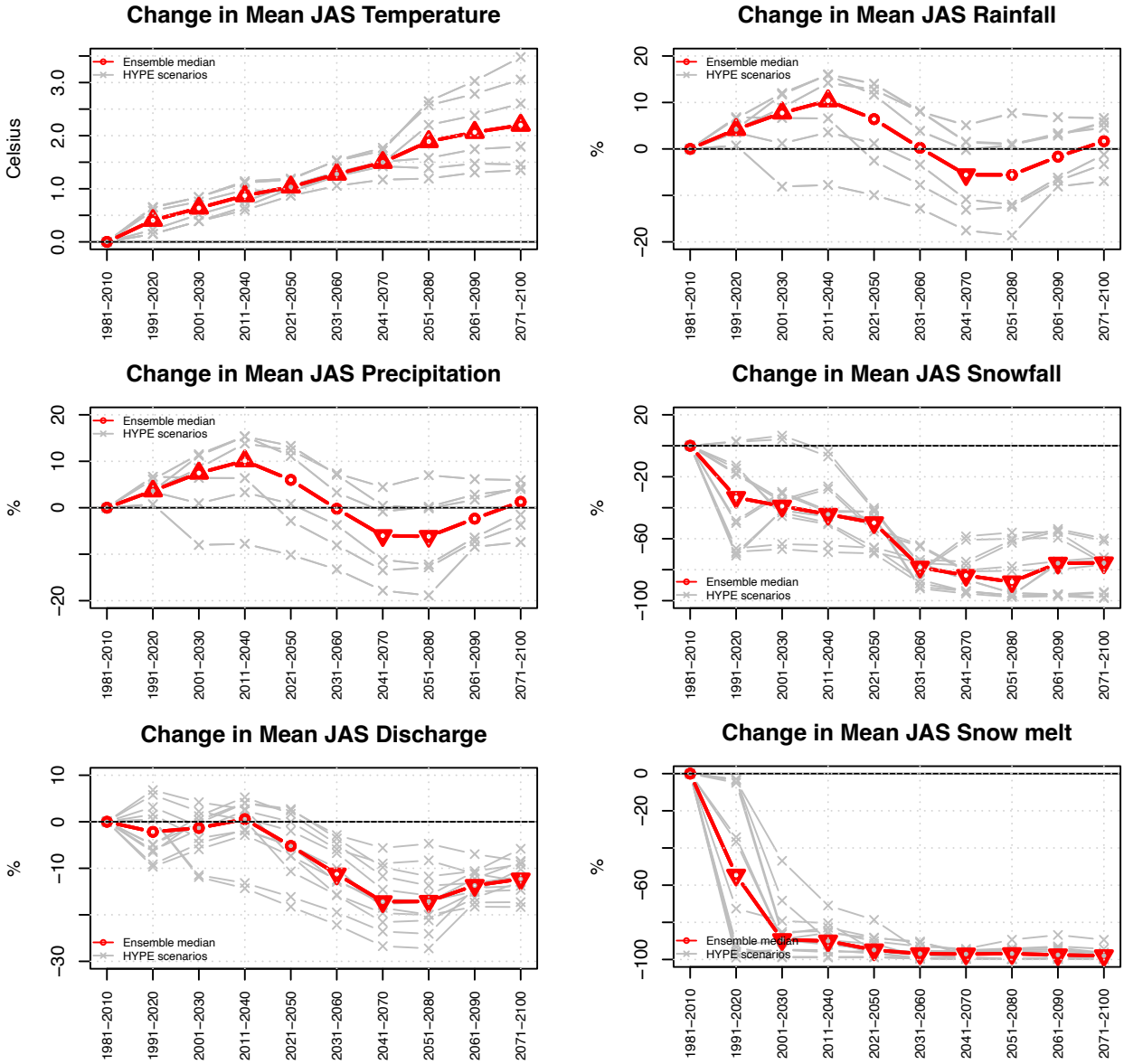

Fig. 48: Laxá catchment (vhm74): Projected changes in 30-year mean JAS temperature, precipitation, rainfall, snowfall, snowmelt and river discharge under the RCP4.5 emission scenario, relative to the 1981-2010 reference period. Ensemble members (grey lines) and ensemble median (red line). The symbols on the ensemble median indicate whether the 30-year mean is likely to increase or decrease significantly or remain unchanged in the future periods compared to the reference period, according to the Mann-Whitney test (triangle point-up=increase; triangle point down=decrease; open circle=no significant change).

RCP8.5

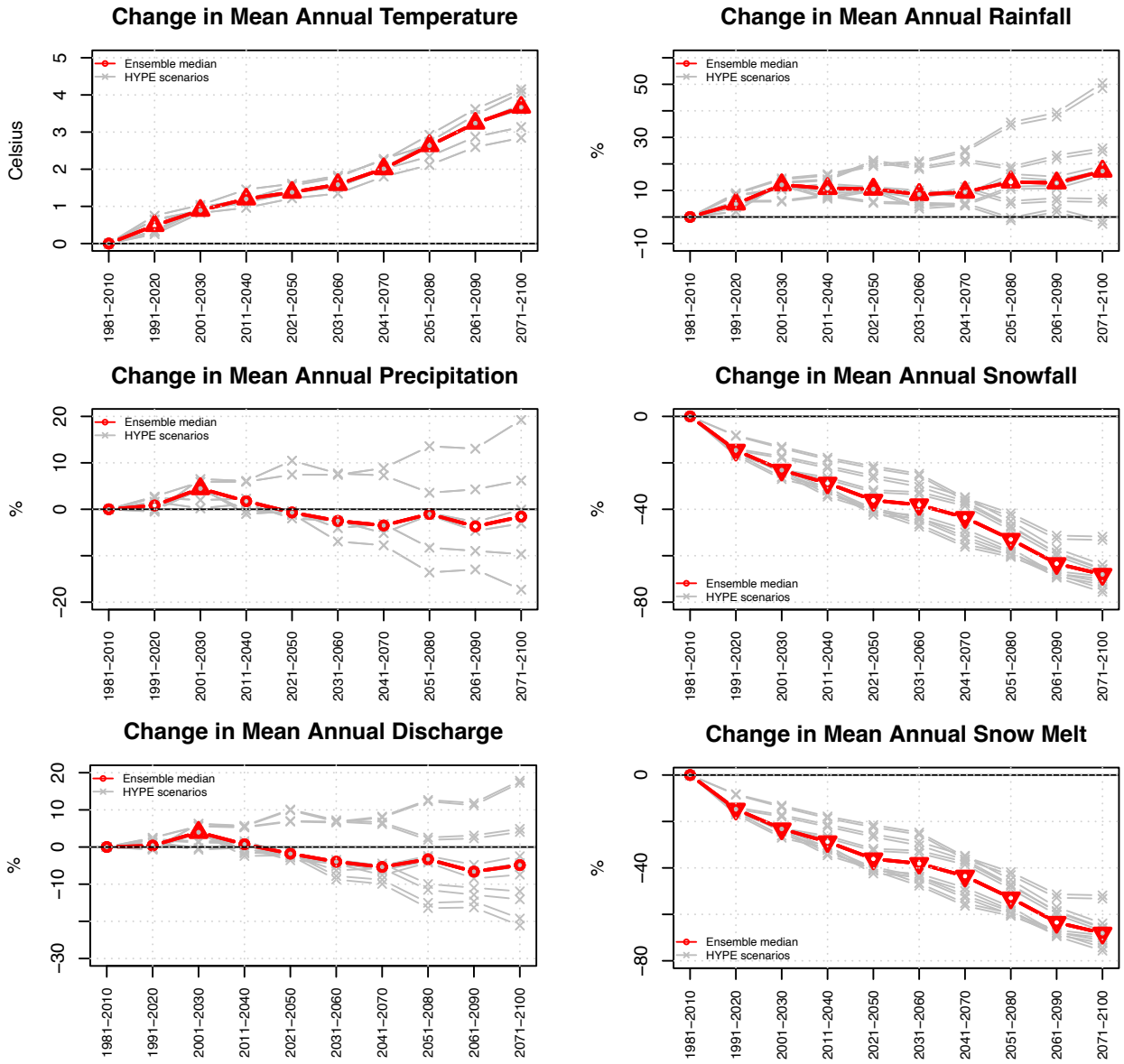

Fig. 49: Laxá catchment (vhm74): Projected changes in 30-year mean annual temperature, precipitation, rainfall, snowfall, snowmelt and river discharge under the RCP8.5 emission scenario, relative to the 1981-2010 reference period. Ensemble members (grey lines) and ensemble median (red line). The symbols on the ensemble median indicate whether the 30-year mean is likely to increase or decrease significantly or remain unchanged in the future periods compared to the reference period, according to the Mann-Whitney test (triangle point-up=increase; triangle point down=decrease; open circle=no significant change).

RCP8.5

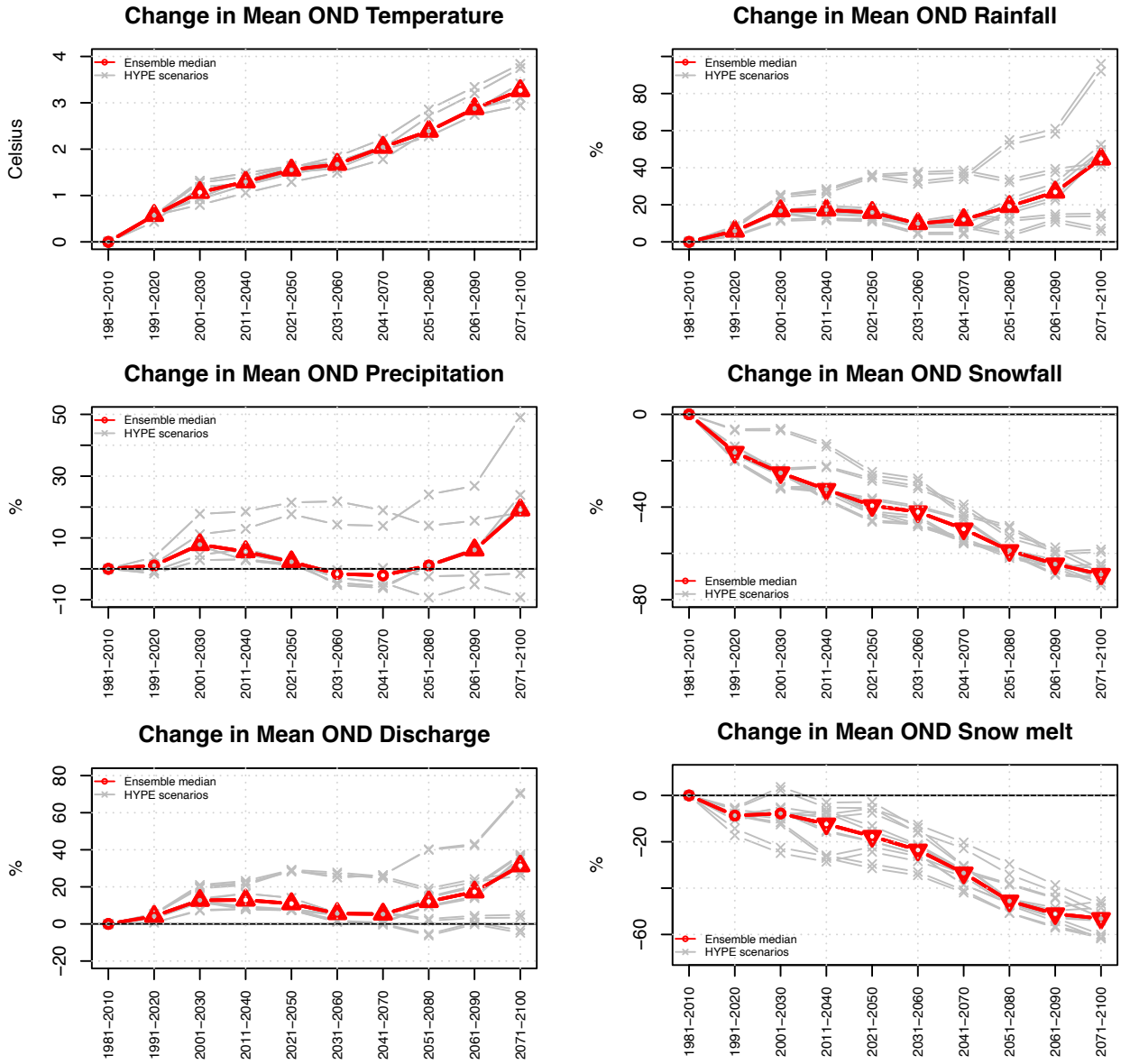

Fig. 50: Laxá catchment (vhm74): Projected changes in 30-year mean OND temperature, precipitation, rainfall, snowfall, snowmelt and river discharge under the RCP8.5 emission scenario, relative to the 1981-2010 reference period. Ensemble members (grey lines) and ensemble median (red line). The symbols on the ensemble median indicate whether the 30-year mean is likely to increase or decrease significantly or remain unchanged in the future periods compared to the reference period, according to the Mann-Whitney test (triangle point-up=increase; triangle point down=decrease; open circle=no significant change).

RCP8.5

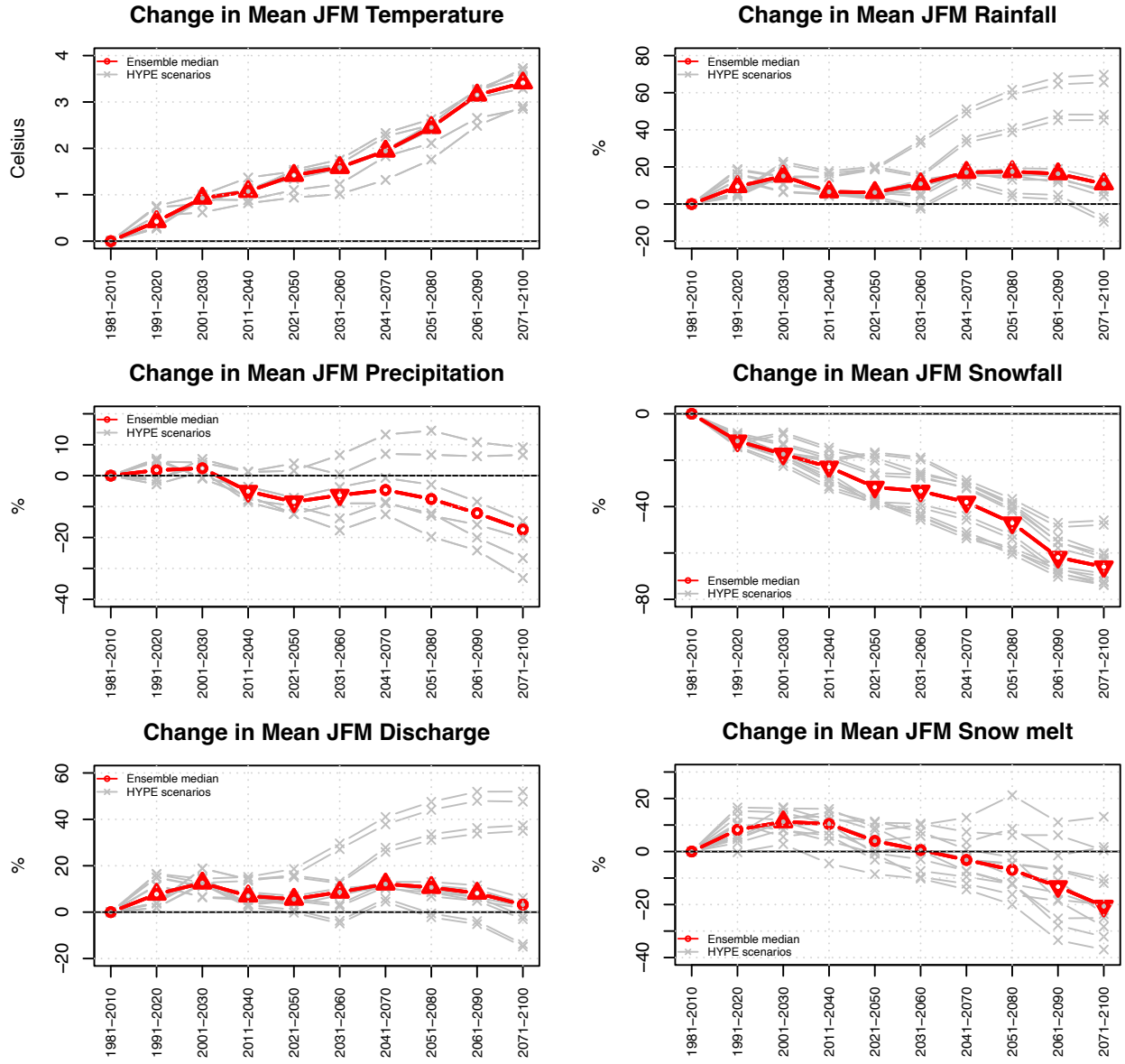

Fig. 51: Laxá catchment (vhm74): Projected changes in 30-year mean JFM temperature, precipitation, rainfall, snowfall, snowmelt and river discharge under the RCP8.5 emission scenario, relative to the 1981-2010 reference period. Ensemble members (grey lines) and ensemble median (red line). The symbols on the ensemble median indicate whether the 30-year mean is likely to increase or decrease significantly or remain unchanged in the future periods compared to the reference period, according to the Mann-Whitney test (triangle point-up=increase; triangle point down=decrease; open circle=no significant change).

RCP8.5

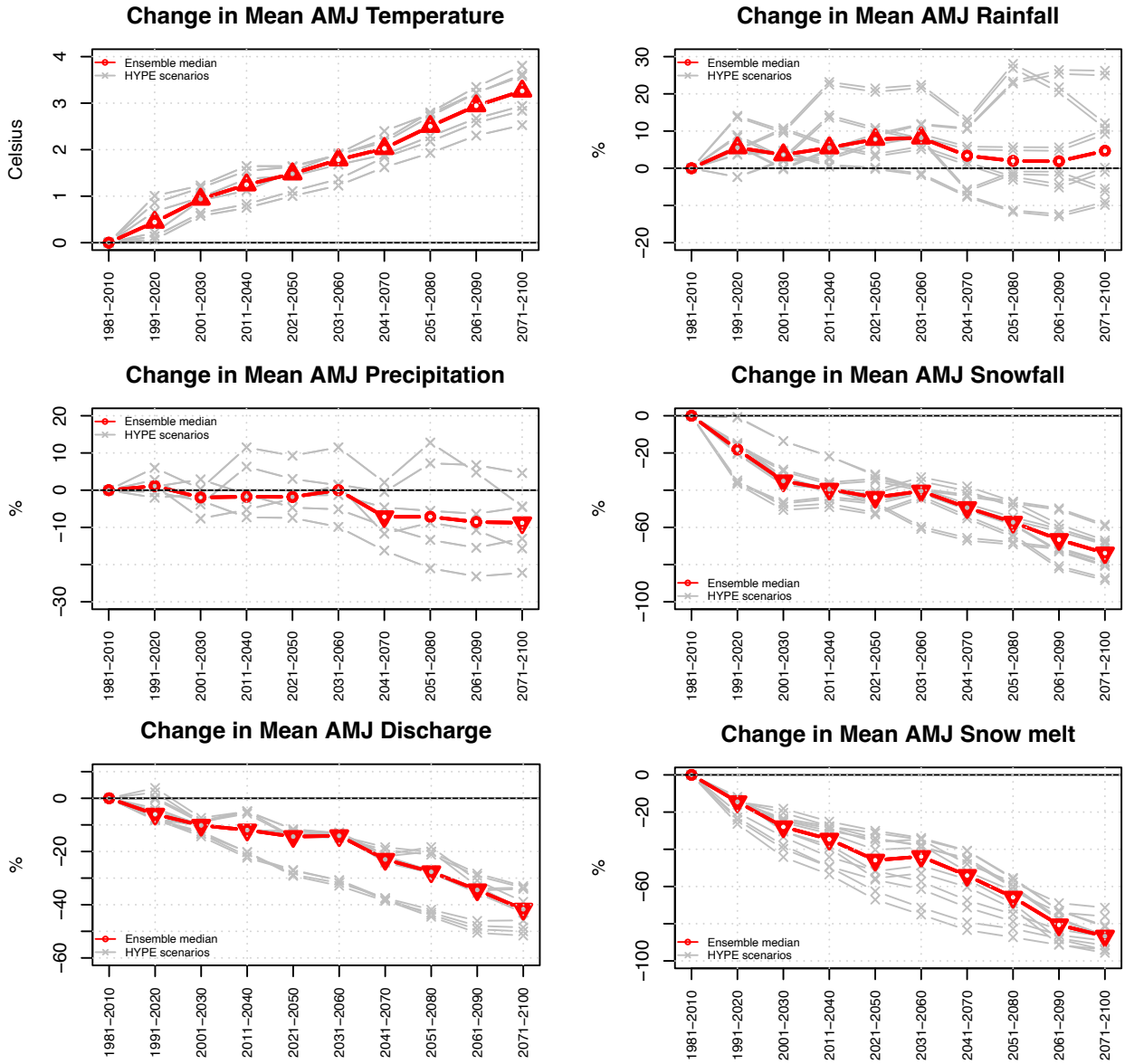

Fig. 52: Laxá catchment (vhm74): Projected changes in 30-year mean AMJ temperature, precipitation, rainfall, snowfall, snowmelt and river discharge under the RCP8.5 emission scenario, relative to the 1981-2010 reference period. Ensemble members (grey lines) and ensemble median (red line). The symbols on the ensemble median indicate whether the 30-year mean is likely to increase or decrease significantly or remain unchanged in the future periods compared to the reference period, according to the Mann-Whitney test (triangle point-up=increase; triangle point down=decrease; open circle=no significant change).

RCP8.5

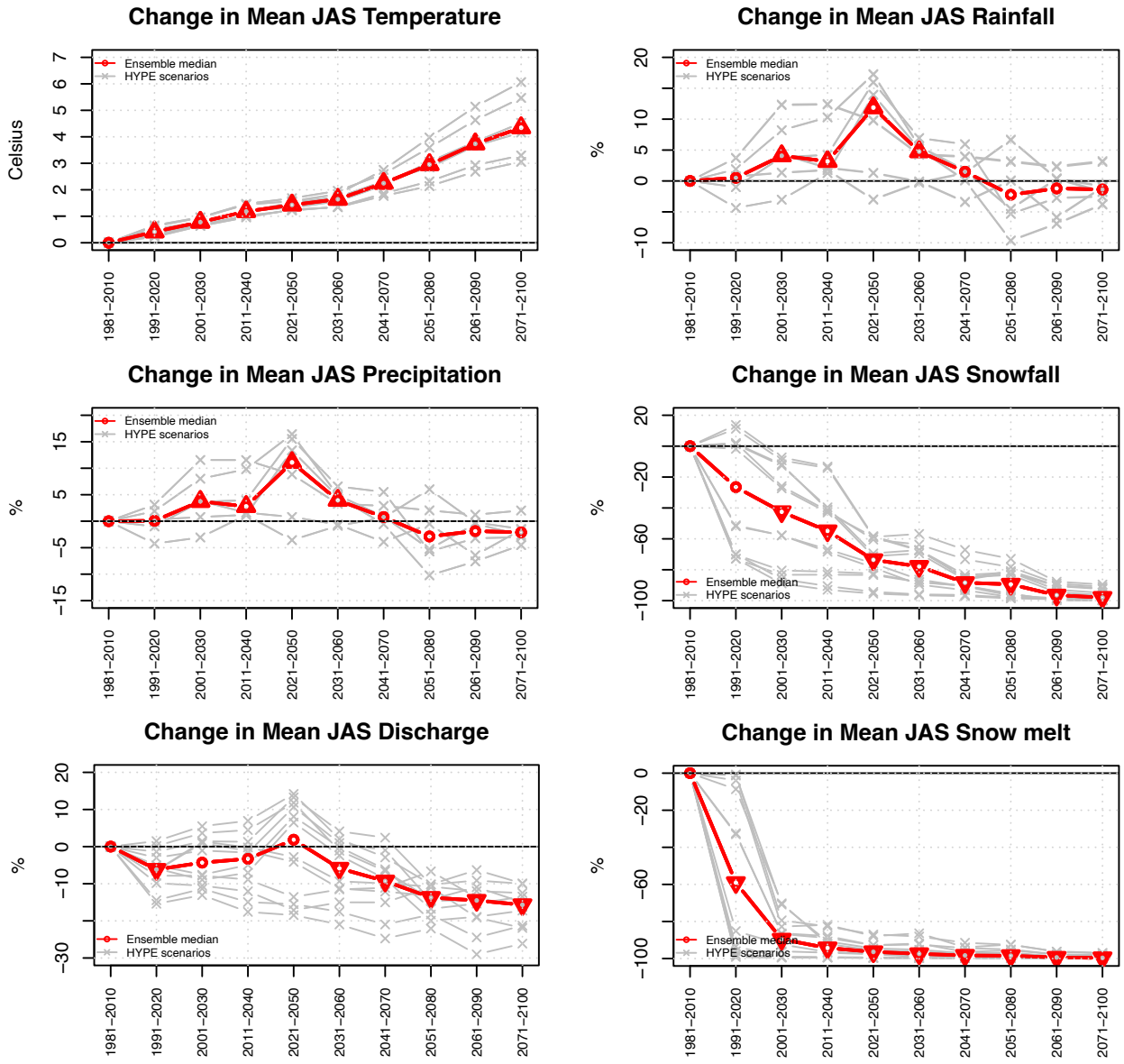

Fig. 53: Laxá catchment (vhm74): Projected changes in 30-year mean JAS temperature, precipitation, rainfall, snowfall, snowmelt and river discharge under the RCP8.5 emission scenario, relative to the 1981-2010 reference period. Ensemble members (grey lines) and ensemble median (red line). The symbols on the ensemble median indicate whether the 30-year mean is likely to increase or decrease significantly or remain unchanged in the future periods compared to the reference period, according to the Mann-Whitney test (triangle point-up=increase; triangle point down=decrease; open circle=no significant change).

6-2-3 Summary and discussion

The projected warming in the 21st century is relatively linear in all seasons and catchments. A greater warming is projected under the RCP8.5 than the RCP4.5 emission scenario, as expected. Spatial variations in projected warming are observed, with the lowest warming projected in the Laxá catchment and the largest one in the Fnjóská catchment. Mean annual and seasonal precipitation projections are mainly characterised by oscillations reflecting long-term natural climate variability. The nature of these oscillations often depends on the driving GCM and the different precipitation projections do not always vary in phase with each other, leading sometimes to large uncertainties in the outcome in some periods. Significant mean precipitation changes (increase or decrease) are projected in some periods, depending on the phase and amplitude of these oscillations. Long-term upward trends are superimposed on top of these oscillations and dominate the mean precipitation variability in JAS and/or OND in the Svartá and Fnjóská catchments, depending on the emission scenario, leading to an increase in mean annual precipitation as well. The warming leads to an increase in mean seasonal rainfall and a decrease in mean seasonal snowfall, in a majority of projection periods. Changes in the phase of precipitation lead to less snow storage and shorter snow seasons. Subsequently, mean seasonal snowmelt is projected to gradually decrease in AMJ and JAS in all catchments. The direction of projected mean snowmelt changes is more variable in OND and JFM and depends on each catchment. An increase in mean snowmelt in JFM is likely caused by an increase in the number of intermittent snowmelt events, and/or a shift earlier in the onset of the snowmelt season, whereas a decrease is likely attributed to a snow storage reduction. Similarly, an increase in mean snowmelt in OND is likely attributed to an increase in the number of intermittent snowmelt events whereas a decrease is likely attributed to a reduction in snow storage and/or a shift later in the start of the snow season.

Projected changes in mean seasonal rainfall and in the snow accumulation and melt cycles, caused by warming, lead, in turn, to changes in the seasonal runoff distribution, along the 21st century, but the timing, magnitude and direction of projected streamflow changes vary with the season, catchment and emission scenario. In summary, mean seasonal flow is projected to i) increase in OND and JFM in all catchments under both emission scenarios, ii) decrease in AMJ in the three catchments under both emission scenarios but the decrease starts later in the Fnjóská catchment, iii) decrease in JAS in the Fnjóská and Laxá catchments under both emission scenarios, whereas in the Svartá catchment, no change is projected under the RCP4.5 emission scenario and a moderate increase is projected under the RCP8.5 emission scenario. The projected changes in mean seasonal flow are not necessarily gradual along the projection horizon, like warming, because precipitation oscillations contribute to modulate these changes. These changes are usually more severe and/or start earlier under the RCP8.5 emission scenario than under the RCP4.5 emission scenario because the warming is greater and is leading to larger changes in the ratio of rainfall and snowfall and to a larger decrease in snow storage.

7 Climate change impact on flood characteristics

This section examines the impact of projected climate change on the timing and magnitude of annual maximum floods (AMFs).

7-1 Changes in the timing of annual maximum floods

To investigate changes in the timing of AMFs, the day of the water year when annual maximum discharge occurred was extracted from the simulated daily streamflow time series and assigned to the corresponding season. The frequency with which AMFs occurred in each season and each 30-year projection period was then calculated for each member and the ensemble median estimated (see Methodology in Section 3-1). Changes in the seasonal frequencies of occurrence of AMFs from the reference to the future periods are considered significant when at least 2/3 of the ensemble members are shifted in the same direction (frequency increase or decrease). The evolution of the seasonal frequencies of occurrence along the projection horizon was analysed. Figs. 54 to 59 present the results for the ensemble median and Appendix 9 presents the results with all ensemble members. It is assumed that AMFs occurring in OND are primarily generated by rainfall; AMFs occurring in JFM are generated by a combination of rainfall and snowmelt; AMFs occurring in AMJ are primarily generated by snowmelt but rainfall may be combined with snowmelt; AMFs occurring in JAS are primarily generated by rainfall but snowmelt may also have some contribution early in the season, depending on the catchment and projection period.

- **Svartá catchment (vhm10)**

In the reference period (1981-2010), AMFs primarily occur in AMJ, followed by JFM and then OND, whereas hardly any event occurs in JAS.

- RCP4.5 emission scenario

As the projection horizon increases, AMFs are projected to occur less and less frequently in AMJ and more and more often in JFM and OND, and later in JAS as well. By the end of the century, the main flood season is still AMJ, but the frequency difference with the other seasons is strongly reduced.

- RCP8.5 emission scenario

Results are similar to those projected with the RCP4.5 scenario but the seasonal changes are greater, especially the frequency decrease in AMJ. Towards the end of the century, AMFs are projected to occur with an equal prevalence in AMJ and JFM.

- **Fnjóská catchment (vhm200)**

In the reference period (1981-2010), AMFs primarily occur in AMJ, followed by JAS, while very few events are occurring in OND and JFM.

- RCP4.5 emission scenario

AMJ is projected to remain the dominant flood season along the entire projection horizon but a significant frequency decrease is projected from 2061-2090 and thereafter. AMFs are also projected to occur less and less frequently in JAS and at the same time, more often in OND. A

moderate median frequency increase is also projected in JFM from 2051-2080 and thereafter. From 2021-2050 and thereafter, AMFs are projected to occur more frequently in OND than in JFM or JAS and from 2041-2070 and thereafter, AMFs are projected to occur more frequently in JFM than in JAS. By the end of the century, very few AMFs are projected in JAS.

- RCP8.5 emission scenario

More changes are projected to take place under this emission scenario. From 2031-2060 and thereafter, AMFs are projected to occur less and less frequently in AMJ but this season remains the main flood season until 2051-2080. AMFs are also projected to occur less frequently in JAS, but the decrease is not as rapid and steady as under the RCP4.5 scenario. AMFs are projected to occur more and more frequently in OND and very quickly, this season becomes the second most frequent flood season, and by the end of the century, the main flood season. From 2041-2070 and thereafter, more AMFs are projected to occur in JFM, and by the end of the century, AMFs have almost the same probability of occurring in AMJ or JFM.

- **Laxá catchment (vhm74)**

In the reference period (1981-2010), AMFs primarily occur in OND, followed by JFM and then by JAS and AMJ.

- RCP4.5 emission scenario

Hardly any change is projected to take place in this catchment, regarding the frequency of occurrence of AMFs. The prevalence of OND followed by JFM persists along most of the entire projection horizon. The main feature characterising the evolution of the median frequency of occurrence of AMFs in the different seasons is an oscillation-like pattern. Changes in the seasonal frequency order are mainly related to the phase and amplitude of the oscillations.

- RCP8.5 emission scenario

Results are very similar to those projected with the RCP4.5 emission scenario. OND is projected to remain the predominant flood season along the entire projection horizon and no change is projected in the seasonal order of the median frequency of occurrence of these extreme events.

- **Discussion**

The flood regime of the Svartá catchment is projected to be less and less governed by spring snowmelt, and more and more influenced by a combination of rainfall and snowmelt in winter, and to a lesser extent by rainfall in autumn and summer, under both emission scenarios. The flood regime of the Fnjóská catchment is projected to remain largely dominated by spring snowmelt under the RCP4.5 emission scenario, because snow storage is large enough to maintain a considerable snowmelt runoff in that season. More drastic changes are projected under the RCP8.5 scenario for this catchment, corresponding to a decreasing dominance of spring snowmelt and an increasing influence of rainfall and snowmelt in autumn and winter. In the Laxá catchment, projected changes in snow storage have little impact on the seasonal frequency of occurrence of AMFs and these extreme events are projected to remain most frequently triggered by rainfall in autumn (ca. 50%) along the entire projection horizon, under both emission scenarios.

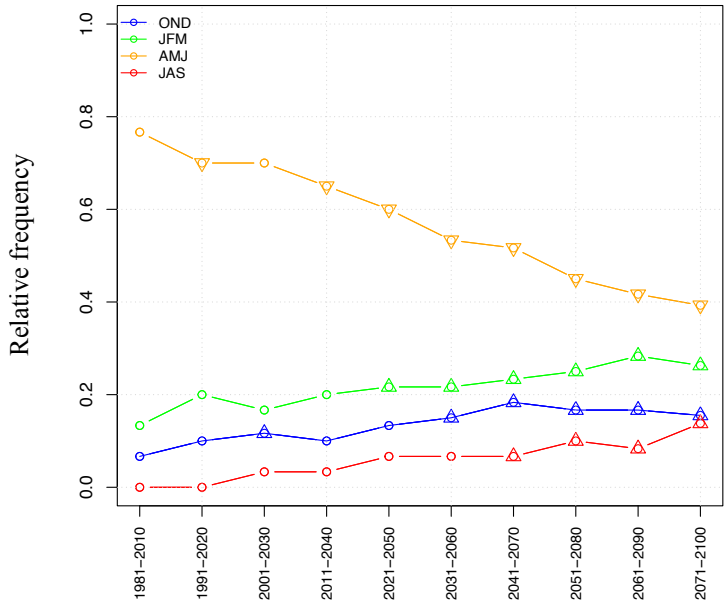

Fig. 54: Svartá catchment (vhm10): Projected median relative frequency of occurrence of AMFs in each season under the RCP4.5 emission scenario. OND (blue), JFM (green), AMJ (orange), JAS (red). The symbols on the ensemble median indicate whether a significant shift in the seasonal frequency ensemble has been detected between the reference and future periods (triangle point-up=freq. increase; triangle point down=freq. decrease; open circle=no significant change).

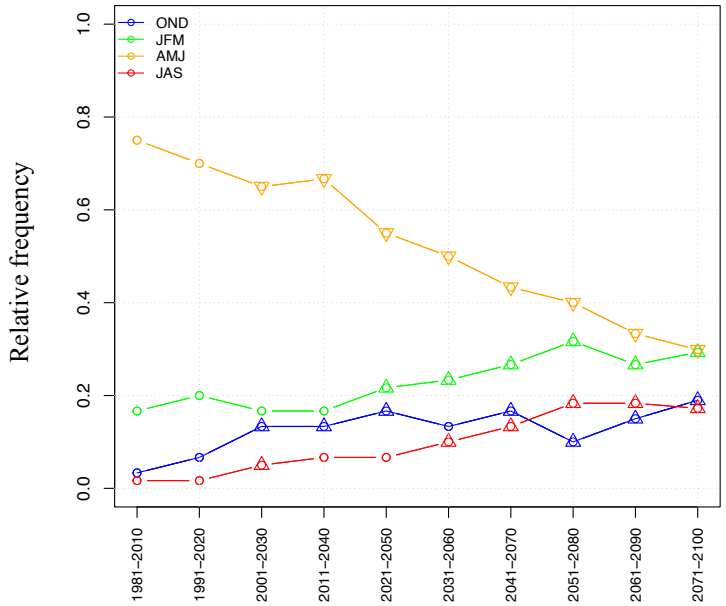

Fig. 55: Svartá catchment (vhm10): as Fig. 54 but under the RCP8.5 emission scenario.

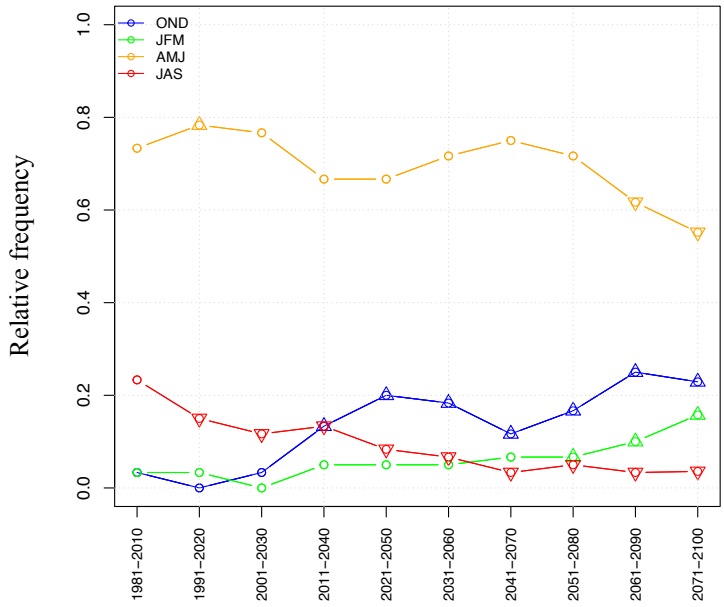

Fig. 56: Fnjóská catchment (vhm200): Projected median relative frequency of occurrence of AMFs in each season under the RCP4.5 emission scenario. OND (blue), JFM (green), AMJ (orange), JAS (red). The symbols on the ensemble median indicate whether a significant shift in the seasonal frequency ensemble has been detected between the reference and future periods (triangle point-up=freq. increase; triangle point down=freq. decrease; open circle=no significant change).

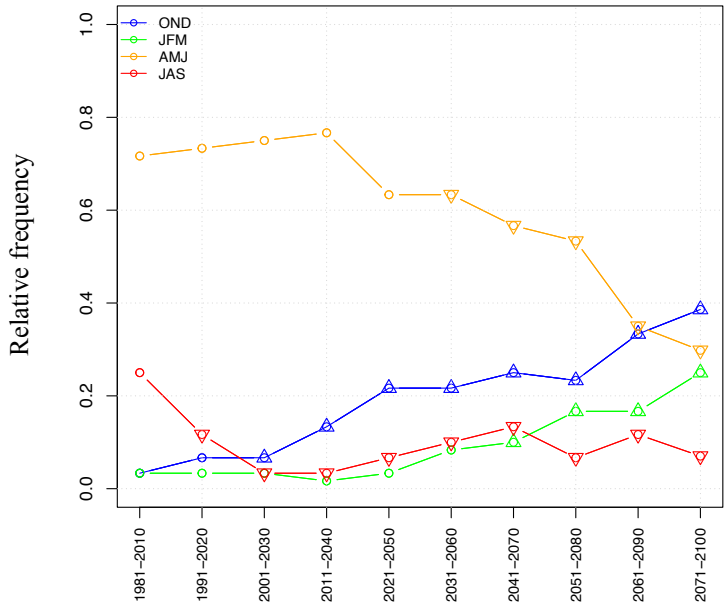

Fig. 57: Fnjóská catchment (vhm200): as Fig. 56 but under the RCP8.5 emission scenario.

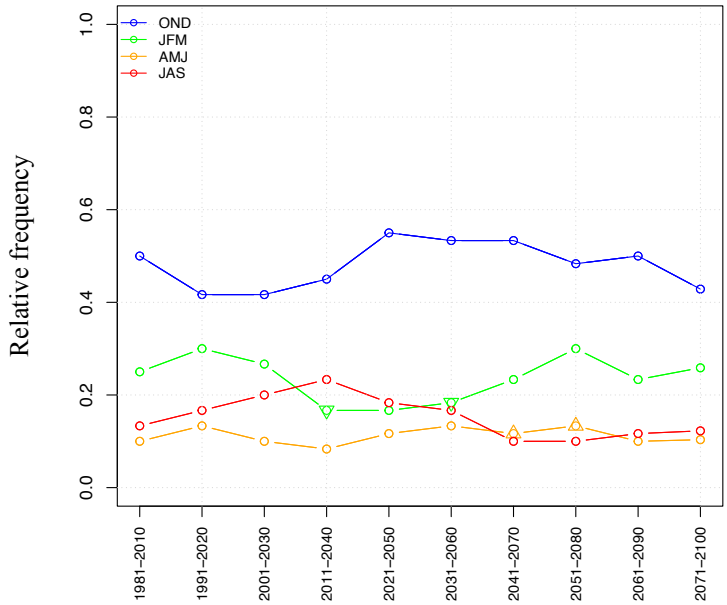

Fig. 58: Laxá catchment (vhm74): Projected median relative frequency of occurrence of AMFs in each season under the RCP4.5 emission scenario. OND (blue), JFM (green), AMJ (orange), JAS (red). The symbols on the ensemble median indicate whether a significant shift in the seasonal frequency ensemble has been detected between the reference and future periods (triangle point-up=freq. increase; triangle point down=freq. decrease; open circle=no significant change).

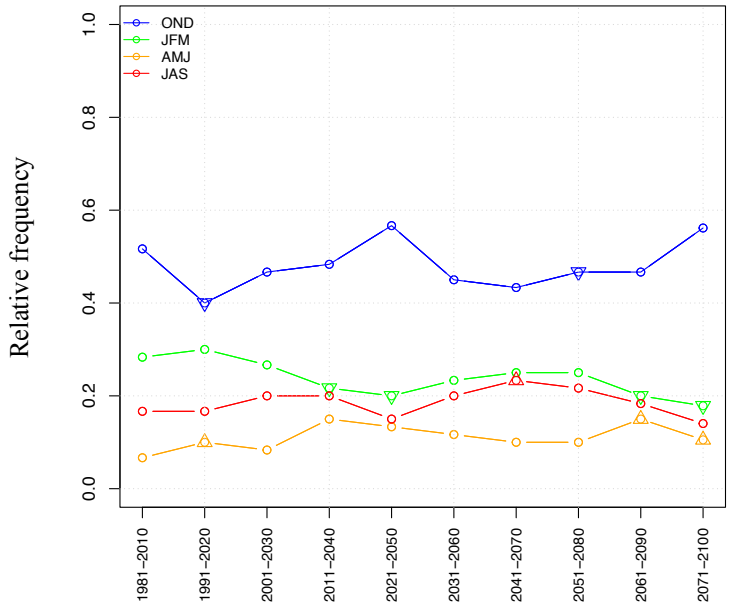

Fig. 59: Laxá catchment (vhm74): as Fig. 58 but under the RCP8.5 emission scenario.

7-2 Changes in the magnitude of annual maximum floods

This section examines the impact of projected climate change on the magnitude of annual maximum floods (AMFs).

7-2-1 Changes in the magnitude of T-year floods

A Gumbel distribution was fitted to the AMFs series in each 30-year projection period (not shown) and the magnitude of the T-year floods estimated for the return periods T=10 and 50 years. The uncertainty associated with the T-year flood estimation is large, including in the reference period, as large variations are often observed between the different ensemble members (see for instance the empirical AMFs frequency distributions for the 1981-2010 reference period presented in Appendix 8 for the two emission scenarios). Projected changes in the magnitude of the T-year floods between reference and future periods are presented in Figs. 60 to 65. The plots also show results from the one-sided Mann-Whitney tests used to compare the ensembles of T-year flood magnitude between the reference and future periods (see Methodology in Section 3-1).

- **Svartá catchment (vhm10)**

See Figs. 60 and 61.

- RCP4.5 emission scenario

No significant change is projected until 2051-2080 and thereafter, a significant magnitude decrease is projected for both T-year floods until the end of the century. The magnitude decrease varies in similar proportions for the two return periods and reaches a median value of about -20% in 2071-2100, relative to the 1981-2010 reference level.

- RCP8.5 emission scenario

The magnitudes of both T-year floods are projected to decrease throughout a large part of the 21st century and in similar proportions. The projected decrease reaches a median value of about -20% in 2071-2100, relative to the 1981-2010 reference level.

- Discussion

Snowmelt runoff in spring plays a primary role in the generation of AMFs in this catchment in the reference period (see Section 7-1). The projected snow storage depletion and the subsequent reduction in spring snowmelt caused by rising temperatures are partly responsible for the projected decrease in the magnitude of T-year floods in this catchment. As these magnitude changes are associated with a shift in the timing of AMFs from spring to the other seasons, these results also indicate that the magnitudes of AMFs occurring in these other seasons in the future periods, tend not to exceed the magnitudes of those generated by snowmelt in spring in the reference period, even though seasonal rainfall and winter snowmelt are projected to increase.

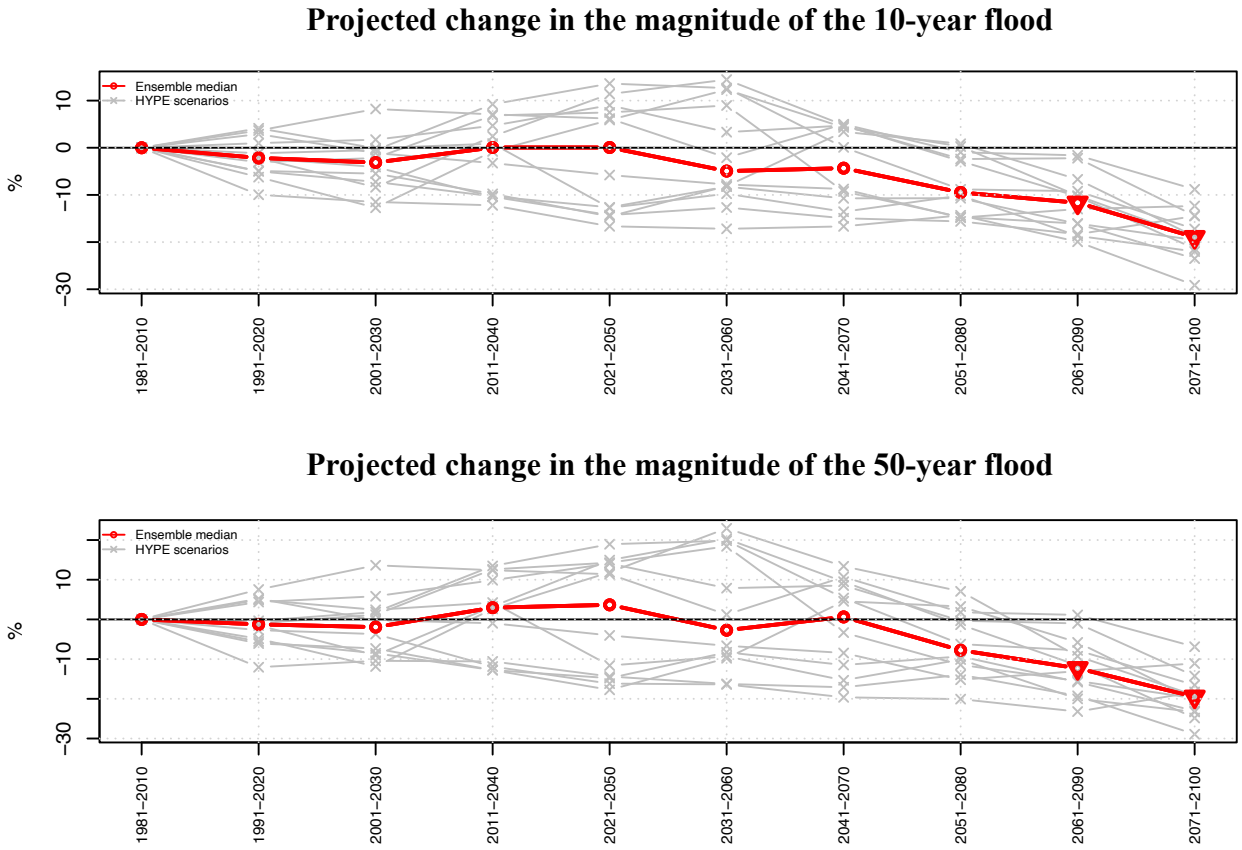

Fig. 60: Svartá catchment (vhm10): Projected changes in the magnitude of the T-year flood relative to the 1981-2010 reference level, under the RCP4.5 emission scenario: 10-year flood (top) and 50-year flood (bottom). Ensemble members (grey lines) and ensemble median (red line). The symbols on the ensemble median indicate whether the magnitude of the T-year flood is likely to increase or decrease significantly or remain unchanged in the future periods compared to the reference period, according to the Mann-Whitney test (triangle point-up=magnitude increase; triangle point down=magnitude decrease; open circle=no significant change).

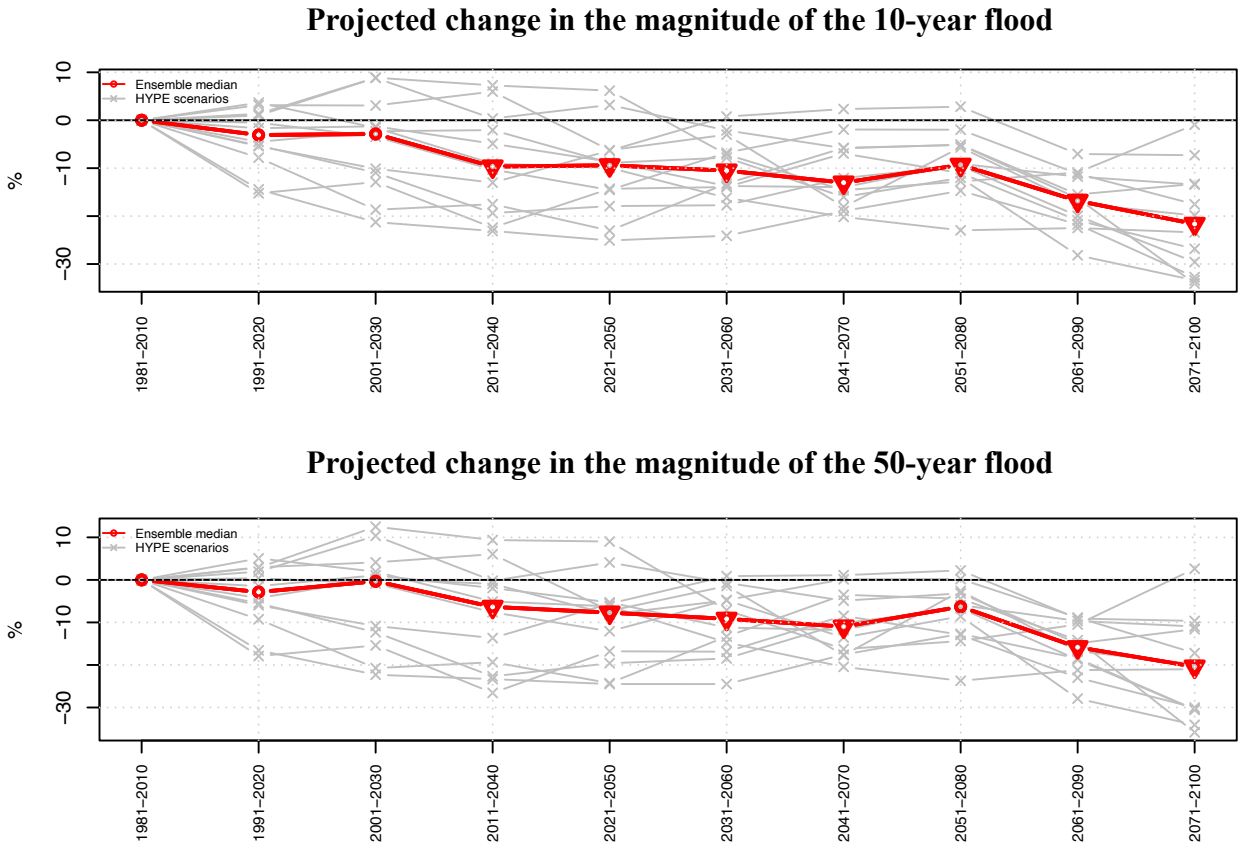

Fig. 61: Svartá catchment (vhm10): As Fig. 60 but under the RCP8.5 emission scenario.

- **Fnjóská catchment (vhm200)**

See Figs. 62 and 63.

- RCP4.5 emission scenario

No significant change is projected until 2021-2050 and thereafter, a significant magnitude decrease is projected for both T-year floods until the end of the century. The magnitude decrease varies in similar proportions for the two return periods and reaches a median value of about -20% in 2071-2100, relative to the 1981-2010 reference level.

- RCP8.5 emission scenario

Results indicate that the magnitudes of both T-year floods are projected to decrease throughout most of the century. The decrease is projected to become significant from 2001-2030 for T=10 years and 2011-2040 for T=50 years, until the end of the century. The magnitude decrease varies in similar proportions for the two return periods and reaches a median value of about -30% in 2071-2100, relative to the 1981-2010 reference level.

- Discussion

Snowmelt runoff in spring plays a primary role in the generation of AMFs in this catchment in the reference period (see Section 7-1). Projected snow storage depletion and the subsequent reduction in spring snowmelt caused by warming are partly responsible for the projected decrease in the magnitude of T-year floods in this catchment. As these changes in T-year flood magnitude are associated with a shift in the timing of AMFs from spring/summer to autumn/winter, especially under the RCP8.5 emission scenario, these results also indicate that the magnitudes of AMFs occurring in autumn and winter in the future periods, tend not to exceed the magnitudes of those generated by snowmelt in spring in the reference period, even though autumn/winter rainfall and winter snowmelt are projected to increase.

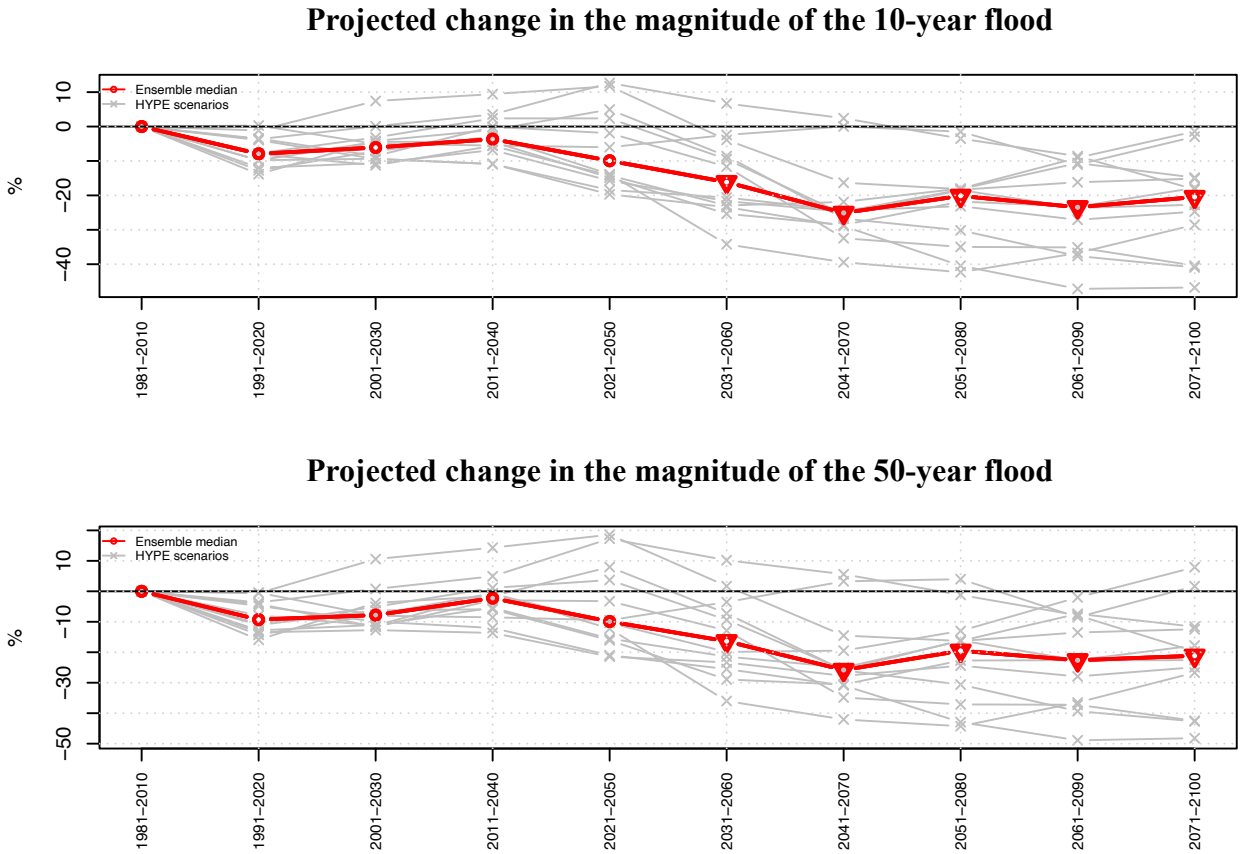

Fig. 62: Fnjóská catchment (vhm200): Projected changes in the magnitude of the T-year flood relative to the 1981-2010 reference level, under the RCP4.5 emission scenario: 10-year flood (top) and 50-year flood (bottom). Ensemble members (grey lines) and ensemble median (red line). The symbols on the ensemble median indicate whether the magnitude of the T-year flood is likely to increase or decrease significantly or remain unchanged in the future periods compared to the reference period, according to the Mann-Whitney test (triangle point-up=magnitude increase; triangle point down=magnitude decrease; open circle=no significant change).

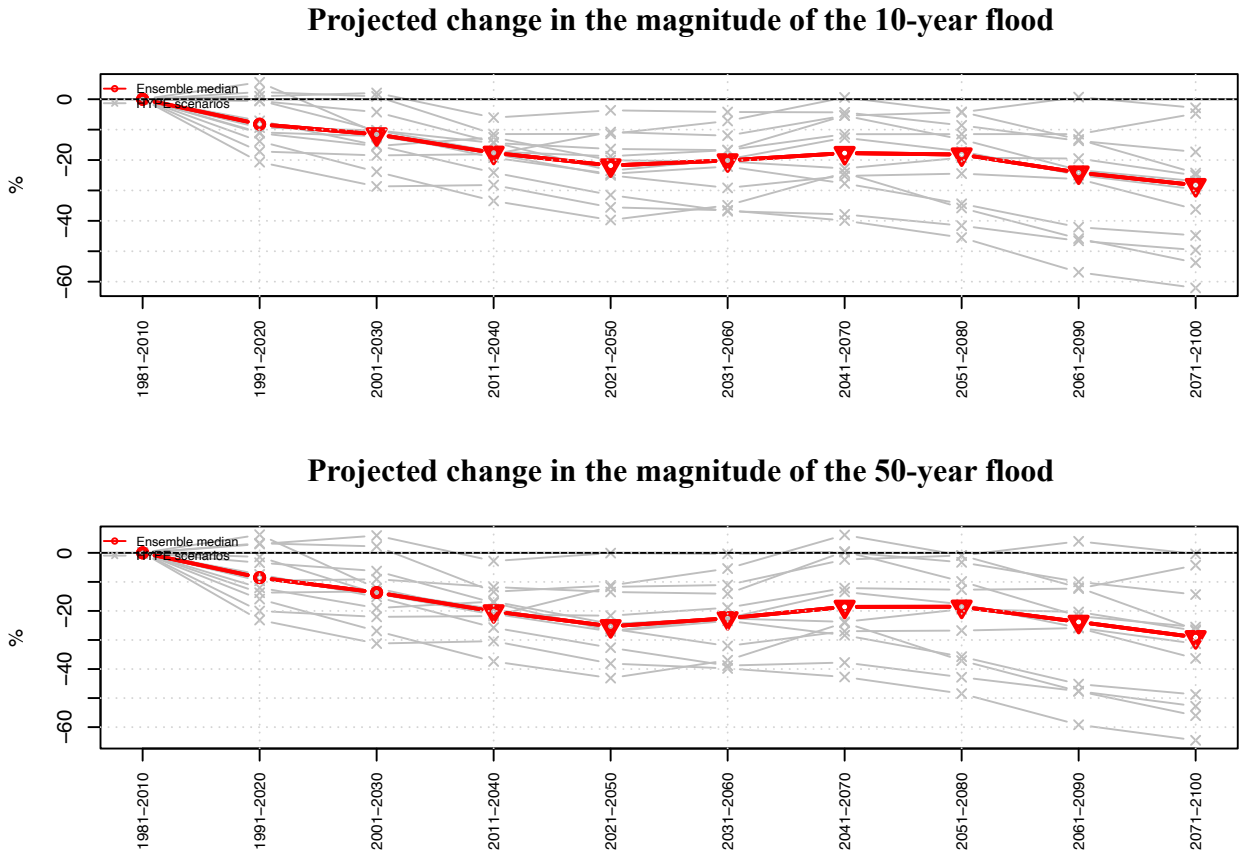

Fig. 63: Fnjóská catchment (vhm200): As Fig. 62 but under the RCP8.5 emission scenario.

- **Laxá catchment (vhm74)**

See Figs. 64 and 65.

- RCP4.5 emission scenario

The magnitudes of both T-year floods are projected to increase significantly in a majority of projection periods. The projected changes are not gradual but oscillate. The magnitude increase varies in similar proportions for the two return periods but seldom exceeds a median value of 10%. The largest median increase is projected in 2061-2090 and reaches a value of about 15% for T=10 years and almost 20% for T=50 years.

- RCP8.5 emission scenario

The magnitudes of both T-year floods are projected to increase significantly from 2021-2050 to 2051-2080. In that period of time, the magnitude increase varies in similar proportions for the two return periods and reaches a median value of about 20% in 2051-2080. Large uncertainties affect the projected changes beyond 2051-2080, making difficult to draw any robust conclusion.

- Discussion

This catchment is projected to remain dominated by rainfall-generated AMFs in autumn (see Section 7-1). Therefore, a rainfall intensification could likely explain the projected increase in the magnitude of T-year floods. However, large uncertainties affect these projections and a large spread is observed in the estimated T-year flood ensembles. These uncertainties originate partly from the large uncertainties affecting the rainfall projections, due to their oscillating nature, making difficult to draw robust conclusions in some projection periods.

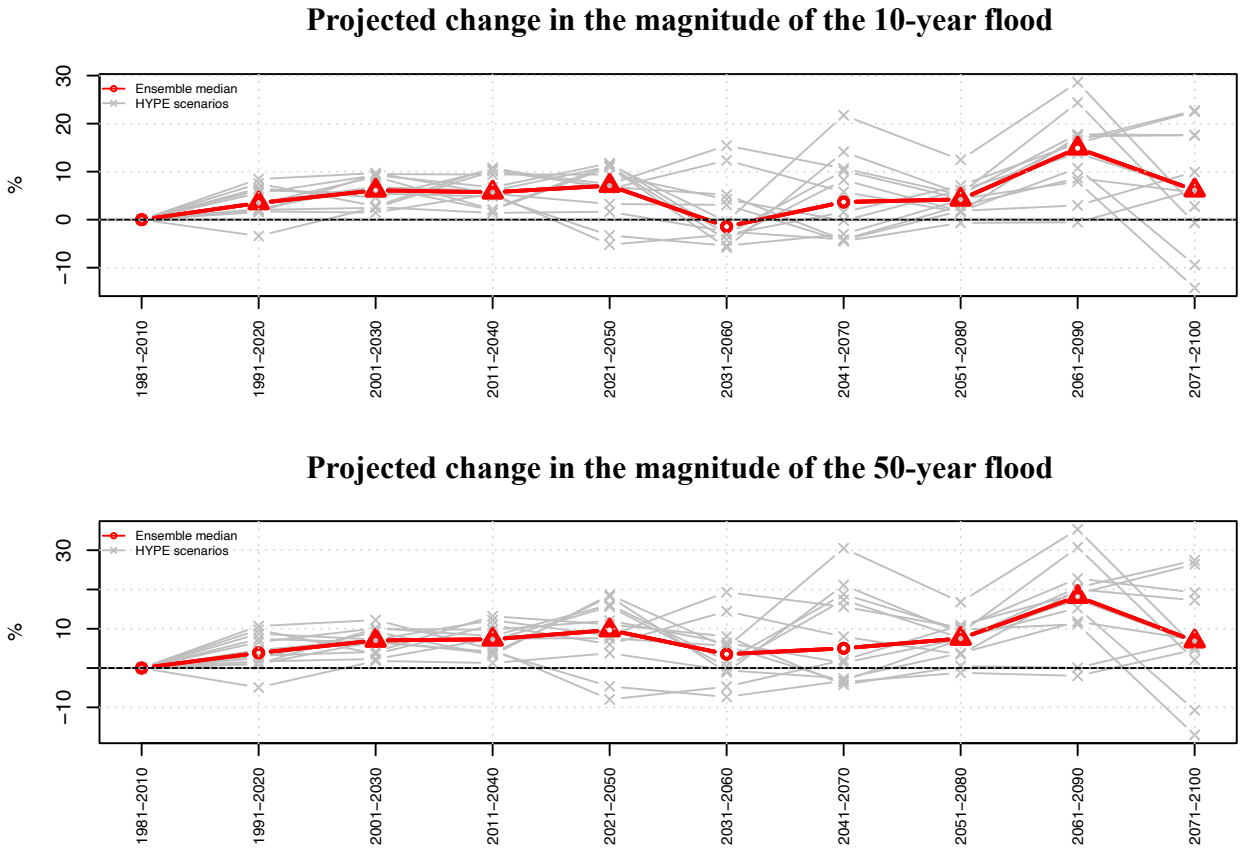

Fig. 64: Laxá catchment (vhm74): Projected changes in the magnitude of the T-year flood relative to the 1981-2010 reference level, under the RCP4.5 emission scenario: 10-year flood (top) and 50-year flood (bottom). Ensemble members (grey lines) and ensemble median (red line). The symbols on the ensemble median indicate whether the magnitude of the T-year flood is likely to increase or decrease significantly or remain unchanged in the future periods compared to the reference period, according to the Mann-Whitney test (triangle point-up=magnitude increase; triangle point down=magnitude decrease; open circle=no significant change).

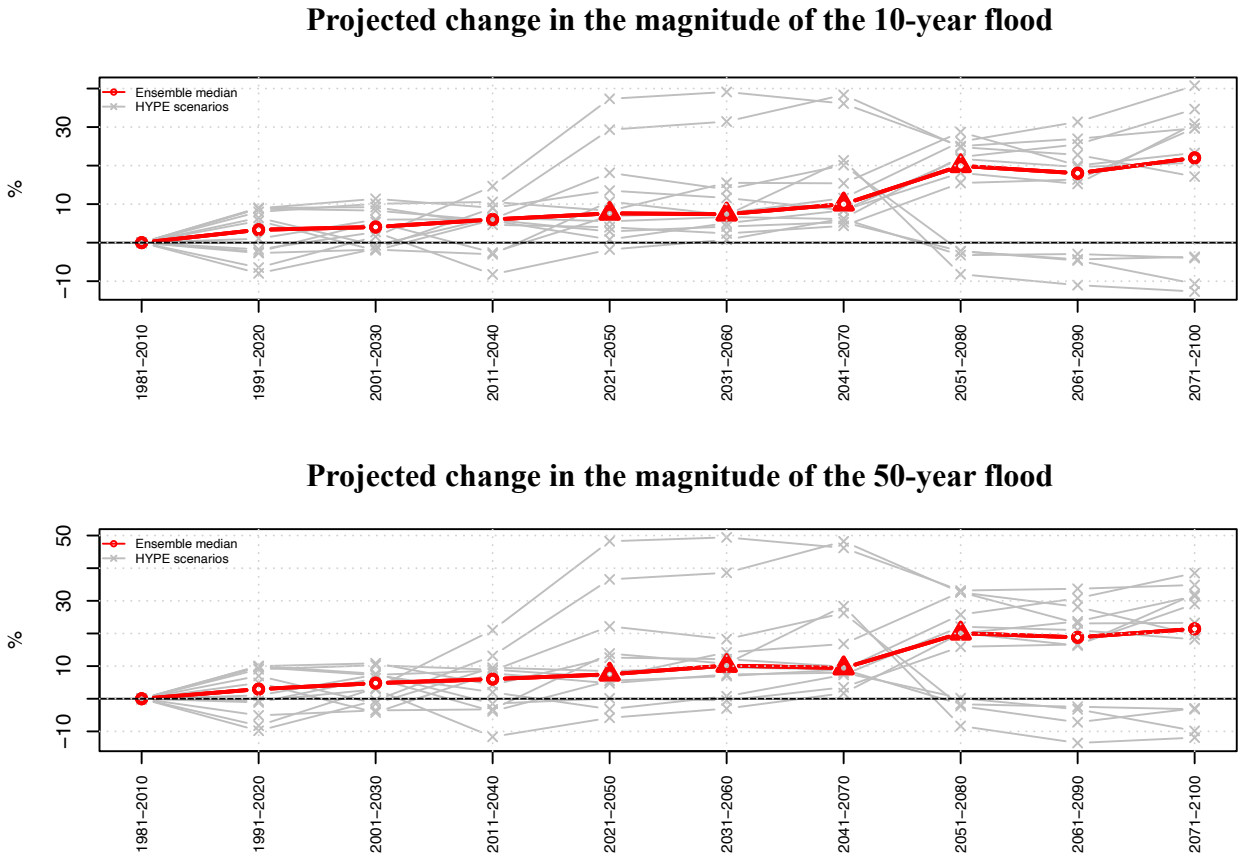

Fig. 65: Laxá catchment (vhm74): As Fig. 64 but under the RCP8.5 emission scenario.

7-2-2 Changes in the return period of annual maximum floods

The flood magnitude (Q) is now fixed and the corresponding return period T(Q) estimated in the 30-year projection periods and compared to T(Q) in the reference period (1981-2010). If the frequency distribution of AMFs is projected to shift towards larger flood discharges in the future, then a flood of magnitude Q will be exceeded more frequently in the future and its return period should decrease:

$$q_2=Q(T=T_i)_{future} > q_1=Q(T=T_i)_{1981\text{-}2010}$$
$$T_2=T(Q=q_1)_{future} < T_1=T(Q=q_1)_{1981\text{-}2010}$$

If the frequency distribution of AMFs is projected to shift towards lower flood discharges in the future, then a flood of magnitude Q will be exceeded less frequently in the future and its return period should increase:

$$q_2=Q(T=T_i)_{future} < q_1=Q(T=T_i)_{1981\text{-}2010}$$
$$T_2=T(Q=q_1)_{future} > T_1=T(Q=q_1)_{1981\text{-}2010}$$

The reference flood magnitude Q is taken as the magnitude of the 10-year flood in the reference period (1981-2010). Here, changes between the reference and future periods are considered significant when at least 2/3 of the ensemble members are shifted in the same direction (T increase or decrease). The temporal evolution of the T(Q) ensembles is presented in Figs. 66 to 68. As expected, the results are found to echo the projected evolution of 10-year floods analysed in Section 7-2-1 above.

- **Svartá catchment (vhm10)**

See Fig. 66.

- RCP4.5 emission scenario

The return period associated with the reference 10-year flood is projected to increase from 2051-2080 to the end of the projection horizon. The spread of the ensemble is large but most members agree with a return period increase. As an example, in 2071-2100, the reference 10-year flood is projected to become a flood with a median return period of about 40 years. Before 2051-2080, the agreement among the ensemble members regarding the direction of change is low, making the outcome very uncertain and leading the median return period to remain close to the reference level of 10 years.

- RCP8.5 emission scenario

Results are similar to those obtained under the RCP4.5 emission scenario, but there is a better consensus within the ensemble regarding a return period increase along most of the 21st century. In 2071-2100, the reference 10-year flood is projected to become a flood with a median return period of about 43 years.

- **Fnjóská catchment (vhm200)**

See Fig. 67.

- RCP4.5 emission scenario

Results indicate that the median return period associated with the reference 10-year flood is projected to increase along the 21st century, especially after 2021-2050. From 2031-2060 to 2071-2100, the reference 10-year flood is projected to become a flood with a median return period varying approximately between 25 and 55 years. The spread of the ensemble is large and increases with the projection horizon, making the projected median return period more and more uncertain, but most members agree with an increase.

- RCP8.5 emission scenario

Results are similar to those obtained under the RCP4.5 emission scenario but the changes are more pronounced, especially before 2031-2060. A large majority of members projects an increase in the return period associated with the reference 10-year flood, along the entire projection horizon. In 2071-2100, the reference 10-year flood is projected to become a flood with a median return period of almost 80 years.

- **Laxá catchment (vhm74)**

See Fig. 68.

- RCP4.5 emission scenario

The median return period associated with the reference 10-year flood is projected to decrease along most of the projection horizon except in the 2031-2060 and 2041-2070 periods, during which the return period is fluctuating close to the initial reference value of 10 years. As an example, the reference 10-year flood is projected to become a flood with a median return period of about 5 years in 2061-2090.

- RCP8.5 emission scenario

The median return period associated with the reference 10-year flood is projected to decrease along most of the projection horizon but this decrease is only considered significant from 2011-2040 to 2041-2070. In that period, the reference 10-year flood is projected to have a median return period varying between approximately 6 and 7 years. Beyond the 2041-2070 period, the spread is large and the consensus among the ensemble members regarding the direction of change of the projected return period is low, making difficult to draw any robust conclusion.

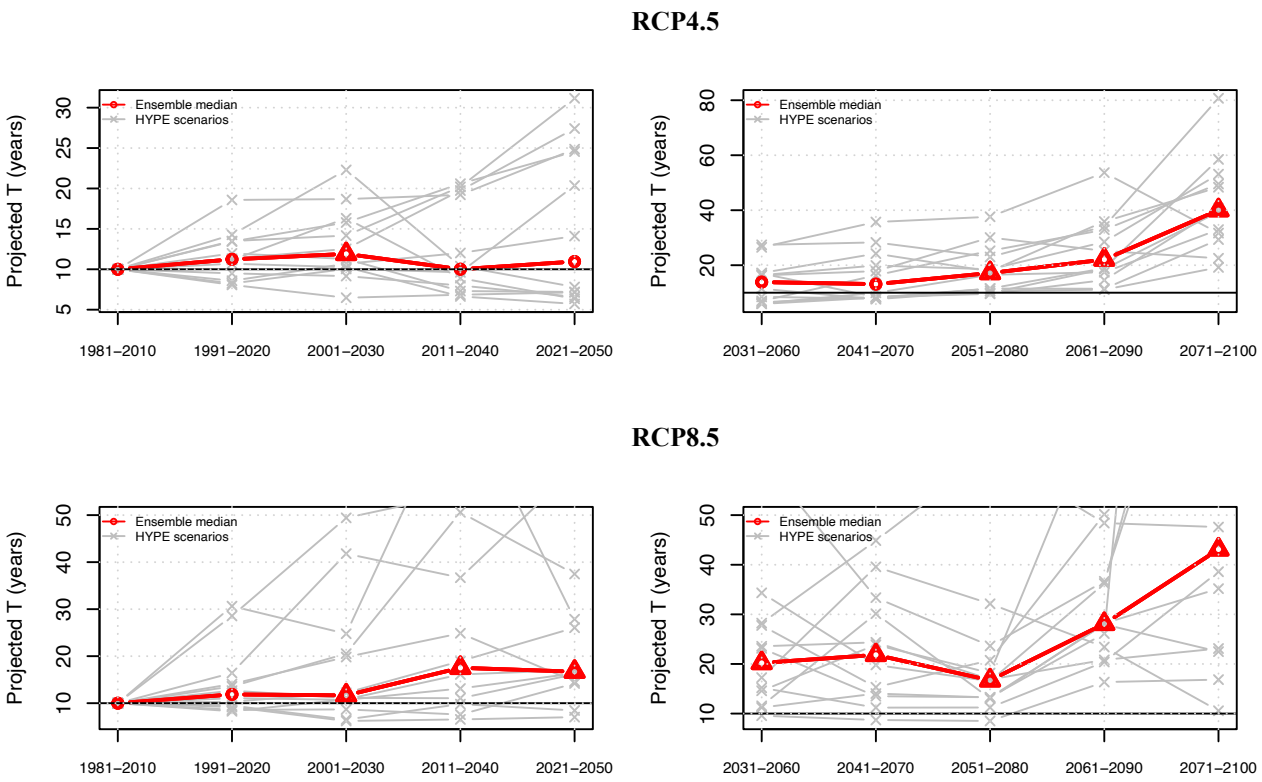

Fig. 66: Svartá catchment (vhm10): Projected return period (T) associated with the reference 10-year flood. Top-panel: RCP4.5 emission scenario; bottom-panel: RCP8.5 emission scenario. Ensemble members (grey lines) and ensemble median (red line). The symbols on the ensemble median indicate whether a significant shift in the T ensemble has been detected between the reference and future periods (triangle point-up=T increase; triangle point down=T decrease; open circle=no significant change).

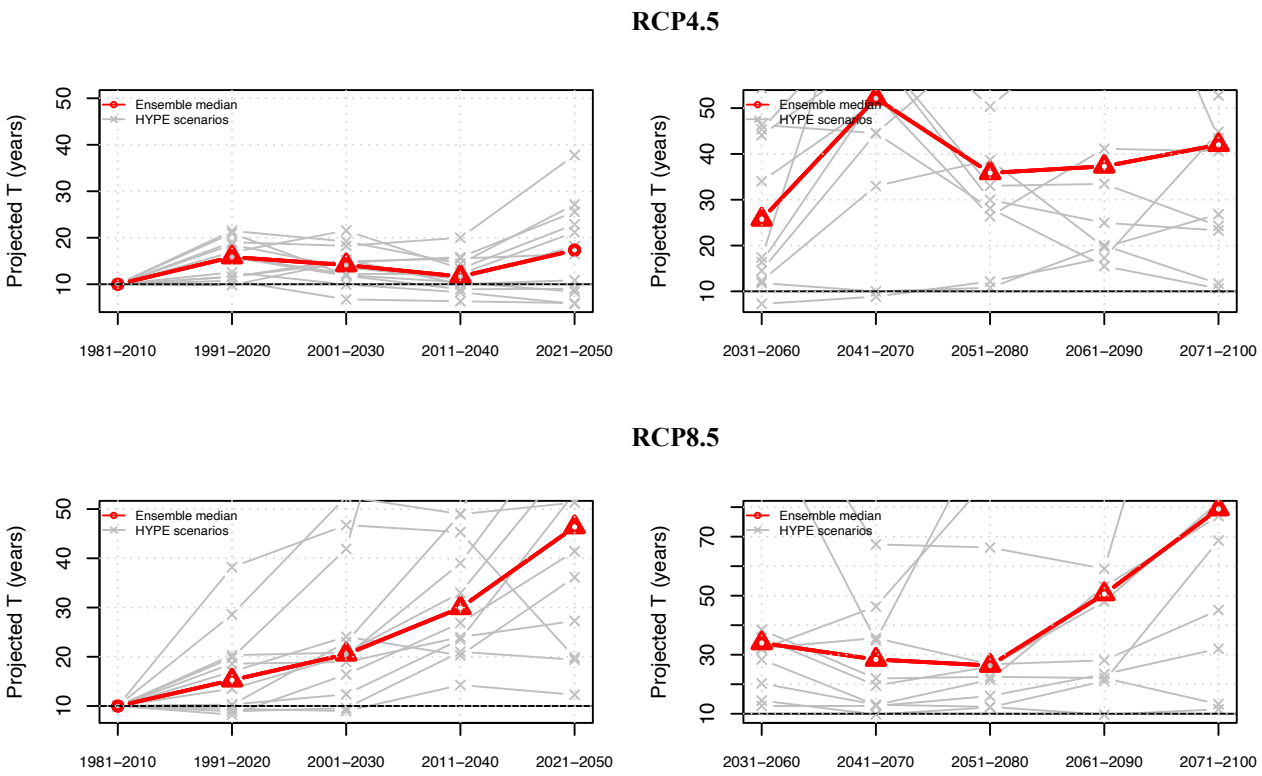

Fig. 67: Fnjóská catchment (vhm200): Projected return period (T) associated with the reference 10-year flood. Top-panel: RCP4.5 emission scenario; bottom-panel: RCP8.5 emission scenario. Ensemble members (grey lines) and ensemble median (red line). The symbols on the ensemble median indicate whether a significant shift in the T ensemble has been detected between the reference and future periods (triangle point-up=T increase; triangle point down=T decrease; open circle=no significant change).

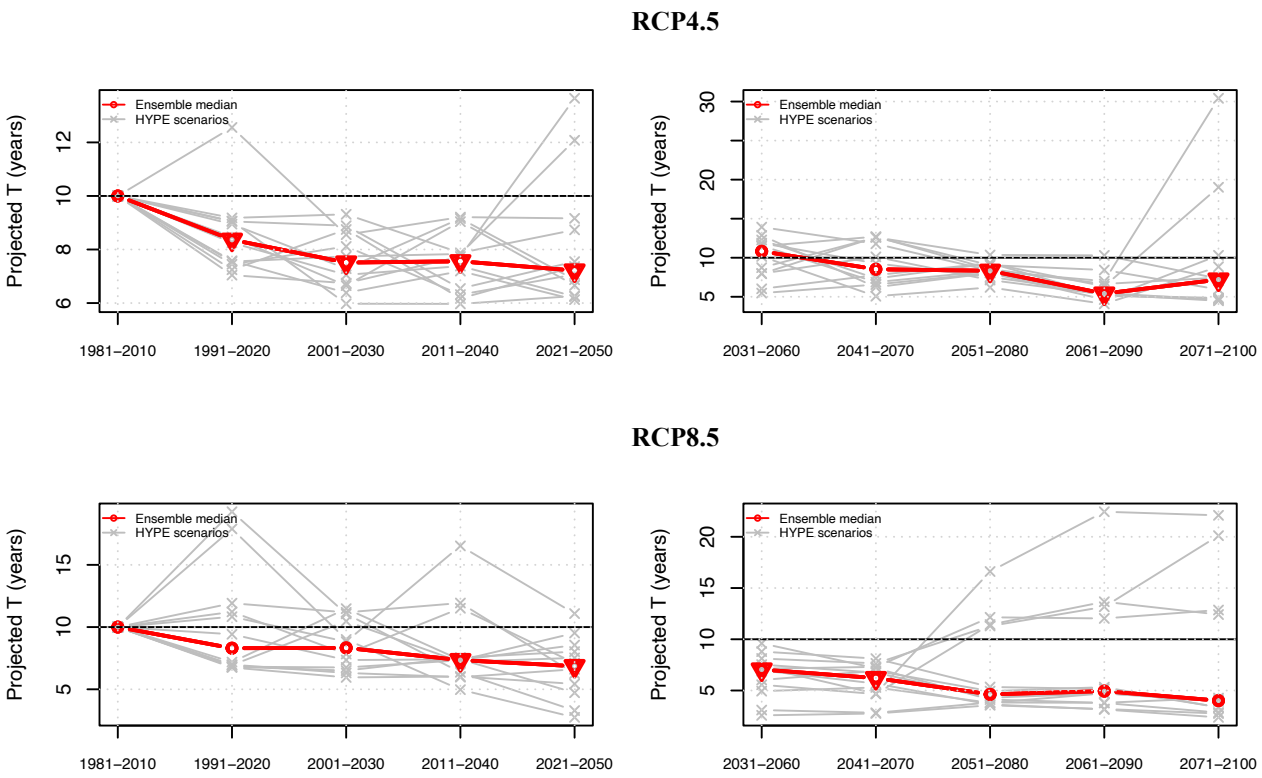

Fig. 68: Laxá catchment (vhm74): Projected return period (T) associated with the reference 10-year flood. Top-panel: RCP4.5 emission scenario; bottom-panel: RCP8.5 emission scenario. Ensemble members (grey lines) and ensemble median (red line). The symbols on the ensemble median indicate whether a significant shift in the T ensemble has been detected between the reference and future periods (triangle point-up=T increase; triangle point down=T decrease; open circle=no significant change).

7-3 Summary and discussion

Projected climate change is expected to have a significant impact on the flood regimes of the three studied catchments in the future, especially those where snowmelt-induced runoff currently plays a dominant role in the generation of annual maximum floods. This impact concerns both the timing and magnitude of these extreme events in the Svartá and Fnjóská catchments and mainly their magnitude in the Laxá catchment.

In the Svartá and Fnjóská catchments, the strong dominance of spring snowmelt on the timing of annual maximum floods is projected to decrease in the future, and the influence of rainfall and/or combined rainfall and snowmelt in autumn and winter increase, owing to the projected increase in temperature. These projected timing changes are associated with a trend towards a decrease in the magnitude of these extreme events. The Laxá catchment is projected to remain dominated by rainfall-generated annual maximum floods in autumn, but a slight magnitude increase is to be expected in some future periods, possibly because of rainfall intensification. Projected changes in the magnitude of T-year floods will have implications in design flood studies.

These results are consistent with findings from hydrological projections in other Icelandic catchments (Crochet 2021), in Norway (Vormoor et al., 2015) and Sweden (Arheimer and Lindström, 2015), which suggest a greater influence of autumn/winter rainfall and a decreasing importance of spring/summer snowmelt on the generation of floods in the future, due to temperature rise.

Projected changes in the timing of annual maximum floods appear to be relatively robust, and the consensus within the ensembles is usually good. On the other hand, projected changes in the magnitude of T-year floods are associated with large uncertainties so these results have to be treated with caution. The overall uncertainty is related to uncertainties affecting extreme discharge projections, uncertainties related to the fitting of the Gumbel distribution and uncertainties in the estimation of flood quantiles or return periods beyond the range of simulated flood values.

8 Conclusions

A methodology based on a multi-model ensemble approach was applied to investigate the impact of projected climate change in the 21st century, on the hydrological characteristics of three river catchments situated in different regions of Iceland. The approach is based on the use of the HYPE hydrological model, calibrated in two different periods, and forced with an ensemble of regional climate projections from CORDEX, under two possible greenhouse gas emission scenarios (RCPs 4.5 and 8.5). In total, twelve daily hydrological projections were obtained for each emission scenario, over the period 1981-2100. The envelope curve of the ensemble of hydrological projections reflects the overall uncertainty associated with the modelling chain. Projected changes affecting near surface air temperature and precipitation and their impact on mean and extreme flow characteristics were analysed, considering moving 30-year periods. The reference period was taken as the 1981-2010 period.

Results indicated that the HYPE hydrological model driven by the ICRA reanalysis provided credible estimates of observed daily discharge characteristics but the magnitude of annual maximum floods was is some cases difficult to simulate properly. The comparisons between discharge simulations obtained with the hydrological model driven by the ICRA reanalysis and by the locally-adjusted CORDEX climate outputs in the reference period showed good agreement, demonstrating the credibility of the modelling chain.

A significant warming is expected throughout the 21st century, more or less pronounced according to the season, catchment location and emission scenario (0.295°C/decade for the RCP4.5 emission scenario and 0.473°C/decade for the RCP8.5 emission scenario, on average over all months and catchments). Mean annual and seasonal precipitation projections are mainly characterised by oscillations reflecting the natural climate variability. These oscillations lead sometimes to significant mean precipitation changes (increase or decrease) in some future periods depending on their phase and amplitude, but no long-term trend is emerging in most cases, except in summer and/or autumn in the Svartá and Fnjóská catchments where an increase is projected, under both emission scenarios, leading to an increase in mean annual precipitation as well.

The projected warming leads to an increase in the fraction of annual precipitation falling as rain, at the expense of snow, which, in turn, leads to shorter snow seasons and less snow storage. The rise in temperature is also expected to lead to an increase in the number of snowmelt events in autumn and/or winter and to contribute to instabilities in the build-up of the snowpack. The projected snow storage reduction leads to a decrease in spring/summer snowmelt.

In the present climate, the hydrological regimes of the Svartá and Fnjóská catchments are strongly influenced by the seasonality of snow accumulation and melt, leading to a strong contrast between low flows in winter when snow accumulates, and high flows in spring when snow melts, whereas the Laxá catchment has a more mixed rainfall/snowmelt regime with high flows in autumn due to rainfall and high flows in spring due to snowmelt. Projected changes in climatic conditions are

expected to impact the streamflow seasonality pattern of the three studied catchments along the 21st century, but the timing, magnitude and direction of changes vary with the catchment, season and emission scenario. Results indicate that mean seasonal river flow is likely to (i) increase in autumn and winter in the three catchments, (ii) decrease in spring in the three catchments, (iii) decrease in summer in the Fnjóská and Laxá catchments, remain unchanged in summer in the Svartá catchment under the lowest emission scenario but increase moderately in the second-half of the 21st century under the highest emission scenario. The peak of mean daily discharge in May/ June is projected to gradually decrease and shift earlier in the three catchments. Note that in spring, mean daily flow is actually projected to increase in April and in the first part of May, depending on the projection horizon and catchment, but the decrease projected in the second part of May and in June leads to an overall decrease in mean flow, when averaged over the season. All these changes reflect the increasing influence of rainfall or the combination of rainfall and snowmelt in autumn/winter, and the decreasing influence of spring snowmelt, on runoff generation, caused by the projected warming. Changes in mean seasonal flow are not necessarily gradual along the projection horizon, like warming, because precipitation fluctuations contribute to modulate these changes.

Projected changes in climatic conditions are also expected to have an impact on flood risk in the future. In the Svartá catchment, annual maximum floods are projected to occur less and less frequently in spring and more and more often in the other seasons, especially winter, and their magnitude is projected to decrease, owing to the projected reduction in snow storage and subsequent decrease in spring snowmelt. In the Fnjóská catchment, annual maximum floods are projected to occur less and less frequently in spring and summer, and more and more frequently in autumn and winter, especially under the highest emission scenario, and their magnitude is projected to decrease. In contrast, the Laxá catchment is projected to remain under the dominating influence of rainfall-generated annual maximum floods in autumn, but a slight magnitude increase is likely to be expected in some future periods, likely because of rainfall intensification. Projected changes in the magnitude of annual maximum floods are associated with large uncertainties whilst changes affecting their timing appear to be more robust.

The projected changes in streamflow characteristics are often more pronounced and/or start earlier under the RCP8.5 emission scenario than under the RCP4.5 emission scenario because the warming is greater and leads to larger changes in the ratio of rainfall and snowfall and to a larger decrease in snow storage.

In conclusion, projected climate change is expected to have a significant impact on the hydrological characteristics of the three studied catchments in the future. The main driver of these changes is the projected warming but the timing, magnitude and direction of the hydrological response vary with the emission scenario, season and catchment characteristics. Therefore, in order to better understand the hydrological response to projected climate change across Iceland, this type of impact assessment study should be extended to other river basins representative of the hydro-climatic conditions encountered in the country.

Acknowledgements

This work was supported by the Icelandic Road and Coastal Administration Research Fund.

The author acknowledges the World Climate Research Programme's Working Group on Regional Climate, and the Working Group on Coupled Modelling, former coordinating body of CORDEX and responsible panel for CMIP5. The author acknowledges the climate modelling groups (listed in Table 2 in this report) for producing and making available their model output. The author also acknowledges the Earth System Grid Federation infrastructure an international effort led by the U.S. Department of Energy's Program for Climate Model Diagnosis and Intercomparison, the European Network for Earth System Modelling and other partners in the Global Organisation for Earth System Science Portals (GO-ESSP).

DEMs were created from DigitalGlobe, Inc., imagery and funded under National Science Foundation awards 1043681, 1559691, and 1542736.

The author wishes to thank the Swedish Meteorological and Hydrological Institute for making the HYPE model available.

Veðurstofa Íslands provided the ICRA climate reanalysis and discharge observations (IMO database, service no. 2019-11-01/01).

Data analysis was performed with the R software (R Core Team, 2016).

9 References

Aðalgeirsdóttir, G., Magnússon, E., Pálsson, F., Thorsteinsson, T., Belart, J.M.C., Jóhannesson, T., Hannesdóttir, H., Sigurðsson, O., Gunnarsson, A., Einarsson, B., Berthier, E., Steffensen Schmidt, L., Haraldsson, H. H., and Björnsson, H. (2020). Glacier Changes in Iceland From ~1890 to 2019. *Front. Earth Sci.* , 8, 1-15, doi: 10.3389/feart.2020.523646.

Arheimer, B. and Lindström, G. (2015). Climate impact on floods: changes in high flows in Sweden in the past and the future (1911–2100). *Hydrol. Earth Syst. Sci.*, 19, 771–784, 2015. doi:10.5194/hess-19-771-2015.

Arnalds, O. (2015). The Soils of Iceland. World Soils Book Series. Springer Netherlands.

Arnalds, Ó., and Óskarsson, H. (2009). Íslenskt jarðvegskort (Soil map of Iceland). Nátturufræðingurinn 78:107-121.

Árnason, K., and Matthíasson, I. (2017). CORINE - landflokkun 2012. Landgerðabreytingar á Íslandi 2006-2012. Landmælingar Íslands.

Benestad, R., Haensler, A., Hennemuth, B., Illy, T., Jacob, D., Keup-Thiel, E., Kotlarski, S., Nikulin, G., Otto, J., Rechid, D., Sieck, K., Sobolowski, S., Szabó, P., Szépszó, G., Teichmann, C., Vautard, R., Weber, T., Zsebeházi G. (2017). Guidance for EURO-CORDEX climate projections data use. EURO-CORDEX Guidelines Version 1.0 - 2017.08. (www.euro-cordex.net)

Björnsson, H., Sigurðsson, B. D., Davíðsdóttir, B., Ólafsson, J., Ástþórssson, Ó. S., Ólafsdóttir, S., Baldursson, T., and Jónsson, T. (2018). Loftslagsbreytingar og áhrif þeirra á Íslandi – Skýrsla vísindanefndar um loftslagsbreytingar 2018. Veðurstofa Íslands.

Brigode, P., Oudin, L., and Perrin, C. (2013). Hydrological model parameter instability: A source of additional uncertainty in estimating the hydrological impacts of climate change? *J. Hydrol.*, 476, 410-425. https://doi.org/10.1016/j.jhydrol.2012.11.012

Climate Change and Energy Systems. Impacts, risks and adaptation in the Nordic and Baltic countries. Th. Thorsteinsson and H. Björnsson Eds. TemaNord (2011):502, 226 pp.

Crochet, P. (2007). A study of regional precipitation trends in Iceland using a high quality gauge network and ERA-40. *J. Climate,* 20(18), 4659-4677.

Crochet, P. (2013). Sensitivity of Icelandic river basins to recent climate variations. *Jökull*, 63, 71-90.

Crochet, P. (2020). Flood frequency analysis in a changing climate - Climate change impact on design flood (160p). Report prepared for the Icelandic Road and Coastal Administration Research Fund. https://www.vegagerdin.is/link_to_report

Crochet, P. (2021). Impact of climate change on mean and high streamflow characteristics in Icelandic watersheds: a case study (166p). Report prepared for the Icelandic Road and Coastal Administration Research Fund. https://www.vegagerdin.is/link_to_report

Dee, D. P., Uppala, S. M., Simmons, A. J., Berrisford, P., Poli, P., Kobayashi, S., Andrae, U., Balmaseda, M. A., Balsamo, G., Bauer, P., Bechtold, P., Beljaars, A. C. M., van de Berg, L., Bidlot, J., Bormann, N., Delsol, C., Dragani, R., Fuentes, M., Geer, A. J., Haimberger, L., Healy, S. B., Hersbach, H., Hólm, E. V., Isaksen, L., Kållberg, P., Köhler, M., Matricardi, M., McNally, A. P., Monge-Sanz, B. M., Morcrette, J.-J., Park, B.-K., Peubey, C., de Rosnay, P., Tavolato, C., Thépaut, J.-N., and Vitart, F. (2011). The ERA-Interim reanalysis: configuration and performance of the data assimilation system, *Q.J.R. Meteorol. Soc.*, 137(656), 553–597, doi:10.1002/qj.828.

Delignette-Muller, M.L., and Dutang, C. (2015). "fitdistrplus: An R Package for Fitting Distributions." *Journal of Statistical Software*, 64(4), 1–34.

Doherty, J. (2021). PEST: Model-independent parameter estimation. User manual part I: PEST, SENSAN and global optimisers. (7th Ed. with latest additions). Watermark Numerical Computing.

Einarsson, B., and Jónsson, S. (2010). The effect of climate change on runoff from two watersheds in Iceland. VÍ-2010-016 report, 34 pp. Veðurstofa Íslands.

Frans, C., Istanbulluoglu, E., Lettenmaier, D.P., Fountain, A.G., and Riedel, J. (2018). Glacier Recession and the response of summer streamflow in the Pacific Northwest United States, 1960-2099. *Water Resour. Res.*, 54, 6202-6225, https://doi.org/10.1029/2017WR021764

Giorgetta, M.A., Jungclaus, J., Reick, C., Legutke, S., Bader, J., Böttinger, M., Brovkin, V., Crueger, T., Esch, M., Fieg, K., Glushak, K., Gayler, V., Haak, H., Hollweg, H., Ilyina, T., Kinne, S., Kornblueh, L., Matei, D., Mauritsen, T., Mikolajewicz, U., Mueller, W., Notz, D., Pithan, F., Raddatz, T., Rast, S., Redler, R., Roeckner, E., Schmid, H., Schnur, R., Segschneider, J., Six, K.D., Stockhause, M., Timmreck, C., Wegner, J., Widmann, H., Weiners, K., Claussen, M., Marotzke, J., and Stevens, B. (2013). Climate and carbon cycle changes from 1850 to 2100 in MPI-ESM simulations for the coupled model intercomparison project phase 5. *Journal of Advances in Modeling Earth Systems* 5:572–597, https://doi.org/10.1002/jame.20038.

Giorgi, F., Jones, C., and Asrar, G. R. (2009). Addressing climate information needs at the regional level: the CORDEX framework, World Meteorological Organization (WMO) Bulletin, 58(3), 175-183.

Gosling, S.N., Taylor, R.G., Arnell, N.W., and Todd, M.C. (2011). A comparative analysis of projected impacts of climate change on river runoff from global and catchment-scale hydrological models. *Hydrol. Earth Syst. Sci.*, 15, 279–294, doi:10.5194/hess-15-279-2011.

Gosseling, M. (2017). CORDEX climate trends for Iceland in the 21st century. VI-report 2017-009. Veðurstofa Íslands.

Graham, L.P., Hagemann, S., Jaun, S., and Beniston, M.. (2007). On interpreting hydrological change from regional climate models. *Climatic Change,* 81 (Suppl 1), 97–122. https://doi.org/10.1007/s10584-006-9217-0.

Gudmundsson, L., Bremnes, J. B., Haugen, J. E., and Engen-Skaugen, T. (2012). Technical Note: Downscaling RCM precipitation to the station scale using statistical transformations – a comparison of methods, *Hydrol. Earth Syst. Sci.*, 16, 3383–3390, https://doi.org/10.5194/hess-16-3383-2012.

Gudmundsson, L. (2016). qmap: Statistical transformations for post-processing climate model output. R package version 1.0-4.

Habets, F., Boé, J., Déqué, M., Ducharne, A., Gascoin, S., Hachour, A., Martin, E., Pagé, C., Sauquet, E., Terray, L., Thiéry, D., Oudin, L., and Viennot, P. (2013). Impact of climate change on the hydrogeology of two basins in northern France. *Climatic Change*, 121: 771-785. DOI 10.1007/s10584-013-0934-x

Hróðmarsson, H.B., and Þórarinsdóttir, T. (2018). Flóð íslanskra vatnsfalla, Flóðagreining rennslisraða. VÍ-2018-003 report, 144 pp. Veðurstofa Íslands.

IPCC, 2021: Summary for Policymakers. In: *Climate Change 2021: The Physical Science Basis. Contribution of Working Group I to the Sixth Assessment Report of the Intergovernmental Panel on Climate Change.* (2021). Masson-Delmotte, V., P. Zhai, A. Pirani, S.L. Connors, C. Péan, S. Berger, N. Caud, Y. Chen, L. Goldfarb, M.I. Gomis, M. Huang, K. Leitzell, E. Lonnoy, J.B.R. Matthews, T.K. Maycock, T. Waterfield, O. Yelekçi, R. Yu, and B. Zhou (eds.). Cambridge University Press, Cambridge, United Kingdom and New York, NY, USA, pp. 3−32, doi:10.1017/9781009157896.001.

Jacob, D., Elizalde, A., Haensler, A., Hagemann, S., Kumar, P., Podzun, R., Rechid, D., Remedio, A.R., Saeed, F., Sieck, K., Teichmann, C., and Wilhelm, C. (2012). Assessing the transferability of the regional climate model REMO to different coordinated regional climate downscaling experiment (CORDEX) regions. *Atmosphere* 3(1): 181-199. https://doi.org/10.3390/atmos3010181.

Jacob, D., Petersen, J., Eggert, B., Alias, A., Christensen, O.B., Bouwer, L.M., Braun, A., Colette, A., Déqué, M., Georgievski, G., Georgopoulou, E., Gobiet, A., Menut, L., Nikulin, G., Haensler, A., Hempelmann, N., Jones, C., Keuler, K., Kovats, S., Kröner, N., Kotlarski, S., Kriegsmann, A., Martin, E., van Meijgaard, E., Moseley, C., Pfeifer, S., Preuschmann, S., Radermacher, C., Radtke, K., Rechid, D., Rounsevell, M., Samuelsson, P., Somot, S., Soussana, J.-F., Teichmann, C., Valentini, R., Vautard, R., Weber, B., and Yiou, P. (2014). EURO-CORDEX: new high-resolution climate change projections for European impact research. *Reg Environ Change* 14:563–578. https://doi.org/10.1007/s10113-013-0499-2.

Jones, C. D., Hughes, J. K., Bellouin, N., Hardiman, S. C., Jones, G. S., Knight, J., Liddicoat, S., O'Connor, F. M., Andres, R. J., Bell, C., Boo, K.-O., Bozzo, A., Butchart, N., Cadule, P., Corbin, K. D., Doutriaux-Boucher, M., Friedlingstein, P., Gornall, J., Gray, L., Halloran, P. R., Hurtt, G., Ingram, W. J., Lamarque, J.-F., Law, R. M., Meinshausen, M., Osprey, S., Palin, E. J., Parsons, Chini, L., Raddatz, T., Sanderson, M. G., Sellar, A. A., Schurer, A., Valdes, P., Wood, N., Woodward, S., Yoshioka, M., and Zerroukat, M. (2011). The HadGEM2-ES implementation of CMIP5 centennial simulations. *Geosci. Model Dev*., 4, 543-570. doi:10.5194/gmd-4-543-2011.

Jóhannesson, T., and co-authors (2007). Effect of climate change on hydrology and hydro-resources in Iceland. OS-2007/011, 91 pp.

Kupiainen, M., Samuelsson, P., Jones, C., Jansson, C., Willén, U., Hansson, U., Ullerstig, A., Wang, S., and Döscher, R. (2011). Rossby Centre regional atmospheric model, RCA4. Rossby Centre Newsletter.

Lane, R.A., and Kay, A.L. (2021). Climate change impact on the magnitude and timing of hydrological extremes across Great Britain. *Front. Water, 3:684982*, https://doi.org/10.3389/frwa.2021.684982.

Lindström, G., Pers, C., Rosberg, J., Strömqvist, J. and Arheimer, B. (2010). Development and testing of the HYPE (Hydrological Predictions for the Environment) water quality model for different spatial scales. *Hydrol. Res.*, 41, 3-4, 295-319.

Nash, J.E., and Sutcliffe, J.V. (1970). River flow forecasting through conceptual models part I - A discussion of principles. *J. Hydrol.*, 10 (3), 282-290. doi:10.1016/0022-1694(70)90255-6.

Nawri, N., Pálmason, B., Petersen, G.N., Björnsson, H., and Þorsteinsson, S. (2017). The ICRA atmospheric reanalysis project for Iceland. VÍ Report, 2017-005. Veðurstofa Íslands.

Naz, B.S., Kao, S.C, Ashfaq, M., Rastogi, D., Mei, R., and Bowling, L.C. (2016). Regional hydrologic response to climate change in the conterminous United States using high-resolution hydroclimate simulations. *Glob. Planet. Chang.,* 143, 100-117.

Osuch, M., Romanowicz, R., and Wong, W.K. (2018). Analysis of low flow indices under varying climatic conditions in Poland. *Hydrol. Res.*, 49 (2), 373-389, https://doi.org/10.2166/nh.2017.021.

Ott, I., Duethmann, D., Liebert, J., Berg, P., Feldmann, H., Ihringer, J., Kunstmann, H., Merz, B., Schaedler, G., and Wagner, S. (2013). High-resolution climate change impact analysis on medium-sized river catchments in Germany: an ensemble assessment. *J. Hydrometeorol.*, 14 (4), 1175-1193, https://doi.org/10.1175/JHM-D-12-091.1.

Porter, C., Morin, P., Howat, I., Noh, M.-J., Bates, B., Peterman, K, Keesey, S., Schlenk, M., Gardiner, J., Tomko, K., Willis, M., Kelleher, C., Cloutier, M., Husby, E., Foga, S., Nakamura, H., Platson, M., Wethington, M. Jr., Williamson, C., Bauer, G., Enos, J., Arnold, G., Kramer, W., Becker, P., Doshi, A., D'Souza, C., Cummens, P., Laurier, F., and Bojesen, M. (2018). "ArcticDEM", https://doi.org/10.7910/DVN/OHHUKH, Harvard Dataverse, V1, [Accessed Nov. 2019].

R Core Team (2016). R: A language and environment for statistical computing. R Foundation for Statistical Computing, Vienna, Austria. URL https://www.R-project.org/.

Rockel, B., Will, A., and Hense, A. (2008). The regional climate model COSMO-CLM (CCLM). *Meteorol Z,* 17(4), 347–348. doi:10.1127/0941-2948/2008/0309.

Samuelsson, P., Jones, C., Willén, U., Ullerstig, A., Gollvik, S., Hansson, U., Jansson, C., Kjellström, E., Nikulin, G., and Wyser, K. (2011). The Rossby Centre Regional Climate Model RCA3: model description and performance. *Tellus* 63A. doi:10.1111/j.1600-0870.2010.00478.x.

Somers, L.D., McKenzie, J.M., Mark, B.G., Lagos, P., Ng., G-H. C., Wickert, A.D., Yarleque, C., Baraër, M., and Silva, Y. (2019). Groundwater buffers decreasing glacier melt in an Andean watershed—but not forever. *Geophysical Research Letters*, 46 (22), 13016-13026, https://doi.org/10.1029/2019GL084730.

Stephenson, A.G. (2002). evd: Extreme Value Distributions. R News, 2(2):31-32, June 2002. URL: http://CRAN.R-project.org/doc/Rnews/.

van Meijgaard, E., van Ulft, L.H., Lenderink, G., de Roode, S.R., Wipfler, L., Boers, R., and Timmermans, R.M.A. (2012). Refinement and application of a regional atmospheric model for climate scenario calculations of Western Europe. Climate changes Spatial Planning publication: KvR 054/12, ISBN/EAN 978-90-8815-046-3, pp 44.

Vetter, T., Huang, S., Aich, V., Yang, T., Wang. X., Krysanova, V., and Hattermann, F. (2015). Multi-model climate impact assessment and intercomparison for three large-scale river basins on three continents. *Earth Syst. Dynam.*, 6, 17-43, https://doi.org/10.5194/esd-6-17-2015.

Vormoor, K., Lawrence, D., Heistermann, M., and Bronstert, A. (2015). Climate change impacts on the seasonality and generation processes of floods – projections and uncertainties for catchments with mixed snowmelt/rainfall regimes. *Hydrol. Earth Syst. Sci.*, 19, 913-931, doi:10.5194/hess-19-913-2015.

Wan, W, Zhao, J., Li, H.-Y., Mishra, A., Hejazi, M., Lu, H., Demissie, Y., and Wang, H. (2018). A holistic view of water management impacts on future droughts: A global multimodel analysis. *J. Geophys. Res.: Atmospheres*, 123, 5947-5972, https://doi.org/10.1029/2017JD027825.

Wanders, N., and Wada, Y. (2015). Human and climate impacts on the 21st century hydrological drought. *J. Hydrol,* 526, 208-220, https://doi.org/10.1016/j.jhydrol.2014.10.047.

Zhao, Q., Ding, Y., Wang, J., Gao, H., Zhang, S., Zhao, C., Xu, J., Han, H., and Shangguan, D. (2019). Projecting climate change impacts on hydrological processes on the Tibetan Plateau with model calibration against the glacier inventory data and observed streamflow. *J. Hydrol.*, 573, 60-81.

Appendix 1

Observed and simulated Annual Maximum Floods

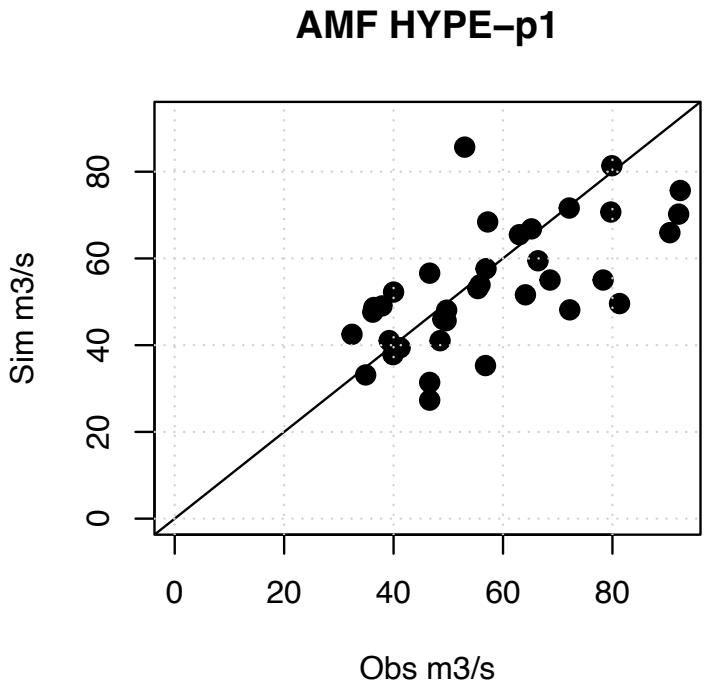

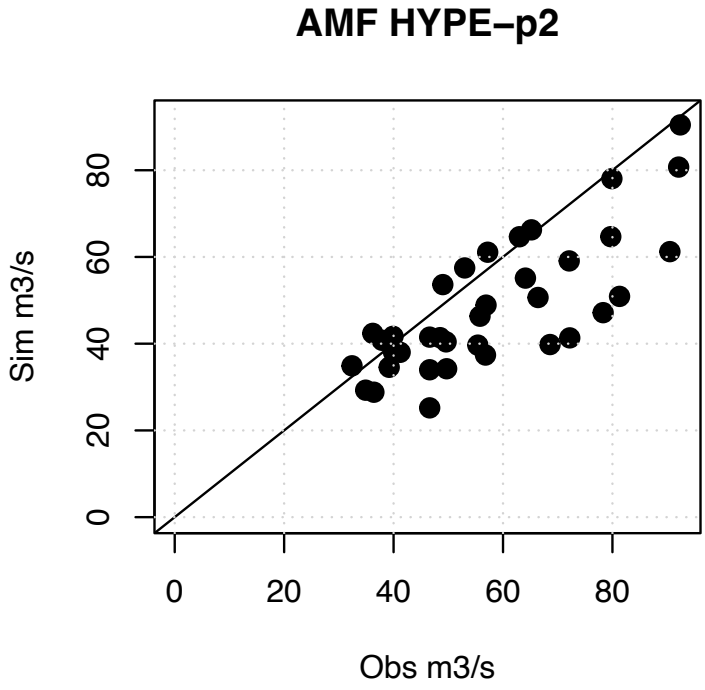

Fig. I-1: Catchment vhm10: Simulated vs. observed AMFs in the water years 1981-2016. Top: HYPE with parameter set calibrated in 1996-2002. Bottom: HYPE with parameter set calibrated in 2003-2009.

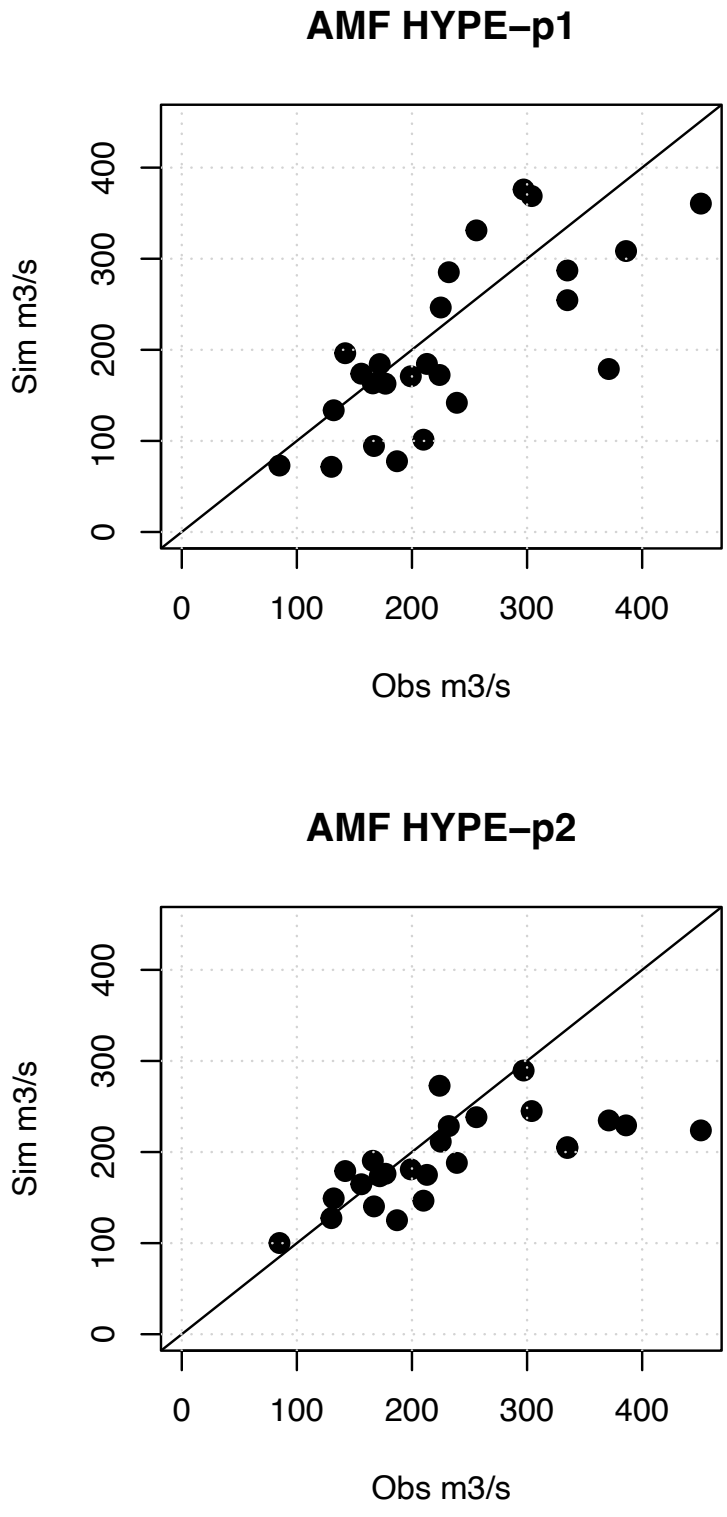

Fig. I-2: Catchment vhm200: Simulated vs. observed AMFs in the water years 1981-2016. Top: HYPE with parameter set calibrated in 1996-2002. Bottom: HYPE with parameter set calibrated in 2003-2009.

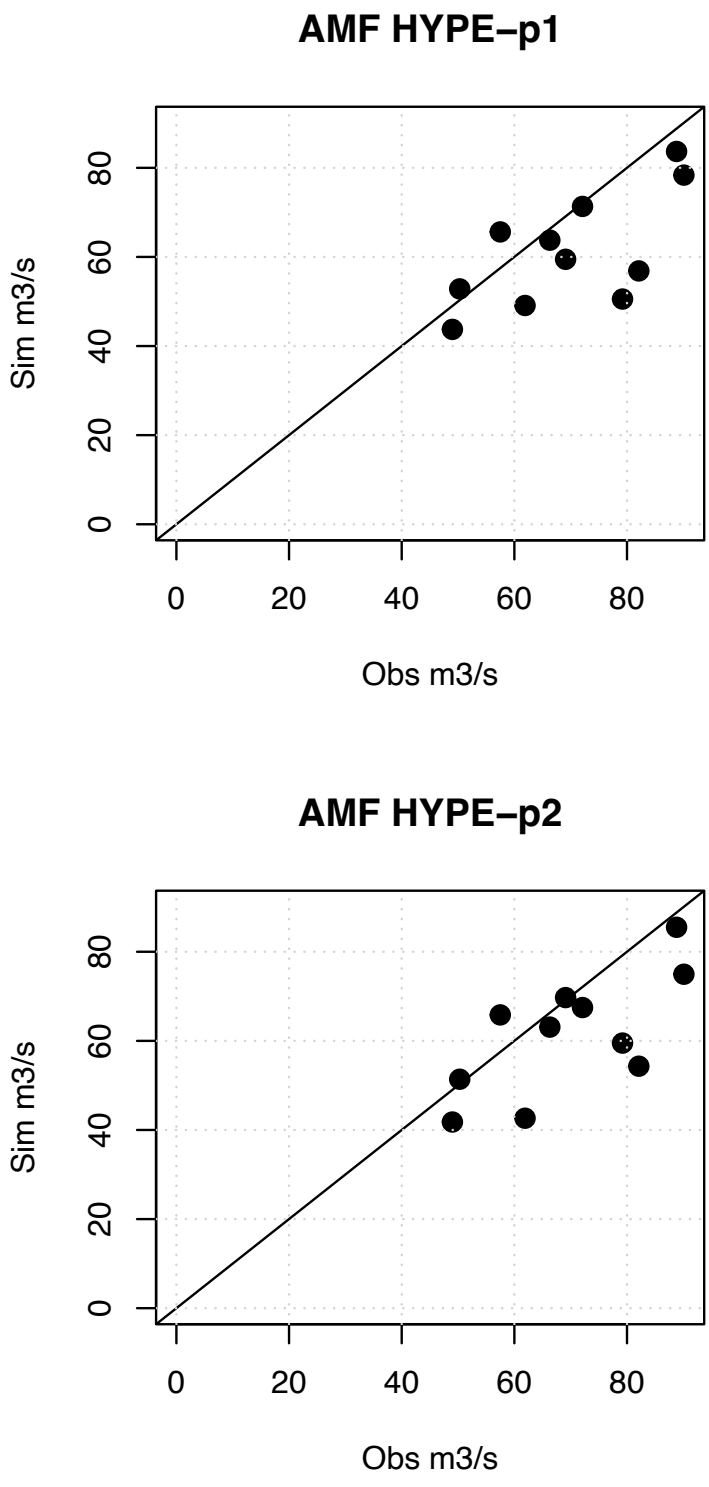

Fig. I-3: Catchment vhm74: Simulated vs. observed AMFs in the water years 2006-2016. Top: HYPE with parameter set calibrated in 2006-2011. Bottom: HYPE with parameter set calibrated in 2012-2016.

Appendix 2

CORDEX air temperature evaluation series

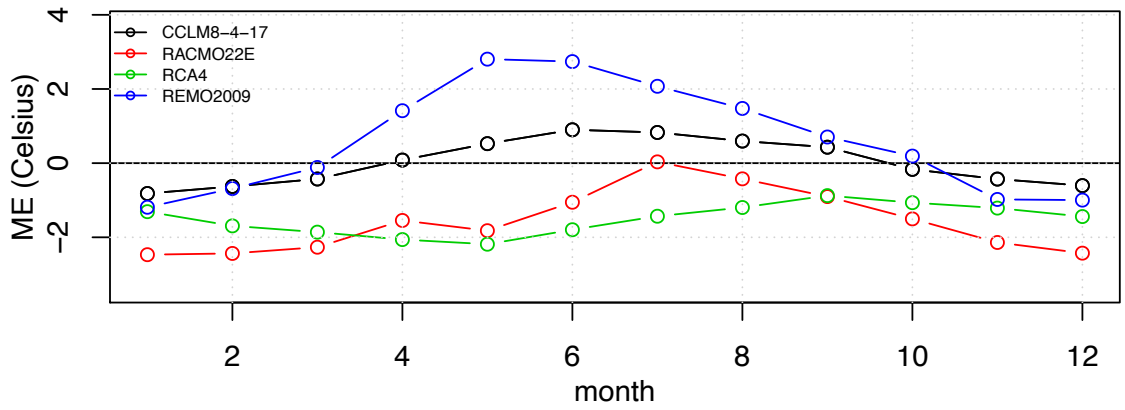

Fig. II-1: Catchment vhm10: Mean error (ME) between original CORDEX evaluation air temperature and ICRA air temperature. Period 1989-2008. Each colour corresponds to a RCM (cf. Table 3). The month=1 for January and 12 for December.

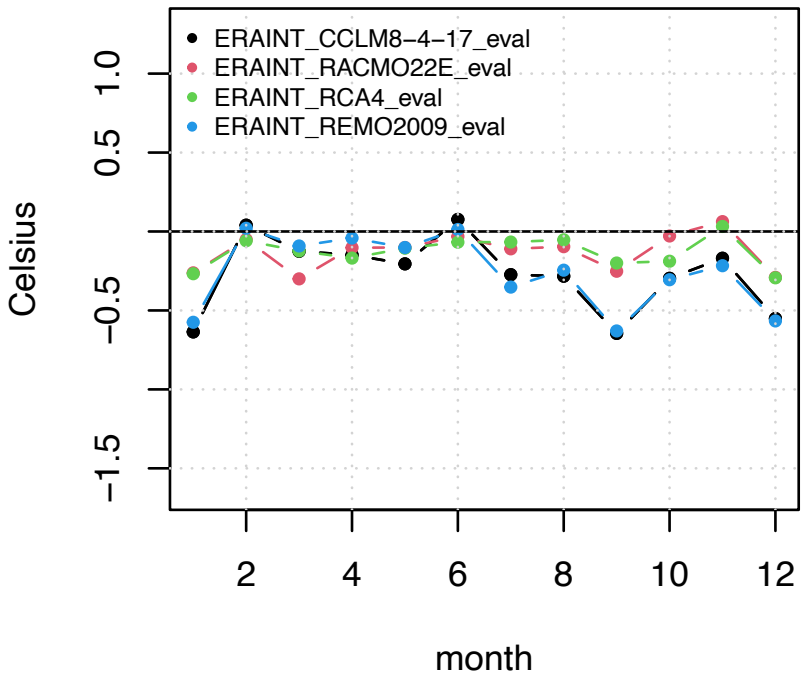

Fig. II-2: Catchment vhm10: Mean error (ME) between locally-adjusted CORDEX evaluation air temperature and ICRA air temperature. Period 1989-2008. The month=1 for January and 12 for December.

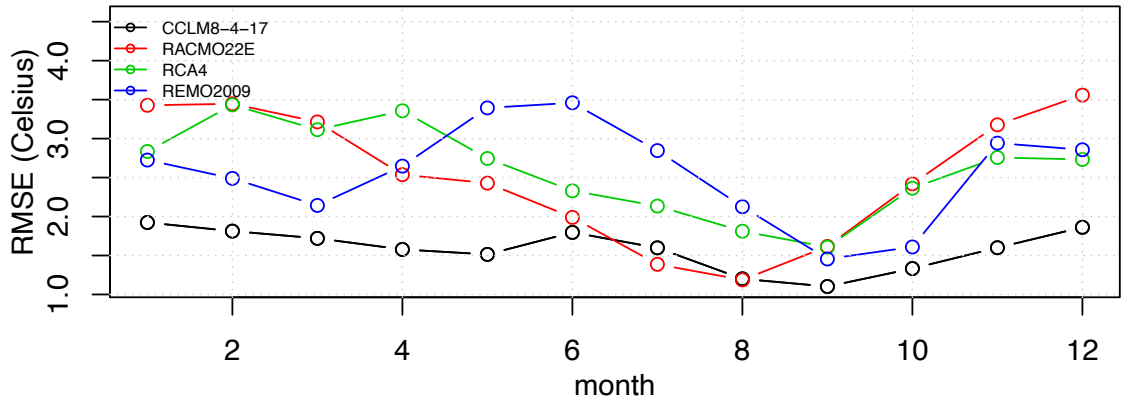

Fig. II-3: Catchment vhm10: Root mean square error (RMSE) between original CORDEX evaluation air temperature and ICRA air temperature. Period 1989-2008. Each colour corresponds to a RCM (cf. Table 3). The month=1 for January and 12 for December.

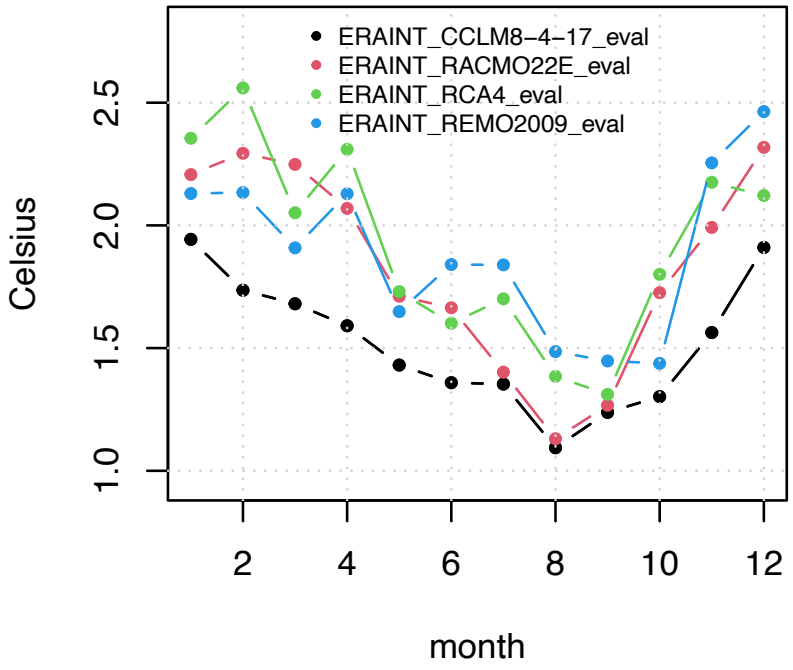

Fig. II-4: Catchment vhm10: Root mean square error (RMSE) between locally-adjusted CORDEX evaluation air temperature and ICRA air temperature. Period 1989-2008. The month=1 for January and 12 for December.

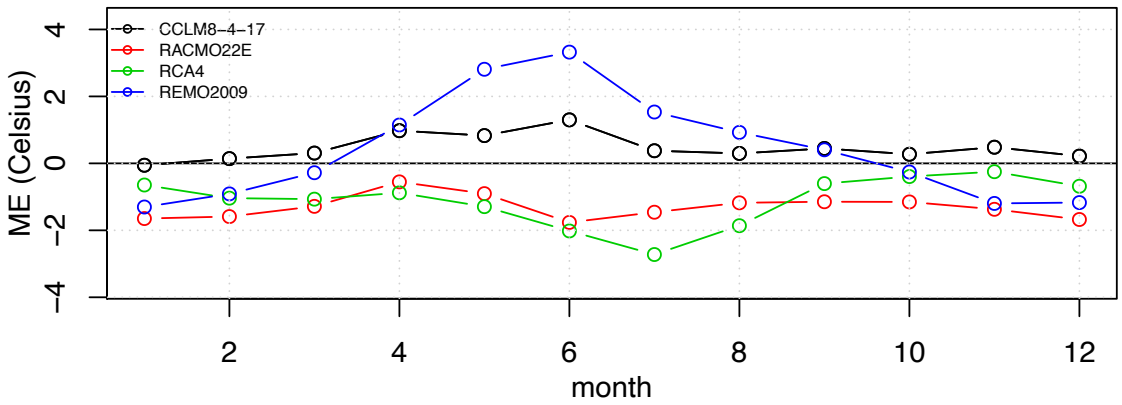

Fig. II-5: Catchment vhm200: Mean error (ME) between original CORDEX evaluation air temperature and ICRA air temperature. Period 1989-2008. Each colour corresponds to a RCM (cf. Table 3). The month=1 for January and 12 for December.

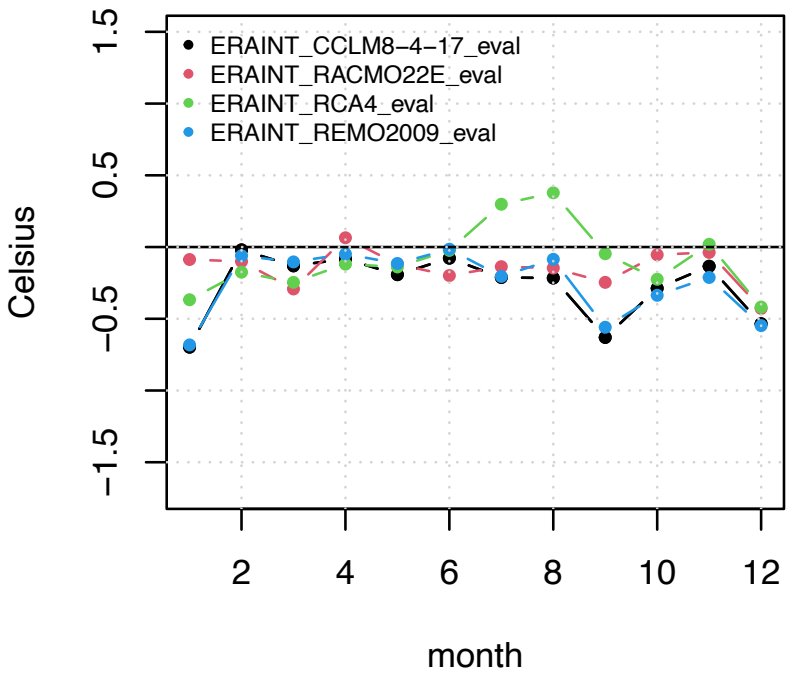

Fig. II-6: Catchment vhm200: Mean error (ME) between locally-adjusted CORDEX evaluation air temperature and ICRA air temperature. Period 1989-2008.The month=1 for January and 12 for December.

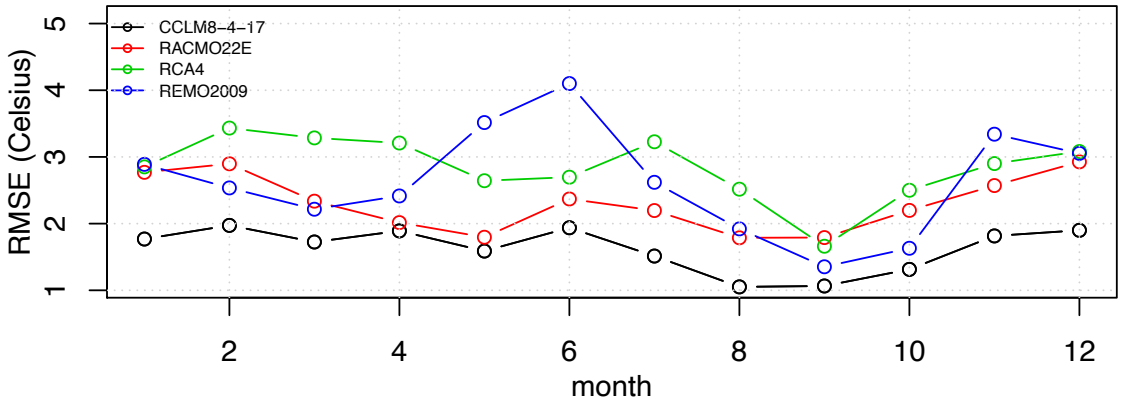

Fig. II-7: Catchment vhm200: Root mean square error (RMSE) between original CORDEX evaluation air temperature and ICRA air temperature. Period 1989-2008. Each colour corresponds to a RCM (cf. Table 3). The month=1 for January and 12 for December.

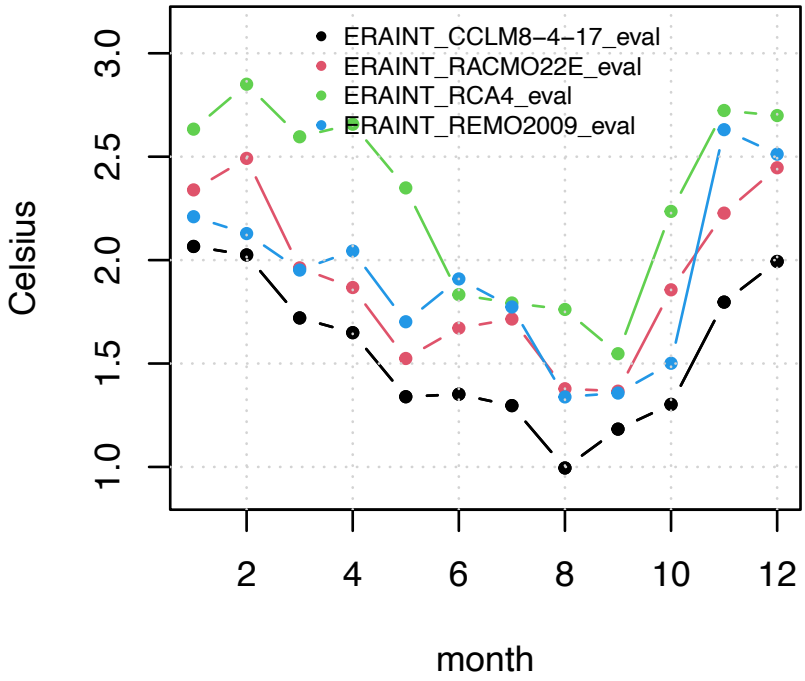

Fig. II-8: Catchment vhm200: Root mean square error (RMSE) between locally-adjusted CORDEX evaluation air temperature and ICRA air temperature. Period 1989-2008. The month=1 for January and 12 for December.

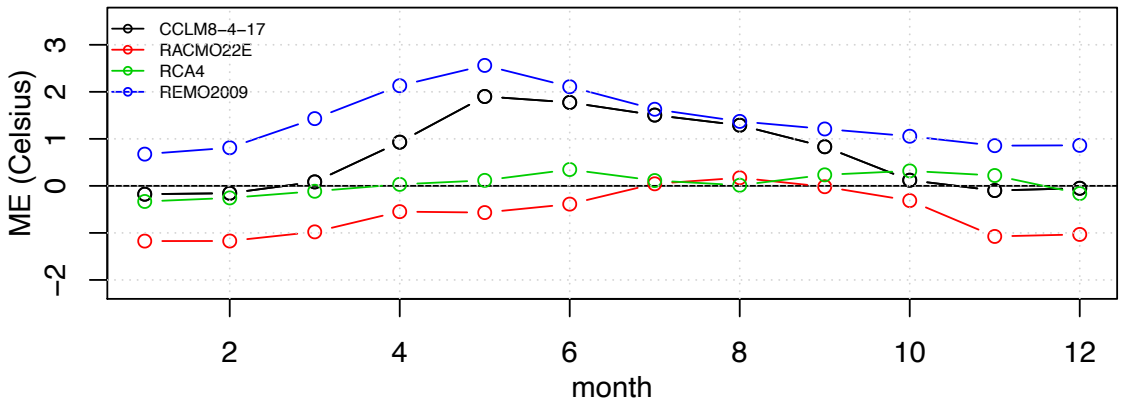

Fig. II-9: Catchment vhm74: Mean error (ME) between original CORDEX evaluation air temperature and ICRA air temperature. Period 1989-2008. Each colour corresponds to a RCM (cf. Table 3). The month=1 for January and 12 for December.

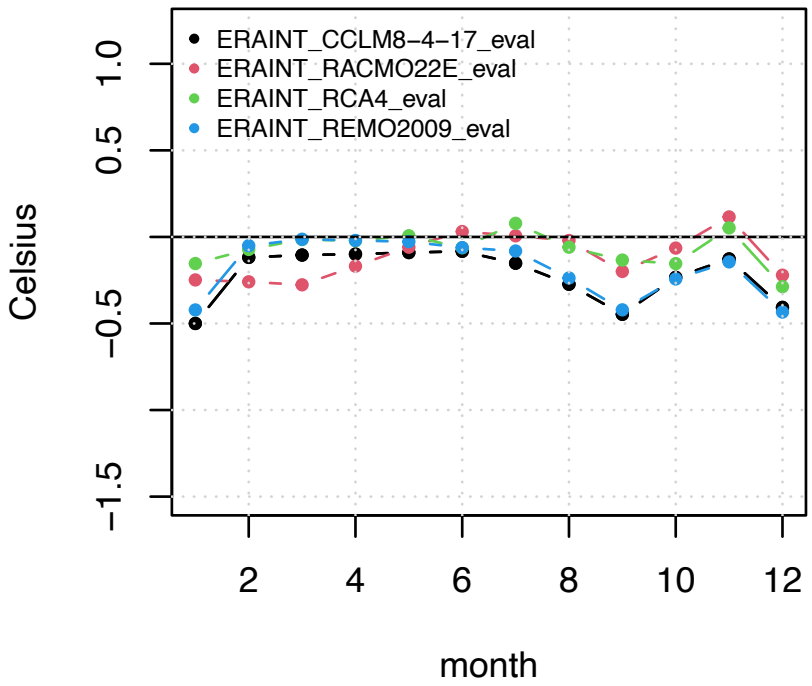

Fig. II-10: Catchment vhm74: Mean error (ME) between locally-adjusted CORDEX evaluation air temperature and ICRA air temperature. Period 1989-2008. The month=1 for January and 12 for December.

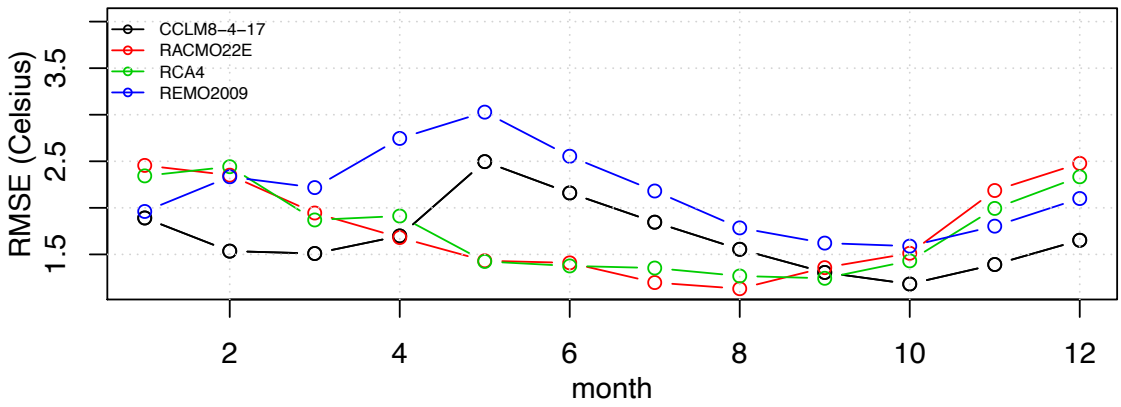

Fig. II-11: Catchment vhm74: Root mean square error (RMSE) between original CORDEX evaluation air temperature and ICRA air temperature. Period 1989-2008. Each colour corresponds to a RCM (cf. Table 3). The month=1 for January and 12 for December.

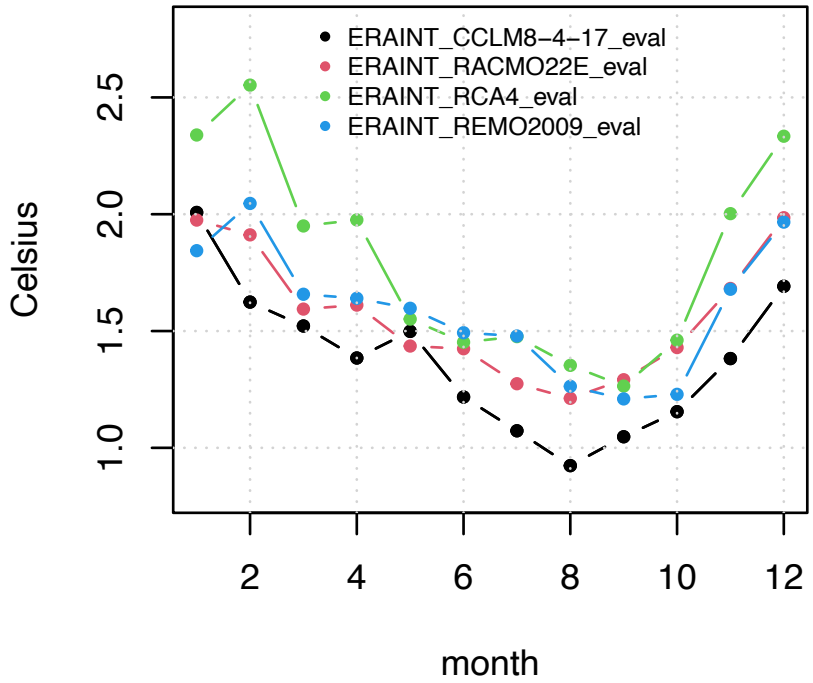

Fig. II-12: Catchment vhm74: Root mean square error (RMSE) between locally-adjusted CORDEX evaluation air temperature and ICRA air temperature. Period 1989-2008. The month=1 for January and 12 for December.

Appendix 3

CORDEX precipitation evaluation series

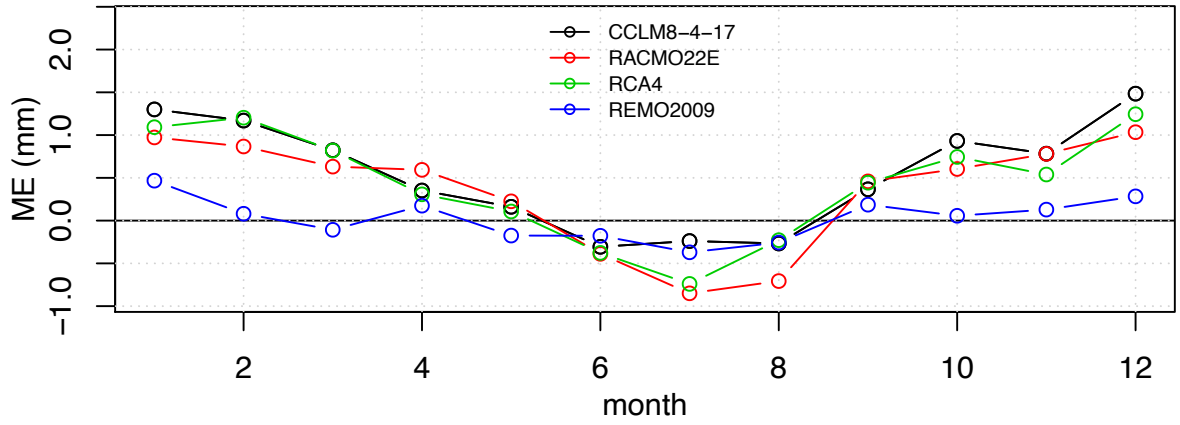

Fig. III-1: Catchment vhm10: Mean error (ME) between original CORDEX evaluation precipitation and ICRA precipitation (mm/d). Period 1989-2008. Each colour corresponds to a RCM (cf. Table 3). The month=1 for January and 12 for December.

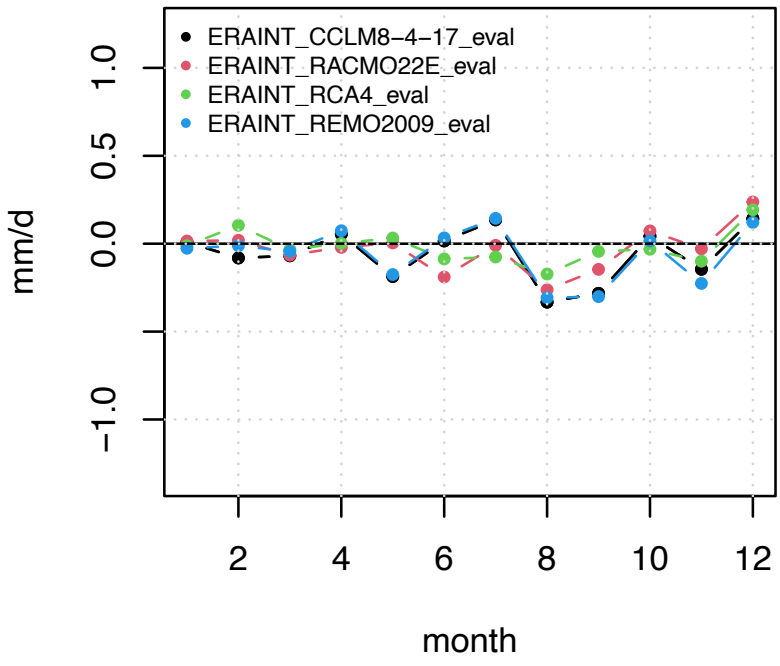

Fig. III-2: Catchment vhm10: Mean error (ME) between locally-adjusted CORDEX evaluation precipitation and ICRA precipitation (mm/d). Period 1989-2008. The month=1 for January and 12 for December.

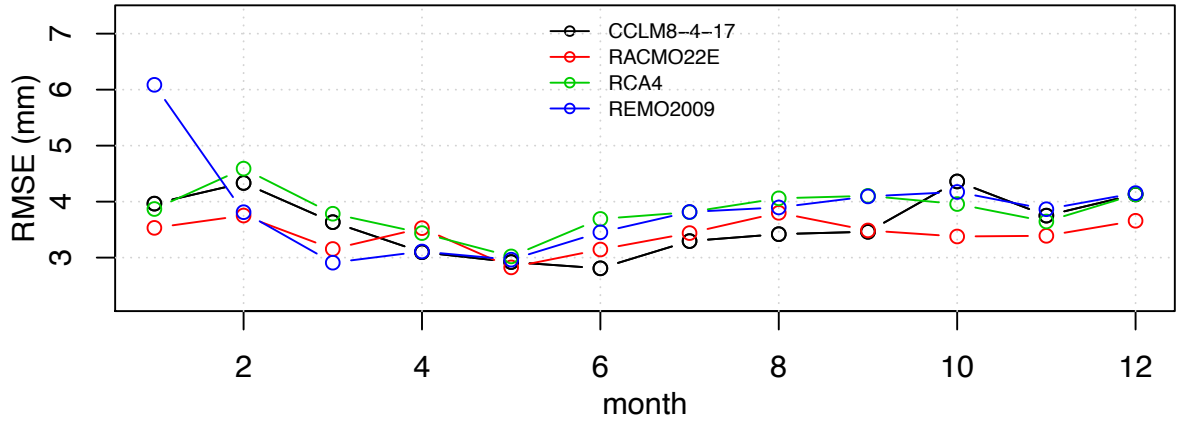

Fig. III-3: Catchment vhm10: Root mean square error (RMSE) between original CORDEX evaluation precipitation and ICRA precipitation (mm/d). Period 1989-2008. Each colour corresponds to a RCM (cf. Table 3). The month=1 for January and 12 for December.

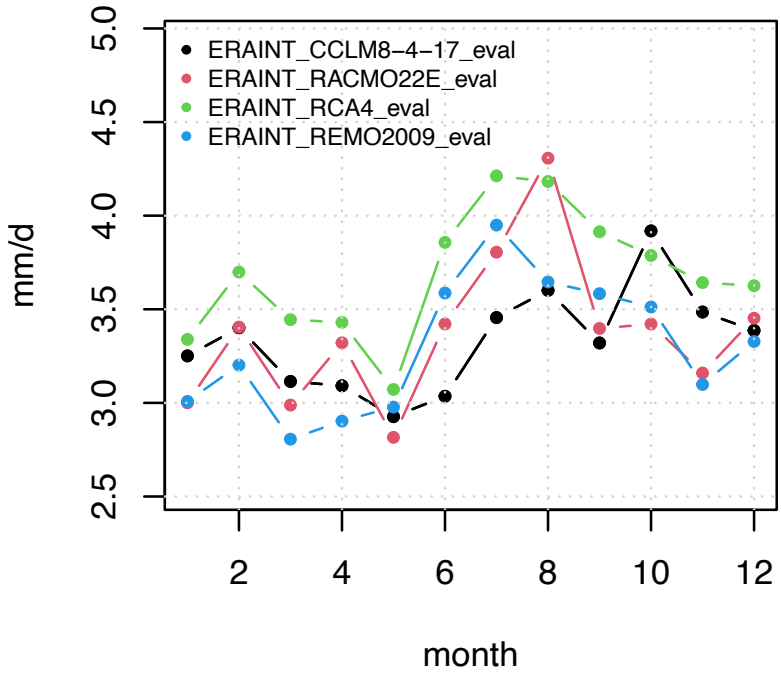

Fig. III-4: Catchment vhm10: Root mean square error (RMSE) between locally-adjusted CORDEX evaluation precipitation and ICRA precipitation (mm/d). Period 1989-2008. The month=1 for January and 12 for December.

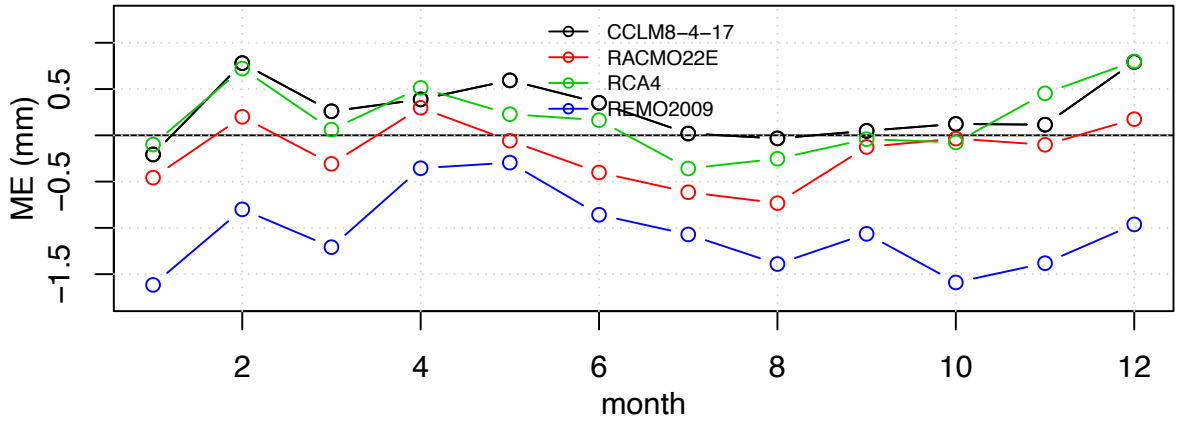

Fig. III-5: Catchment vhm200: Mean error (ME) between original CORDEX evaluation precipitation and ICRA precipitation (mm/d). Period 1989-2008. Each colour corresponds to a RCM (cf. Table 3). The month=1 for January and 12 for December.

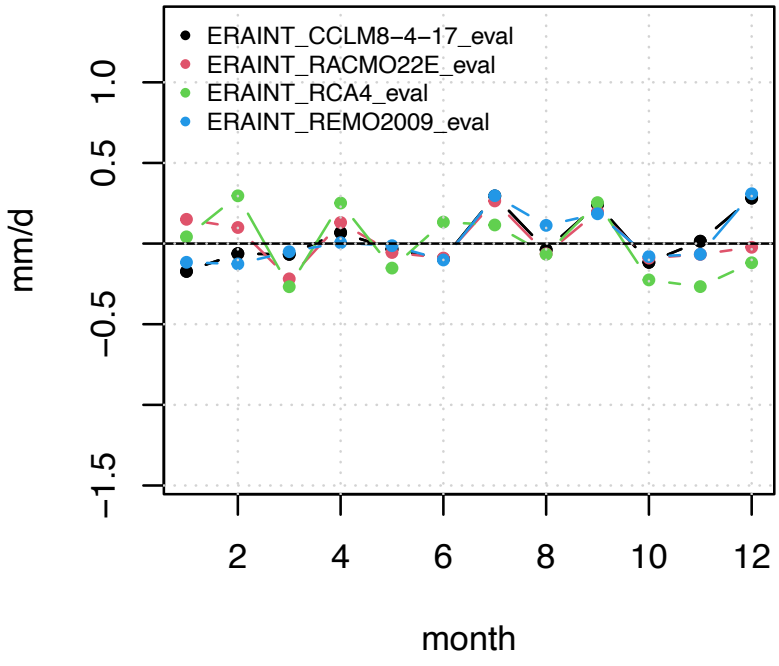

Fig. III-6: Catchment vhm200: Mean error (ME) between locally-adjusted CORDEX evaluation precipitation and ICRA precipitation (mm/d). Period 1989-2008. The month=1 for January and 12 for December.

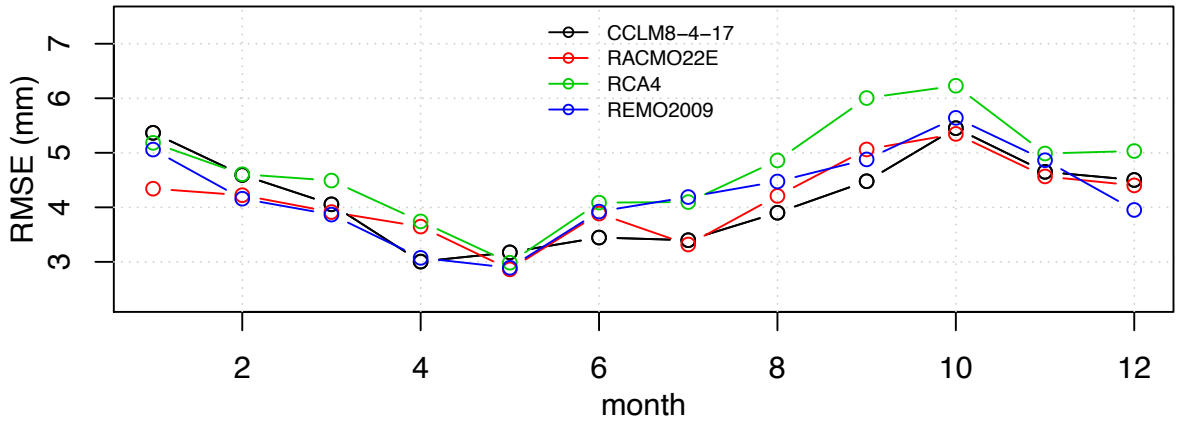

Fig. III-7: Catchment vhm200: Root mean square error (RMSE) between original CORDEX evaluation precipitation and ICRA precipitation (mm/d). Period 1989-2008. Each colour corresponds to a RCM (cf. Table 3). The month=1 for January and 12 for December.

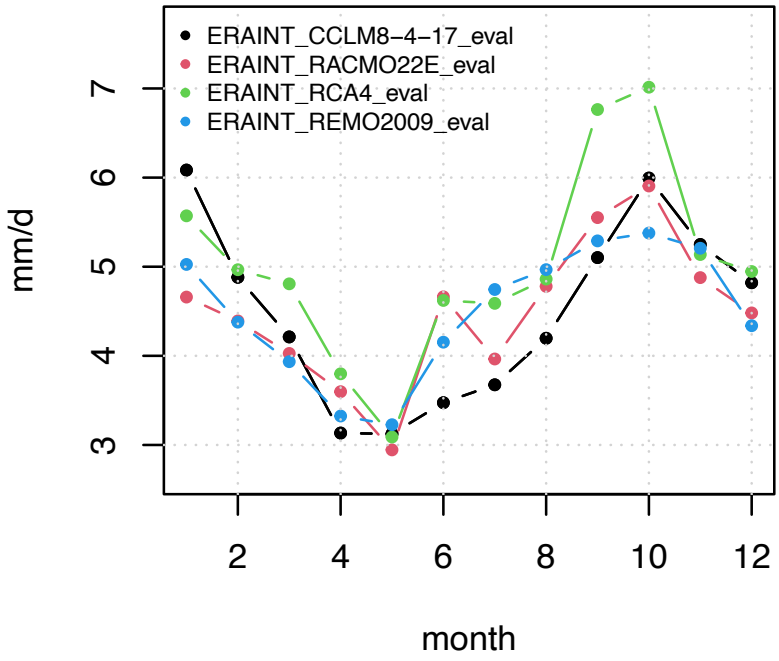

Fig. III-8: Catchment vhm200: Root mean square error (RMSE) between locally-adjusted CORDEX evaluation precipitation and ICRA precipitation (mm/d). Period 1989-2008. The month=1 for January and 12 for December.

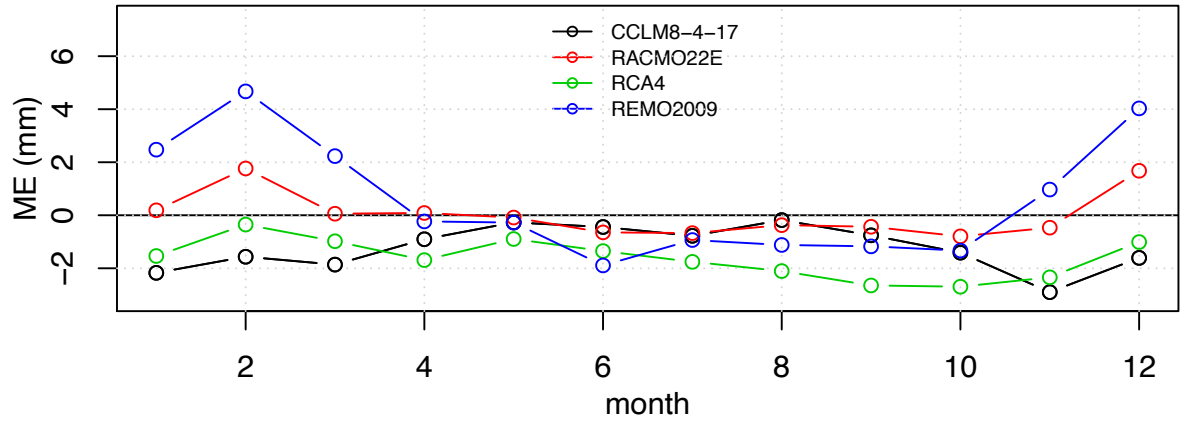

Fig. III-9: Catchment vhm74: Mean error (ME) between original CORDEX evaluation precipitation and ICRA precipitation (mm/d). Period 1989-2008. Each colour corresponds to a RCM (cf. Table 3). The month=1 for January and 12 for December.

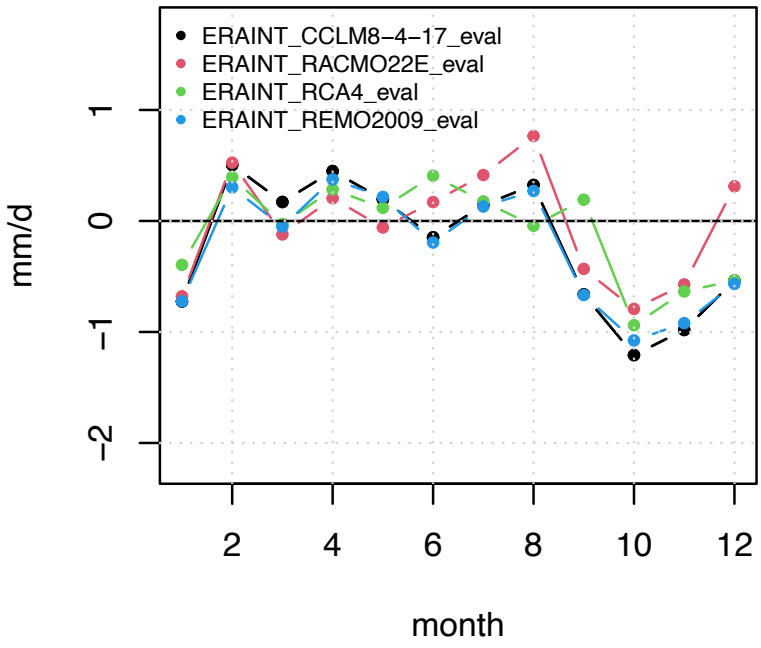

Fig. III-10: Catchment vhm74: Mean error (ME) between locally-adjusted CORDEX evaluation precipitation and ICRA precipitation (mm/d). Period 1989-2008. The month=1 for January and 12 for December.

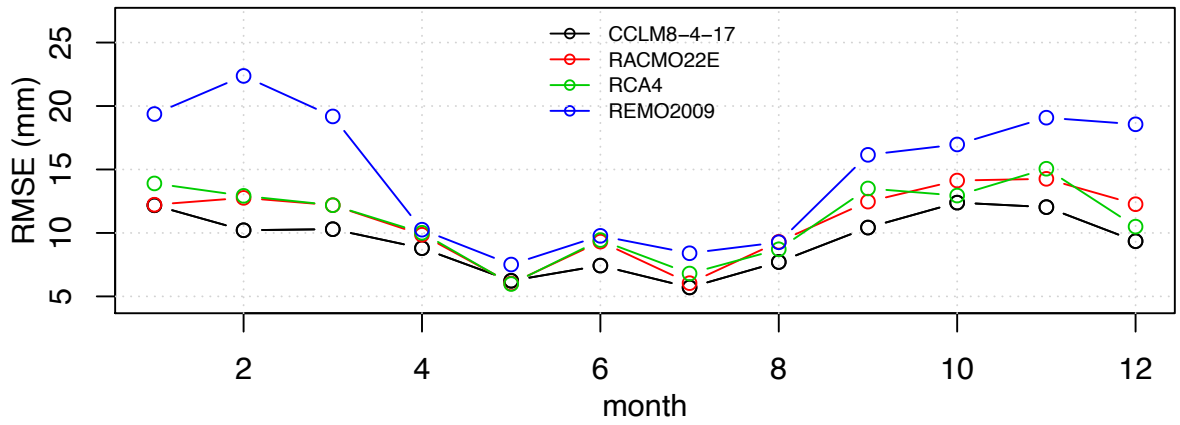

Fig. III-11: Catchment vhm74: Root mean square error (RMSE) between original CORDEX evaluation precipitation and ICRA precipitation (mm/d). Period 1989-2008. Each colour corresponds to a RCM (cf. Table 3). The month=1 for January and 12 for December.

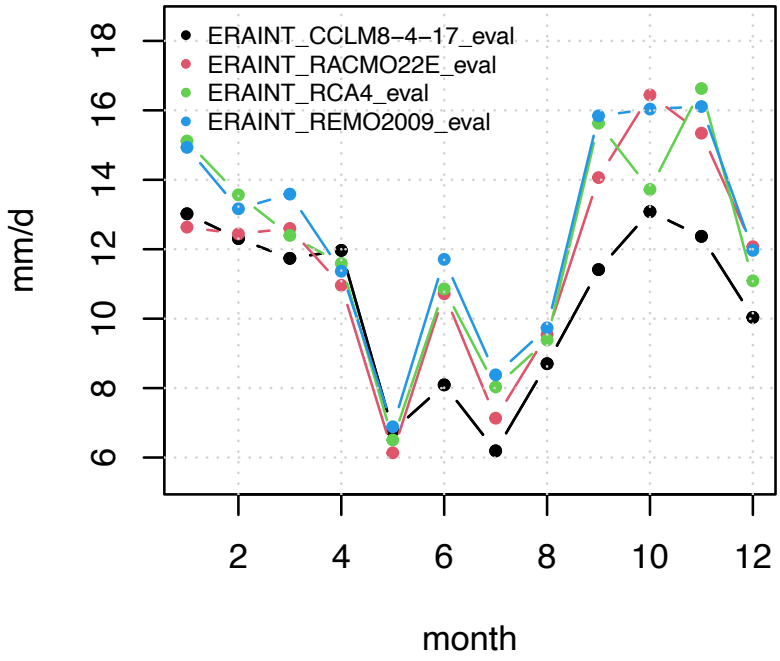

Fig. III-12: Catchment vhm74: Root mean square error (RMSE) between locally-adjusted CORDEX evaluation precipitation and ICRA precipitation (mm/d). Period 1989-2008. The month=1 for January and 12 for December.

Appendix 4

Mean monthly air temperature in the reference period (1981-2010)

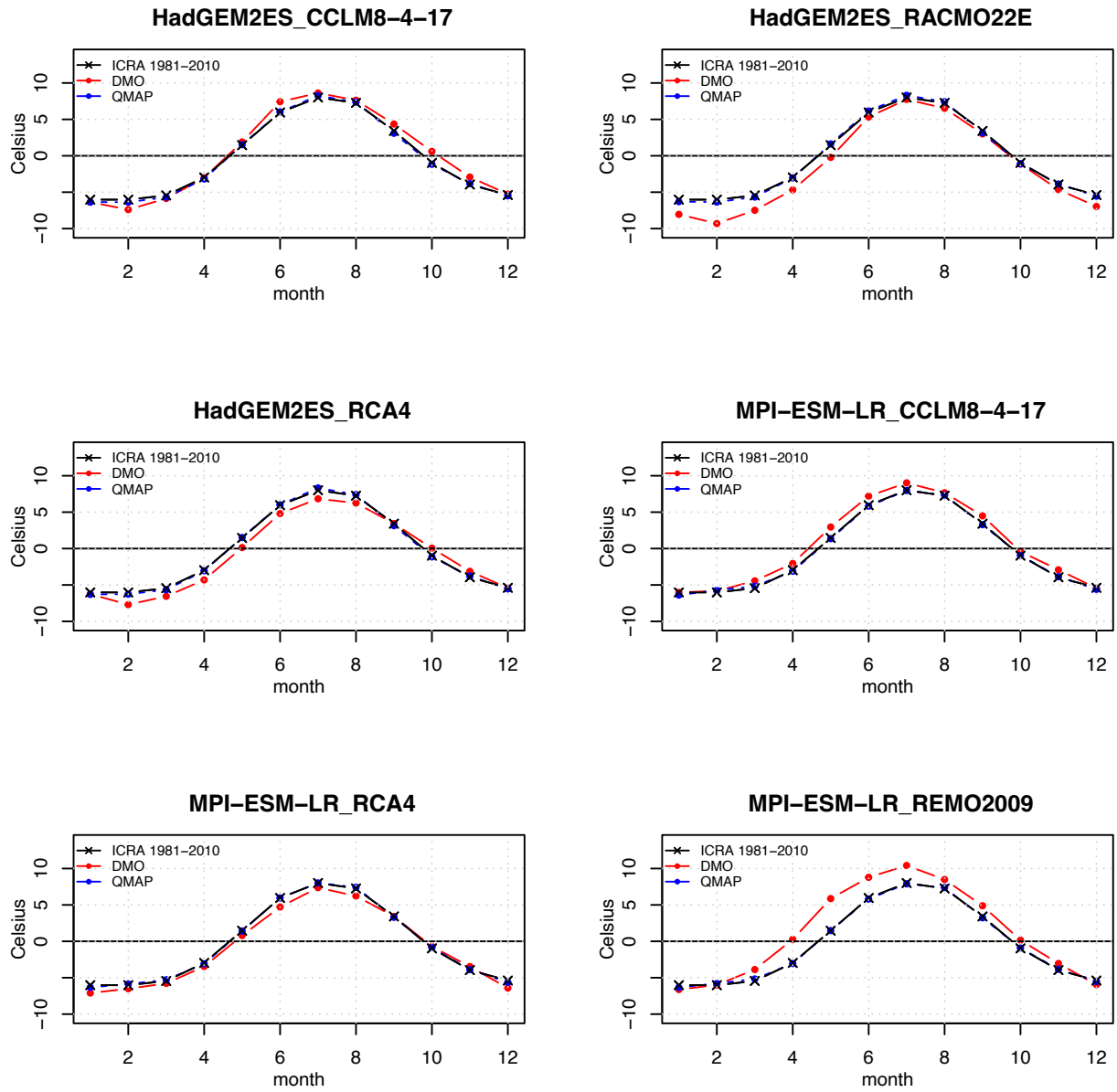

Fig. IV-1: Catchment vhm10: Mean monthly surface air temperature in the reference period (1981-2010). Each panel corresponds to a GCM-RCM combination (cf. Table 3). ICRA-reference (black line), original CORDEX projections (red line), locally-adjusted CORDEX projections (blue line). For the CORDEX projections, the period 2006-2010 is taken from the RCP4.5 scenario. The month=1 for January and 12 for December.

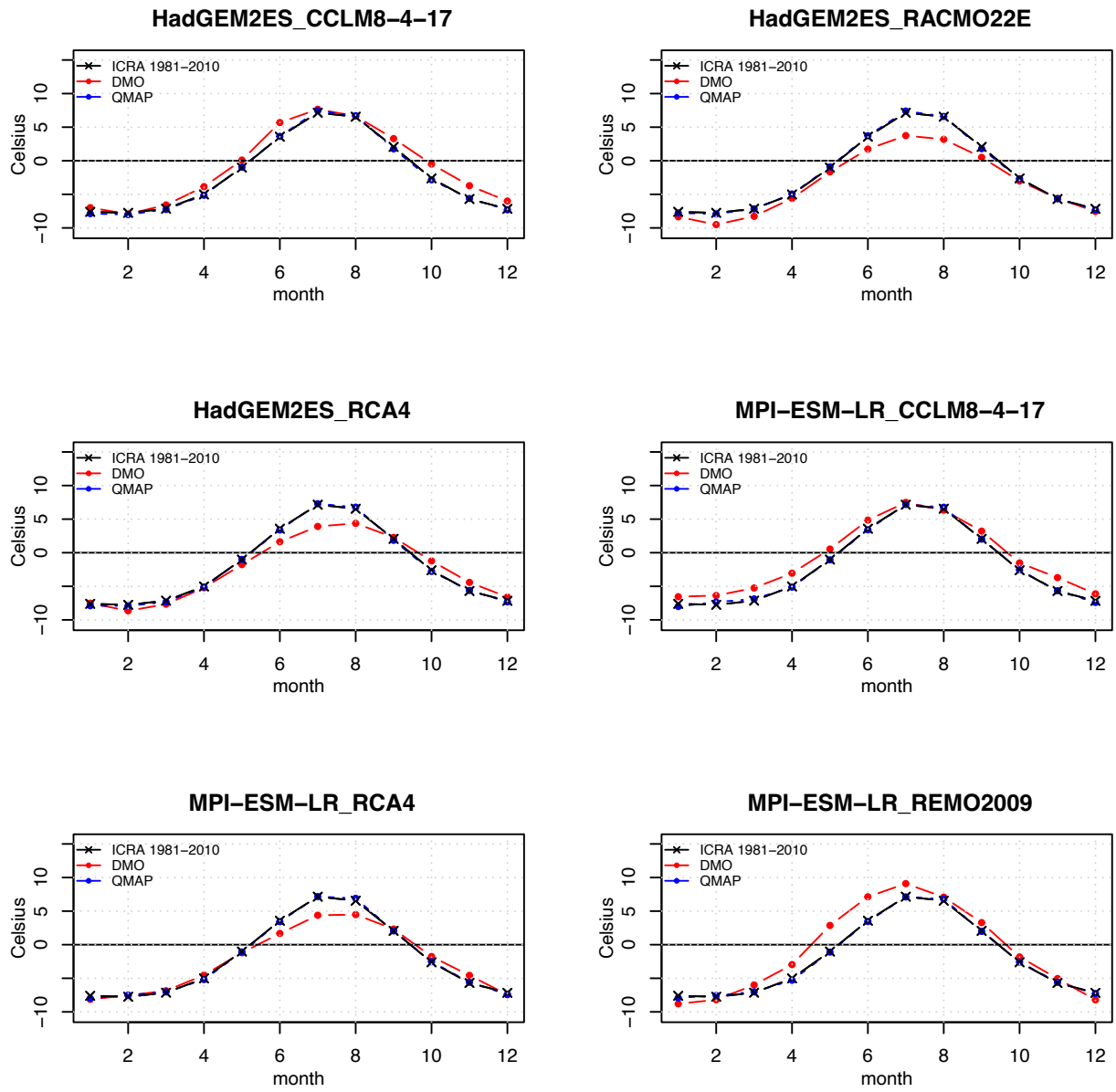

Fig. IV-2: Catchment vhm200: Mean monthly surface air temperature in the reference period (1981-2010). Each panel corresponds to a GCM-RCM combination (cf. Table 3). ICRA-reference (black line), original CORDEX projections (red line), locally-adjusted CORDEX projections (blue line). For the CORDEX projections, the period 2006-2010 is taken from the RCP4.5 scenario. The month=1 for January and 12 for December.

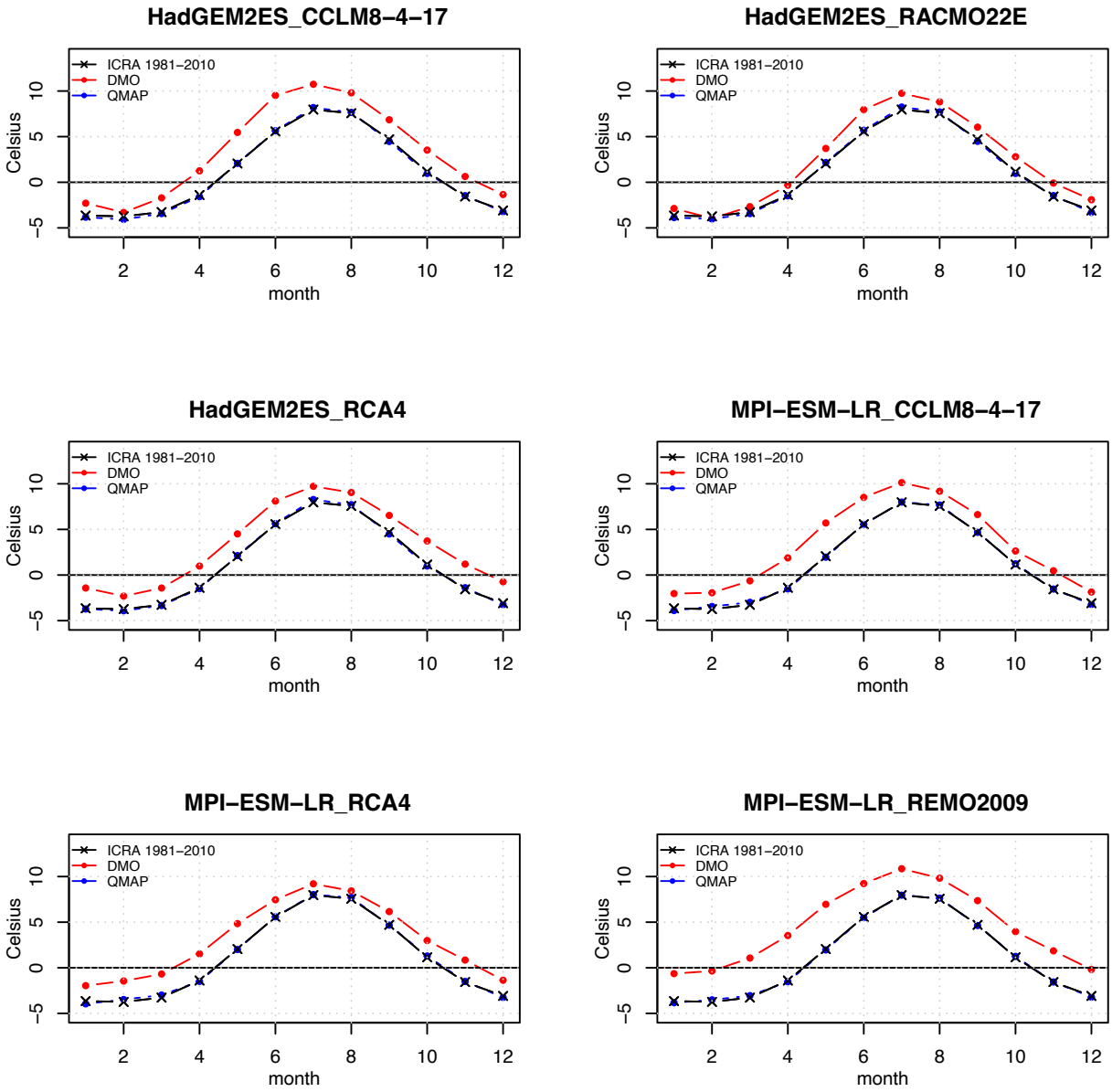

Fig. IV-3: Catchment vhm74: Mean monthly surface air temperature in the reference period (1981-2010). Each panel corresponds to a GCM-RCM combination (cf. Table 3). ICRA-reference (black line), original CORDEX projections (red line), locally-adjusted CORDEX projections (blue line). For the CORDEX projections, the period 2006-2010 is taken from the RCP4.5 scenario. The month=1 for January and 12 for December.

Appendix 5

Mean monthly precipitation in the reference period (1981-2010)

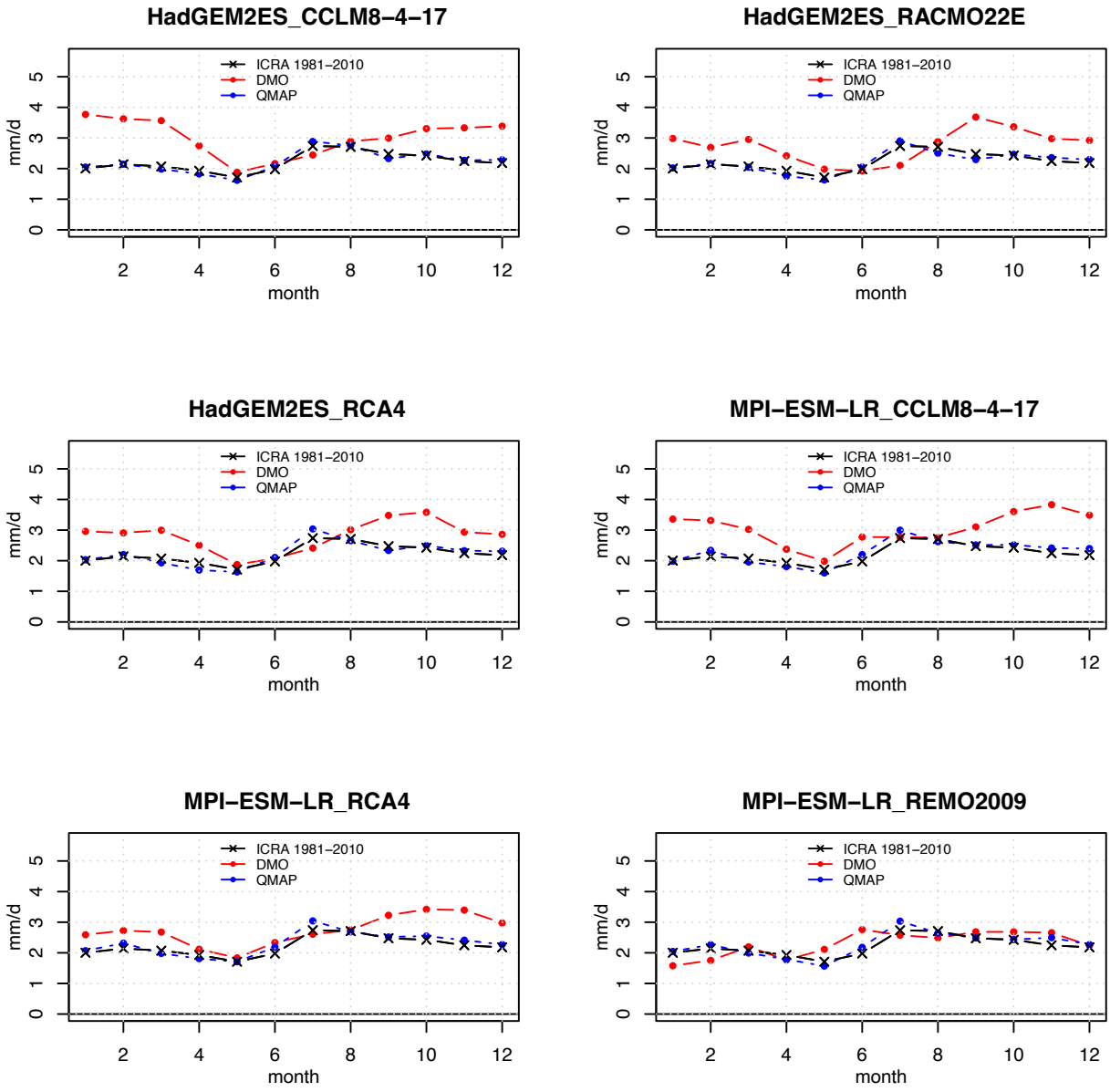

Fig. V-1: Catchment vhm10: Mean monthly precipitation in the reference period (1981-2010). Each panel corresponds to a GCM-RCM combination (cf. Table 3). ICRA-reference (black line), original CORDEX projections (red line), locally-adjusted CORDEX projections (blue line). For the CORDEX projections, the period 2006-2010 is taken from the RCP4.5 scenario. The month=1 for January and 12 for December.

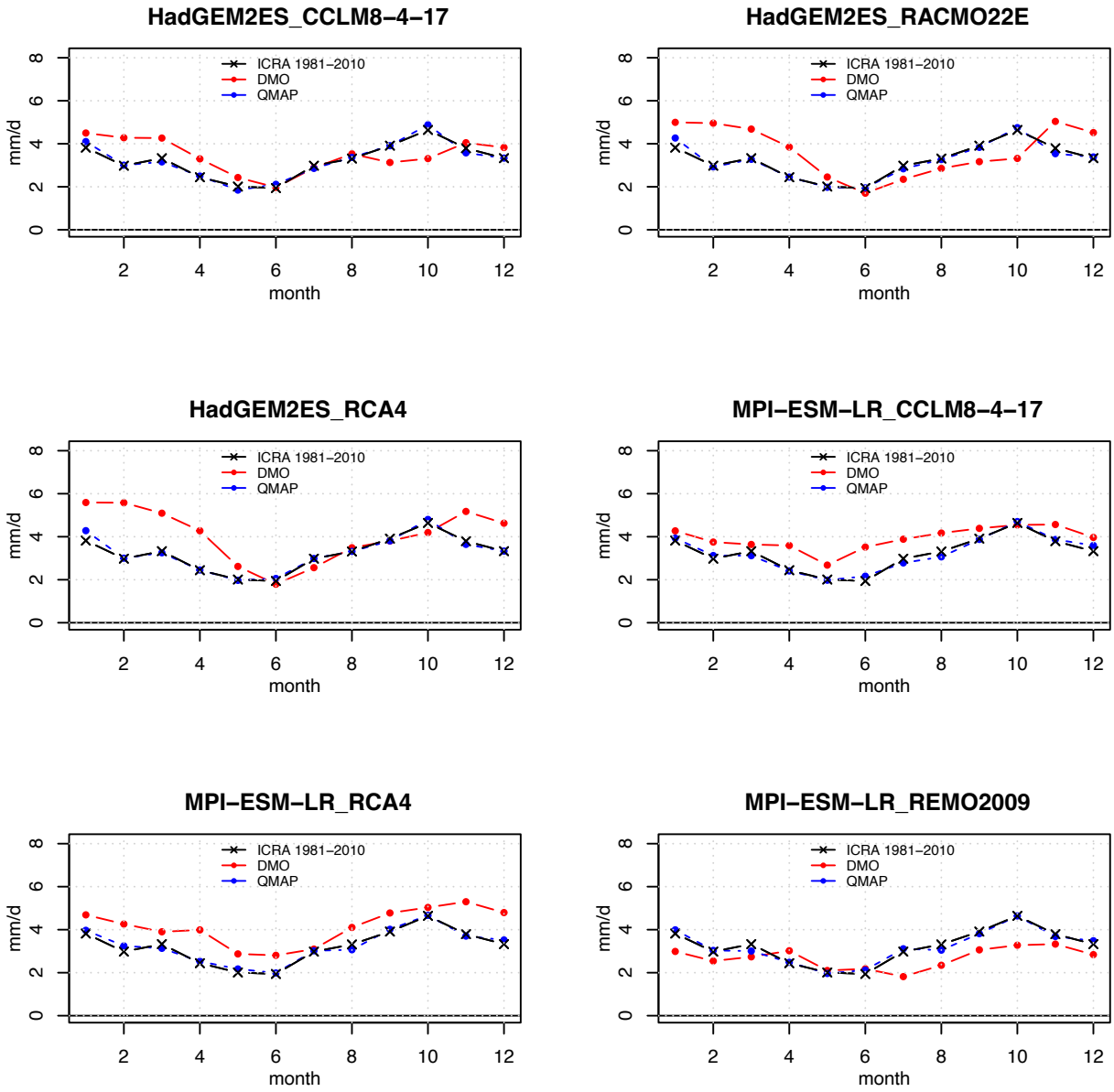

Fig. V-2: Catchment vhm200: Mean monthly precipitation in the reference period (1981-2010). Each panel corresponds to a GCM-RCM combination (cf. Table 3). ICRA-reference (black line), original CORDEX projections (red line), locally-adjusted CORDEX projections (blue line). For the CORDEX projections, the period 2006-2010 is taken from the RCP4.5 scenario. The month=1 for January and 12 for December.

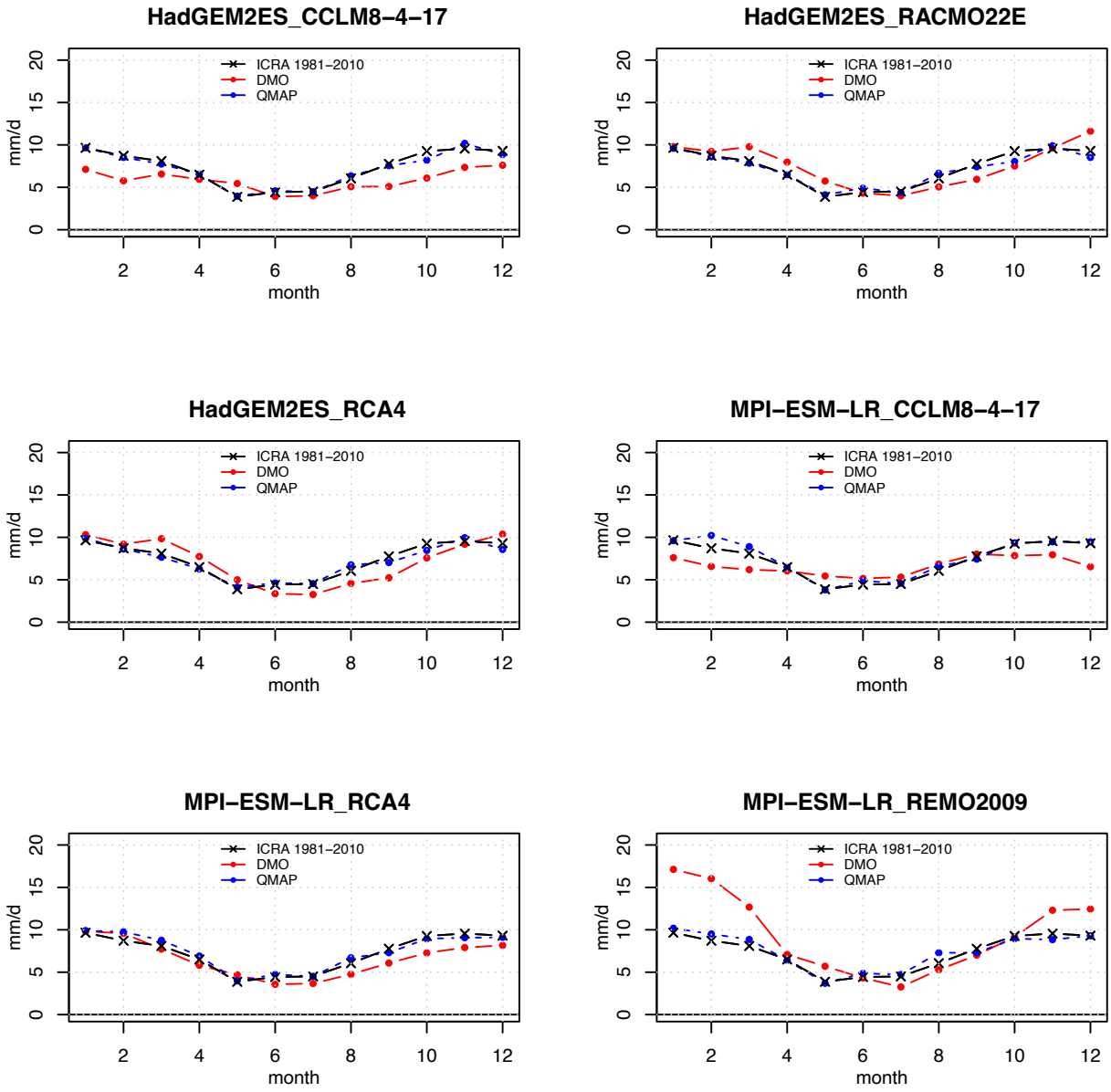

Fig. V-3: Catchment vhm74: Mean monthly precipitation in the reference period (1981-2010). Each panel corresponds to a GCM-RCM combination (cf. Table 3). ICRA-reference (black line), original CORDEX projections (red line), locally-adjusted CORDEX projections (blue line). For the CORDEX projections, the period 2006-2010 is taken from the RCP4.5 scenario. The month=1 for January and 12 for December.

Appendix 6

Projected locally-adjusted 30-year mean monthly air temperature

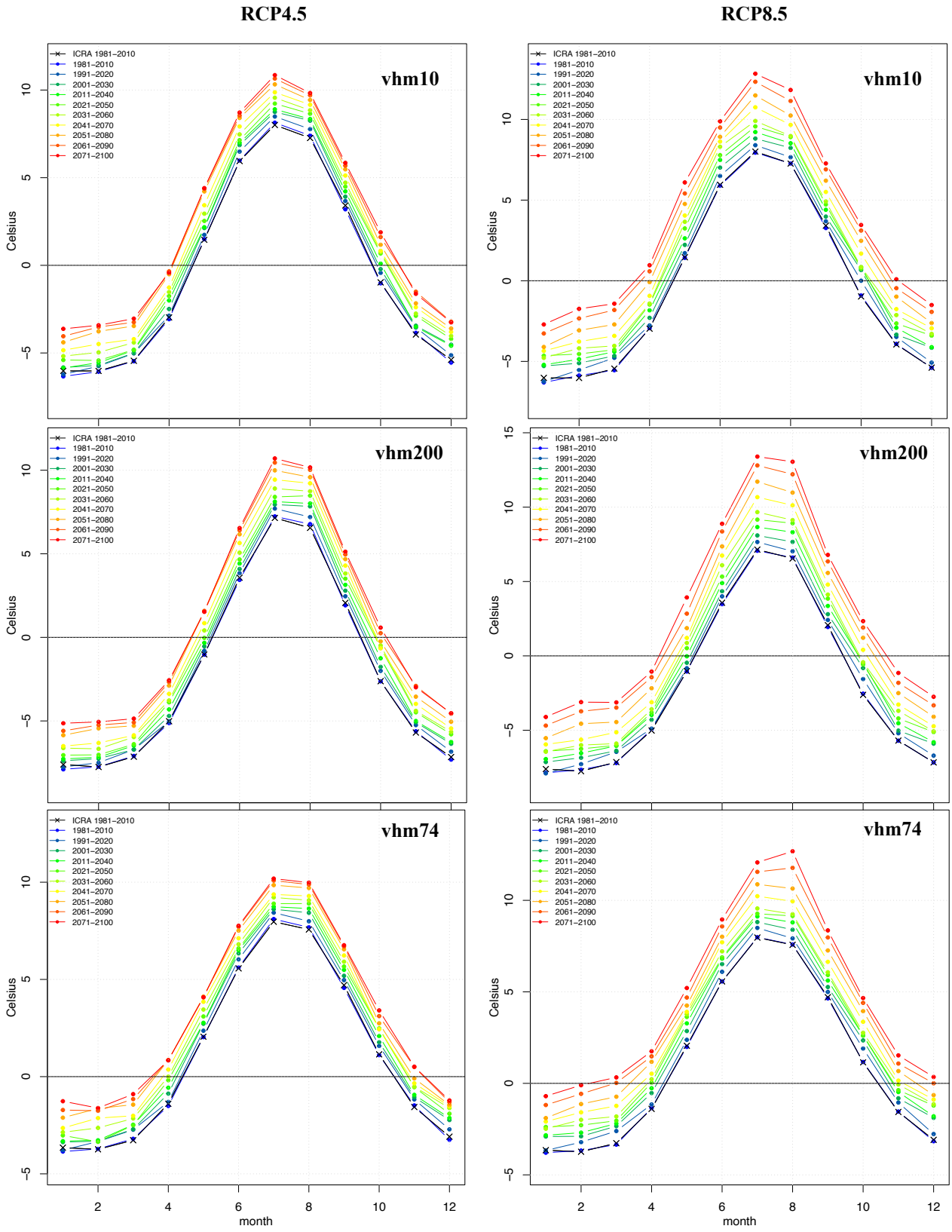

Fig. VI-1: Ensemble median of the projected seasonality of 30-year mean monthly surface air temperature under the RCP4.5 emission scenario (left panel) and RCP8.5 emission scenario (right panel). Catchments vhm10 (top panel), vhm200 (middle panel), vhm74 (bottom panel). ICRA-reference (1981-2010) (black line). Each colour corresponds to a 30-year period: from dark blue (1981-2010) to red (2071-2100). The month=1 for January and 12 for December.

Appendix 7

Projected locally-adjusted monthly precipitation under the RCP4.5 emission scenario

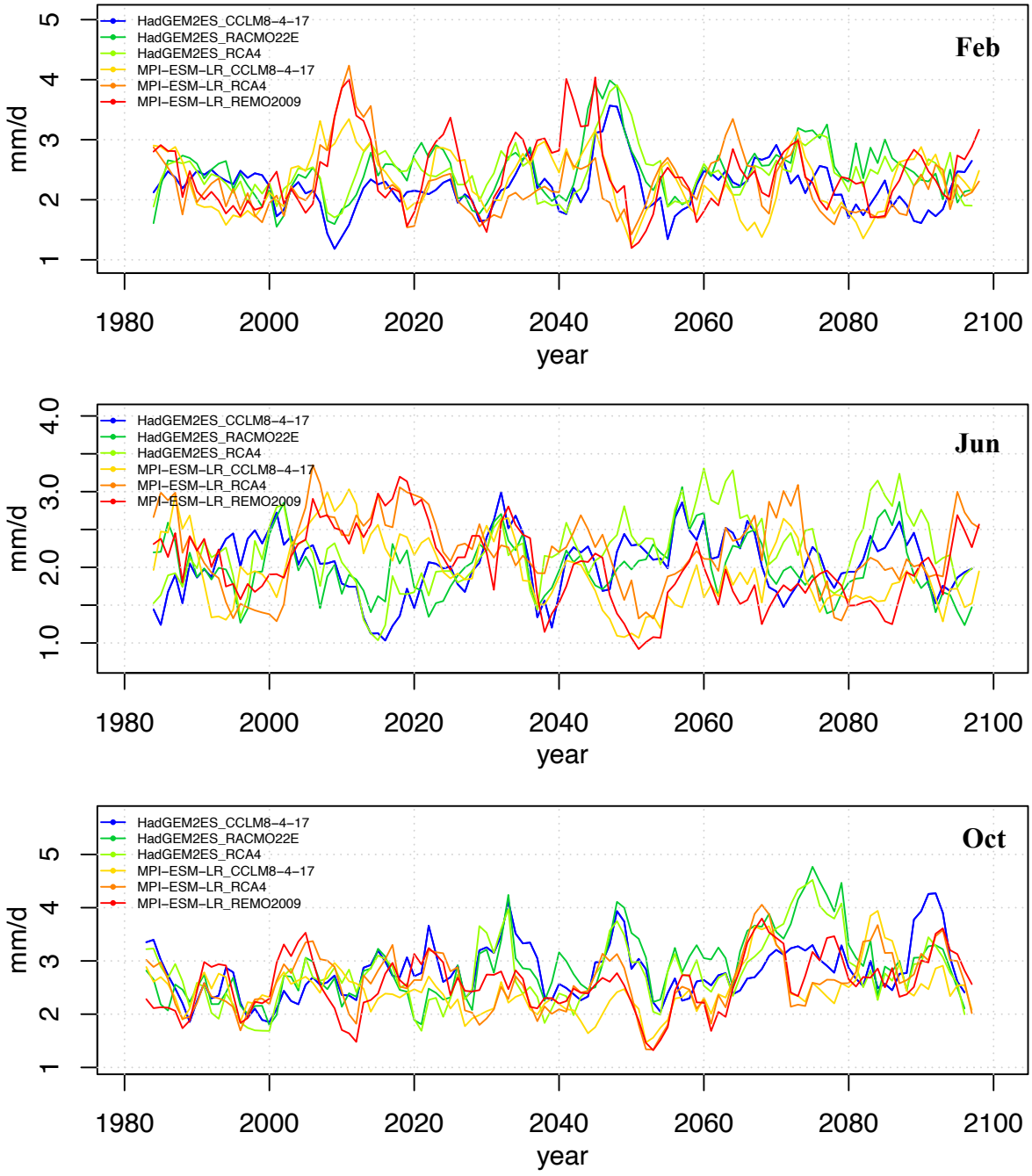

Fig. VII-1: Catchment vhm10: Projected CORDEX monthly precipitation under the RCP4.5 emission scenario. Top (February); Middle (June); Bottom (October). A 5-year running mean was applied. Each colour corresponds to a GCM-RCM combination (cf. Table 3).

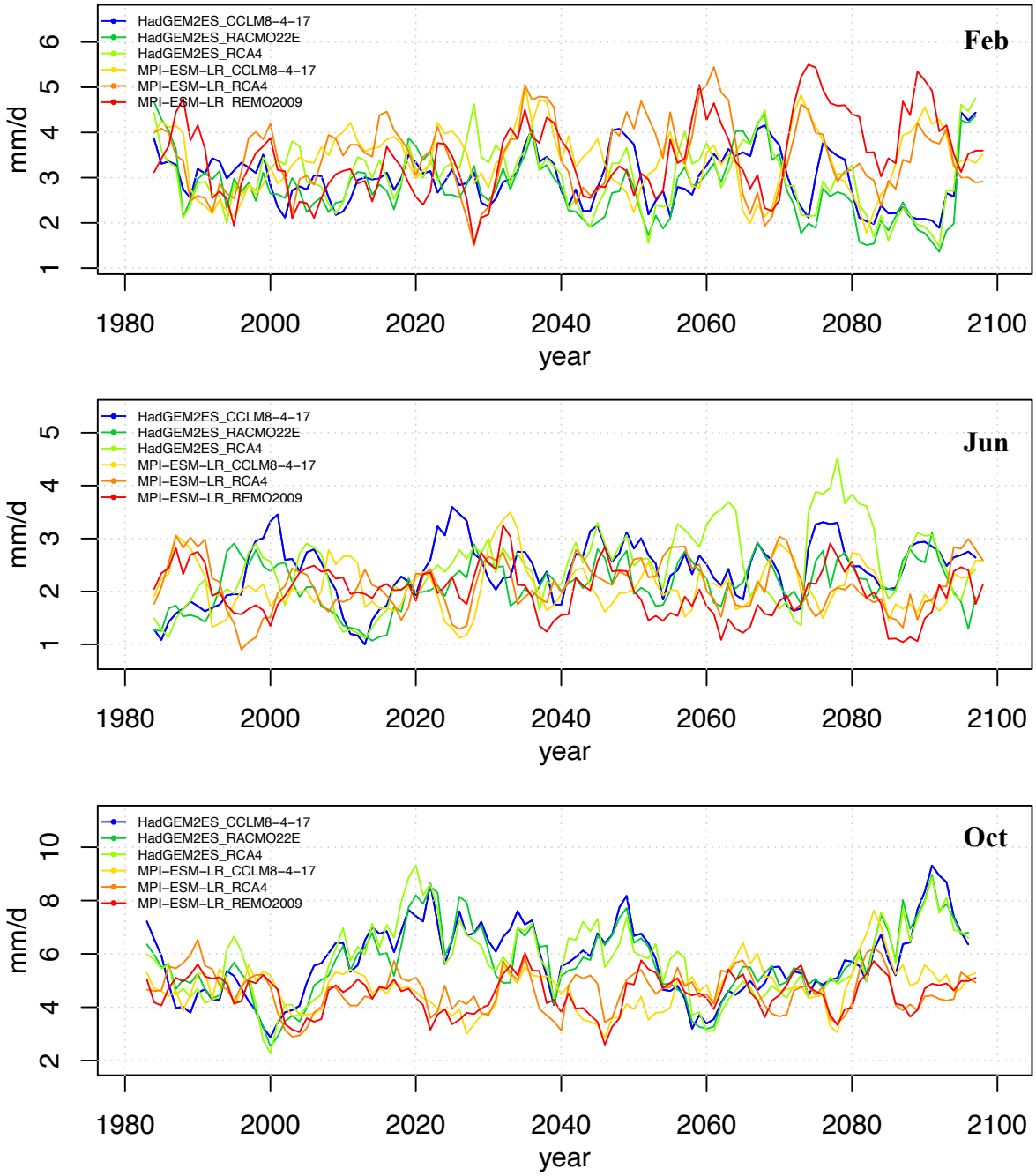

Fig. VII-2: Catchment vhm200: Projected CORDEX monthly precipitation under the RCP4.5 emission scenario. Top (February); Middle (June); Bottom (October). A 5-year running mean was applied. Each colour corresponds to a GCM-RCM combination (cf. Table 3).

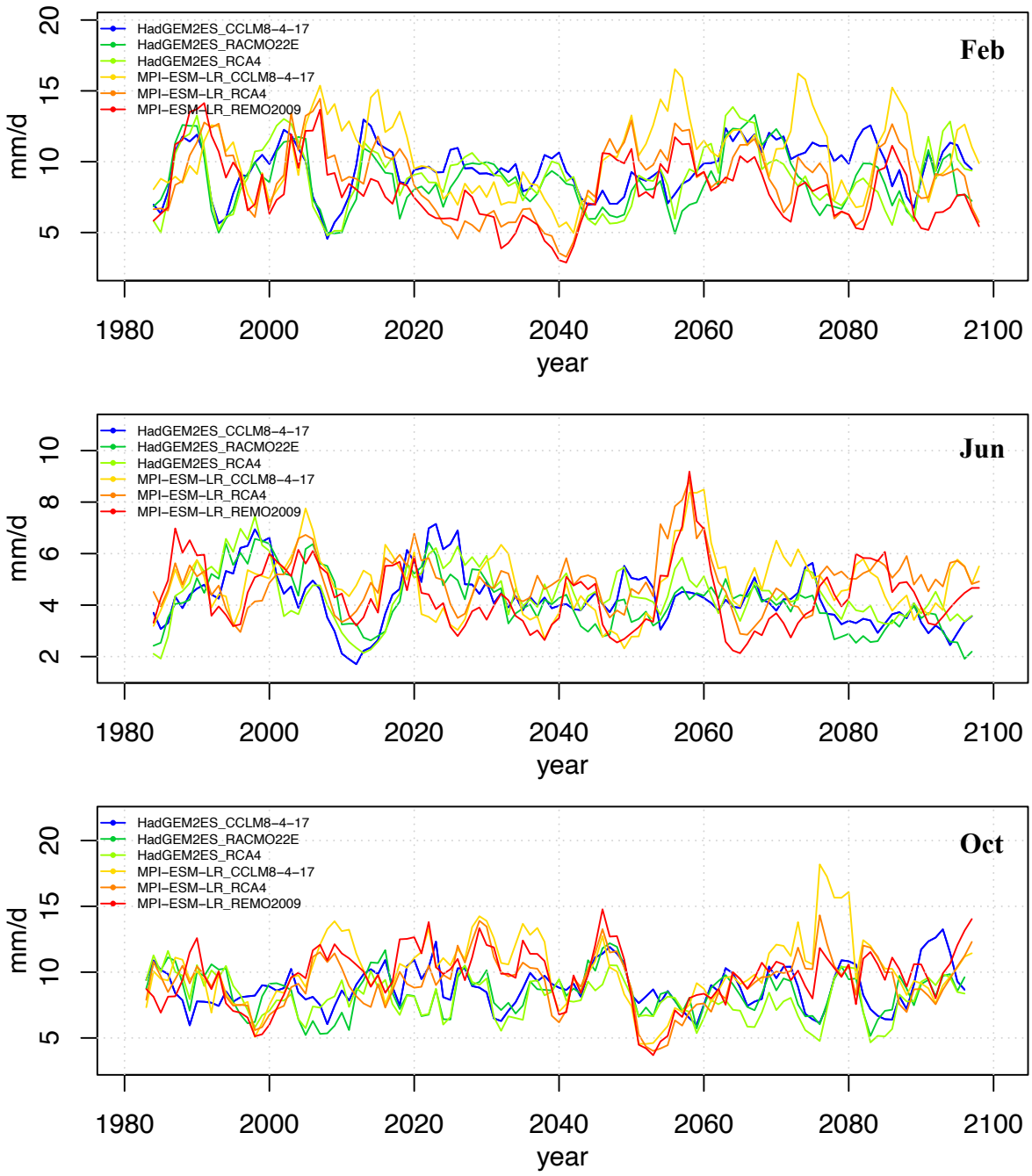

Fig. VII-3: Catchment vhm74: Projected CORDEX monthly precipitation under the RCP4.5 emission scenario. Top (February); Middle (June); Bottom (October). A 5-year running mean was applied. Each colour corresponds to a GCM-RCM combination (cf. Table 3).

Appendix 8

Hydrological projections in the reference period (1981-2010): magnitude and seasonal frequency of occurrence of AMFs

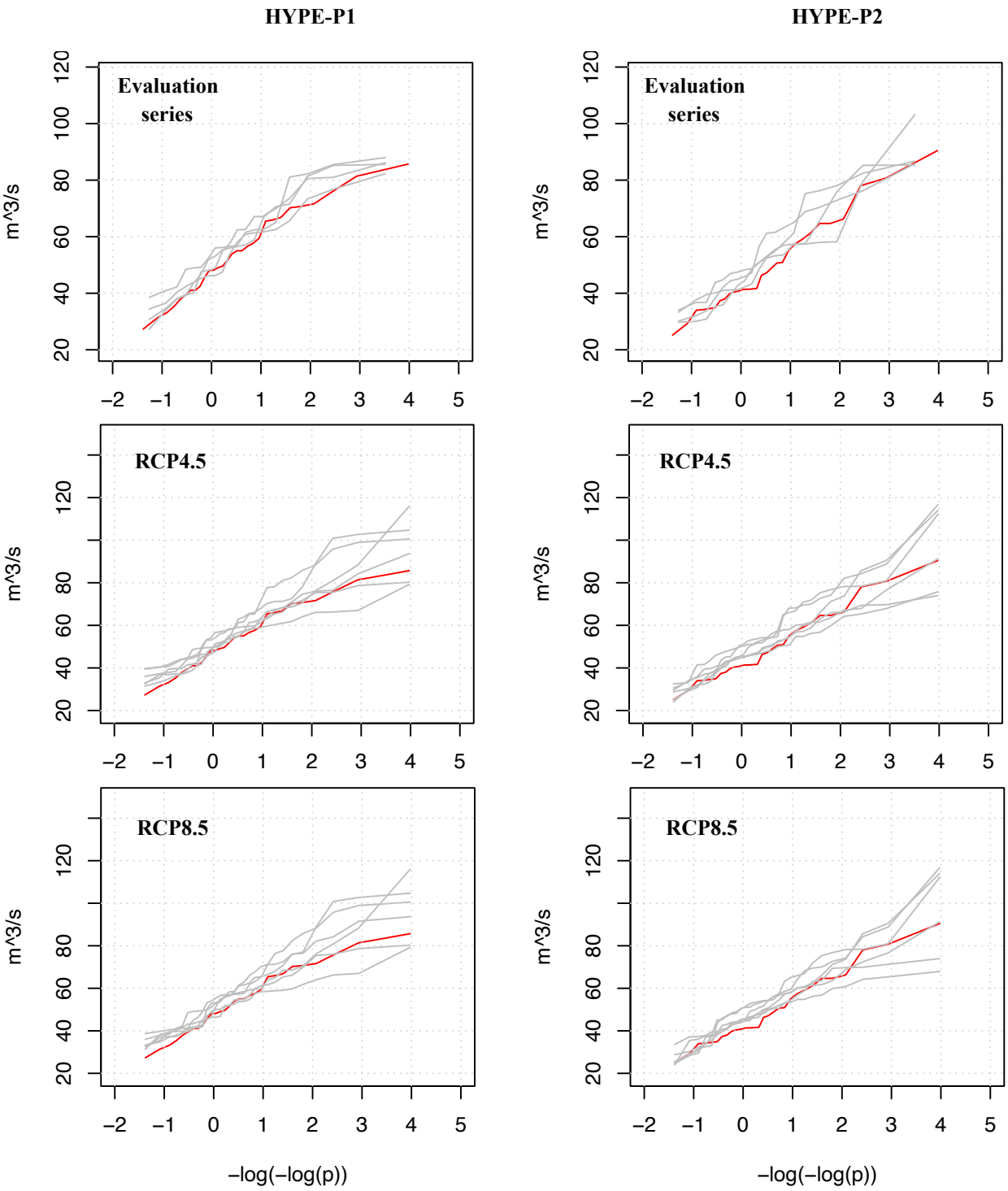

Fig. VIII-1: Catchment vhm10: Empirical cumulative distribution function of AMFs in the reference period. Estimations derived from the HYPE model forced with the ICRA reanalysis (red line) and with the locally-adjusted CORDEX projections (grey lines) in the 1989-2007 period (evaluation series) and 1981-2010 period (RCPs 4.5 & 8.5). Hydrological model forced with CORDEX evaluation series (top), CORDEX RCP4.5 series (middle), CORDEX RCP8.5 series (bottom). Left-panel: HYPE with parameter set calibrated in 1996-2002. Right-panel: HYPE with parameter set calibrated in 2003-2009.

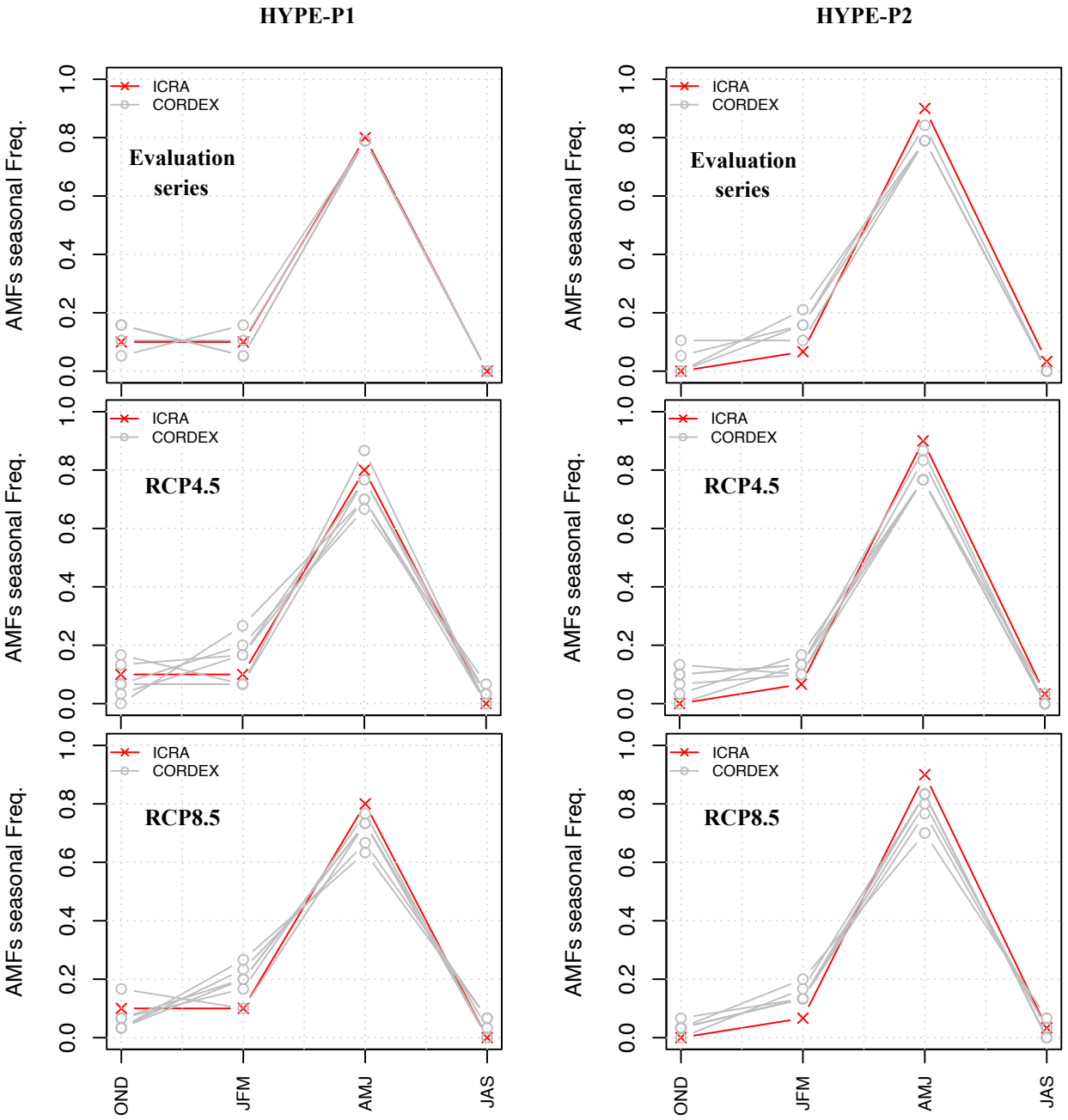

Fig. VIII-2: Catchment vhm10: Relative seasonal frequency of occurrence of AMFs in the reference period. Estimations derived from the HYPE model forced with the ICRA reanalysis (red line) and with the locally-adjusted CORDEX projections (grey lines) in the 1989-2007 period (evaluation series) and 1981-2010 period (RCPs 4.5 & 8.5). Hydrological model forced with CORDEX evaluation series (top), CORDEX RCP4.5 series (middle), CORDEX RCP8.5 series (bottom). Left-panel: HYPE with parameter set calibrated in 1996-2002. Right-panel: HYPE with parameter set calibrated in 2003-2009.

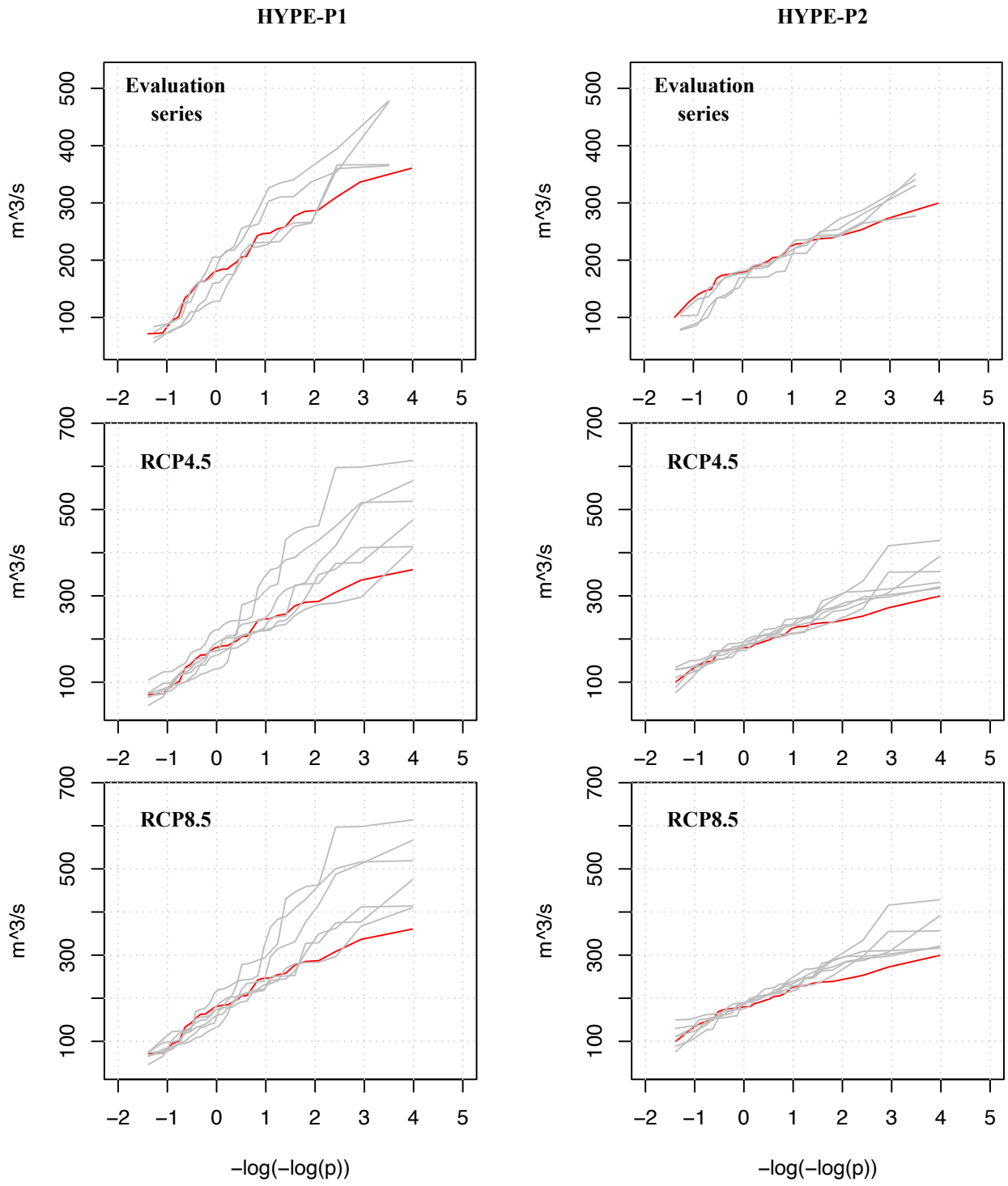

Fig. VIII-3: Catchment vhm200: Empirical cumulative distribution function of AMFs in the reference period. Estimations derived from the HYPE model forced with the ICRA reanalysis (red line) and with the locally-adjusted CORDEX projections (grey lines) in the 1989-2007 period (evaluation series) and 1981-2010 period (RCPs 4.5 & 8.5). Hydrological model forced with CORDEX evaluation series (top), CORDEX RCP4.5 series (middle), CORDEX RCP8.5 series (bottom). Left-panel: HYPE with parameter set calibrated in 1996-2002. Right-panel: HYPE with parameter set calibrated in 2003-2009.

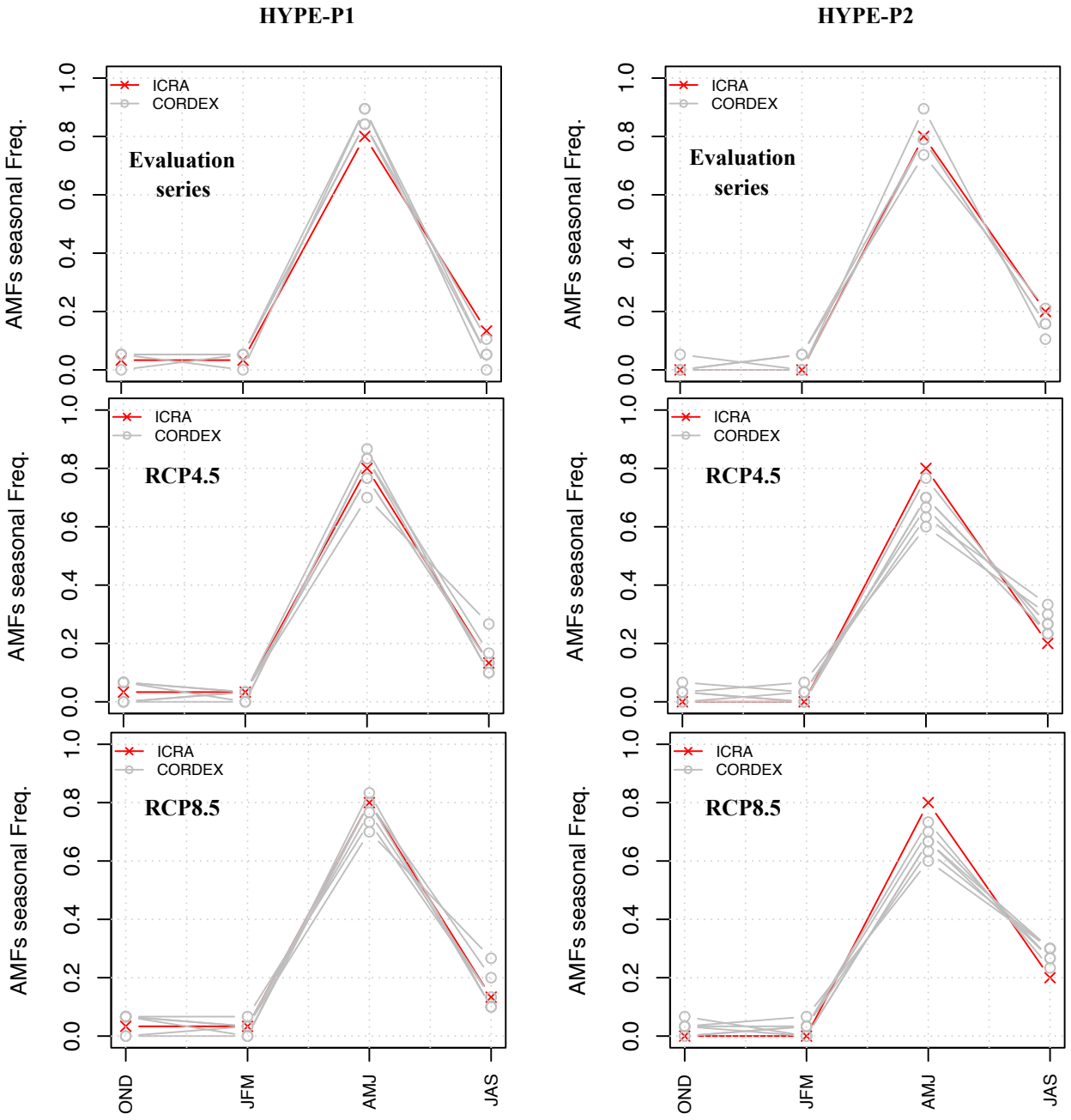

Fig. VIII-4: Catchment vhm200: Relative seasonal frequency of occurrence of AMFs in the reference period. Estimations derived from the HYPE model forced with the ICRA reanalysis (red line) and with the locally-adjusted CORDEX projections (grey lines) in the 1989-2007 period (evaluation series) and 1981-2010 period (RCPs 4.5 & 8.5). Hydrological model forced with CORDEX evaluation series (top), CORDEX RCP4.5 series (middle), CORDEX RCP8.5 series (bottom). Left-panel: HYPE with parameter set calibrated in 1996-2002. Right-panel: HYPE with parameter set calibrated in 2003-2009.

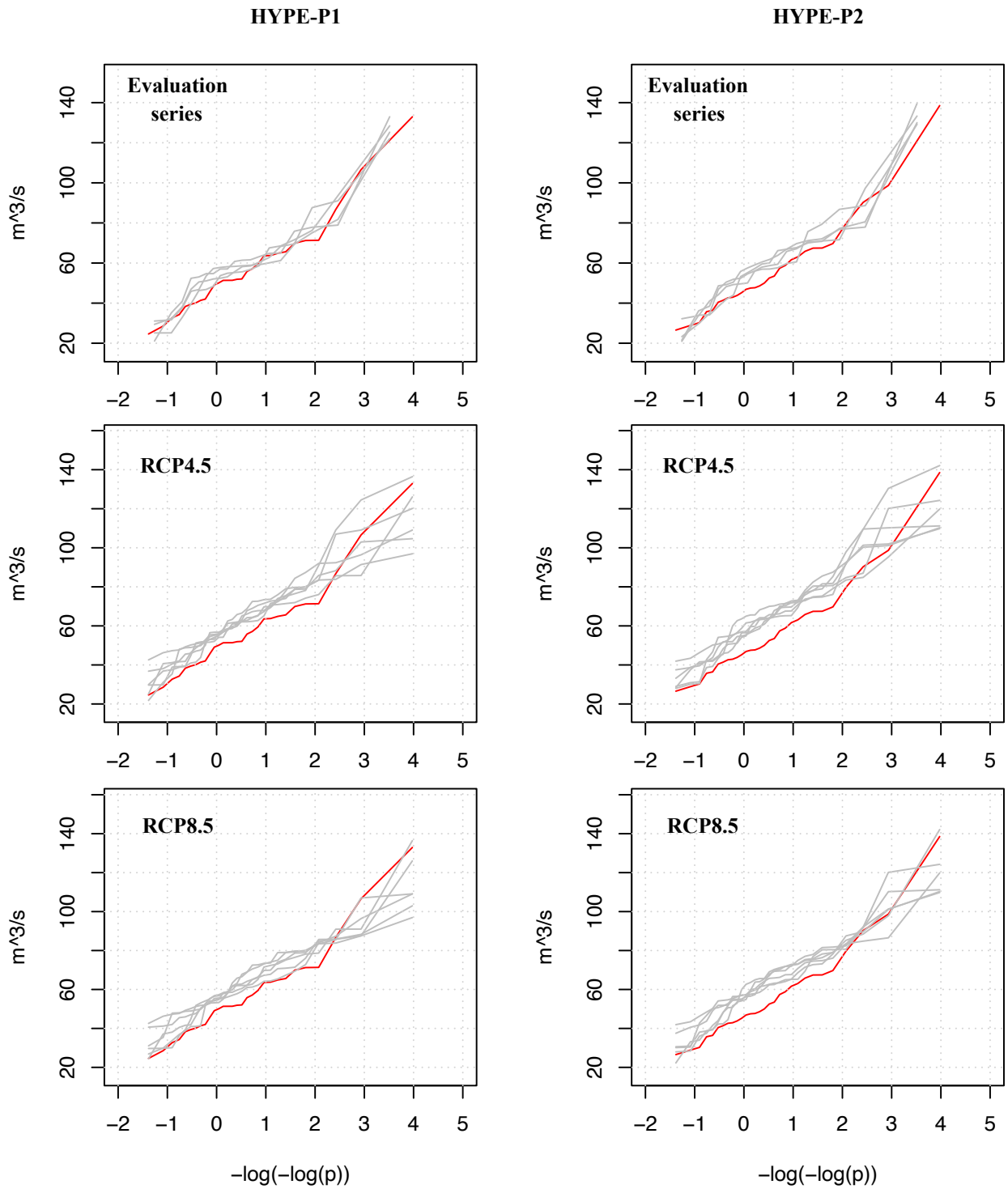

Fig. VIII-5: Catchment vhm74: Empirical cumulative distribution function of AMFs in the reference period. Estimations derived from the HYPE model forced with the ICRA reanalysis (red line) and with the locally-adjusted CORDEX projections (grey lines) in the 1989-2007 period (evaluation series) and 1981-2010 period (RCPs 4.5 & 8.5). Hydrological model forced with CORDEX evaluation series (top), CORDEX RCP4.5 series (middle), CORDEX RCP8.5 series (bottom). Left-panel: HYPE with parameter set calibrated in 2006-2011. Right-panel: HYPE with parameter set calibrated in 2012-2016.

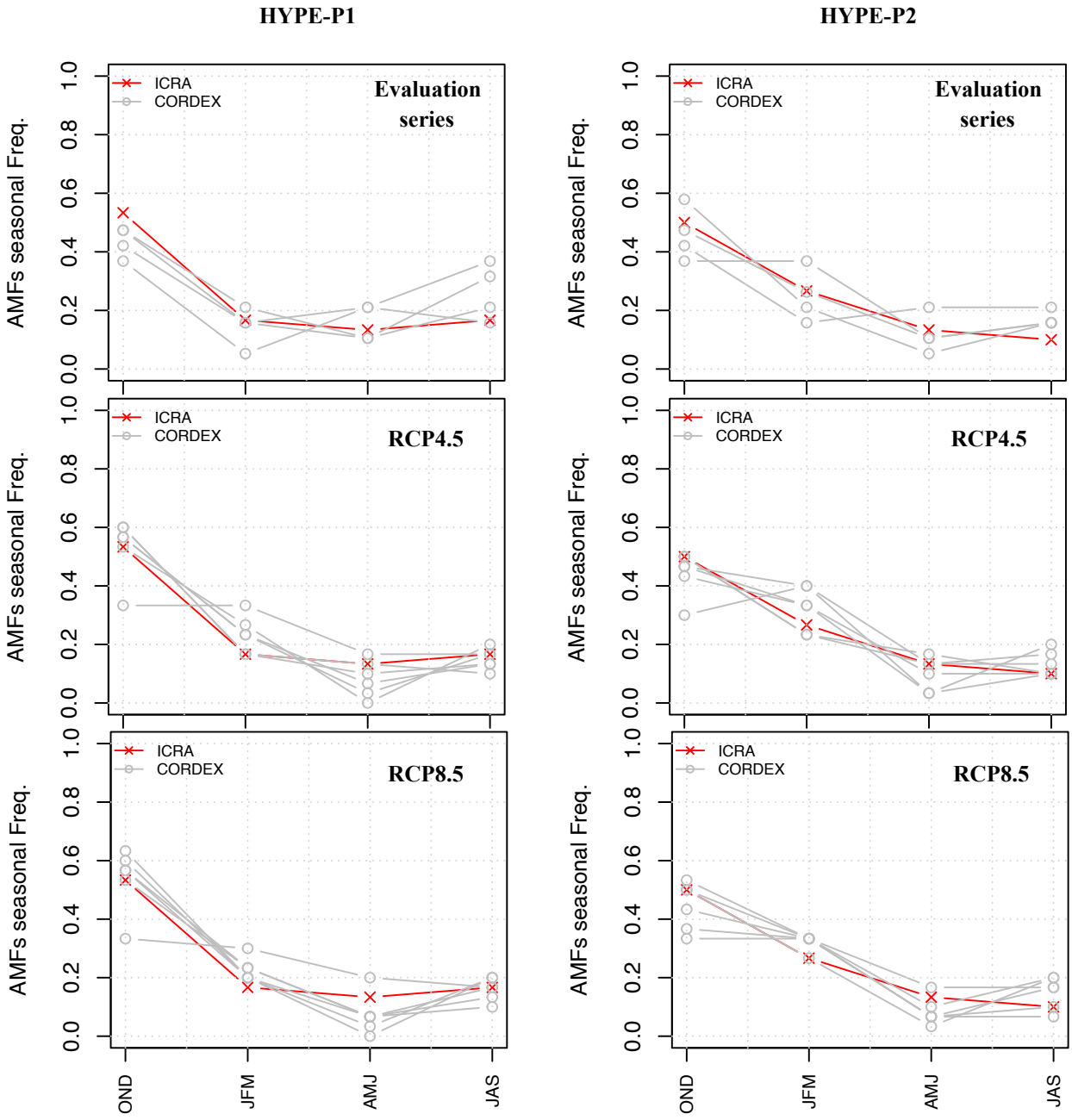

Fig. VIII-6: Catchment vhm74: Relative seasonal frequency of occurrence of AMFs in the reference period. Estimations derived from the HYPE model forced with the ICRA reanalysis (red line) and with the locally-adjusted CORDEX projections (grey lines) in the 1989-2007 period (evaluation series) and 1981-2010 period (RCPs 4.5 & 8.5). Hydrological model forced with CORDEX evaluation series (top), CORDEX RCP4.5 series (middle), CORDEX RCP8.5 series (bottom). Left-panel: HYPE with parameter set calibrated in 2006-2011. Right-panel: HYPE with parameter set calibrated in 2012-2016.

Appendix 9

Projected seasonal frequency of occurrence of AMFs

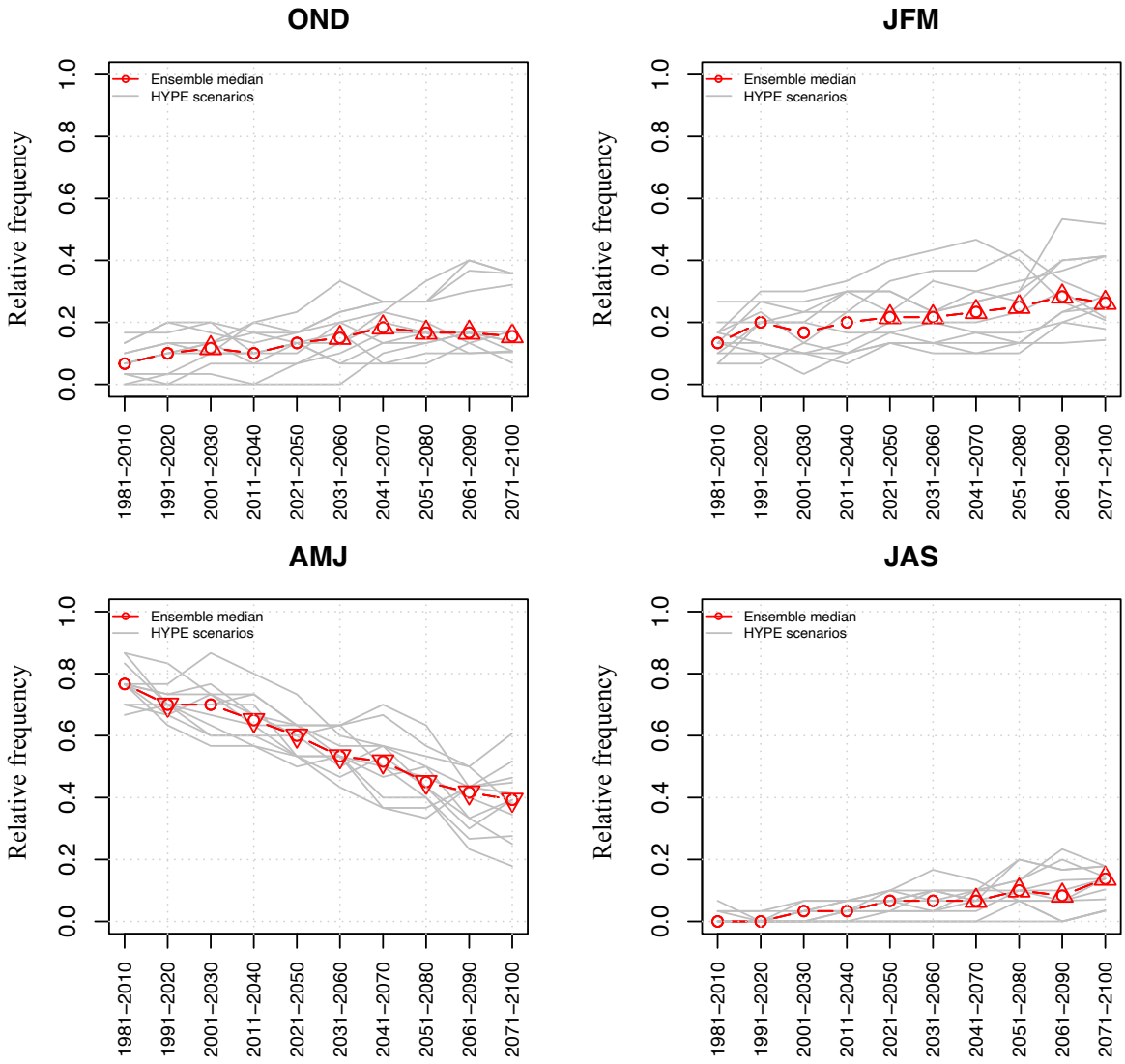

Fig. IX-1: Catchment vhm10: Projected relative seasonal frequency of occurrence of AMFs under the RCP4.5 emission scenario. Ensemble members (grey lines) and ensemble median (red line). The symbols on the ensemble median indicate whether a significant shift in the seasonal frequency ensemble has been detected between the reference and future periods (triangle point-up=freq. increase; triangle point down=freq. decrease; open circle=no significant change).

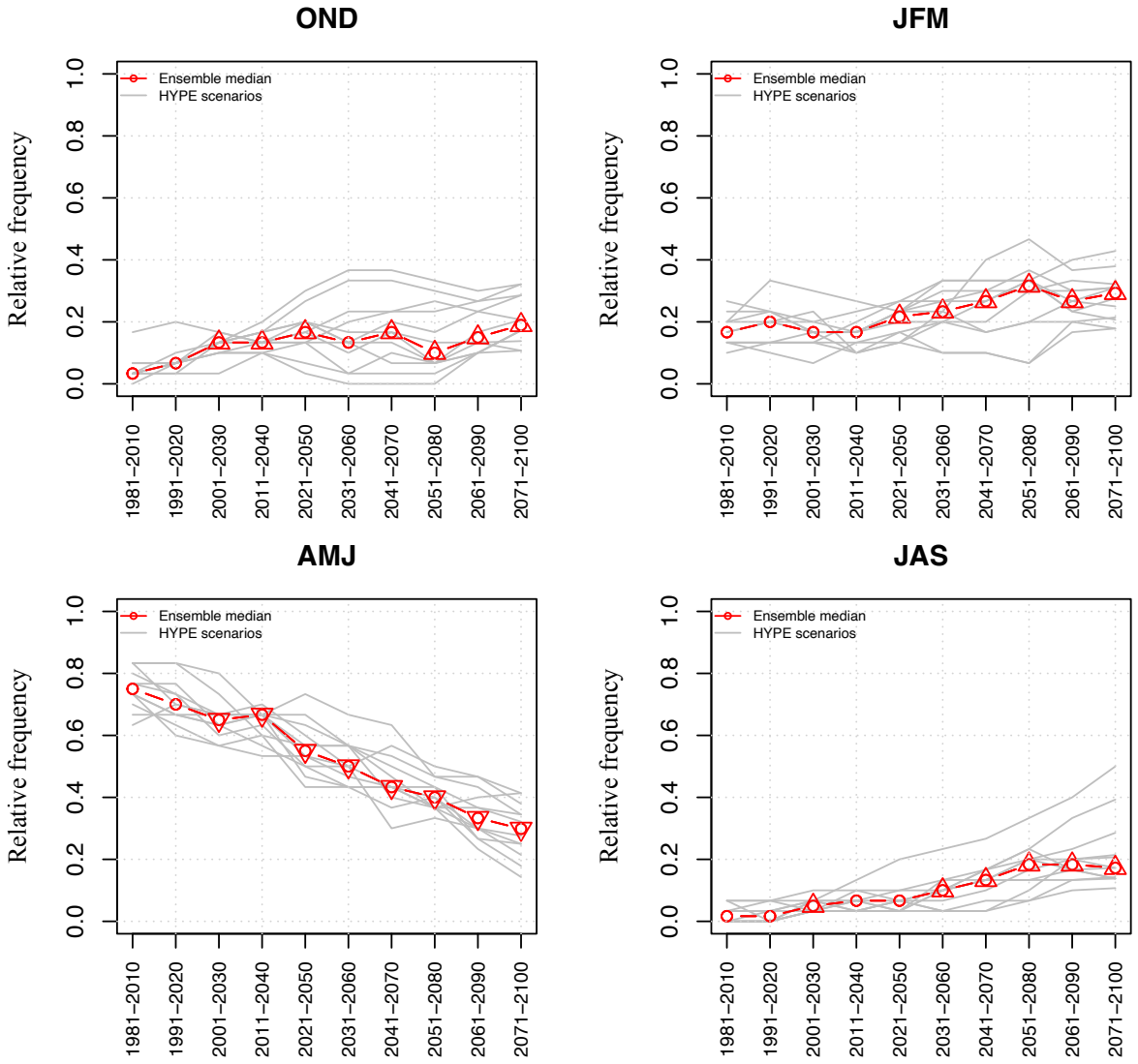

Fig. IX-2: Catchment vhm10: Projected relative seasonal frequency of occurrence of AMFs under the RCP8.5 emission scenario. Ensemble members (grey lines) and ensemble median (red line). The symbols on the ensemble median indicate whether a significant shift in the seasonal frequency ensemble has been detected between the reference and future periods (triangle point-up=freq. increase; triangle point down=freq. decrease; open circle=no significant change).

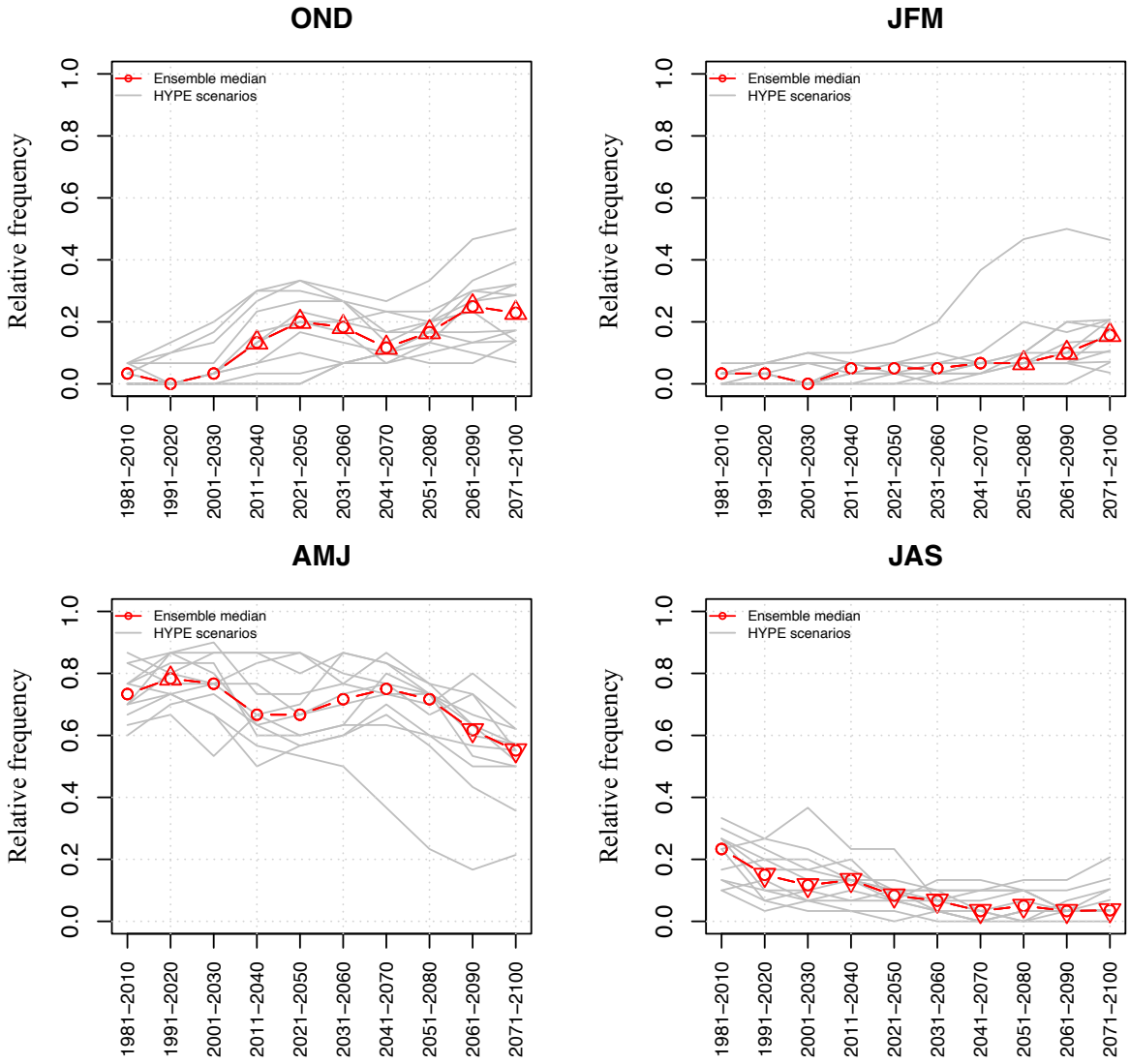

Fig. IX-3: Catchment vhm200: Projected relative seasonal frequency of occurrence of AMFs under the RCP4.5 emission scenario. Ensemble members (grey lines) and ensemble median (red line). The symbols on the ensemble median indicate whether a significant shift in the seasonal frequency ensemble has been detected between the reference and future periods (triangle point-up=freq. increase; triangle point down=freq. decrease; open circle=no significant change).

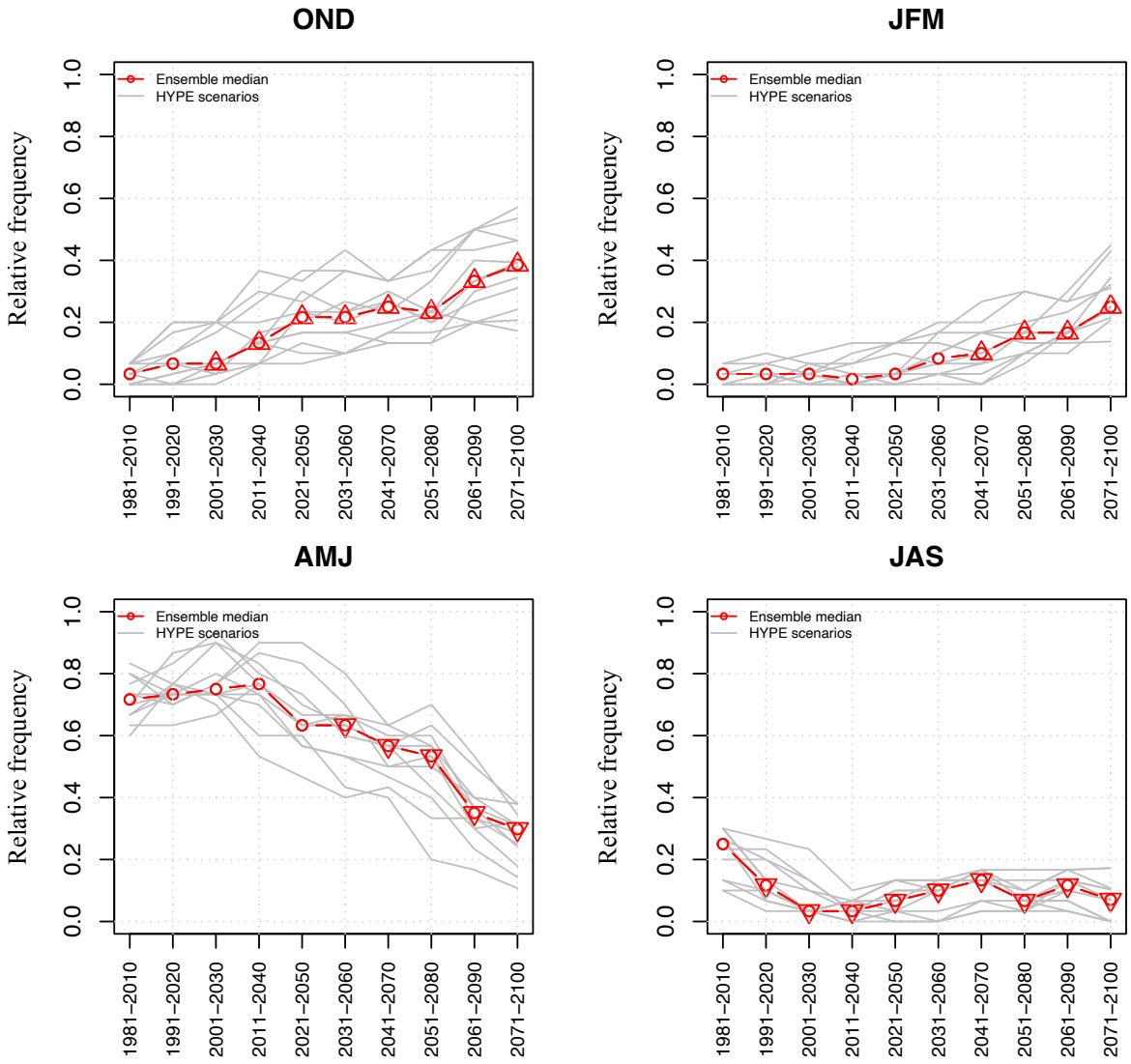

Fig. IX-4: Catchment vhm200: Projected relative seasonal frequency of occurrence of AMFs under the RCP8.5 emission scenario. Ensemble members (grey lines) and ensemble median (red line). The symbols on the ensemble median indicate whether a significant shift in the seasonal frequency ensemble has been detected between the reference and future periods (triangle point-up=freq. increase; triangle point down=freq. decrease; open circle=no significant change).

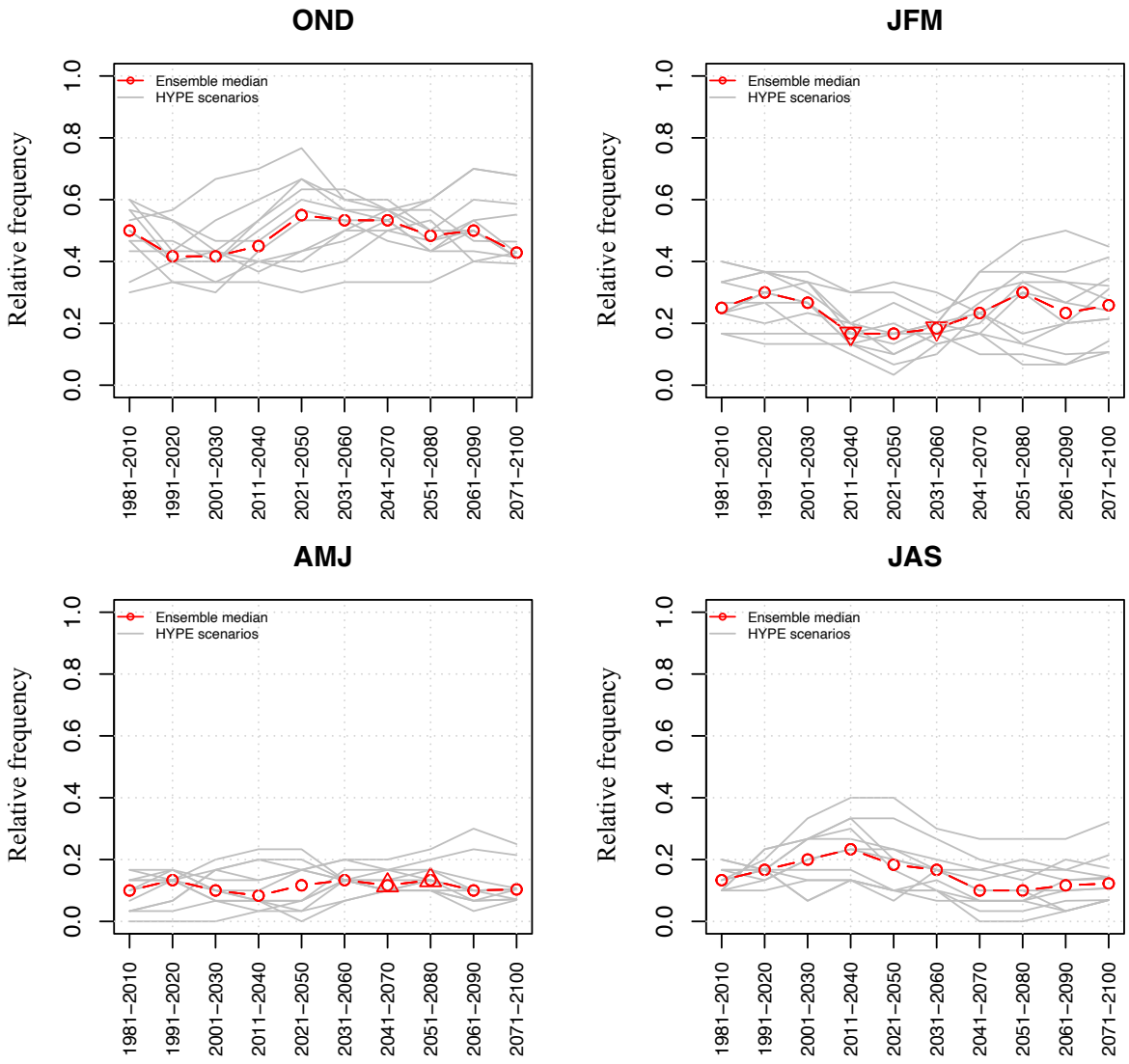

Fig. IX-5: Catchment vhm74: Projected relative seasonal frequency of occurrence of AMFs under the RCP4.5 emission scenario. Ensemble members (grey lines) and ensemble median (red line). The symbols on the ensemble median indicate whether a significant shift in the seasonal frequency ensemble has been detected between the reference and future periods (triangle point-up=freq. increase; triangle point down=freq. decrease; open circle=no significant change).

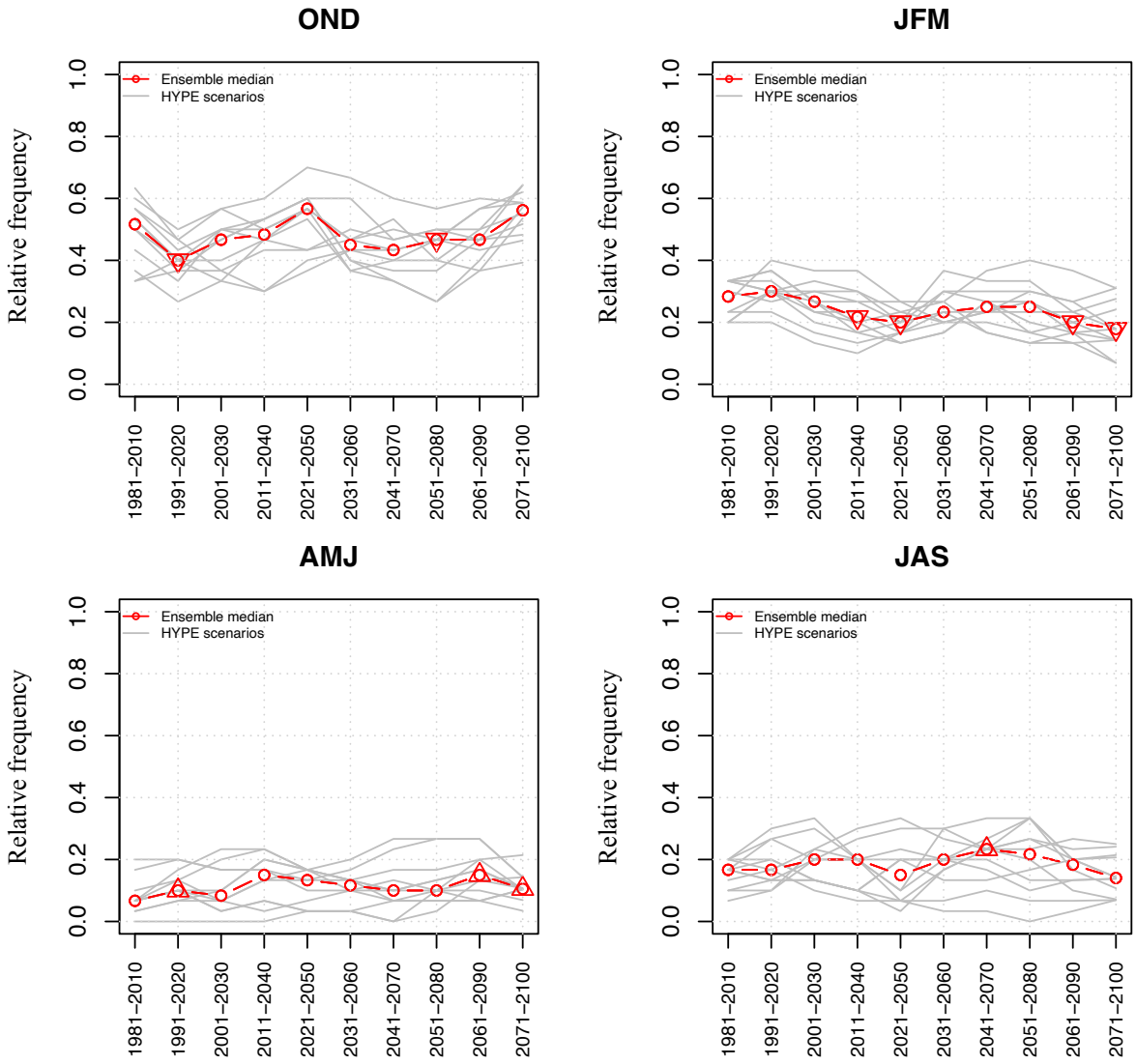

Fig. IX-6: Catchment vhm74: Projected relative seasonal frequency of occurrence of AMFs under the RCP8.5 emission scenario. Ensemble members (grey lines) and ensemble median (red line). The symbols on the ensemble median indicate whether a significant shift in the seasonal frequency ensemble has been detected between the reference and future periods (triangle point-up=freq. increase; triangle point down=freq. decrease; open circle=no significant change).